13th INTERNATIONAL BOLOGNA CONFERENCE ON MAGNETIC RESONANCE IN POROUS MEDIA

Bologna 2016

Conference Handbook and Book of Abstracts

3-4 September 2016 – NMR School

4-8 September 2016 – MRPM13 Conference

http://eventi.unibo.it/mrpm13 - http://www.mrpm.org

How to cite this work:
Bortolotti, Villiam; Fantazzini, Paola; Brizi Leonardo (Eds), (2016) *13th Internationl Bologna Conference on Magnetic Resonance in Porous Media - Bologna 2016: Conference Handbook and Book of Abstracts*.
DOI: http://doi.org/10.6092/unibo/amsacta/5446

Welcome to Bologna *MRPM13*, the 13th International Bologna Conference on Magnetic Resonance in Porous Media, an AMPERE Event organized under the auspices of Alma Mater Studiorum, University of Bologna. The Conference will be held at the University's prestigious School of Engineering and Architecture, which has made available its excellent facilities.

The conference series was founded by the University of Bologna, where the first meeting was held in 1990. MRPM2, held in 1993, was hosted by the University of Kent, Canterbury, UK, MRPM3 in 1995 at the Université Catholique of Louvain-la-Neuve, Belgium, and MRPM4, in 1997, in Trondheim, Norway. The conference returned to Bologna for its fifth edition in 2000. MRPM6 was organized in 2002 at the University of Ulm, Germany, and MRPM7 in 2004 in Palaiseau, France. After MRPM7, the community joined the *Groupement Ampere* as the *MRPM Division*, and the Conferences, now called the "*Bologna MRPM Conferences*," became *Ampere Events*. MRPM8 returned to Bologna in 2006; MRPM9 in 2008 was hosted by the Schlumberger Research Center (Cambridge, MA, USA); MRPM10 in 2010 at the University of Leipzig, Germany; MRPM11 in 2012 at the University of Surrey (Guildford, UK); and MPM12 in 2014 at the University of Wellington, NZ.

MRPM Conference Proceedings were initially published as special issues of *Magnetic Resonance Imaging* (MRPM1 to MRPM8) while MRPM9 and MRPM10 came out as part of the *AIP Conference Proceedings* Series. Since MRPM11, proceedings have been published as special issues of *Microporous and Mesoporous Materials*. In addition, since MRPM8 (2006), poster presenters may submit papers based on their posters for inclusion in special issues of the open-access on-line journal *Diffusion Fundamentals*. As was the practice at previous conferences, all authors of the Invited and Oral communications are invited to prepare a manuscript for inclusion in the MRPM13 Proceedings. After review, contributions will be published in a special issue of *Microporous and Mesoporous Materials*. The manuscripts should be no more than four printed pages and comply precisely with the Journal's editorial indications.

MRPM conferences look at progress achieved by magnetic resonance in furthering understanding porous media and fluids inside the pore-space. The meetings are also intended to encourage contact among people from different academic and industrial backgrounds. Researchers in Physics, Chemistry, Engineering, Life Sciences, Mathematics, Computer Sciences, and Industrial Applications will benefit from the exchange of ideas, experiences and new approaches. Topics of MRPM13 will include innovative techniques to study structures, the behavior of fluids and their interactions in a wide range of natural and artificial materials, including rocks, cements, biological tissues, foodstuffs, wood, particle packs, sediments, pharmaceuticals, zeolites, and bioconstructs. Advances in hardware, methodology, data acquisition and processing are also on the agenda for discussion.

The *Giulio Cesare Borgia Prize for Young Researchers* will be awarded at the end of the Conference. The Prize (three thousand Euro offered by our DICAM and DIFA Departments, University Bologna) was established in "*memory of the contribution made by Giulio Cesare Borgia to the development of Magnetic Resonance in Porous Media and for the particular attention he always paid to the enthusiasm, passion, and courage of young people who undertook the difficult and adventurous path of scientific investigation in this fascinating area of research"*. The award will be presented to an emerging (usually under 35 year old) scientist whose presentation at the Conference shows greatest promise for future scientific leadership.

Contributions to the Conference are as follows: Invited speeches (20 minutes + 5 minute discussion), Oral presentations (12 minutes + 3 minute discussion), and Poster presentations during the Poster Session. Posters will be numbered; the numbered poster list is printed in the Scientific Programme.

The Organizing Committee would like to thank all sponsors and donors for their support. These include: Università di Bologna (IT); Dipartimento di Fisica e Astronomia (DIFA, U. Bologna, IT); Dipartimento DICAM (U. Bologna, IT); Scuola di Ingegneria e Architettura (U. Bologna, IT); Stelar s.r.l. (IT); Bruker Biospin GmbH (DE, IT); Niumag (China); Oxford Instruments (UK); MR Solutions (UK); Pure Devices GmbH (DE); Jeol S.p.A. (IT); Lab-Tools Ltd (UK).

The Organizing Committee is also very grateful to Prof. Ezio Mesini, President of the School of Engineering and Architecture, for making available the conference venue at the School, and to Professors Ezio Mesini and Ferruccio Trifirò, President of the *Accademia dell'Istituto delle Scienze di Bologna*, for hosting the NMR School in the Academy's Ulisse Hall.

On behalf of the Organizing Committee, I wish you an enjoyable and fruitful time in Bologna.

August 21st 2016

William Bortolotti Chair, Bologna MRPM13
DICAM, University of Bologna

International Scientific Advisory Committee

Rodolfo Acosta (AR)
Matthias Appel (USA)
Christoph Arns (AU)
Bruce Balcom (CA)
Martin Bencsik (UK)
Bernhard Blümich (DE)
Villiam Bortolotti (IT)
Clifford Russell Bowers (USA)
Melanie Britton (UK)
Sarah Codd (USA)
Andrew Coy (USA)
Paola Fantazzini (IT)
Marc Fleury (FR)
Edmund Fordham (UK)
Eiichi Fukushima (USA)
Petrik Galvosas (NZ)
Ravinath Kausik (USA)
Peter McDonald (UK)
Nikolaus Nestle (DE)
Bill Price (AU)
Dimitris Sakellariou (FR)
Igor Sersa (SI)
Frank Stallmach (DE)
Daniel Topgaard (SE)
Rustem Valiullin (DE)
Dagmar Van Dusschoten (DE)
Sergey Vasenkov (USA)
Lizhi Xiao (CN)

Organizing Committee

Villiam Bortolotti, Chairman (IT)
Paola Fantazzini (IT)
Leonardo Brizi (IT)
Francesco Tinti (IT)
Stefano Bonduà (IT)
Ester Maria Vasini (IT)
Rebecca Steele (UK)

Steering Committee

Christoph Arns (AU), Chair
Villiam Bortolotti (IT)
Paola Fantazzini (IT)
Petrik Galvosas (NZ)
Frank Stallmach (DE)

SPONSORSHIPS and DONATIONS (The Organizing Committee thanks:)

Università di Bologna (IT)

Dipartimento di Fisica e Astronomia (University of Bologna, IT)

Dipartimento DICAM (University of Bologna, IT)

Scuola di Ingegneria e Architettura (University of Bologna, IT)

Bruker Biospin GmbH (DE, IT)

Bruker Corporation is the global market and technology leader in analytical magnetic resonance instruments including NMR, preclinical MRI and EPR. The Bruker BioSpin Group of companies develop, manufacture and supply technology to research establishments, commercial enterprises and multi-national corporations across countless industries and fields of expertise.
For more information please visit https://www.bruker.com

Stelar s.r.l. (IT)

Stelar's mission is to develop, manufacture and market innovative scientific electronic instrumentation for Nuclear Magnetic Resonance (NMR) research and industrial applications. Stelar specializes in unique instrumentation for Fast Field Cycling (FFC) NMR Relaxometry and is focused on continuous development of this technology and diffusion of the FFC NMR method for both academic and industrial research and for process and QC applications. Stelar is an independent company which was established in 1984 in Mede, Italy. Since 1994 Stelar embarked on a research and development project aimed at the development of advanced instrumentation for a novel low-field NMR technique, called Fast Field Cycling (FFC) NMR relaxometry. This challenging development allowed Stelar to introduce the first commercial FFC NMR instrument to the market since the 1997. Stelar's experience and unique innovative technology has gained the company a strong reputation as the absolute leader in FFC NMR relaxometry. Indeed, Stelar is dedicated to continuous development of FFC NMR instrumentation by employing methods which exploit the latest technologies in electronics design and by integrating FFC NMR with other related techniques. The FFC NMR method has been adopted in many NMR laboratories around the world and successfully applied in fields such as materials science (polymers, liquid crystals, porous materials, etc.), biomedical research (MRI contrast agents, proteins, pharmaceutical and cosmetic formulations, etc.) and food science. Stelar is keenly focused on the development of new applications for FFC NMR which can lead to the increased awareness and use of FFC NMR for industrial research, development and manufacturing.
For more information please visit http://www.stelar.it

Niumag (CN)

Niumag Corporation is an international high-tech corporation focusing on development and application spread of low-field NMR (Nuclear Magnetic Resonance), with strong development ability, Completed customer service system and sophisticated internal management system. Niumag Corporation now has three core product lines, multiple invention patents and software copyrights.The NMR imaging system pioneered by Niumag Corporation has obtained several national certificates, and it has been widely used and unanimously approved in agriculture and food, petroleum prospecting, chemical fiber industry, biomedical, etc. Niumag Corporation has developed a dozen series low-field NMR system, for example Online NMR Automation Oil Seed Sorting System, NMR Drilling Fluid Analyzer, NMR Shale Analyzer, Small Animal MRI System, NMR Cross Link Density Analyzer, 1 T NMR spectrometer and so on. After years of sales, Niumag Corporation has been successfully installed more than 300 sets products all over the world. Niumag Corporation has set up offices in the United States, and it has been listed in China at 2015. The stock code is 836507.We are proud to say Niumag Corporation has grown up to the most promising and dynamic enterprise in low-field NMR industry.
For more information please visit http://en.niumag.com

Oxford Instruments (UK)

Oxford Instruments manufactures the market-leading **GeoSpec** range of nuclear magnetic resonanance (NMR) analysers for porous media and rock core studies. The original **GeoSpec** 2MHz range has been progressively extended and improved, first with the addition **Q-Sense** technology for enhanced sensitivity and shorter echo spacings, and now with a **Q-Sense** 12MHz version for even greater sensitivity for low porosity materials such as shales. The **GeoSpec**12 also has the capability for simple 3D imaging. All **GeoSpec** models use exclusively Green Imaging Technologies software for either simple routine core measurements or for SCAL measurements including capillary pressure and 2D data analysis. For non-rock samples we are now introducing the **MQR** range of 20MHz instruments for research requiring short pulses, short echo times, variable sample temperature, and diffusion capabilities. Finally, we offer the **Pulsar** 60MHz high resolution cryogen-free NMR spectrometer for teaching and for monitoring organic synthesis processes.
For more information please visit www.oxford-instruments.com or email: industrial@oxinst.com

MR Solutions (UK)

MR Solutions combines its MR Imaging technology with Green Imaging's software products to provide the Imacore 3D imaging system for rock core analysis. The system has the latest 3D imaging pulse sequences and variable field capability proving to be the imaging tool for the porous media industry.
For more information please visit http://www.mrsolutions.com

Pure Devices GmbH (DE)

Pure Devices is a manufacturer of state-of-the-art benchtop MRI scanners.
Since 2011, the headquarters is located in Würzburg in the heart of Europe. From here the research and development, project planning, construction, testing and finally sale takes place. All our products are designed and made in Germany. Our company is known for our benchtop MRI scanners research lab and portable lab which are optimized for scientific as well as educational use. Their compact design and the easy-to-use software offer great opportunities in the scientific laboratory setting. Especially teaching and learning laboratory classes will profit from the hands-on examples made possible with the portable lab. Scientists familiar to Matlab will enjoy the use of the research lab. Furthermore Pure Devices provides external gradient and RF amplifiers especially for applications in bench-top MRI. Feel free to visit our booth for a live demonstration.

WWW: www.pure-devices.com
Email: info@pure-devices.com
Phone #: 0049-931-71053590

Jeol SpA (IT)

JEOL is a leading global supplier of scientific instruments used for research and development in the fields of nanotechnology, life sciences, pharma, forensics, biotechnology and food. Utilizing its unique technologies, and knowledge, JEOL helps its customers make significant breakthroughs in product development and scientific research.
www.jeol.it

Lab-Tools Ltd (UK)

Lab-Tools: nano-science, nano-metrology and instrumentation design.

- **Nano-science:**
  - Nano-scale properties of liquids in pores and at interfaces;
- **Nano-metrology:**
  - Nano- to micro-scale characterisation;
  - NMR Cryoporometric PSDs;
- **Instrumentation:**
  - Peltier cooled probes.
  - USB&FPGA instruments.

AMPERE event

Organized under the auspices of

ALMA MATER STUDIORUM
UNIVERSITÀ DI BOLOGNA

MRPM13
13th International Bologna Conference
on Magnetic Resonance in Porous Media
4 - 8 September 2016
Bologna, Italy

NMR School Programme

and

Abstracts

13.00 SATURDAY 3th SEPTEMBER

and

10.00 SUNDAY 4th SEPTEMBER

Ulisse Room
Accademia delle Scienze
dell'Istituto di Bologna
Via Zamboni 31, Bologna

SATURDAY 3th SEPTEMBER

Accademia delle Scienze dell'Istituto di Bologna

13.00 **Registration**

13.45 **Welcome**
Ferruccio Trifirò
President of the Academy of Science

14:00 **Bernhard Blümich**
The NMR phase: k and q

15:30 **Coffee Break**

16:00 **Jean-Pierre Korb**
17.30 Principles and Applications of Fast Field Cycling NMR Relaxation

SUNDAY 4th SEPTEMBER

Accademia delle Scienze dell'Istituto di Bologna

10:00 **Ville-Veikko Telkki**
Laplace NMR

11:30 **Coffee Break**

12:00 **Lizhi Xiao**
Nuclear Magnetic Resonance in Shale Gas and Tight Gas Reservoirs

13:30
14.30 Lunch

The NMR Phase: *k* and *q*

B. Blümich

Institut für Technische und Makromolekulare Chemie, RWTH Aachen University, Worringerweg 1, D-52056 Aachen, Germany.

The competitive edge of NMR with respect to other spectroscopic methods is the ability to measure the signal phase. This not only enables multi-dimensional spectroscopy but also imaging and the measurement of flow and transport phenomena. In a tutorial lecture, the phase of the transverse magnetization evolving in an inhomogeneous magnetic field is analyzed for spins at rest and in translational motion. This analysis naturally leads to the foundations of imaging, flow and diffusion measurement. The analogy of NMR with short gradient-field pulses with differentiation schemes from numerical analysis is demonstrated [1]. This lecture honors the contributions of the late Paul Callaghan to NMR of translation motion (Fig. 1) [2].

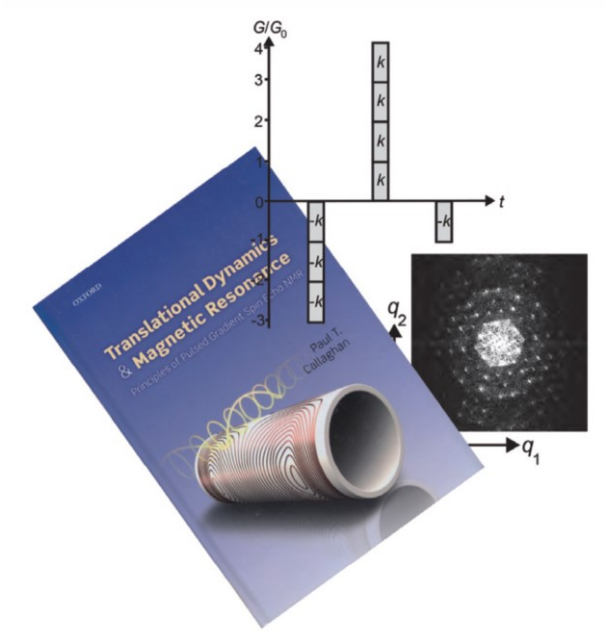

Figure 1 – Cover page of the Journal of Magnetic Resonance 267 (6) (2016) showing Paul Callaghan's book on Translational Dynamics & Magnetic Resonance along with the scattering function derived from MRI data of a regular array of capillaries stacked in water and a finite-difference derived PFG sequence to measure accelleration-compensated coherent displacements.

References

[1] B. Blümich, *k* and *q* Dedicated to Paul Callaghan, J. Magn. Reson. 267 (2016) 79-85.
[2] P.T. Callaghan, Translational Dynamics and Magnetic Resonance, Oxford University Press, Oxford, 2011.

Principles and applications of fast field cycling NMR relaxation

J.-P. Korb[a,b]

[a]Physique de la Matière Condensée, Ecole Polytechnique-CNRS, 91128 Palaiseau, France; [b] Phenix-UMR CNRS UPMC 8234, 75252 Paris, France.

We present an introduction to the main principles and applications in porous materials of fast field cycling (FFC) NMR relaxation. Since the pioneering works [1, 2], numerous improvements and applications have been proposed [3]. The FFC technique concerns the magnetic-field dependence of the longitudinal nuclear-spin-lattice relaxation rate $1/T_1$, often refered as "Nuclear Magnetic Relaxation Dispersion (NMRD) because it leads to a frequency-dispersion of $1/T_1$. Basically, NMRD techniques offer a large variety of opportunities for characterizing the molecular dynamics and transport properties of fluids embedded in confined environments. Systems of interest are high surface-area microporous materials, chromatographic supports, heterogeneous catalytic materials, plasters, cements and natural microporous organic kerogens and clays minerals in shale oils and macroporous materials such as porous petroleum rocks (sandstones and carbonates). Varying the magnetic field changes the Larmor frequency, and thus, the fluctuations to which the nuclear spin relaxation is sensitive. Moreover, this method permits a more complete characterization of the dynamics than the usual measurements as a function of temperature at fixed magnetic field strength because many common solvent liquids have phase transitions that may alter significantly the character of the dynamics over the temperature range usually studied. Further, the magnetic field dependence of the spin-lattice relaxation rate, $1/T_1$, provides a good test of the theories that relate the measurement to the micro-dynamical behavior of the fluid. This is especially true in spatially confined systems where the effects of reduced dimensionality may force more frequent reencounters of spin-bearing molecules that may alter the correlation functions that enter the relaxation equations in a fundamental way [4, 5]. The FFC technique can also follow the progressive setting of cement-based material [6]. It allows studying the dynamics of hydrocarbons at proximity of asphaltene nanoaggregates and macroaggregates [7] on heavy crude oils when varying the concentration of asphaltenes. It gives also new information on the wettability of petroleum fluids (brine and oil) embedded in organic shale rocks [8]. It is also useful for understanding the relations and correlations between NMR relaxation times T_1 and T_2, diff usion coefficients D, and viscosity η of heavy crude oils [9]. In these latter case, the NMRD data allow interpreting $2D$ T_1-T_2 and D-T_2 correlation spectra that could be made down-hole, thus giving a valuable tool for investigating *in situ* the molecular dynamics of petroleum fluids [9].

References

[1] A.G. Redfield, W. Fite, H.E. Bleich, Rev. Sci. Instrum. 39 (1968) 710.
[2] F. Noack, Prog. Nucl. Magn. Reson. Spectrosc. 18 (1986) 171.
[3] R. Kimmich, E. Anoardo, Progr. Nucl. Magn. Reson. Spectrosc. 44 (2004) 257-320.
[4] J.-P. Korb, M. Whaley-Hodges, R.G. Bryant, Phys. Rev. E, (1997), **56**, 1934.
[5] J.-P. Korb, M. Whaley-Hodges, T. Gobron, R.G. Bryant, Phys. Rev. E, 1999, **60**, 3097.
[6] F. Barberon, J.-P. Korb, D. Petit, V. Morin, E. Bermejo, Phys. Rev. Lett. 90 (2003) 116103-4
[7] L. Benamsili, J.-P. Korb, G. Hamon, A. Louis-Joseph, B. Bouyssiere, H. Zhou, and R. G. Bryant, Energy Fuels (2014), 28, 1629−1640
[8] J.-P. Korb, B. Nicot, A. Louis-Joseph, S. Bubicci, G. Ferrante, J. Phys. Chem. C. 118 (2014) 23212-23218.
[9] J.-P. Korb, N. Vorapalawut, B. Nicot, R.G. Bryant, J. Phys. Chem. C 119 (2015) 24439-24446.

Laplace NMR

V.-V. Telkki

NMR Research Group, University of Oulu, P.O.Box 3000, FIN-90014 University of Oulu, Finland;

NMR is one of the very few methods for measuring molecular self-diffusion coefficient without an invasive tag, even inside opaque samples. Relaxation experiments, in turn, reveal the rates of recovery of the initially perturbed magnetization to the thermal equilibrium, mainly due to random rotational motion of molecules. Diffusion and relaxation experiments provide versatile information about the dynamics of substances. Furthermore, they offer chemical resolution not available in the traditional NMR spectra.

While the frequency content of conventional, oscillating NMR signal is analyzed by a Fourier transform, the relaxation and diffusion data consist of exponentially decaying components, and the distribution of diffusion coefficients or relaxation times can be extracted from the experimental data by an inverse Laplace transform. Consequently, these methods are referred to as Laplace NMR (LNMR).

This lesson offers an overview how the inverse Laplace transform, which is an ill-posed problem, becomes feasible with the use of regularization. Furthermore, in addition to conventional 1D methods, the lesson elucidates the principles of 2D LNMR methods, enabling one to correlate various LNMR parameters as well as to investigate chemical exchange phenomena. Recent efforts in the development of single-scan, ultrafast multidimensional LNMR methods will be also highlighted.

Nuclear Magnetic Resonance in Shale Gas and Tight Gas Reservoirs

Lizhi Xiao

State Key Lab. of Petroleum Resources and Prospecting, China University of Petroleum, Beijing, China 102249. Prof. Lizhi Xiao is currently on sabbatical at Harvard University, the Faculty of Arts and Sciences.

In this presentation, I will first discuss the characteristics of shale gas and tight gas reservoirs from the point of view of rocks and pores with core samples and digital imaging results on different scales. Comparing to conventional sandstone or carbonates, both shale gas and tight gas reservoirs have much smaller pore sizes and complicated structure, which make the NMR responses much more difficulty to characterize.

Second I will emphases on the pore systems and propose different types of pore models. NMR responses to pore fluids in the rock and are affected by the physical chemical properties of the pore surfaces. For theoretic treatment and simulation, proper pore system models are critical. There are many different kinds of pore models available in the literature, but no one of them is good for both shale gas and tight gas reservoirs.

Third I will review the progress of NMR in shale gas and tight gas reservoirs in both experimental and simulation studies. There are many nice works in NMR in shale and tight gas reservoirs in the literature regarding NMR pulse sequences and theoretical and experimental results, but few of them actually works for routine measurements or down hole.

And finally I will introduce NMR logging examples in both shale gas and tight gas reservoirs. We have run many down hole NMR logs in both shale gas and tight gas reservoirs. The trends of responses with statistical analysis demonstrate the correlation of NMR to Petrophysics and fluids typing, but the relations are not so obvious. Detailed analysis suggests that an integration of NMR with other measurements such as resistivity and acoustic will be helpful and sometimes are necessary.

AMPERE event

Organized under the auspices of

ALMA MATER STUDIORUM
UNIVERSITÀ DI BOLOGNA

MRPM13
13th International Bologna Conference
on Magnetic Resonance in Porous Media
4 - 8 September 2016
Bologna, Italy

Conference
Scientific Programme

from
13.00 SUNDAY 4th SEPTEMBER
to
13.00 THURSDAY 8th SEPTEMBER

Conference Room

Sunday 4th September: Oratorio di San Filippo Neri,
Via Manzoni, 5, Bologna

From Monday 5th September to Thursday 8th September:
Room 6.1 – 6.2, School of Engineering and Architecture,
Viale del Risorgimento 2, Bologna

SUNDAY 4th SEPTEMBER

Oratorio di San Filippo Neri

13.00 — **Registration**

15.30 — **Opening session**
Chairpersons: Villiam Bortolotti and Paola Fantazzini

15.40 — **WELCOME**
Ezio Mesini
(President of School of Engineering and Architecture)

15.50 — KEYNOTE — FLUID DYNAMICS IN PORES: CHALLENGES AND PERSPECTIVES
Rainer Kimmich

16.30 — KEYNOTE — GETTING BIG WITH LARGE BECOMING SMALL?
Bernhard Blümich

17.10 — **Welcome party**

19.00

MONDAY 5th SEPTEMBER

School of Engineering and Architecture

SESSION I

Connected porous systems and NMR relaxometry

Chairpersons: Ernst Roessler and Ioan Ardelean

9.00 **I01** DYNAMICS AND WETTABILITY OF COMPLEX FLUIDS PROBED BY FAST FIELD CYCLING NMR RELAXATION
J.-P. Korb, B. Nicot

9.25 **O01** CHARACTERIZATION OF POROUS POLYMER MATERIALS BY TIME DOMAIN AND SINGLE-SIDED NMR
M.I. Velasco, E.V. Silletta, C.G. Gomez, M.C. Strumia, S. Stapf, G.A. Monti, C. Mattea, **R. Acosta**

9.40 **O02** SHALE ORGANIC POROSITY AND TOTAL ORGANIC CARBON (TOC) BY COMBINING SPIN ECHO, SOLID ECHO AND MAGIC ECHO
Z. Jia, L. Xiao, Z. Wang, C. Liang, L.Guo

9.55 **O03** LOW-FIELD NMR LABORATORY MEASUREMENTS OF HYDROCARBONS CONFINED IN ORGANIC AND NON-ORGANIC NANOPOROUS MEDIA AT VARIOUS PRESSURES
H. Thern, C. Horch, F. Stallmach, B. Li, A. Mezzatesta, H. Zhang, R. Arro

10.10 **O04** A MULTIDISCIPLINARY APPROACH FOR THE MULTI-SCALE STRUCTURAL STUDY OF ECO-COMPATIBLE MGO/CAO-BASED CEMENTS
S. Borsacchi, **F. Martini**, M. Geppi, M. Tonelli, F. Ridi, P. Baglioni, L. Calucci

10.25 – 10.55 **Coffee Break**

10.55 **O05** MULTI-DIMENSIONAL NMR EXPERIMENTS FOR CHARACTERIZATION OF PORE STRUCTURE HETEROGENEITY AND LIQUID SATURATIONS
R.T. Lewis, **J.G. Seland**

11.10 **O06** LOCALIZATION IN A SINGLE PORE
E.J. Fordham, J. Mitchell

11.25 **O07** A NEW MODEL FOR THE INTERPRETATION OF T_1^{-1} DISPERSION MEASUREMENTS
D. Faux, P.J. McDonald

SESSION II

Plants, soils, and environmental sciences

Chairperson: Siegfried Stapf

11.40 **I02** IMAGING OF ROOT ZONE PROCESSES
S. Haber-Pohlmeier, C. Totzke, S. Oswald, A. Pohlmeier, B. Blümich

12.05 **O08** EFFECT OF MUCILAGE ON WATER PROPERTIES IN THE RHIZOSPHERE MONITORED BY 1H-NMR RELAXOMETRY
M. Brax, C. Buchmann, G. E. Schaumann

12.20 **O09** APPLICATION OF MR MICROSCOPY FOR RESEARCH IN WOOD SCIENCE
U. Mikac, I. Serša, M. Žlahtič, M. Humar, M. Merela, P. Oven

12.35

Lunch

14.25

SESSION III
Chemical engineering and related materials
Chairperson: Nikolaus Nestle

14.25 **I03** CHARACTERIZING GELS BY NMR POROUS MEDIA METHODS: DIRECT MEASUREMENT OF GLASS DYNAMICS AND MESH SIZE IN A SOLVENT POLYMER SYSTEM BY MULTIDIMENSIONAL RELAXOMETRY AND DIFFUSOMETRY
S.L. Codd, N.H. Williamson, A.M. Dower, A.L. Broadbent, D. Gross and J.D. Seymour

14.50 **O10** IN SITU VISUALIZATION OF FLOW AND FOULING LAYER FORMATION DURING ALGINATE FILTRATION
F. Arndt, S. Schuhmann, G. Guthausen, S. Schütz, H. Nirschl

15.05 **O11** MASS TRANSPORT IN MICROFLUIDICS: HOW FLOW-MRI CAN HELP UNDERSTAND FLOW PHENOMENA
S. Benders, M. Wiese, M. Küppers, M. Wessling, B. Blümich

15.20 **O12** INFLUENCE OF FLUID DYNAMICS ON POLYMERIZATION KINETICS MEASURED BY RHEO-NMR
E. Laryea, G. Guthausen, T. Oerther, N. Schuhardt, M. Kind

15.35 **O13** LITHIUM ION DIFFUSION IN A SOLID CONDUCTOR OF AMORPHOUS $(LI_2S)_8(P_2S_5)_2$ STUDIED BY PULSED-GRADIENT SPIN-ECHO ^{7}LI NMR SPECTROSCOPY
K. Hayamizu, S. Ito, Y. Aihara

15.50 **O14** NMR IMAGING OF HYDROGENATION IN MICRO-SCALE POROUS CATALYST LAYERS
V. V. Zhivonitko, V-V. Telkki, I V. Koptyug

16.05 **O15** SOLID-STATE AND FIELD-CYCLING NMR RELAXOMETRY STUDIES ON THE DYNAMICS OF GLASS FORMING LIQUIDS AND POLYMERS IN NANOPROUS SYSTEMS
M. Hofmann, Th. Körber, S. Gradmann, B. Hartmann-Azanza, M. Steinhart, **E. Rössler**

16.20

Coffee Break

&

POSTER SESSION 1
(with authors present)
From P01 to P47

17.45

TUESDAY 6th SEPTEMBER

SESSION IV
Diffusion and applications
Chairpersons: Mike Johns and Yiqiao Song

9.00 **I04** LOCAL AND GLOBAL ANISOTROPY – RECENT RE-IMPLEMENTATION OF 2D ILT DIFFUSION METHODS
F. Zong, N. Spindler, L.R. Ancelet, I.F. Hermans, **P. Galvosas**

9.25 **O16** ULTRAFAST LAPLACE NMR OF HYPERPOLARIZED XENON IN CPG MATERIALS
O. Mankinen, J. Hollenbach, S. Ahola, J. Matysik, V.-V. Telkki

9.40 **O17** NONINVASIVE RELAXOMETRY EVIDENCE OF LINEAR PORE SIZE DEPENDENCE OF WATER DIFFUSION IN NANOCONFINEMENT
H. Chemmi, **D. Petit**, P. Levitz, R. Denoyel, A. Galarneau, J.-P. Korb

9.55 **O18** DIFFUSION MRI/NMR AT HIGH GRADIENTS: CHALLENGES AND PERSPECTIVES
D.S. Grebenkov

10.10 **O19** MULTIDIMENSIONAL CORRELATION OF NUCLEAR RELAXATION AND DIFFUSION TENSOR SIZE, SHAPE, AND ORIENTATION
J.P. de Almeida Martins, D. Topgaard

10.25 – 10.55 **Coffee Break**

10.55 **O20** SINGLE-FILE DIFFUSION OF GAS MIXTURES BY HIGH FIELD DIFFUSION NMR
A. R. Dutta, P. Sekar, M. Dvoyashkin, C. R. Bowers, K. J. Ziegler, **S. Vasenkov**

11.10 **O21** UNDERSTANDING DEACTIVATION IN POROUS CATALYSTS USING NMR DIFFUSION TECHNIQUES
C. D'Agostino, Y. Ryabenkova, G. J. Hutchings, M. D. Mantle, L. F. Gladden

11.25 **O22** MARGINAL DISTRIBUTIONS CONSTRAINED OPTIMIZATION (MADCO) USED TO ACCELERATE 2D MRI RELAXOMETRY
D. Benjamini, P. J. Basser

SESSION V
Advances in technology and hardware
Chairperson: Rustem Valiullin

11.40 **I05** NMR TECHNOLOGY: RECENT HISTORY, EMERGING POSSIBILITIES AND NEW CHALLENGES
S. Sykora

12.05 **O23** MAGNETIC RESONANCE IMAGING WITH A VARIABLE FIELD SUPERCONDUCTING MAGNET THAT CAN BE ROTATED FOR VERTICAL OR HORIZONTAL OPERATION
B. Balcom

12.20 **O24** A NEW DOWNHOLE MRI TOOL
W. Liu, L. Xiao, X. Li, S. Luo

12.35 **O25** A COMPACT X-BAND RESONATOR FOR DNP-ENHANCED FAST-FIELD-CYCLING NMR AT 340 mT
O. Neudert, C. Mattea, S. Stapf

12.50 – 14.25 **Lunch**
MRPM Committee meeting & Lunch
Room 5.5

SESSION VI
Petrophysics and flow
Chairperson: Edmund Fordham

14.25 **I06** SODIUM-23 NMR IN POROUS MEDIA
J. Mitchell, E.J. Fordham

14.50 **O26** A ROBUST NMR METHOD TO MEASURE POROSITY OF LOW POROSITY ROCKS
J.M. Sun, W.C. Yan, T. Li

15.05 **O27** EMERGING NMR APPROACHES FOR CHARACTERIZING ROCK HETEROGENEITY
H. Liu, L. Xiao, P. Galvosas

15.20 **O28** LOW FIELD NMR SURFACE RELAXIVITY STUDIES OF CHALK AND ARGILLACEOUS SANDSTONES
K. Katika, **H. Fordsmand**, I.L. Fabricius

15.35 **O29** MEASUREMENT OF INTERFACIAL AREA FROM NMR TIME DEPENDENT DIFFUSION AND RELAXATION MEASUREMENTS
M. Fleury

15.50 **O30** PERMEABILITY FROM TIME DEPENDENT METHANE SATURATION MONITORING IN SHALES
A. Valori, S. Van den Berg, F. Ali, R. Taherian, W. Abdallah

16.05 **O31** ACCURATE PHASE-SHIFT VELOCIMETRY IN POROUS MEDIA: THE IMPORTANCE OF PROPAGATOR ASYMMETRY
A. Vallatos, M.N. Shukla, V.R. Phoenix, W.M. Holmes

16.20 – 17.45 **Coffee Break**
&
POSTER SESSION 2
(with authors present)
From P48 to P92

WEDNESDAY 7th SEPTEMBER

SESSION VII

Advances in methodology and new areas of research

Chairpersons: Bruce Balcom and Susanna Ahola

9.00 **I07** MULTIFREQUENCY-MULTINUCLEAR NMR OF SHALE ROCKS
K. Ravinath, Y. Donghan

9.25 **O32** WATER SPRAY MEASUREMENTS WITH MAGNETIC RESONANCE IMAGING: THE NEAR-NOZZLE REGION
I. Mastikhin, S. Ahmadi, K.M. Bade

9.40 **O33** AN ON-LINE NMR FOR DRILLING FLUID ANALYSIS SYSTEM
S. Li, L. Xiao, X. Li, Z. Wang

9.55 **O34** A NOVEL SPATIALLY RESOLVED 2D LAPLACE NMR METHOD FOR POROUS MATERIALS AT LOW MAGNETIC FIELD
Y. Zhang, L. Xiao

10.10 **O35** REMOTE DETECTION NMR GAS ADSORPTION METER
A. Selent, V. V. Zhivonitko, V.-V. Telkki

10.25 – 10.55 **Coffee Break**

10.55 **O36** NMR CRYOPOROMETRY: WHAT HAVE WE OVERLOOKED?
D. Kondrashova, **R. Valiullin**

11.10 **O37** EFFECTS OF COHERENCE PATHWAYS ON THE PERFORMANCE OF THE MODULATED GRADIENT SPIN ECHO SEQUENCE
I. Serša, F. Bajd, A. Mohorič

11.25 **O38** DEVELOPMENT OF CONTINUOUS FLOW XENON-129 FOR GAS PHASE NMR FLOW AND VELOCIMETRY STUDIES IN POROUS MEDIA
F. Hill-Casey, S. P. Rigby, T. Meersmann, G. E. Pavlovskaya

11.40 **O39** RECENT PROGRESS IN MAGNETIC RESONANCE IMAGING OF HARD AND SOFT SOLIDS
S. Barrett

SESSION VIII

Biomedicine and food

Chairperson: Andrea Valori

11.55 **I08** USING DIFFUSION MRI TO STUDY TISSUE MICROSTRUCTURE IN TRAUMATIC BRAIN INJURY (TBI)
M. E. Komlosh, E.B. Hutchinson, M. Haber, D. Benjamini, A.V. Avram, P.J. Basser

12.20 **O40** LOAD-DEPENDENT LOW-FIELD PROFILING AND RELAXOMETRY OF OSTEOARTHRITIC ARTICULAR CARTILAGE
E. Rössler, C. Mattea, M. T. Nieminen, S. Karhula, S. Saarakkala, **S. Stapf**,

12.35 **O41** SINGLE-SIDED NMR ON A QUASI-REAL MODEL OF BONE FOR THE DIAGNOSIS OF OSTEOPOROSIS
M. Barbieri, L. Brizi, M. Nogueira d'Eurydice, S. Obruchkov, H. Liu, V.Bortolotti, P. Fantazzini, P. Galvosas

12.50

14.25

Lunch

SESSION IX

Colloquium on mobile magnetic resonance

Chairperson: Stanislav Sykora

14.25 **I09** MOLECULAR TRANSPORT IN IONIC LIQUIDS UNDER CONFINEMENT STUDIED BY LOW FIELD NMR
C. Mattea, S. Stapf and A. Ordikhani-Seyedlar

14.50 **O42** APPLICATION OF EARTH'S FIELD NUCLEAR MAGNETIC RESONANCE TO MULTIPHASE FLOW METERING
M.L. Johns, K.T. O'Neill, P.L. Stanwix and E.O. Fridjonsson

15.05 **O43** A MODULAR SINGLE-SIDED NMR SENSOR DESIGN WITH MULTIFUNCTION
Z. Sun, L. Xiao, G. Liao, Y. Zhang

15.20 **O44** NMR AND X-RAY µCT STUDY OF PLASTICIZER (HEXAMOLL® DINCH®) IN PVC
N. Nestle, A. Sandor, M. Pfeiffer

15.35 **O45** VISUALIZING THE SENSITIVE VOLUME OF A UNILATERAL NMR SENSOR
C. Rehorn, R. Höhner, B. Blümich

15.50

16.20

Coffee Break

WEDNESDAY 7th SEPTEMBER

Guided Tour in Bologna

16:50 – 18:50

City redbus

http://cityredbus.com

20.00 CONFERENCE DINNER

Cantina Bentivoglio

Via Mascarella 4/B, Bologna

http://www.cantinabentivoglio.it

THURSDAY 8th SEPTEMBER

SESSION X
Non-destructive testing and cultural heritage
Chairperson: Rodolfo Acosta

9.15 **I10** NON-DESTRUCTIVE AND NON-INVASIVE NMR IN CULTURAL HERITAGE
D. Capitani, V. Di Tullio, N. Proietti

9.40 **O46** MULTI ION TRANSPORT IN CONCRETE AS STUDIED BY MULTI-NUCLEI NMR
L. Pel, P.A.J. Donkers

9.55 **O47** PROBING INTO THE POROUS STRUCTURE OF HYDRATED CEMENT PASTE WITH THE NMR RELAXOMETRY OF CYCLOHEXANE AND ETHANOL MOLECULES UNDER PARTIALLY SATURATED CONDITIONS
I. Ardelean, A. Bede, A. Scurtu

10.10 **O48** ONE AND TWO-DIMENSIONAL NMR STUDIES FOR CULTURAL HERITAGE: EVALUATION OF CONSOLIDANTS PERFORMANCE
L. Brizi, M. Camaiti, V. Bortolotti, P. Fantazzini, B. Blümich, S. Haber-Pohlmeier

10.25 – 10.55 **Coffee Break**

SESSION XI
Simulation and multidimensional inversion
Chairperson: Ville-Veikko Telkki

10.55 **I11** XRAY-CT ENHANCED INTERPRETATION OF HIGH-DIMENSIONAL INVERSE LAPLACE NMR EXPERIMENTS
C. H. Arns, I. Shikhov, M. Nogueira d'Eurydice

11.20 **O49** RECOVERING 2-DIMENSIONAL T_1-T_2 DISTRIBUTION FUNCTIONS FROM 1-DIMENSIONAL T_1 AND T_2 MEASUREMENTS
N. H. Williamson, M. Röding, S.J. Miklavcic, M. Nydén

11.35 **O50** MEMORY EFFICIENT MULTIDIMENSIONAL NMR INVERSION WITHOUT KRONECKER PRODUCTS
D. Medellin, V. R. Ravi, C. Torres-Verdin

12.50 **O51** IMPROVED INVERSION OF TWO-DIMENSIONAL NMR RELAXATION DATA WITH THE UPEN PRINCIPLE
V. Bortolotti, R. J. S. Brown, P. Fantazzini, G. Landi, **F. Zama**

12.05	**GIULIO CESARE BORGIA PRIZE**
12.20	**MRPM GENERAL ASSEMBLY**
13.10	**CLOSING CEREMONY END OF CONFERENCE**
13:20 14:30	**Lunch**

POSTER SESSION 1
16:20 – 17:50 - Monday 5th

P01 Ultrafast multidimensional Laplace NMR for a rapid and sensitive chemical analysis.
S. Ahola, V.-V. Telkki.

P02 Accurate T_2 distribution of fluids in porous media measured with Phase Incremented Echo Train Acquisition.
D.J. Srivastava, **A.G. de Araujo Ferreira**, D.R. Cole, J.H. Baltisberger, T.J. Bonagamba, P.J. Grandinetti.

P03 Topological stydy of porous media through µCT imaging and complex networks.
M.B. Andreeta, R.S. Polli, E. Lucas-Oliveira, F.A. Rodrigues, T.J. Bonagamba.

P04 Parameterization of multi-exponential NMR relaxation in terms of logarithmic moments of an underlying relaxation time distribution.
O.V. Petrov, S. Stapf.

P05 Application of principal component analysis in NMR relaxometry.
O.V. Petrov, M. Vogel.

P06 Real-time NMR data processing and management.
Y. Shi, L.Z. Xiao, G.Z. Liao, Y. Zhang, S.J. Jiang, L. Gao.

P07 Proper coherence pathways selection in echo train acquisition for T_2 measurements.
R. Shakhovoy, **V. Sarou-Kanian**, M. Yon, F. Fayon.

P08 Ring dynamics in functionalized UiO66(Zr) MOFs via SLF solid-state NMR.
J. Damron, J. Ma, K. Saalwächter, A. Matzger, A. Ramamoorthy.

P09 Homodyne relaxation analysis.
S. Huber, A. Joos, B. Gleich, A. Haase.

P10 ^{129}Xe NMR methodology for complex porous matter.
J. Hollenbach, V. Kotolup, R. Valiullin, D. Enke, J. Matysik.

P11 Confined fluids: nanotechnology-driven quest for new physics.
S. Mascotto, **R. Valiullin**.

P12 Online NMR measurements and parameter optimization by fluid analysis system.
W. Chen, L.Z. Xiao, Y. Zhang, G.Z. Liao.

P13 A home-built NMR core analytic system based on the OPENCORE spectrometer.
G. Yang, L. Xiao, W. Liu.

P14 Machine learning for magnetic resonance.
Y. Song, M. D. Hurlimann, D. Cory.

P15 A new side-looking design for downhole NMR probe.
S. Luo, L. Xiao, G. Liao, Y. Zhang

P16 A new proof and applications in NMR inversions of the Tikhonov method.
Y. Gao, L. Xiao, B. Wu

P17 Biocompatible silicon nanoparticles as MRI contrast agents for cancer diagnosis.
Yu.V. Kargina, M.B. Gongalsky, L.A. Osminkina, A.M. Perepukhov, M.V. Gulyaev, Yu.A. Pirogov, A.V. Maximychev, V.Yu. Timoshenko.

P18 Diffusion quantifications in MR-mammography by threshold isocontouring.
F. Zong, S. Bickelhaupt, T. A. Kuder, W. Lederer, H. Daniel, A. Stieber, H.-P. Schlemmer, P. Galvosas, F. B. Laun.

P19 Monitoring the animals' health status during vivisection by low-field NMR.
J. Viess, J. Flohr, D. Weidener, P. Keschenau, H. Simons, H. Klingel, **M. Küppers**, J. Kalder, B. Blümich.

P20 Intra-aneurysmal flow and thrombosis.
J. Flohr, J. Viess, J. Clauser, G. Cattaneo, M. Küppers, B. Blümich.

P21 Fast field cycling NMR as a method to study protein dynamics and aggregation of therapeutic proteins.
G. Ferrante, R. Steele, M. Pasin, C. Luchinat, M. Fragai, E. Ravera, G. Parigi

P22 Developing fingerprinting systems to identify fake paintings and assign ancient wall paintings through NMR relaxation studies.
C. Rehorn, W. Zia, T. Meldrum, C. Kehlet, E. Del Federico, G. Zolfo, J. Thompson, B. Blümich.

P23 Noninvasive examination of an ancient tear bottle.
S. Benders, B. Blümich, I. Bohm, J. Ehling, A. Eterović, N. Gross-Weege, V. Schulz, D. Truhn, J. Wehner.

P24 Cyclic hygro-expansion of oak studied by NMR.
T. Arends, L. Pel.

P25 Spatially resolved NMR: MRI and single-sided profiles on samples treated with environmentally safe fluorinated compounds to preserve Cultural Heritage porous media.
V. Bortolotti, **L. Brizi**, M. Camaiti, P. Fantazzini.

P26 Changes of water status in relation to strawberry fruit development and ripening.
J. Li, W. Jia, L. Xiao.

P27 Imaging of ^{23}Na accumulation in the soil-root region due to root water uptake.
A. Pohlmeier, A. Perelman, S. Haber-Pohlmeier, J. Vanderborght, N. Lazarovich.

P28 Applications of 2D NMR to soils with slim-line logging tool.
B. Guo, B. Blümich.

P29 Magnetic resonance probes as a tool to monitor long term clogging in constructed wetlands.
R. H. Morris, T. Hughes-Riley, E. R. Dye, S. Parslow, P. Hawes, J. García, E. Uggetti, J. Puigagut, M. I. Newton.

P30 The emerging use of MRI to study River Bed dynamics.
H. Haynes, S. Lakshmanan, A. Ockelford, E. Vignaga, **W.M. Holmes**.

P31 Quo vadis Surface-NMR – adiabatic pulses?
R. Dlugosch, M. Müller-Petke.

P32 Non-invasive Magnetic Resonance Imaging of nanoparticle migration and water velocity inside sandstone.
M.N. Shukla, A.Vallatos, M. Riley, J. Tellam, V. Phoenix and **W. Holmes**.

P33 Mobile NMR-Lab for field phenotyping of oilseed rape leaves.
M. Musse, F. Mariette, W. Debrandt, C. Sorin, C. Mireille, A. Bouchereau, L. Leport.

P34 Soil moisture mapping in the field with a slim-line logging tool.
X. Cai, B. Guo, M. Küppers, B. Blümich.

P35 Effect of water entrapment by a hydrogel on the structural stability of artificial soils.
C. Buchmann, G.E. Schaumann.

P36 Hardware and software for embedded compact broadband low field NMR spectrometers (ECBLFNMR).
A. Louis-Joseph, A. Nauton, D. Coupvent-Desgravier, J.-P. Korb.

P37 Visualizing the 1-D fluid distribution using FT-NMR in fibrous porous media over time.
B. Mohebbi, J. Claussen, B. Blümich.

P38 Development of a robust mobile plant imager.
M. Meixner, M. Tomasella, P. Först, C.W. Windt.

P39 A compact and mobile NMR platform.
J. Zhen, **R. Dykstra**, G. Gouws, S. Obruchkov.

P40 Real-time multidimensional NMR inversion using compressed sensing.
S. Gu, L. Xiao, G. Liao.

P41 Fast Laplace Inverse Transform (FLINT)
P.D. Teal.

P42 The effect of microstructure of semi-permeable barriers onto diffusion MRI: A one-dimensional theoretical study.
N. Moutal, D.S. Grebenkov.

P43 What are, and what are not, Inverse Laplace Transforms.
E. Fordham, L. Venkataramanan, J. Mitchell, A. Valori.

P44 Local analysis of single-phase flow through complex porous media using flow propagators.
Y. Zheng, I. Shikhov, M.N. d'Eurydice, **C. H. Arns**.

P45 Performance Evaluation of Improved 2DUPEN algorithm.
V. Bortolotti, L. Brizi, P. Fantazzini, G. Landi, **F. Zama**.

P46 Hydrodynamics and 2D NMR characterization of wettability in saturated rocks.
J. Wang, L. Xiao, L. Guo, G. Liao, Y. Zhang, F. Xiao.

P47 NMR solid state spin-echo simulation for water absorption in SWCNT.
L. Guo, L. Xiao, Z. Jia.

POSTER SESSION 2
16:20 – 17:50 Tuesday 6th

P48 Micrometer lithium ion diffusion in a garnet-type cubic $Li_7La_3Zr_2O_{12}$ (LLZO) for pellet and powder samples studied by ^7Li NMR spectroscopy.
K. Hayamizu, S. Seki and T. Haishi.

P49 Water transport in Nafion membranes under various conditions studied by NMR.
J.-C. Perrin, A. El Kaddouri, M. Klein, **S. Leclerc**, J. Dillet, L. Guendouz, O. Lottin.

P50 Low field NMR relaxivity as a fast characterization method for mesoporous alumina.
H. Fordsmand, M. Lutecki.

P51 Liquid and gas phase velocity measurements of foam using motion-sensitized SPRITE.
A. Adair, B. Newling.

P52 Investigation of the influence of DNP spin probes on the NMR relaxation and diffusion properties of water molecules in Nafion.
O. Neudert, **T. Überrück**, J. Granwehr, S. Han, S. Stapf, B. Blümich.

P53 In situ NMR imaging: a tool for characterizing ion transport properties in Li-Ion battery electrolyte solutions.
S. Krachkovskiy, J. Bazak, **B. Balcom**, I. Halalay, G. Goward.

P54 Monitoring steady state moisture distribution during wick action in mortar by MRI.
R. Enjilela, P. F. de J. Cano-Barrita, A. Komar, A. Boyd, B. J. Balcom.

P55 Multidimensional relaxation and diffusion studies of a halogen free ionic liquid.
M.A. Javed, S. Ahola, K. Aslam, O. Mankinen, A. Filippov, F.U. Shah, S. Glavatskih, O.N. Antzutkin, V.-V. Telkki.

P56 Investigation of CH_4 motional behavior in isoreticular M_2 MOF-74.
V.J. Witherspoon, J. Bachman, J. Long, B. Blümich, J.A. Reimer.

P57 Fast field cycling NMR applied to understand dynamics of polypropylene and polyethylene polymers.
M. Pasin, G. Ferrante, R. Steele, A. Marchi Netto, M. Farah, M. Flämig, E.A. Rössler.

P58 Revealing the porous structure of cement materials via the NMR relaxometry and diffusometry of cyclohexane molecules.
A. Bede, C. Badea, **I. Ardelean**.

P59 A computational approach for understanding nuclear spin diffusion in porous media.
E. Lucas-Oliveira, A.G. Araújo-Ferreira, W.A. Trevisan, M.N. D'Eurydice, C.A. Fortulan, T.J. Bonagamba.

P60 T_2-Encoded Fast-Field-Cycling Relaxometry.
O. Neudert, C. Mattea, S. Stapf.

P61 Comparison of NMR porosity and water imbibition porosity (WIP): A case study of Paleocene limestone and associated rocks from Eastern Dahomey Basin.
O.B. Olatinsu, B. Clennell, L. Esteban.

P62 Obtaining surface relaxivity from NMR-only data.
Z. Luo, J. Paulsen, V. Vembusubramanaian, and **Y. Song**.

P63 Wettability determination of porous media from T_1-T_2 method.
C. Liang, L.Z. Xiao, C.C. Zhou, L. Guo, Z.J. Jia.

P64 Free induction decay rates of water suspensions and water-saturated densely packed particles with varying volume fractions of solid phases.
O. Kishenkov, L. Menshikov, A. Maximychev.

P65 Superdiffusion in porous media.
A.M. Perepukhov, D.A. Alexandrov, A.V. Maximychev, L.I. Menshikov, P.L. Menshikov.

P66 Particle motion in porous materials during capillary suction.
C.J. Kuijpers, H.P. Huinink, N. Tomozeiua, O.C.G. Adan.

P67 Detecting microbially induced calcite precipitation (MICP) in a model well-bore using downhole low-field NMR.
C. M. Kirkland, S. Zanetti, A.J. Phillips, E. Grunewald, D.O. Walsh, S.L. Codd.

P68 Assessment of multiscale hybrid network structures of defibrillated plant fiber dispersions.
G.-J. W. Goudappel, K.P. Velikov, R. den Adel, J.P.M. van Duynhoven.

P69 Chirality and kinetics of a self-assembled Fe_4L_6 metallosupramolecular cage with guests.
S. Komulainen, J. Jayapaul, J. Zhu, K. Rissanen, L. Schröder, V.-V. Telkki.

P70 The mechanism of NMR relaxometry of tight porous media with multi-scale digital rock.
G. Liao, L. Xiao, J. Wang, L. Guo, W. Chen.

P71 Development of a compact bench-top NMR system for Fast Field Cycling relaxometry in rock cores and large volume samples.
M. Polello, R. Rolfi, A. Provera, Y. Xia, **G. Ferrante**.

P72 New instrumental platforms for the exploitation of the field-dependence of T_1, T_2 and 2D correlation spectra T_1-T_2 for probing the dynamics and wettability of petroleum fluids in rock cores and shale oils.
J.-P. Korb, G. Ferrante, R.Steele, D. Pooke.

P73 Tortuosity estimate through paramagnetic gas diffusion in multi-phase fluid systems saturating reservoir rock using T_2 (z, t) low-field NMR.
I. Shikhov, **C. H. Arns**.

P74 A new application of ionic liquid in predicting tortuosity factor in hierarchically porous silica monolith by means of PFG NMR.
S. Hwang, R. Valiullin, J. Haase, J. Kärger.

P75 Molecular translational dynamics in glycerol/water mixtures by MGSE method.
J. Stepisnik, **C. Mattea**, S. Stapf.

P76 NMR diffusometric droplet sizing in nanoemulsions.
J.-H. Sommerling, A. J. Simon, **G. Guthausen**, G. Leneweit, H. Nirschl.

P77 Restricted diffusion and higher order relaxation modes – A combined approach utilizing DT2 to extract pore-sizes without calibration.
M. Müller-Petke, R. Dlugosch, A. Obert.

P78 Self-diffusion in Polymer Solutions Measured with PFG NMR.
X. Guo, E. Laryea, M. Wilhelm, B. Luy, H. Nirschl, G.Guthausen.

P79 ^{1}H PFG NMR for characterizing interactions of potential electrolytes and electrode materials.
S. Merz, P. Jakes, H. Tempel, H. Kungl, M.F. Graf, R.-A. Eichel, J. Granwehr.

P80 Diffusion of carboxylate molecules in nanosilica suspensions: from the monomer to polyelectrolytes.
C. Dolce, **G. Meriguet**.

P81 Spatially resolved, under-sampled propagators and imaging of carbonate rock dissolution.
A.A. Colbourne, A.J. Sederman, M.D. Mantle, L.F. Gladden.

P82 Enhanced gas recovery NMR measurements.
M.L. Johns, M. Zecca, A. Honari, S.J. Vogt, B. Bijilic and E.F. May

P83 Improvement of NMR-based measurement accuracy in tight sandstone porosity and pore distribution.
Y.L. Zhang, Y.W. Gao, F. Wu, Y. Yang, P.Q. Yang.

P84 Low-field (LF) NMR-based characterization of active pore distribution during natural gas accumulation.
F. Wu, Y.L. Zhang, Y. W. Gao, Z.Y. Xie, P.Q. Yang.

P85 High temperature fast field cycling study of crude oil.
A. Lozovoi, M. Hurlimann, R. Kausik, S. Stapf, C. Mattea.

P86 Petrophysical study of reservoir rocks by magnetic resonance imaging with spirical method.
B.B. Bam, B. Balcom, B. MacMillan, F. Marica.

P87 Hydrodynamics and 2D NMR characterization of wettability and viscosity in saturated rocks.
J. Wang, L. Xiao, L. Guo, G. Liao, Y. Zhang, F. Xiao

P88 Pore scale analysis of NMR response in laminated rock with digital rock.
Z. Tian, L. Xiao, G. Liao, J. Wang.

P89 Permeability of water flow in CH_4 hydrate-bearing quartz sand.
E. Kossel, C. Deusner, N. Bigalke, M. Haeckel

P90 A new method for measuring the wettability of porous media by In-situ NMR water vapor isotherm technique.
H. T. Kwak, A. Harbi, Y. Chong, Z.-X.Luo, P. R. Doyle, A. Kleinhammes, Y. Wu.

P91 Asphaltene porous aggregates in crude oil investigated by aromatic and fluorine containing tracers: a relaxometry and DNP study.
S. Stapf, A.Ordikhani-Seyedlar, A. Lozovoi, C. Mattea, O. Neudert, R. Kausik, D. E. Freed, Y.Song, M. D. Hürlimann.

P92 Optimising digital filters in low-field NMR.
E. Fordham, A. Valori, J. Mitchell.

AMPERE event

Organized under the auspices of

ALMA MATER STUDIORUM
UNIVERSITÀ DI BOLOGNA

MRPM13

13th International Bologna Conference on Magnetic Resonance in Porous Media

4 - 8 September 2016

Bologna, Italy

Abstracts

KEYNOTE
&
INVITED

Fluid Dynamics in Pores: Challenges and Perspectives

Rainer Kimmich

University of Ulm, Ulm, Germany, rainer.kimmich@uni-ulm.de

Since the first meeting "Recent Advances in NMR Applications to Porous Media" held in Bologna 26 years ago, the MRPM conferences developped to a most successful periodic forum for our common research area. Actually, this manifests that mutual interests exist which are stable enough over the years to establish what one calls a 'scientific community'. The materials and systems that can be categorized as 'porous' are ubiquitous in nature and technology. Actual and potential applications of the expertise accumulated by the community can be seen all over. As illustrated in the graphical abstract below, the corner-stones limiting our research efforts may be circumscribed by

- pore space topology
- transport properties
- dynamic phenomena at solid/liquid interfaces

These are the key terms I will try to underpin with selected and typical examples from the recent literature. Any such review will unavoidably be incomplete. I therefore ask to bear with me here for any view and repertory appearing to be too subjective.

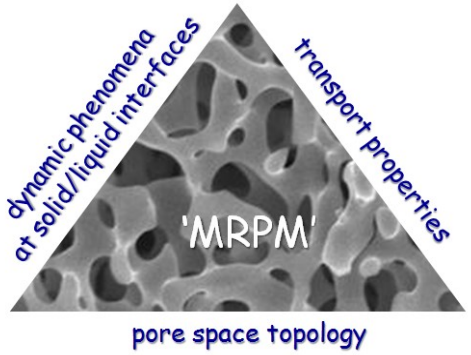

Figure 1 – Graphical abstract tentatively circumscribing the predominant research interests of the MRPM community.

There have been numerous attempts to assess the texture of pore spaces with the aid of three-dimensional magnetic-resonance microscopy. However, even fast techniques such as 3d echo-planar imaging are time consuming and the spatial resolution remains relatively poor. The use of diffraction-like patterns arising in diffusion studies of fluid-filled pore spaces became legend for elucidating structural dimensions on a 10 micrometer length scale. More recently, modifications of pulsed gradient diffusometry methods even promise to overcome the so-called phase problem of such studies. Pore-size distributions have been determined based on diffusion in internal, susceptibility-induced magnetic fields by selectively referring to higher diffusion modes. NMR cryoporometry using fluid/matrix material combinations suitable for size-dependent melting-point depressions serves the same purpose.

Transport through pore spaces is of paramount importance for numerous phenomena and applications in the context of porous media. This category implies not only inter-pore diffusion, pressure-driven or electroosmotic flow or hydrodynamic dispersion and thermal convection, but can also refer to ionic currents and heat conduction. NMR provides an extensive repertoire of techniques for the spatial assessment of the more or less anomalous transport properties suspected in porous media. An ideal and ultimate objective of spatially-resolved transport examinations would be to link characteristic structural and dynamic pore space parameters. A compromise could be on the one hand to measure local transport properties with NMR methods and, on the other, the pore space texture with X-ray techniques. Structure/transport interrelations of this sort can be supplemented by computer simulations based on boundary conditions deduced from the pore space structure. For the same purpose, it may be helpful to examine porous model objects of a predetermined structure instead of measuring it. Such 'percolation' objects can be modeled based on certain generation algorithms and then be fabricated with the aid of milling, 3d-printing or lithographical techniques.

From the molecular-dynamics point of view, all physics specific for saturated porous media happens at or near fluid/solid interfaces. This is the realm of field-cycling NMR relaxometry which permits us to record dynamic features in a particularly wide time/frequency range. It turned out that rotational and translational dynamics intertwine at surfaces. Model concepts used to interpret field-cycling data sets therefore imply features of translational diffusion. In this sense, conclusions from relaxation data are amazingly well in accordance with results obtained with pulsed-gradient spin-echo studies. The proper relaxation mechanisms are mainly dipolar coupling to diamagnetic and/or paramagnetic, intra- and/or inter-molecular partners depending on the system background. Adsorption and exchange properties are crucial for understanding the surface diffusion.

Analogous to the interdependence of transport features and pore space texture, surface topology influences reorientational dynamics of adsorbate molecules at solid/liquid interfaces. Results of this sort shed new light on the old question whether 'stick' or 'slip' boundary conditions are relevant for flow along solid surfaces. The circle opened above is thus closed again: The main issues of our work, 'structure', 'transport' and 'molecular dynamics', in a sense belong to the same research complex and cannot be considered independent of each other.

Getting big with large becoming small?

B. Blümich[a]

[a] Institut für Technische und Makromolekulare Chemie, RWTH Aachen University, Worringerweg 2, D-62056 Aachen, Germany

For about 65 years since the disovery of NMR, the overriding goal of instrument developers was to develop magnets with higher field strengths in an effort to gain sensitivity and chemical shift dispersion for NMR spectroscopy. To achieve this goal, the magnet size steadily increased whereas the sample size rather decreased than increased. Efforts to make the NMR spectrometer smaller have been successful for individual components [1,2] while the NMR magnet remains the largest component still today. Nevertheless, the last decade has witnessed the appearance of commercial NMR spectrometers with permanent magnets, which are small enough to be operated on the table top in the chemistry laboratory and under the fume hood [3,4], so that today the number of studies conducted with compact NMR instruments [5] employing spectroscopy, tomography and relaxometry reported in the literature is reapidly expanding. Before the advent of compact, permanent high-resolution NMR magnets the major applications of compact NMR instruments were for materials testing with tabletop relaxometers and mobile relaxometers like the NMR-MOUSE [6]. Since about the year 2010 the use of compact NMR spectrometers is being explored for teaching, chemical analysis and reaction monitoring in academia as well as in industry [7]. Yet in a longer run, tabletop instruments are also just an intermediate step towards even smaller NMR analyzers [8]. Such analyzers might find use as web-interfaced health monitors that employ NMR spectroscopy among other analytical methods to analyze body fluids following microfluidic sample preparation. Key elements in such a device are likely to be signal amplifiers that selectively hyperpolarize marker molecules, and miniature magnets with homogeneous magnetic fields for spectroscopic detection. Following an introduction to the world of compact NMR [5], advances in contact-mediated para-hydrogen hyperpolarization in water [9] and the fabrication of small magnets [10,11] will be reported.

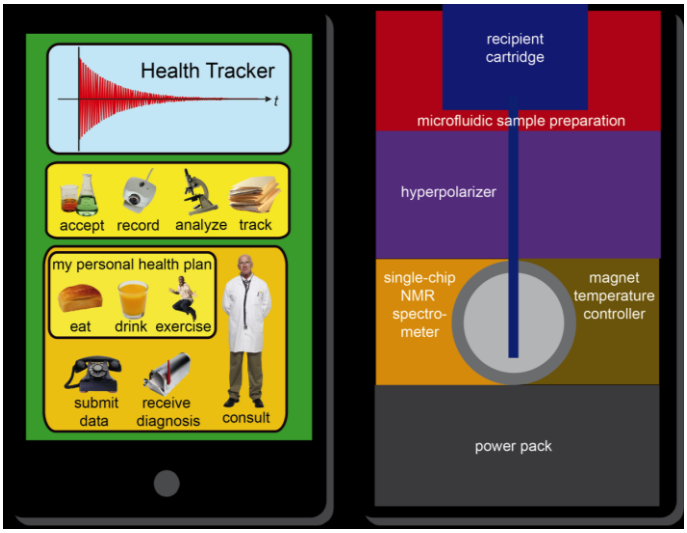

Figure 1 – Vision of an NMR-spectroscopy based analyzer for body fluids [5]

References

[1] M. Johns, E.I. Fridjonson, S. Vogt, A. Haber, Mobile NMR and MRI, R. Soc. Chem., Cambridge, 2016.
[2] S.S. Zalesskiy, E. Danieli, B. Blümich, V.P. Ananikov, Miniaturization of NMR Systems: Desktop Spectrometers, Microcoil Spectroscopy, and "NMR on a Chip" for Chemistry, Biochemistry, and Industry, Chemical Reviews 114 (2014) 5641-56894.
[3] B. Blümich, Miniature and Tabletop Nuclear Magnetic Resonance Spectrometers, in: R.A. Meyers, ed., Encyclopedia of Analytical Chemistry, John Wiley, Chichester, DOI: 10.1002/9780470027318.a9458
[4] B. Blümich, Introduction to compact NMR: A review of methods, Trends Anal. Chem. (2016), doi: 10.1016/j.trac.2015.12.012
[5] B. Blümich, S. Haber-Pohlmeier, W. Zia, Compact NMR, de Gruyter, Berlin, 2000.
[6] B. Blümich, J. Perlo, F. Casanova, Mobile Single-Sided NMR, Prog. Nucl. Magn. Reson. Spectr. 52 (2008) 197-269.
[7] E. Pretsch, B. Blümich, eds., Special issue on Compact NMR, Trends Anal. Chem. xx (2016), Elsevier, New York.
[8] D. Ha, J. Paulsen, N. Sun, Y.-Q. Song, D. Ham, Scalable NMR Spectroscopy with Semiconductor Chips, Proc. Nat. Acad. Sci. 111 (2014) 11955–11960.
[9] P. Spannring, I. Reile, M. Emondts, P.P.M. Schleker, N.K.J. Hermkens, N.G.J. van der Zwaluw, B.J.A. van Weerdenburg, P. Tinnemans, M. Tessari, B. Blümich, F.P.J.T. Rutjes, M.C. Feiters, A new Ir-NHC catalyst bearing di(ethyleneglycol)benzyl groups for organic solvent-free NMR signal amplification by reversible exchange in D_2O, Chemistry Europ. J. xxx (2016) xxx-xxx.
[10] A.J. Parker, W. Zia, C.W.G. Rehorn, B Blümich, Improving the homogeneity of the Halbach magnet making use of material imperfections, J. Magn. Reson. 265 (2016) 83-89.
[11] E.P. Danieli, B. Blümich, W. Zia, H. Leonards, Method for a targeted shaping of the magnetic field of permanent magnets, WO 2015043684 A1 pending, published 2. April 2015.

Dynamics and wettability of complex fluids probed by fast field cycling NMR relaxation

J.-P. Korb[a,b], B. Nicot[c]

[a]Physique de la Matière Condensée, Ecole Polytechnique-CNRS, 91128 Palaiseau, France; [b] Phenix-UMR CNRS UPMC 8234, 75252 Paris, France ; [c]Total EP, Centre Scientifique et Technique Jean Feger (CSTJF), 64018 Pau, France.

It is critical to probe *in situ* the dynamics and wettability of complex fluids in the complex micro- and meso-structures of porous systems. However, usual techniques cannot separate easily these fluids in confinement. On the contrary, the magnetic-field dependence of the longitudinal nuclear-spin relaxation rate $1/T_1$ probed by the fast field cycling NMRD relaxometry is a rich source of dynamical information [1]. It provides a good test of the theories that relate the measurement to the microdynamical behavior of the confined fluids specifically at proximity of pore surfaces. It gives information on the wettability of the embedded fluids. Here, we present our recent results on the frequency dispersion behaviors of the longitudinal relaxation rates $1/T_1$ for oil and brine confined in different petroleum rocks (sandstones, carbonates, organic shales) for probing non invasively these dynamics and wettability in confinement [2,3]. These NMRD data allow also interpreting our 2D T_1-T_2 and D-T_2 correlation spectra that could be made down-hole, thus giving a valuable tool for investigating *in situ* the molecular dynamics of petroleum fluids.

References

[1] R. Kimmich, E. Anoardo, Progr. Nucl. Magn. Reson. Spectrosc. 44 (2004) 257-320.
[2] J.-P. Korb, B. Nicot, A. Louis-Joseph, S. Bubicci, G. Ferrante, J. Phys. Chem. C. 118 (2014) 23212-23218.
[3] J.-P. Korb, N. Vorapalawut, B. Nicot, R.G. Bryant, J. Phys. Chem. C 119 (2015) 24439-24446.

Imaging of root zone processes

S. Haber-Pohlmeier[a], C. Tötzke[b], S. Oswald[b], A. Pohlmeier[c], B. Blümich[a]

[a]RWTH Aachen University, ITMC, Worringer Weg 1, 52074 Aachen, Germany, [b]Univ. of Potsdam, Inst. of Earth and Environmental Science, Karl-Liebknecht-Str. 24-25, 14476 Potsdam, Germany, [c]Research Center Jülich, IBG-3, 52425 Jülich, Germany.

Against the background of climate change and exploding world population we need an efficient and sustainable use of our resources soil and water but at the same time a higher crop yield. Typically, the latter is achieved by breeding and genetic eneginering with subsequent control by screening for phenotypes mostly of the above ground plant part. However, in addition to the genetic disposition there is also the possibility to improve the interactions in the soil-root compartment for nutrient and water uptake. For this one needs exact knowledge about available structures and the involved root-zone processes. Classically these processes are investigated in rhizotrones which restrict growth and observation in a very thin 2D layer or one concludes only indirectly by analysing breakthrough curves, treating the soil-root compartment as black box. This type of macroscopic characterization fails to see the details to unambigiously resolve root-zone processes like water uptake, solute transport and changes in hydraulic properties.

In the first part of the talk we will demonstrate with examples and in comparison with neutron imaging how low-field MRI can be used to visualize with high accuracy the root system architecture, which is a prerequisite for the subsequent investigation of root-zone processes. One of the most important but also challenging root-zone processes is solute transport. We show that MRI in combination with inversion-recovery preparation can quantitatively map in 3D concentration changes of a model solute, Gd-DTPA and thus allows to draw conclusions on the underlying solute uptake mechanisms. The presentation concludes with first data from the complementary use of MRI and neutron imaging on the same plant. While neutron imaging is extremely sensitive to the proton density and therefore guarantees accurate measurements of the total water content, MRI provides synergistic information about local water dynamics based on relaxation times and relaxation time contrast. The experiments focus on changes in hydraulic properties of the root zone occuring during drying and rewetting scenarios, which are relevant for root-water uptake.

Characterizing Gels by NMR Porous Media Methods: Direct measurement of glass dynamics and mesh size in a solvent polymer system by multidimensional relaxometry and diffusometry

Sarah L. Codd[a,b], Nathan H. Williamson[c], April M. Dower[c,d], Amber L. Broadbent[d], Dieter Gross[e] and Joseph D. Seymour[b,c]

[a]Department of Mechanical and Industrial Engineering, Montana State University, Bozeman, MT, 59717 USA

[b]Center for Biofilm Engineering, Montana State University, Bozeman, MT, 59717 USA

[c]Department of Chemical and Biological Engineering Montana State University, Bozeman, MT, 59717 USA

[d]Bend Research Incorporated, Capsugel, Bend, OR 97701 USA

[e]Bruker Biospin Corp., Karlsruhe Germany

Phase transitions during solvent evaporation drying of biopolymer solutions (*e.g.* HPMC) are important in food science and pharmaceutical production processes. The characterization of the structure of glassy polymer solutions and gels can provide insight into the transport processes within these systems. Displacement time dependent PGSE NMR, as has been used to characterize pore sizes in porous media, is shown to directly provide data on a mesoscale gel mesh size or glass free volume domain size. The application of 2D relaxation time T_1-T_2 correlation data and T_2-T_2 exchange data are applied to further study the molecular dynamics of phase transitions during solvent evaporative drying. The NMR data and analysis, applied in the context of porous media characterization approaches, provide unique data on structural length scale size and connections between gelation and glass transitions.

Local and global anisotropy - recent re-implementation of 2D ILT diffusion methods.

F. Zong[a], N. Spindler[b,c], L.R. Ancelet[d,e], I.F. Hermans[d,e,f], P. Galvosas[a]

[a]MacDiarmid Institute for Advanced Materials and Nanotechnology, School of Chemical and Physical Sciences, Victoria University of Wellington, Wellington, New Zealand; [b]Tecan Schweiz AG, 8708 Männedorf, Switzerland; [c]Forschungszentrum Jülich, Institute of Bio- and Geosciences - Agrosphere, 52425 Jülich, Germany; [d]Malaghan Institute of Medical Research, Wellington, New Zealand; [e]Maurice Wilkins Centre, Auckland, New Zealand; [f]School of Biological Sciences, Victoria University of Wellington, Wellington, New Zealand.

Multidimensional Inverse Laplace Transform (ILT) NMR methods have established themselves over the last two decades in material science, engineering, medical research and industry [1]. Like multidimensional Fourier Transform (FT) NMR it enables one to correlate parameters in at least two independent domains, to separate distributions which would collapse in only one dimension or to study exchange processes [2]. However, unlike FT NMR it lends itself to the processing of (multi-) exponential decays and therefore to the study of NMR relaxation times and diffusional dynamics of mobile species in the sample. More specifically ILT NMR enables one to correlate mobility or transversal relaxation times at subsequent time intervals for the study of molecular exchange [3-5] or to study molecular displacements in different spacial directions which allows the characterization of the sample anisotropy [3,4].

Here we report on **two variants** of the two-dimensional (2D) Diffusion-Diffusion Correlation Spectroscopy (DDCOSY) [3,4]. This method is a so called double Pulsed Gradient Spin Echo (dPGSE) experiment which performs two NMR diffusion experiments in close succession but different spatial directions. This allows for the correlation of molecular displacements associated with the two directions, thus sampling local mobility and confinement. Identical displacements in the two subsequent measurements indicate isotropic diffusion. In contrast, different displacements in the two directions are a signature for local diffusion anisotropy which may manifest itself as off-diagonal features in 2D correlation maps.

The **first variant** aims to measure Fractional Anisotropy (FA) averaged over the whole sample. FA is commonly derived from the diffusion tensor (DT) measured via Diffusion Tensor Imaging (DTI) [6]. The core idea of DTI is to sample diffusion in at least six independent spatial directions which is sufficient to reconstruct the DT. Transferring the approach of sampling six spatially independent directions to DDCOSY results in the acquisition of at least three independent DDCOSY experiments, thus sampling diffusion along a particular choice of gradient directions and obtaining corresponding 2D correlation maps [7]. Sample averaged FA can be extracted subsequently from the DDCOSY results [7]. We will demonstrate that this method is robust and returns averaged FA values for a number of biological samples which are consistent with DTI measurements. We will further discuss the potential of sample averaged FA values for the discrimination of healthy and cancerous biological tissue [7].

The **second variant** concerns a shortened version of the DDCOSY (sDDCOSY) experiment for which gradients in the two different directions are applied at the same time but incremented independently [8]. This pulse sequence structure is a single PGSE (more akin to DTI) and fundamentally different from the dPGSE scheme used for DDCOSY. We will report on the relationships between DTI, DDCOSY and sDDCOSY. The particular focus is on the additional attenuation of the echo signal. This attenuation occurs for sDDCOSY due to cross terms between the two gradients applied in different directions. In the case of conventional DDCOSY the echo signal is affected by the displacement correlation tensor [9] which is typical for dPGSE experiments in general. We will demonstrate that sDDCOSY is able to return results consistent with simulations and DDCOSY experiments if contributions arising from the cross terms are compensated. This shortened DDCOSY version may proof indispensable for samples with short T_2 relaxation times. Furthermore, true correlation is sampled with sDDCOSY since displacements in different directions are traced simultaneously. sDDCOSY may also provide further insight into diffusion mechanisms in anisotropic porous materials because it should allow to extract and study the off-diagonal elements in the 2D correlation maps alone.

References

[1] P. Galvosas and P.T. Callaghan, C. R. Physique, 11 (2010) 172–180.
[2] R.R. Ernst, G. Bodenhausen and A. Wokaun, Principles of Nuclear Magnetic Resonance in one and two Dimensions, Clarendon Press, 1987.
[3] P.T. Callaghan, S. Godefroy and B.N. Ryland, Magn. Reson. Imaging, 21, (2003) 243–248.
[4] P.T. Callaghan and I. Furo, J. Chem. Phys., 120, (2004) 4032–4038.
[5] P.J. McDonald, J.P. Korb, J. Mitchell and L. Monteilhet, Physical Review E, 72 (2005) 011409.
[6] P.J. Basser, J. Mattiello and D. LeBihan, Biophys. J., 66 (1994) 259–67.
[7] F. Zong, L.R. Ancelet, I.F. Hermans and P. Galvosas, Magn. Reson. Chem., accepted (2016).
[8] N. Spindler, Diffusion and Flow Investigations in Natural Porous Media by Nuclear Magnetic Resonance, RWTH Aachen University, 2011.
[9] S.N. Jespersen and N. Buhl, J. Magn. Reson. 208 (2011) 34–43.

NMR Technology: Recent History, Emerging Possibilities and New Challenges

Stanislav Sykora

Extra Byte, Via Raffaello Sanzio 22c, 20022 Castano Primo, Italy.

In this presentation I will review the development in MR technology and its 'neighborhood areas' over the last 25 years. The following scheme attributes one to five stars to each 'plank' according to how much it has progressed. The stars reflect my personal perceptions and reveal that, in my opinion, there is a lot to be less than happy about. I will of course try and substantiate these 'scores'.

_A. Progress in fields other than MR but with a strong MR impact (****)
- _1. Small signal electronics: revolutionary progress (*****)
  - Miniaturization and components density (*****)
  - Computing technology and computer science (*****)
  - RF synthesis and management (****)
  - Broad-band RF designs instead of tuned designs (****)
- _2. Power electronics: steady evolution (***)
  - RF power units (***)
  - Power supplies for magnets and field gradients (**)
- _3. Magnetic fields generation and handling: lackluster evolution (**)
  - Main field generation: materials and methods (**)
  - Field stabilization (**) and homogeneity control (*)
- _4. Recent 'revival' of low-field and bench-top instrumentation (**)

_B. Progress in areas involving specific NMR phenomena over the last 30 years: (**)
- _1. Sensors such as coils, micro-coils and macro-coils, near-field antennas: slow evolution (**)
  - Inductive: micro-coils, broad-band coils (***)
  - Non-inductive: SQUIDs, electric, optical, thermal noise, ... (*)
- _2. S/N enhancement (**): Dynamic nuclear polarization, DNP (**), cryo probes (*)
- _3. MAS and CP (***) : Ultra-fast spinning (***), cryo-MAS probes (*)
- _4. Very-low and zero field MR detection: few signs of life (*)

_C. Progress in developing new application areas (**)
- MRI: no longer young, but still moving quite fast (***)
- MRI spectroscopy: no major breakthrough (**)
- NMR and Bio-NMR spectroscopy: BMS = Big, Mature, and Smug (*)
  - Some real progress in complex-systems (metabolomics, foodstuffs)(**)
  - Appreciable progress in software (***) and automation (**)
- Geophysical and petrological MR: slow evolution (*)
- Relaxometry: slow evolution (*)
- Other: timid signs, lots of competition from other methodologies (*)

The above overview raises many follow-up questions, to which I will attempt to give some answers (no doubt just partial ones) biased, where possible, towards MR in porous media.

- Why was progress in areas _B and _C so disappointing, compared with _A1 ?
- Why is there a slowdown in R&D targeted on pure MR phenomenology and technology (lack of 'faith') ?
- Why we keep talking most of the time about the same old applications and developing so few new ones ?
- **Which are presently the most outstanding technical obstacles hindering a faster progress ?**
- **Which technical approaches might lead to significant performance gains in short/mid term ?**
- **Which technical approaches might lead to breakthrough results in mid/ long-terms ?**
- **Are we facing a growing need of a fundamental shift in the MR paradigm?**
  from the Instrument to the Application, to the Best Instrument for My Application: **I => A => BIMA**

References

[1] R.M. Fratila, M.V. Gomez, S. Sykora, A. Velders, Multinuclear nanoliter one-dimensional and two-dimensional NMR spectroscopy with a single non-resonant microcoil, Nature Communications, 5, Article number 3025 (2014). DOI: 10.1038/ncomms4025.
[2] S. Sykora, A new paradigm streamlining the analysis of NMR spectra of small molecules,
Presentation at GERMN 2013, Stan's Library IV, DOI 10.3247/SL4Nmr13.007.
[3] S. Sykora, Some Thermodynamic and Quantum Aspects of NMR Signal Detection,
Lecture at BFF6, 2011, Stan's Library IV, DOI 10.3247/SL4nmr11.002.
[4] S. Sykora, Do we really understand Magnetic Resonance?,
Invited Lecture at MMCE 2011, Stan's Library IV, DOI 10.3247/SL4nmr11.001.
[5] S. Sykora, The Many Walks of Magnetic Resonance: Past, Present and Beyond,
Seminar at Uni Cantabria, 2010, Stan's Library III, DOI 10.3247/SL3Nmr10.005.
[6] S. Sykora, NMR hardware and the New Electronics: a boat in a hurricane,
Presentation at 24-th Valtice NMR, 2009, Stan's Library III, DOI 10.3247/SL3Nmr09.006.
[7] S. Sykora, Spin Radiation, remote MR Spectroscopy, and MR Astronomy,
Presentation at 50-th ENC, 2009, Stan's Library III, DOI 10.3247/SL3Nmr09.008.

Sodium-23 NMR in porous media

J. Mitchell, E.J. Fordham

Schlumberger Gould Research, High Cross, Madingely Road, Cambridge CB3 0EL, UK.

The enhancement in relaxation of ^{1}H spins adsorbed at pore walls is well known, described by the famous solutions of Brownstein and Tarr to the Bloch-Torrey diffusion equation with a partially absorbing boundary [1]. This theory has been applied successfully to interpret longitudinal (T_1) and transverse (T_2) relaxation time distributions in a variety of materials, from biological cells [1] to oil field reservoir rocks [2]. In the case of NMR applied to oil field systems, ^{1}H spins are ubiquitous in both the oleic and aqueous fluid-phases. The usual contrast mechanisms of relaxation time and diffusion coefficient available at low-field are used to separate these components and hence quantify the saturation state (relative fraction of oil and water) of the porous rock [3]. However, situations are encountered (e.g., light oil and brine in small pores) where these contrast mechanisms fail to provide the necessary fluid-phase discrimination. An alternative is the detection of sodium (^{23}Na), a spin-3/2 nucleus found uniquely in the aqueous-phase [4]. Together, quantitative ^{1}H and ^{23}Na NMR signal amplitudes provide robust oil and brine volumetrics, independent of pore geometry or liquid viscosity.

The ability to access ^{23}Na is advantageous for many applications: salt crystallization is known to damage construction materials such as stone and concrete [5], and sodium content is a quality control indicator in the food industry [6]. However, very few articles address interpretation of sodium relaxation at the pore surface. Rijniers *et al.* attempted to apply the theory of Brownstein and Tarr to sodium relaxation in order to extract a pore size information [7]. The results were unsatisfactory and, as will be shown in this paper, the "fast diffusion" model for ^{1}H spin relaxation in a pore cannot be extended, unaltered, to ^{23}Na. The sodium nucleus has four Zeeman energy levels, resulting in two probabilities of transition for excited spins. Outside the motional narrowing regime, the transition probabilities for the inner and satellite levels differ, leading to complex relaxation behavior of the quadrupole nucleus [8,9].

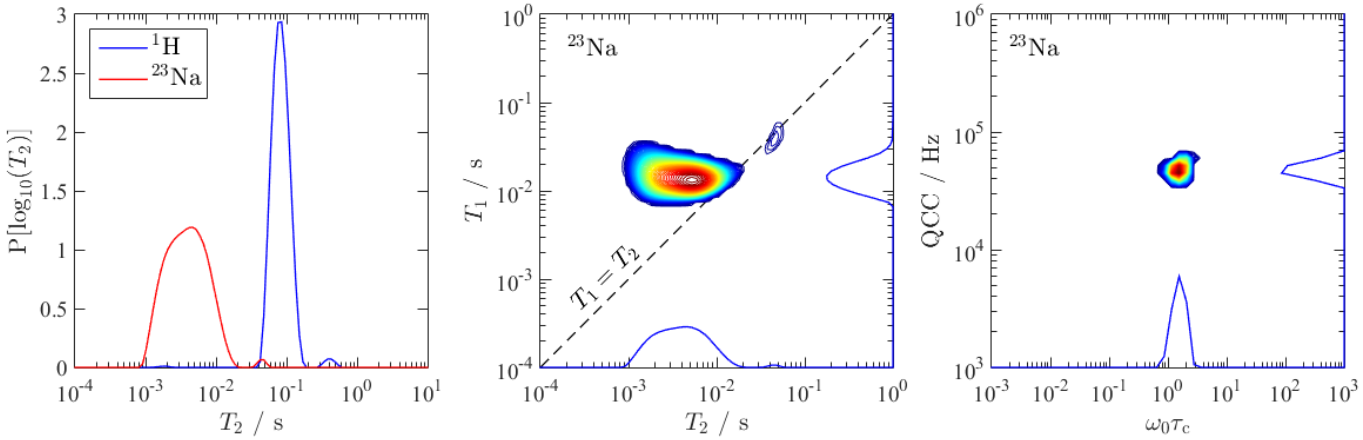

Figure 1 – Sodium relaxation of NaCl brine (5 mol dm^{-3}) in a porous chalk. The ^{1}H and ^{23}Na T_2 distributions are compared (left), where the ^{1}H T_2 distribution reflects the narrow, monomodal pore size distribution as expected, but the ^{23}Na T_2 distribution does not. A ^{23}Na T_1-T_2 correlation plot (middle) suggests that multiple relaxation components are present. Marginal T_1 and T_2 plots are included for clarity. The low-intensity peak at $T_1 = T_2 \approx 40$ ms corresponds to bulk brine on the outside of the sample. Inverting the ^{23}Na T_1-T_2 data for QCC and τ_c [9] (right, $\omega_0 = 2.1 \times 10^7$ rad s^{-1}) provides a narrow, monomodal distribution in each dimension, suggesting the relaxation is governed by single values of QCC $\approx$ 50 kHz and $\tau_c \approx$ 70 ns. These values are substantially different from the bulk brine QCC = 1.1 MHz and τ_c = 10 ps [10].

To explore ^{23}Na in porous media, we consider brine in a chalk (limestone) selected for its monodisperse pore size distribution and low paramagnetic content. The ^{1}H T_2 distribution is narrow and monomodal, reflecting the pore size distribution as expected, see Figure 1(left). In contrast, the ^{23}Na T_2 distribution spans well over an order of magnitude. A T_1-T_2 correlation plot for ^{23}Na is equally unhelpful, see Figure 1(middle). To start interpreting the ^{23}Na relaxation, it is necessary to explore the fundamental parameters that describe quadrupole relaxation in liquids and soft solids, namely the quadrupole coupling constant QCC and the rotational correlation time τ_c. The measured QCC and τ_c values suggest that the liquid-state relaxation equations for the quadrupole nucleus continue to apply for ^{23}Na spins in the pores, albeit with a QCC significantly modified from the bulk solution, see Figure 1(right). In this paper we explore these initial observations, possible mechanisms for the relaxation behavior, and call for a new interpretation of ^{23}Na relaxation in porous materials.

References

[1] K.R. Brownstein, C.E. Tarr, J. Magn. Reson. 26 (1977) 17-24.
[2] J.A. Brown, L.F. Brown, J.A. Jackson, J.V. Milewski, B.J. Travis, SPE/DOE-10813 paper presented at the SPE/DOE Unconventional Gas Recovery Symposium of the Society of Petroleum Engineers, Pittsburgh, PA, 16-18 May, 1982.
[3] M.D. Hürlimann, L. Venkataramanan, C. Flaum, J. Chem. Phys. 117 (2002) 10223-10232.
[4] K.E. Washburn, G. Madelin, J. Magn. Reson. 202 (2010) 122-126.
[5] L.A. Rijners, H.P. Huinink, L.Pel, K. Kopinga, Phys. Rev. Lett. 94 (2005) 075503.
[6] J. Mitchell, L. F. Gladden, T.C. Chandrasekera, E.J. Fordham, Prog. Nucl. Magn. Reson. Spectrosc. 76 (2014) 1-60.
[7] L.A. Rijniers, P.C.M.M. Magusin, H.P. Huinink, L. Pel, K. Kopinga, J. Magn. Reson. 167 (2004) 25-30.
[8] P. S. Hubbard, J. Chem. Phys. 53 (1970) 985-987.
[9] D. E. Woessner, Concepts Magn. Reson. 13 (2001) 294-325.
[10] W.S. Price, B.E. Chapman, P.W. Kuchel, Bull. Chem. Soc. Jpn. 63 (1990) 2961-2965.

Multifrequency-multinuclear NMR of shale rocks

Ravinath Kausik, Donghan Yang

Schlumberger-Doll Research, 1 Hampshire street, Cambridge, Ma 02039, USA

The reservoir quality (RQ) of tight-oil organic shale is a function of the quantities of the producible light oil, bitumen and kerogen. The producible light oil is a positive RQ indicator, whereas the bitumen and the kerogen, which clog the pores and adsorb the oil respectively, can have negative RQ properties [1]. In this paper we demonstrate a methodology for fluid typing using NMR T_1-T_2 experiments at multiple frequencies and discuss the response of different components of gas and tight-oil organic shales based on their relaxation mechanisms [2,3]. We describe how the NMR relaxation dispersion of the various components differ due to the intrinsic relaxation mechanisms such as spin rotation, inter and intra molecular dipolar relaxation, and how this can be taken advantage of for the identification and quantification of these components, and therefor for reservoir quality estimations. We also demonstrate how 2D NMR T_1-T_2 methodology provides information about the confining geometries such as organic versus inorganic pore types based on the fluid wettability.

In addition, we demonstrate ^{23}Na-^{1}H-combined, high-field 2D NMR relaxometry to be a quantitative method for separately characterizing the brine and hydrocarbon contents in various porous materials, from porous glass, to conventional rocks, clays, and shale [3]. We discuss new features in the 2D relaxation maps for the sodium nuclei, due to the relaxation of quadrapolar spins in nanoporous geometries, and the associated interpretations. In summary we present the combination of multi frequency-multinuclear NMR for superior fluid typing and salinity information in unconventional shale, which is presently a great challenge in formation evaluation.

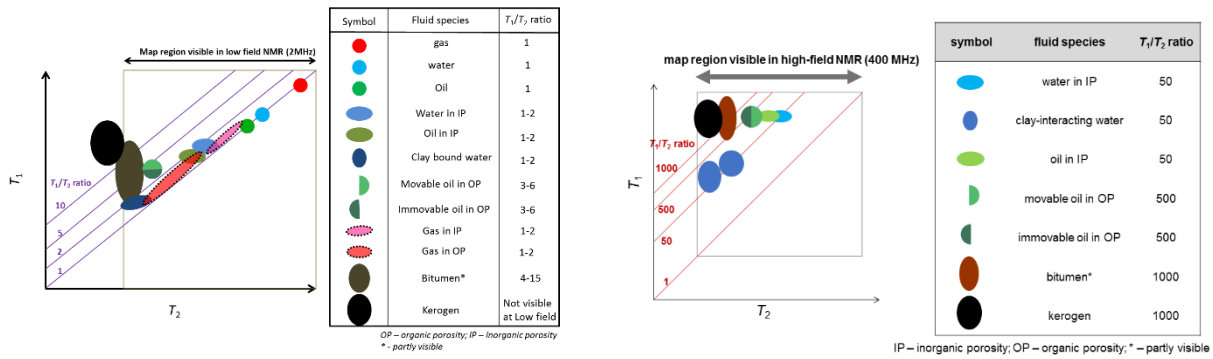

Fig.1 The low-field NMR (2MHz) ^{1}H T_1-T_2 map for all the components in unconventional shale rocks is summarized in left while the corresponding map at high-field (400 MHz) is shown in the right [2,3].

References

[1] Kausik, R., Craddock, P.R., Reeder, S.L., Kleinberg, R.L., Pomerantz, A.E., Shray, F., Lewis, R.E., Rylander, E., 2015, SPE-178622, Unconventional Resources Technology Conference, San Antonio, Texas, USA, 20–22 July.

[2] Kausik, R.; Fellah, K.; Rylander, E.; Singer, P. M.; Lewis, R. E.; Sinclair, S. M., *SPWLA 56th Annual Logging Symposium*, Society of Petrophysicists and Well-Log Analysts: Long Beach, California, USA, 2015..

[3] Donghan Yang and Ravinath Kausik, *Energy & Fuels* (2016) DOI: 10.1021/acs.energyfuels.6b00130

[4] Papaioannou, A., Kausik, R. *Phys. Rev. Applied* 4, (2015) 024018

Using diffusion MRI to study tissue microstructure in traumatic brain injury (TBI)

M. E. Komlosh[a,b], E. B. Hutchinson[a,b], M. Haber[b], D. Benjamini[a], A. V. Avram[a], P. J. Basser[a]

Eunice Kennedy Shriver National Institute of Child Health and Human Development, National Institutes of Health, Bethesda, MD, USA; The Henry M. Jackson Foundation for the Advancement of Military Medicine, Inc, Bethesda, MD, USA

Traumatic brain injury (TBI) is a major cause of disability and death worldwide, accounting for about 30% of all injuries and deaths in the USA [1]. The pathology, which ranges from severe to mild, can cause microstructural changes (some on the scale of microns) within the brain, including cell varicosities, micro-glia cell migration, and tissue loss [2,3]. While clinical MRI is routinely used to detect robust physiological and vascular abnormalities, more subtle cellular alterations are challenging to observe, identify, and characterize using conventional MRI methods. TBI can often only be detected at autopsy. Diffusion MRI methods, which are sensitized to the local microdynamics of tissue water, are promising techniques to probe subtle changes in brain microstructure and advances in the measurement and modeling of higher order diffusion may improve both sensitivity or specificity for the detection of brain abnormalities following injury. In this talk we will evaluate how diffusion tensor imaging (DTI) [4], mean apparent propagator (MAP-MRI) [5] and double-pulsed field gradient (d-PFG) [6] are being employed to quantitate microstructural features in the brain. We will also examine evidence from phantom [7] and tissue MRI studies and assess their value and potential for the detection of cellular alterations that accompany TBI [8,9].

References

[1] M. Faul, L. Xu, M. M. wald, V. G. Coronado, Centers for Disease Control and Prevention, National Center for Injury Prevention and Control; 2010.
[2] M. Gaez, E.B. Clin. Neuropathol. 115 (2004) 4-18.
[3] D. R. Namjoshi, et. al., Mol. Neurodegener. 9 (2015) 55
[4] P. J. Basser, J. Mattiello, D. LeBihan, Biophys J. 66(1994) 259–267
[5] E. Özarslan, et. al., Neuroimage (2013) 78:16-32.
[6] P. P. Mitra, Phys Rev B 51 (1995) 15074-15078.
[7] A. V. Avram, et al., The 23rd Annual meeting of the International Society for Magnetic Resonance in Medicine., Toronto, Canada. (2015).
[8] E.B. Hutchinson, et. al., Society for Neuroscience, San Diego, CA (2015)
[9] M. Haber, et. al., Capital Region TBI Research Symposium, Bethesda, MD, 2016.

Molecular transport in ionic liquids under confinement studied by low field NMR

C. Mattea [a], S. Stapf [a] and A. Ordikhani-Seyedlar [a]

[a] Department of Technical Physics II, TU Ilmenau, P.O. Box 100 565, 98684 Ilmenau, Germany.

The development of materials based on polymeric matrices combined with room temperature ionic liquids (RTILs) has gained considerable interest during recent years due to their applications as conducting films [1] and as electrochemical actuators [2]. The functionality and properties of these materials can be tuned using different types of RTILs and hosting polymers. For instance, the combination of RTILs with biopolymers expands these applications towards the field of biosensors. The knowledge of dynamical and structural properties in these systems is necessary in order to characterize the transport of the mobile ions responsible for conductivity.

The development of single-sided mobile NMR scanners in recent years [3] allows the study of films during its formation process up to the final state, with microscopic resolution as it has been demonstrated in the case of biopolymer gelatin and PVOH films [4, 5]. The preparation of the films requires the evaporation of the solvent after casting of the solution. Due to their geometrical characteristics, these systems are suitable to be measured with single-sided NMR (see figure 1), which allows evaporation in an open environment. In addition, the high field gradient strength of devices permits the discrimination between the two different nuclei ^{1}H and ^{19}F. This is particularly suitable because in many RTILs, ^{1}H is found in the cations and ^{19}F, in the anions forming these solvents.

In this contribution a short overview of the use of single-sided mobile NMR device for studies of film formation processes in biopolymers will be given as well as the recent advances in the dynamical studies of ionic liquid confined in gelatin film matrices.

Films from solutions of different concentration of ionic liquid in 10% solution of gelatin of 140 bloom in water, were studied. After casted, the water is allowed to evaporate until the film is ready, while the ionic liquid remains in the structure because of the negligible vapor pressure that characterizes these solvents. Relaxation times T_2, T_1 and diffusion coefficient of the films, at different layers were determined with single-sided mobile NMR scanners (Magritec, Germany/New Zealand) with static magnetic field gradients of 490 kHz/mm and 920 kHz/mm.

The results reveal different dynamics of the RTIL under confinement in the gelatin film porous matrix, depending on concentration and type of ions. Strong deviations could be expected comparing dynamics of ionic liquids in bulk [6] and confined in a porous gelatin matrix. Interestingly, restricted dynamics is observed in certain cases, while bulk dynamics is retained when the RTIL shows more non-polar character.

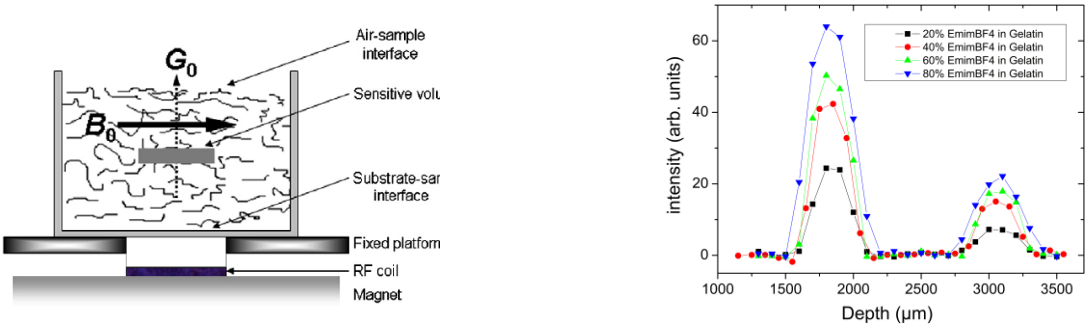

Figure 1 – (Left) Illustration of the experimental setup. B_0 is the external magnetic field. G_0 is the magnetic field gradient. (Right) Profile showing the signal intensity of cations (lower layers) and anions (higher layers) in gelatin-RTIL film at different concentrations.

References

[1] T. Ueki and M. Watanabe, Macromolecules, 41 (2008) 11.
[2] S. Imaizumi, Y. Ohtsuki, T. Yasuda, H. Kokubo, and M. Watanabe, ACS Appl. Mater. Interfaces 5 (2013) 6307.
[3] B. Blümich, J. Perlo, F. Casanova, Prog. Nucl. Magn. Reson. Spectrom. 52 (2008) 197.
[4] S. Ghoshal, C. Mattea, P. Denner, S. Stapf, J. Phys. Chem. B, 114 (2010) 16356.
[5] S. Ghoshal, P. Denner, S. Stapf, C. Mattea, Macromolecules, 45 (2012) 1913.
[6] A. Ordikhani-Seyedlar, S. Stapf, C. Mattea, Phys. Chem. Chem. Phys., 17 (2015) 1653.

Non-destructive and non-invasive NMR in cultural heritage

D. Capitani, V. Di Tullio, N. Proietti

Istituto di Metodologie Chimiche, CNR Area della Ricerca di Roma, Via Salaria km 29,300, 00015 Monterotondo, Roma

The characterization of materials and the causes of their degradation, the development of new methods and materials aimed at lengthening the life time of artefacts, are mandatory in the correct safeguard of cultural heritage. A breakthrough in the application of NMR in the cultural heritage field has surely been the development of portable NMR instrumentation [1-3]. These devices can be applied directly in situ on large objects fully preserving the integrity and the dimension of the object under investigation. NMR parameters measured by these devices give information about the state of degradation of materials, the performances of consolidation and water repellent treatments on porous materials, the ^{1}H NMR stratigraphy of paintings, the quantitative map of the dampness in wall paintings. The study of cleaning methods of materials of interest in the cultural heritage field is another new application. Water transport and kinetics of water penetration from the hydrogel throughout the material may be studied in a fully non-invasive and non-destructive way with portable NMR devices. This study is a fundamental step to develop and improve (with complexants and enzymes) the effectiveness of hydrogels as cleaning materials.

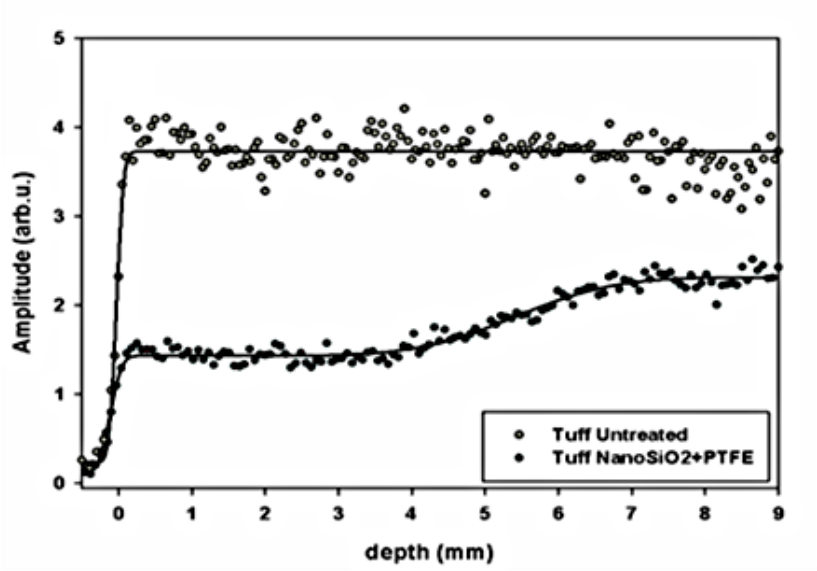

Figure 1. Non invasive, non-destructive NMR depth profiles of untreated tuff and tuff treated with silica and polytetrafluoroethylene nanoparticles.

[1] Bernard Blümich, Juan Perlo, Federico Casanova,. *Progr. Nucl. Magn. Reson. Spectrosc.* **2008**, *52*, 197-269.
[2] Donatella Capitani, Valeria Di Tullio, Noemi Proietti, *Progr. Nucl. Magn. Reson. Spectrosc*. **2012**, *64*, 29-69.
[3] Jonathan Mitchell, Peter Blümer, Peter McDonald, *Progr. Nucl. Magn. Reson* **2006**, *48*, 161-181.

Xray-CT enhanced interpretation of high-dimensional inverse Laplace NMR experiments

C.H. Arns[a], I. Shikhov, M. Nogueira d'Eurydice[a,b]

[a]School of Petroleum Engineering , University of New South Wales, Sydney, 2052, Australia; [b]School of Chemical and Physical Sciences, Victoria University of Wellington, New Zealand

For NMR in porous media internal gradients can present a major problem in the interpretation of both T_2-relaxation curves and higher-dimensional correlation maps (e.g. T_2-D, T_2-D-DG_0^2). Understanding these challenges is particular important when NMR is used for fluid-typing and/or spectral structure quantification. For rocks with relatively weak susceptibility contrast but sharp corners and for many sandstones, internal gradients can range in strength to a point where they become as strong as the applied gradient. This leads to apparent diffusion coefficients and T_2 relaxation times, complicating petrophysical interpretation. If a high-resolution Xray-CT image is available, the internal gradient field can be calculated for linear media (magnetic permeability $\mu \approx 1$) through a Poisson equation with scalar magnetic potential and appropriate internal and external boundary conditions. Knowledge of the internal field allows making corrections to the diffusion coefficients measured by NMR e.g. through a PGSE pulse sequence by considering applied gradient strength and cross-terms between internal and applied gradients. Experimentally, high-dimensional measurements may be carried out to derive the internal field distributions directly, aiding the development of better corrections for internal field effects. In a different context the characterisation of rock samples by NMR methods may be enhanced by considering a T_1-D-T_2 experiment.

In this work we review some of the signal processing challenges these 3D inverse problems pose, noting the ill-conditioned nature of the problem and the concept of separability of acquisition kernels. We compare a set of solution methods for both experiment and simulation in terms of accuracy, resolution, and computational resource requirements. Simulations and low field NMR measurements on model/artificial media, Mt Gambier limestone and a sandstone are used to illustrate concepts for the decomposition of additive contributions to the distribution functions for a selected set of pulse sequences. An example for a decomposition of magnetisation decay for a 1D simulation is given in Figure 1; a Euclidean distance transform is used to record the transfer of magnetisation from one rock-type into another.

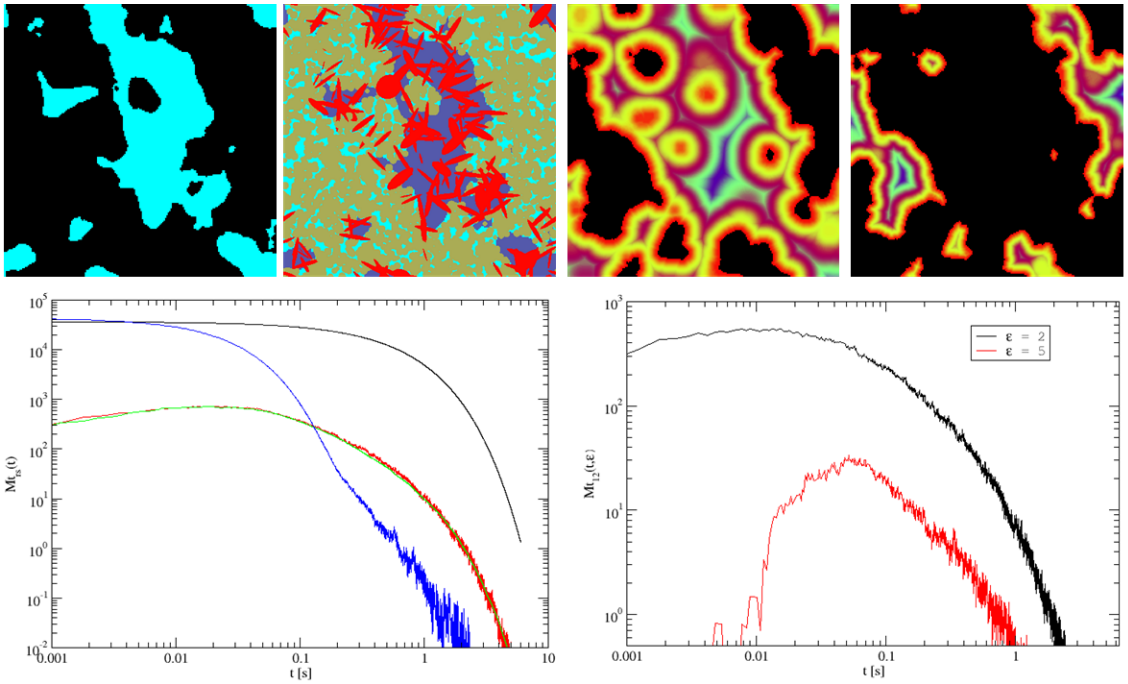

Figure 1 – Illustration of magnetisation coupling analysis using a Euclidean distance map as order field (slices through 3D model). *Top:* spatial distribution of micro-structure type, micro-structure, and Euclidean distance maps with reference to the surface beween micro-structure types. *Bottom:* Magnetisation decay for each pure rock-type (no mixing) and integrated mixing term (left, green and red curves starting with M0=0 at t=0) and distance based analysis of mixing (right).

References

[1] R.C. Wilson and M. D. Hürlimann, J. Magn. Res., 183 (2006) 1-12.
[2] J.D. Jackson, Classical Electrodynamics, John Wiley & Sons, New York, 1962.

ORAL

O01

Characterization of porous polymer materials by time domain and single-sided NMR

M.I. Velasco[a], E.V. Silletta[a], C.G. Gomez[b], M.C. Strumia[b], S. Stapf[c], G.A. Monti[a], C. Mattea[c], R.H. Acosta[a]

[a] FaMAF-Universidad Nacional de Córdoba and IFEG-CONICET, 5000 Córdoba, Argentina.

[b] Departamento de Química Orgánica, Facultad de Ciencias Químicas, (IMBIV-CONICET) Universidad Nacional de Córdoba, Haya de la Torre y Medina Allende, Edificio de Ciencias II - Ciudad Universitaria, 5000 Córdoba, Argentina.

[c] Department of Technical Physics II/Polymer Physics, Ilmenau University of Technology, 98684 Ilmenau, Germany

Porous polymer matrices are widely used in several areas such as catalysis, enzyme immobilization, HPLC, adsorbents or drug controlled release. These polymers have pores in their structures both in the dry and swollen state. Although it is well known that the structures and properties greatly differ between these two states, only few analytical methods provide information about the swollen state, even though most of the applications involve swollen matrices and in nearly every case its performance is a sensitive function of the distribution of internal pore size. Nuclear Magnetic Resonance is a suitable tool for the study of the molecular dynamics of different liquids spatially confined in macro, meso and nanopores through changes in relaxation times, thus providing information of the porosity of the systems in the state of further applications. Macroporous adsorption resins are porous cross-linked polymer beads that have been developed as useful adsorbents. They have shown high physical and chemical stabilities, large specific surface area, high adsorption capacities, easy regeneration, and long service life. Pore architecture leads to effective separation and reorientation of fluid elements, creating a high interfacial area between the immiscible phases for mass transfer to occur in liquid−liquid extraction. The particular systems used in this work are stable netwoks that do not collapse, with high porosity values of up to 85 % in the dry state. The pore size distribution however changes upon swelling when the systemas are fludded with polar liquids.

In this work, we describe the study of the pore structure of the macroporous polymer of ethylene glycol dimethacrylate and 2-hydroxyethyl methacrylate [poly(EGDMA-co- HEMA)] in the dry and in the swollen state by determination of properites of liquids contained in the polymer network [1,2]. This information allows the characterization of the matrices in terms of pore distribution, water uptake, and swelling under different conditions of synthesis. The behaviour of polar liquids during evaporation and deswelling dynamics is monitored and described by combining transverse relaxation data acquired in homogeneous magnetic fields, with spatial and time dependent water content determined with single sided NMR. We find that if the system has a relatively low amount of crosslinker content, an internal migration of water from the swollen polymer mesh into expanding pores takes place. With this procedure, it is possible to obtain information about the microscopic morphology behaviour of the matrix during evaporation and deswelling [3]. Additionally, the pore diameter can be determined by measuring diffusion which is encoded though magnetic field distortions that arise due to heterogeneities in the magnetic field, which are produced by changes in magnetic susceptibilities in going from the pore wall to the pore void (DDIF - Decay due to Diffusion in Internal Field) [4]. Comparison of the relaxation times present in different pore sizes provides information on surface interaction [5,6], in particular the influence of hydrogen bond between water and hydroxyl groups as a function of the amount of crosslinker is determined.

Experiments were carried out at room temperature and ambient pressure. The results presented are obtained by combining data acquired at 1.4 Tesla, 7 Tesla, with NMR-MOUSE and with a Fast Field Cycling relaxometer.

References

[1] Gomez, C.G., G. Pastrana, D. Serrano, E. Zuzek, M.A. Villar, and M.C. Strumia, *Macroporous poly(EGDMA-co-HEMA) networks: Morphological characterization from their behaviour in the swelling process.* Polymer, 2012. **53** (14): p. 2949-2955.
[2] Silletta, E.V., M.I. Velasco, C.G. Gomez, R.H. Acosta, M.C. Strumia, and G.A. Monti, *Evaporation kinetics in swollen porous polymeric networks.* Langmuir, 2014. **30**(14): p. 4129-36.
[3] M.I. Velasco, E.V. Silletta, C.G. Gomez, M.C. Strumia, S. Stapf, G.A. Monti, C. Mattea, R.H. Acosta, *Spatially resolved monitoring of drying of hirearchical porous organic networks.* Langmuir, 2016. **32**: p. 2067-2074.
[4] Song, Y.Q., S. Ryu, and P.N. Sen, *Determining multiple length scales in rocks.* Nature, 2000. **406** (6792): p. 178-181.
[5] Mitchell, J., L.M. Broche, T.C. Chandrasekera, D.J. Lurie, and L.F. Gladden, *Exploring Surface Interactions in Catalysts Using Low-Field Nuclear Magnetic Resonance.* The Journal of Physical Chemistry C, 2013. **117** (34): p. 17699-17706.
[6] S. Stapf, R. Kimmich, R. Seitter, *Proton and deuteron Field-cycling NMR relaxometry of liquids in porous glasses: evidence for Lévy-Walk statistics,* Physical Review Letters, 1995. **75** (15) p. 2855-2858.

O02

Shale organic porosity and total organic carbon (TOC) by combining spin echo, solid echo and magic echo

Zijian Jia[a], Lizhi Xiao[a]*, Zhizhan Wang[b], Can Liang[a], Long Guo[a]

[a]State Key Laboratory of Petroleum Resources and Prospecting, China University of Petroleum, Beijing, China; [b]SINOPEC Research Institute of Petroleum Engineering, Beijing, China;

Unconventional shale resources may contain a significant amount of hydrogen in organic solids such as kerogen, but it is difficult to detect the solids component directly with NMR method. Current methods measurements of organic porosity and structure are expensive and time-consuming. This paper presents a new method for determining organic porosity and structure by low field NMR combining spin echo, solid echo and magic echo. We proposed a new multi-magic echo sequence for the T1 -T2 measurement. To the authors' knowledge, this is the first instance of an inversion recovery and T1-T2 measured from a magic echo.

A recent study has shown that a significant amount of transverse relaxation in organic rich systems may arise from homonuclear dipolar coupling. In contrast, the majority of dipolar interactions in conventional reservoirs arise from heteronuclear dipolar coupling between fluid molecules and paramagnetic impurities on the pore surface. Unfortunately, the spin echo only recovers magnetization lost due to chemical shift anisotropy, underlying magnetic field inhomogeneity, and heteronuclear dipolar coupling. When homonuclear dipolar coupling is present, this signal intensity will still be lost in spin echo measurement. For systems containing heteronuclear and homonuclear dipolar coupling, the solid echo will refocus both types of couplings. But the solid-echo is only able to completely refocus dephasing due to isolated spin pairs and will be less efficient at refocusing the magnetization of a hydrogen atom undergoing multiple homonuclear dipolar interactions. This isolated spin pairs often occur in organic pore surface. Multiple homonuclear dipolar interactions often occur in organic matrix. Magic echo will recover the multiple homonuclear dipolar interactions and get additional signal of organic matrix. The different samples show different increases in signal intensity by spin-, solid- and magic-echo. Per gram, kerogen with small porosity produces fewer homonuclear dipolar interactions between pairs of spins and more between many spins.

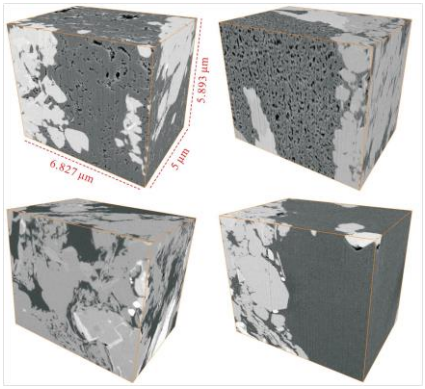

Figure 1 – Shales with different kerogen structure and TOC

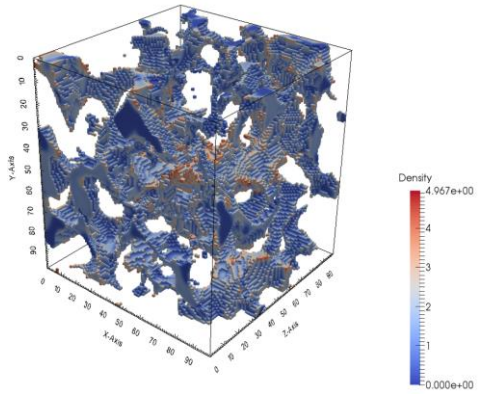

Figure 2 –Reconstruct digital core

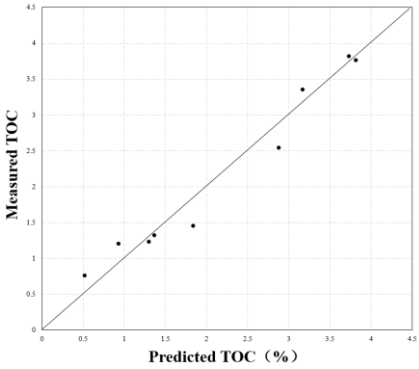

Figure 3 –TOC Result form NMR predicted and TOC analyzer

We use Lattice Boltzmann Method (LBM) to do the NMR response simulation of the liquid in nanopores. Based on the analysis of the core slice, digital cores are reconstruct from shale samples. Three type echos simulation depends on the fact that liquid molecules encounter the pore surface and stick for a short time. For solid echo and magic echo, every liquid molecule on organic surface experience homonuclear dipolar interaction. And there is multiple homonuclear dipolar interaction in kerogen matrix with magic echo. Previous work with benzene in zeolites produced that the adsorbed fluid molecules in shales are in the rigid-lattice approximation may be common.

For shales containing heteronuclear and homonuclear dipolar coupling, the different of spin echo and solid echo signal:

$$E_s(t) - E_c(t) = 2t\tau(2M_2^{II} - M_2^{IS}) / 2! + M_4^{II}(t - \tau)^4 / 4! \quad (1)$$

where $M_2^{II} = \frac{1}{3} I(I+1) \frac{1}{N_I} \sum_{j,k} B_{jk}^2$ $M_2^{IS} = \frac{1}{3} S(S+1) \frac{1}{N_I} \sum_{k,\beta} C_{k\beta}^2$

Where Es is solid echo amplitude, Ec is spin echo amplitude. I,S are different spins species. NI is the number of hydrogen absorbed on organic surface.Where j, k represent different hydrogen atoms, β represents different impure atoms. B and C are the factors related to the relative positions of molecules. And the magic echo is similar. The result show that we can get the organic porosity and TOC from the difference of three echo simulation intensity. The real shale samples were analysed by NMR. We get the organic porosity and structure by FIB-SEM. The TOC of samples were obtain by TOC analyzer. The result proved that we can get the shale organic porosity and TOC by combining spin echo, solid echo and magic echo.

References

[1] J. G. Powles, J. H. Strange, *PROC. FHYS.* SOC.VOL. 82 (1963)
[2] W.-K. Rhim, A. Pines and J.S. Waugh, Phys. Rev. 3 (1971) 684.
[3] Kathryn E. Washburn, Justin E. Birdwell, J. Magn. Reson. 233 17–28. (2013)

O03

Low-Field NMR Laboratory Measurements of Hydrocarbons Confined in Organic and Non-Organic Nanoporous Media at Various Pressures

H. Thern[a], C. Horch[b], F. Stallmach[b], B. Li[c], A. Mezzatesta[c], H. Zhang[c], R. Arro[c]

[a]Baker Hughes Incorporated, Baker-Hughes-Str. 1, 29221 Celle, Germany; [b]U. of Leipzig, Dept. of Physics of Interfaces, Linnestr. 5, 04103 Leipzig, Germany; [c]Baker Hughes Incorporated, Rankin Rd. 2001, Houston, TX 77073, USA.

The commercial production of hydrocarbons from unconventional shale reservoirs on a large scale developed since approximately 5 years. The potential of NMR measurements for probing core samples in the laboratory and sub-surface formations by logging tools was identified early on. NMR is sensitive to rock and fluid properties, both being critical for understanding the storage and production behavior of shale reservoirs. Despite a large number of research works and publications (e.g., [1], [2]) there are still questions and uncertainties on how to best acquire, process, and interpret NMR data in shale reservoirs.

We present laboratory data on organic and non-organic nano-porous media filled with hydrocarbon gas at various pressures. Main goals were the characterization of the adsorption-desorption process including capillary condensation, as well as the interpretation of NMR data with respect to hydrocarbon and water present in organic and non-organic pores.

Laboratory measurements were conducted in a low-field NMR setup [3] with water-wet porous glass, with oil-wet polymer-based spherical activated carbon (PBSAC) beads, and with a crushed shale core sample. NMR relaxation times were used to observe the occurrence of capillary condensation for mixtures of methane and propane at room temperature under controlled pressure conditions for the PBSAC beads (Figure 1). A PVT (pressure, volume and temperature in an equation of state) simulation software, incorporating a novel phase equilibrium model, was developed [4], showing good agreement between acquired NMR data and simulation results.

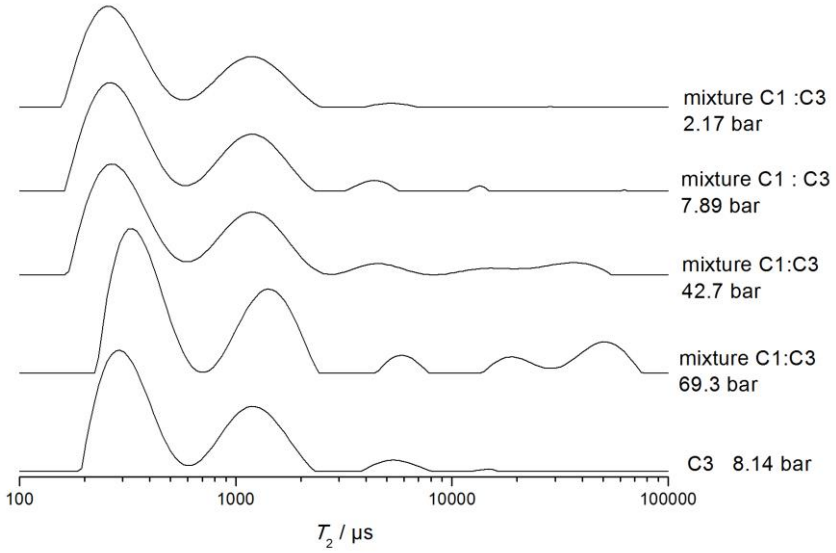

Figure 1 – NMR T_2 response of propane (bottom) and propane-methane mixtures in PBSAC beads at varying total pressure.

The NMR data indicate a strong dependence on wettability of the hydrocarbon system in nano-porous media. Hydrocarbon in water-wet porous glass shows long relaxation times in contrast to much shorter relaxation times observed for the oil-wet PBSAC beads. An observed bi-modal T_2 distribution of the adsorbed gas phase in the PBSAC is interpreted with respect to pore size distribution, exchange between the micro- and meso-pores and the interparticle voids, and hydrocarbon mixture compostion. The NMR data from the shale core sample, which contains a combination of water-wet non-organic and oil-wet organic components, are interpreted for pore fluid and rock properties using the results from the synthetic samples.

References

[1] K. E. Washburn, Concepts in Magnetic Resonance 43A (2014) 57-78.
[2] J. P. Korb, B. Nicot, A. Louis-Joseph, S. Bubici, G. Ferrante, J. Phys. Chem. C (2014) 118 (40), 23212–23218.
[3] C. Horch, S. Schlayer, F. Stallmach, J. Magnet. Resonan. 240 (2014) 24–33.
[4] B. Li, A. Mezzatesta, Y. Li, Y. Ma, A. Jamili, Petrophysics (2015) 57 (1), 121-139.

A multidisciplinary approach for the multi-scale structural study of eco-compatible MgO/CaO-based cements

S. Borsacchi[a], F. Martini[a], M. Geppi[a,b], M. Tonelli[c], F. Ridi[c], P. Baglioni[c], L. Calucci[a]

[a]Istituto di Chimica dei Composti OrganoMetallici, Consiglio Nazionale delle Ricerche − CNR S.S. di Pisa, Via G. Moruzzi 1, 56124 Pisa, Italy; [b]University of Pisa, Dept. of Chemistry and Indusrial Chemistry, Via G. Moruzzi 13, 56124 Pisa, Italy; [c]University of Florence, Dept. of Chemistry "Ugo Schiff" & CSGI, Via della Lastruccia 3, 50019 Sesto Fiorentino (FI), Italy;

The development of cement formulations alternative to the traditional Portland (CaO-based) cement is currently object of great interest in the field of building materials research both with the aim of reducing the environmental impact associated with the CO_2 emissions [1] and in view of solving specific needs required for particular applications, such as that of radioactive waste encapsulation [2-4]. In this field, low-pH cements are researched in order to overcome the problems related to the high alkalinity of Portland cement pore solution, which can cause the corrosion of the radioactive wastes and the degradation of the clayey materials used for waste storage [3,4].

One of the most promising alternative is rapresented by MgO-based cements, which, beside developing pH values lower than those typical of Portland cements [5], also respond to the eco-suistainability requirement of reducing CO_2 emissions [refs]. Indeed, abundant natural sources, as for example the magnesium silicates present in the Earth Crust, can be employed to derive reactive periclase (MgO), used as starting material in these formulations [5]. MgO-based cements can be obtained from the hydration of MgO in the presence of silica sources, which leads to the formation of a binder phase called Magnesium Silicate Hydrate (MSH) analogous to the binder phase Calcium Silicate Hydrate (CSH), formed in CaO-based cements. Even if the interest in MgO-based cements is growing, as demonstrated by the large number of papers recently appeared in the literature [3-8], a full comprehension of their properties, such as hydration kinetics, the nature of the hydrated products and their multi-scale structure and organization, is still lacking. The investigation of these properties, as well as the research for new formulations with improved performances, is fundamental to achieve the industrial breakout of these materials, whose mechanical properties are still inferior to those of traditional Portland cements.

In this work novel MgO-based cements obtained by hydration of a 1:1 molar mixture of MgO and silica fumes (MgO/SiO_2) and mixed-formulations containing different amounts of MgO/SiO_2 and Portland cement were developed. The muti-scale structural properties and hydration kinetcs of the prepared systems were investigated in detail by means of solid-state NMR spectroscopy (SSNMR) and Fast Field Cycling (FFC) relaxometry, which already proved to be very powerful for the study of cements [9-11], with the support of complementary techniques such as X-Ray Diffraction (XRD), thermogravimetry (TGA), IR spectroscopy, Scanning Electron Microscopy (SEM) and calorimetric techniques. The nature and the structure at the sub-nanometric scale of the formed hydrated phases, as well as their formation kinetics, were investigated on samples liophilized at different times of hydration by means of high-resolution SSNMR experiments for the observation of ^{1}H, ^{29}Si and ^{27}Al nuclei. In particular, mono- and bi-dimensional ^{29}Si MAS experiments allowed the different silicon sites, Q^1, Q^2 and Q^3, characterized by different connectivity to –OSi, -OH, –OMg or -OCa groups, to be identified and quantified. In the case of mixed systems, it was also possible to distinguish between MSH and CSH domains, and to study their properties and relative amounts as a function of composition and hydration times.The state of water in the pastes and the evolution of the porous structure with hydration time, a property that is strongly related to the final mechanical properties of a cementitious material, were investigated directly on the cement pastes by means of ^{1}H T_1 Fast Field Cycling relaxometry and the measurements of ^{1}H T_2 relaxation times at low magnetic fields (proton Larmor frequency of 20 MHz) [10].

This work was financially supported by MIUR (FIR2013 Project RBFR132WSM).

References

[1] R. J. Flatt, N. Roussel, C. R. Cheeseman, J. Eur. Ceram. Soc. 32 (2012) 2787–2798.
[2] A. Dauzeres, P. Le Bescop, P. Sardini, C. Cau Dit Coumes, Cem. Concr. Res. 40 (2010) 1327–1340.
[3] A. Dauzeres, G. Achiedo, D. Nied, E. Bernard, S. Alahrache, B. Lothenbach, Cem. Concr. Res. 79 (2016) 137–150.
[4] S. A. Walling, H. Kinoshita, S. A. Bernal, N. C. Collier, J. L. Provis, Dalton Trans. 44 (2015) 8126–8137.
[5] M. Tonelli, F. Martini, L. Calucci, E. Fratini, M. Geppi, F. Ridi, S. Borsacchi, P. Baglioni, Dalton Trans 45 (2016) 3294–3304.
[6] B. Lothenbach, D. Nied, E. L'Hôpital, G. Achiedo, A. Dauzères, Cem. Concr. Res. 77 (2015) 60–68.
[7] C. Roosz, S. Grangeon, P. Blanc, V. Montouillout, B. Lothenbach, P. Henocq, E. Giffaut, P. Vieillard, S. Gaboreau, Cem. Concr. Res. 73 (2015) 228–237.
[8] D. Nied, K. Enemark-Rasmussen, E. L'Hopital, J. Skibsted, B. Lothenbach, Cem. Concr. Res. 79 (2016) 323–332.
[9] A. Rawal, B.J. Smith, G.L. Athens, C.L. Edwards, L. Roberts, V. Gupta, B.F. Chmelka, J. Am. Chem. Soc. 132 (2010) 7321-7337.
[10] V. Bortolotti, L. Brizi, R. J. S. Brown, P. Fantazzini, M. Mariani, Langmuir 30 (2014) 10871–10877.
[11] F. Barberon, J.P. Korb, D. Petit, V. Morin, E. Bermejo, Phys. Rev. Lett., 90 (2003) 116103-1-116103-4.

Multi-dimensional NMR experiments for characterization of pore structure heterogeneity and liquid saturations.

R. T. Lewis, J. G. Seland

Department of Chemistry, University of Bergen, Allegaten 41, N-5007, Bergen, Norway

Dynamical NMR measurements of spin bearing molecules in liquid saturated porous materials are influenced by the physical and chemical surroundings, in particular the longitudinal (T_1) and transverse (T_2) relaxation time constants. In addition, the inhomogeneous internal magnetic field generated on the pore level depends on the strength of the static magnetic field, the differences in magnetic susceptibilities ($\Delta\chi$), but also on the geometry of the porous network [1, 2]. To thoroughly investigate how the internal field and it spatial dependence (the internal gradient G_0) can be used to determine various properties of the porous structure and the confined liquids, we present multi-dimensional Inverse Laplace NMR experiments that enable measurements of several dynamic correlations, and where all of the correlations involve the internal magnetic field and its dependence on the geometry of the porous network.

First, we describe how the Decay due to Diffusion in the Internal Field - CPMG (DDIF-CPMG) experiment designed by Liu et al. [3], resulting in a correlation between pore size (d) and T_2, also can be used to separate signals from water and oil in a porous sample. Thus, the confining geometry of the water phase and its correlation to T_2 can be determined. The results clearly demonstrate that in a rock core plug saturated with water and oil, water is mainly found in smaller pores and is confined to the walls in the larger pores [4].

Second, we present a novel multi-dimensional NMR experiment (shown in Figure 1) that enables us to measure the following correlations: $T_1 - \Delta\chi$, $G_0 - \Delta\chi$, $G_0 - T_1$, and $G_0 - d$ in one experiment [5]. We discuss how the obtained correlations can be an indicator for pore structure heterogeneity. For instance, compared to a water saturated packing of mono-sized glass beads, there is a clear negative $G_0 - d$ correlation in a water-saturated rock core sample, indicating a more heterogeneous pore stucture in the rock material. We also discuss how to take into account the different time scales involved in the measurement of the different dynamic parameters.

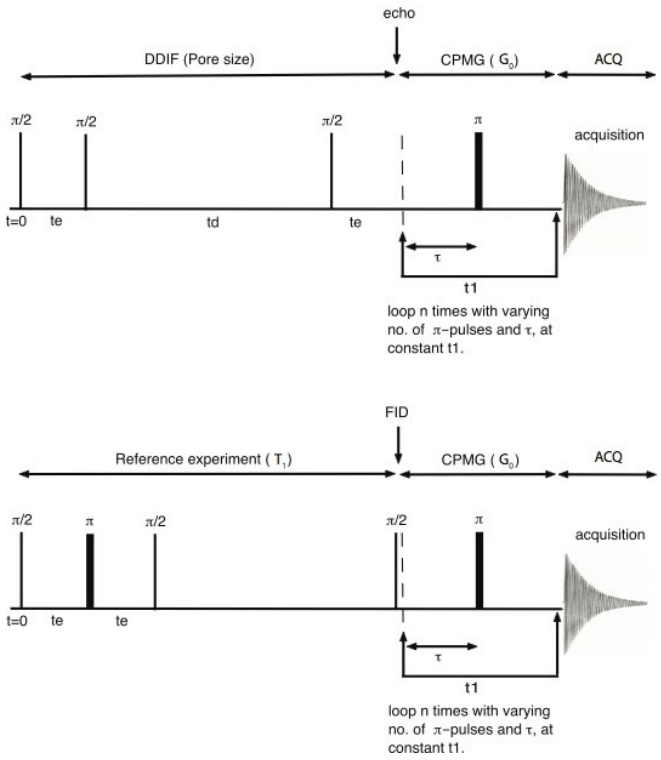

Figure 1 – Multi-dimensional NMR experiment that enables determination of $T_1 - \Delta\chi$, $G_0 - T_1$, $G_0 - \Delta\chi$ and $G_0 - d$ correlations.

References

[1] R. Brown, Phys. Rev. 121 (5) (1961), 1379–1382.
[2] Y.-Q. Song, Concepts Mag. Reson. 18A (2) (2003), 97–110.
[3] R. H. Liu, M. Nogueira d'Eurydice, S. Obruchkov, P. Galvosas, J. Mag. Reson. 246 (2014), 110–118.
[4] R. T. Lewis, K. Djurhuus, J. G. Seland, J. Magn. Reson., 259 (2015), 1-9.
[5] R. T. Lewis, J. G. Seland, J. Magn. Reson. 263 (2016), 19-32.

Localization in a single pore

E. J. Fordham[a], J. Mitchell[a]

[a]Schlumberger Gould Research, High Cross, Madingley Road, Cambridge CB3 0EL, UK.

Multi-dimensional NMR designed to elucidate pore structure heterogeneity offers ingenious sequences [1,2] with simultaneous interpretations for various combinations of pore size ℓ_s, T_1, susceptibility contrast $\Delta\chi$ and induced internal gradients g_{int}. That the latter cannot in general be ignored is well-known. However quantitative interpretation requires *models* for magnetization decay from diffusion in the internal fields; but well-founded models are available from theory only in a few asymptotic limits. Furthermore the consequences [3,4] of the so-called dephasing length ℓ_g being shorter than both the pore size ℓ_s and the inter-echo diffusion distance ℓ_E are not so commonly recognized. Magnetization is then "Localized" to small pockets of surviving magnetization which may be only a small fraction of the fluid-filled pore [3,5].

We explore, by direct simulations in a single pore, magnetization decay by "diffusion in a gradient". We model directly the internal field within a representative pore image taken from X-ray microtomography, for various $\Delta\chi$. For given solutions of the magnetostatic problem, molecular diffusion, and decay of total magnetization, can then be simulated. Analytical results are available only in two out of three asymptotic limits, generally called "Short Time" (ST), "Motionally Averaged" (MAV) and "Localization" (LOC), determined by the competition between the length scales ℓ_s, ℓ_E and ℓ_g [3,4]. The three asymptotes are explored directly, by choice of parameters, with extension to intermediate cases for which no analysis exists. Simulation also provides the magnetization *distribution* (dominant mode shapes) within the pore space, of which only the total is directly measured.

The LOC regime is shown to be qualitatively different from both the ST and MAV limits, where the dominant diffusion eigenmode is uniform. In the LOC regime the intra-pore magnetization is rapidly distorted; surviving magnetization is confined to small pockets either by restriction at the pore walls, or around saddle points where the internal field is locally flat. Experimental NMR obtains signal only from an unrepresentative fraction of the pore space.

These features are in agreement with the limited analytical results available. A general asymptote is available only for a 1D restriction [4,5], confirmed experimentally [3] and of theoretical interest for this reason [7]. It is arguable whether an asymptotic LOC regime is experimentally observable on more typical porous media, with 2D or 3D restrictions [5]. The limited theoretical base does show that behavior in the LOC regime is strongly geometry-dependent [8]. This paucity of analytical results makes quantitative interpretation of experiments in the LOC regime difficult. Where a porous system behaves in a "pre-asymptotic LOC" manner, the best basis for data analysis currently available is from Mitchell [9] involving an empirical power law in the decay exponent. This approach remains heuristic.

In qualitative terms, the asymptotic limits are typical for: ST: short echo spacings; MAV: small pores; and LOC: strong internal gradients. For many sedimentary rocks, the ST or MAV regimes may be accessible in low-field petrophysical platforms. In spectroscopy systems typical field strengths may push the system strongly toward the LOC regime (nano-porous shales excepted). The experimenter is thus deprived of useful results for data analysis, just where characterizations including susceptibility and internal gradients would be of greatest value.

To escape the LOC regime, with a given sample and ℓ_E at the instrumental limit, the experimenter has just one option: reduce B_0. This may conflict with much conventional judgment.

References

[1] Lewis, R.T. & Seland, J.G., J. Magn. Reson. 263 (2016), 19–32
[2] Lewis, R.T., Djurhuus, K., Seland, J.G., J. Magn. Reson. 259 (2015), 1–9
[3] Hürlimann, M.D., Helmer, K.G., de Swiet, T.M., Sen, P.N. & Sotak, C.H., J. Magn. Reson. Ser. A 113 (1995), 260–264
[4] Mitchell, J., Chandrasekera, T.C., Johns, M.L., Gladden, L.F. & Fordham, E.J., Phys Rev. E. 81 (2010), 026101
[5] de Swiet, T. M & Sen, P.N., J. Chem. Phys. 100 (1994), 5597
[6] Sen, P.N., Andre, A. & Axelrod, S., J. Chem Phys. 111 (1999), 6548
[7] Grebenkov, D.S., Rev. Mod. Phys. 79, (2007), 1077–1137
[8] Zielinski, L.J. & Sen, P.N., J. Magn. Reson. 147 (2000) , 95
[9] Mitchell, J. & Chandrasekera, T.C., J. Chem. Phys. 141 (2014), 224201

A new model for the interpretation of T_1^{-1} dispersion measurements

D. A. Faux, P. J. McDonald

Department of Physics, University of Surrey, Guildford, GU2 7XH, UK.

Fast-field-cycling NMR dispersion (NMRD) relaxometry has been applied, for decades, to a broad range of systems including cement-based materials, bio-polymers, glass, plaster, rock and more [1-3]. NMRD has the potential to measure the nano-scale transport properties of fluids in porous material. To interpret the T_1^{-1} dispersions, a simple model due to Korb and co-workers [1-3] has been widely used and has proved successful at fitting dispersions across this broad range of systems. The basic physics of the Korb model is that relaxation is due to the interaction of mobile surface and bulk spins with paramagnetic impurities. The model generates a dipolar spin-diffusion correlation function $G(t)$ which is Fourier transformed to obtain T_1^{-1}. The output of the fitting process is two transport parameters, τ_ℓ and τ_d, the surface layer diffusion correlation time and the spin layer-to-bulk desorption time constant respectively, and a constant T_1^{-1} rate to account for the bulk contribution. However, the breadth of applications has revealed that values of τ_ℓ and τ_d are surprisingly unchanging from system to system, and hard to justify based on any physically-reasonable diffusion model [4].

We believe that the basic physics of the Korb model is correct. We have therefore taken this physics and developed a new model which makes four key adaptations compared to Korb:

- paramagnetic impurities are treated as a plane of uniform density *within the crystal*, as illustrated in Fig. 1, rather than located within the surface layer. This leads to $G(t) \propto t^{-2}$ compared to t^{-1} for the Korb model and leads to a fundamentally-different T_1^{-1} dispersion,
- $G(t)$ is calculated by explicitly taking into account the functional dependence on z across the layer thickness, where z is the distance from the layer of paramagnetic impurities. This is important because $G(t) \propto z^{-4}$.
- explicit calculation of T_1^{-1} is undertaken for bulk spins characterised by diffusion correlation time τ_b, rather than assuming a constant contribution, as in the Korb model,
- desorbed spins are permitted to re-enter the surface layer by the incorporation of Lévy dynamics.

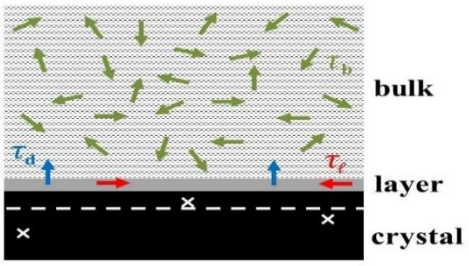

Figure 1 – a representation of a pore surface showing surface diffusion events (red), desorption (blue) and bulk diffusion (green). Paramagnetic impurities are indicated by white crosses modelled by a single layer below the pore surface (dashed line).

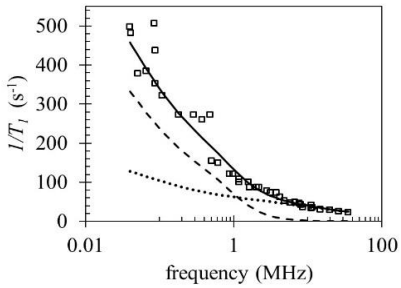

Figure 2 – shows the fit to the relaxation dispersion for the oil component of an oil shale (□) [3]. The fit (solid line) is the sum of the bulk (dotted) and surface (dashed) components.

The new model and associated theory is fit to NMRD measurements spanning three decades of frequency and, simultaneously, the T_1/T_2 ratio (where available) for a mortar, a plaster paste and for water and oil in oil shale [1-3]. The model contains the same number of fit parameters as the Korb model. Results for τ_ℓ, τ_d and τ_b are shown in the table.

System	τ_ℓ (μs)	τ_d (μs)	τ_b (ps)
Hydrated mortar [1,5]	0.2-1.0	0.8-1.1	33-40
Plaster paste [2]	35-45	60-70	19-21
Oil in oil shale [3]	0.1-0.5	0.2-0.3	20-40
Water in oil shale [3]	n/a	n/a	10-40

The application of the model yields:

(i) physically-realistic transport parameters for all systems,

(ii) parmeter sets that change between systems.

In the presentation, the new model will be explained, the new fits shown and the criticality of the different adaptations explained. We will show that the application of our model plus associated theory yields a wealth of physically-meaningful and consistent nano-scale transport parameters, insight into diffusion mechanisms and pore morphology. We believe that this work develops NMRD as the most powerful experimental tool for finding nano-scale dynamic properties of fluids in porous systems.

References

[1] F. Barberon, J.-P. Korb, D. Petit, V. Morin, E. Bermejo, Phys. Rev. Lett. 90 (2003) 116103.
[2] J.-P. Korb, New J. Phys. 13 (2011) 035016.
[3] J.-P. Korb, B. Nicot, A. Louis-Joseph, S. Bubici, G. Ferrante,, J. Phys. Chem. C 118 (2014) 23212-8.
[4] D. A. Faux, S.-H. P. P. Cachia, P. J. McDonald, N. C. Howlett, J. S. Bhatt, S. V. Churakov, Phys. Rev. E., 91, (2015) 032311.
[5] P. J. McDonald, J.-P. Korb, J. Mitchell, L. Monteilhet, Phys. Rev. E 72 (2005) 011409.

O08

Effect of mucilage on water properties in the rhizosphere monitored by ^{1}H-NMR relaxometry

Mathilde Brax[a], Christian Buchmann[a], Gabriele E. Schaumann[a]

[a] University Koblenz-Landau, Institute for Environmental Sciences, Group of Environmental and Soil Chemistry, Fortstrasse 7, 76829 Landau, Germany.

Mucilage is mainly produced at the root tips and has a high water holding capacity derived from highly hydrophilic gel-forming substances. Neutron radiography showed that for young roots of lupins growing in sandy soils, the rhizosphere was wetter than the bulk soil during drying, but after severe drying and subsequent irrigation it remained markedly dry and required more than two days to rewet [1]. The objective of the MUCILAGE project is to understand the mechanistic role of mucilage for the regulation of water supply for plants. Our subproject investigates the chemical and physical properties of mucilage as pure gel and mixed with soil.

^{1}H-NMR Relaxometry represents a non-intrusive powerful method for soil scientific research by allowing both the quantification of water distributions and the monitoring of the water mobility in soil pores and gel phases, respectively. The objective of our study was first to distinguish water in a gel phase from pore water in a simplified soil system. From this knowledge, we demonstrate how mucilage drying and rewetting alter the properties of water in the respective gel phases and pore systems in the rhizosphere.

To distinguish gel-inherent processes from classical processes, we investigated how the water mobility varied as function of the water content in pure chia mucilage and how the wettability of dried chia mucilage changed by using ^{1}H-NMR relaxometry. Using model soils, the signals coming from pore water and gel water were differentiated. Mucilage-containing model soils were consecutively dried and rewetted in order to characterize the swelling and shrinking of the mucilage gel in the soil matrix and the potential effects on the soil water mobility. The water properties for mucilage-rich soils were shown to evolve in function of the mucilage history. Further, by affecting the mobility of water entrapped in the mucilage network, we show that mucilage can modulate the rhizosphere hydraulic properties. Several factors influence the effect of mucilage such as its drying-wetting history, the soil particle distribution and the soil solution composition.

Based on these findings, we discussed the potential and limitations of ^{1}H-NMR relaxometry for following natural swelling and shrinking processes of a natural biopolymer in soil.

References

[1] Carminati, A., Moradi, A.B., Vetterlein, D., Vontobel, P., Lehmann, E., Weller, U., Vogel, H.-J., Oswald, S.E. Plant and Soil 332 (2010) 163-176.

Application of MR microscopy for research in wood science

U. Mikac[a], I. Serša[a], M. Žlahtič [b], M. Humar [b], M. Merela [b], P. Oven [b]

[a]Jožef Stefan Institute, Jamova 39, 1000 Ljubljana, Slovenia; [b] University of Ljubljana, Biotechnical Faculty, Dept. of Wood Science and Technology Jamnikarjeva 101, SI-1000 Ljubljana, Slovenia.

Moisture content (MC) of wood has a pronounced effect on its physical and mechanical properties [1]. Namely, resistance of wood against wood destroying organisms is always a combined effect of toxic or inhibiting ingredients on the one hand, and of anatomical or chemical exclusion of moisture, which is one of the most important factors for biodeterioration. For this reason, the information on distribution and concentration of water in wood is of great importance. Large variability in wood structure and therefore distribution of MC is expected among different tree species. The feasibility of MR imaging for a non-destructive characterization of the moisture content and moisture distribution in tree tissues was tested and used in different applications, as for example in an *in-vivo* study of tree response to a mechanical wounding and in a study of efficacy of non-biocidal solutions for wood preservation (wax and oil based solutions).

Wood is a porous material whose matrix includes macromolecules that link water by hydrogen bonds [2]. Therefore, wood has three different kinds of hydrogen nuclei and thus three different ^{1}H MR signal sources: protons in solid wood, the cell-wall water protons and protons of free water in cell lumens, the later when the total moisture content is above fibre saturation point (FSP). The correlation between the MC and relaxation times was measured on samples of beech (*Fagus sylvatica L.*) branches from different trees at different MC. The correlation was used to determine the MC distribution in the wounded part of a beech branch *in-vivo* from MR images obtained at different times after the mechanical wounding. The results indicate that in the margins of wounded wood in beech, not only cell wall alterations, but also intensive water accumulation represents integral part of protective mechanism for underlying sound wood [3]. MRI revealed that xylem at the wound was dehydrated in a cone-shaped pattern reaching approximately 4.5 mm deep in the branch. Dehydration was delimited from the underlying sound wood with a layer of tissue with a high MRI signal and hence a high moisture content. This layer corresponds in position to the reaction zone. Moisture contents determined from MRI for the reaction zone in beech were greater than in healthy wood by factor of 1.5±0.3.

Water repellents as environment-friendly treatments are gaining their popularity as non-biocidal solutions for wood protection. One of the most important water repellents for wood besides waxes and organosilicon compounds are drying oils. Tung oil is one of the best performing oil. However, tung oil, similarly as other oils, does not penetrate deeply into wood, due to its high viscosity. In order to improve penetration of oil into wood, vacuum-pressure procedure was applied. MRI was used to determine the penetration depth and distribution of the oil into the wood samples of different species that are important in Central Europe: sweet chestnut heartwood, European larch heartwood, Scots pine heartwood, and Norway spruce heartwood (Fig. 1).

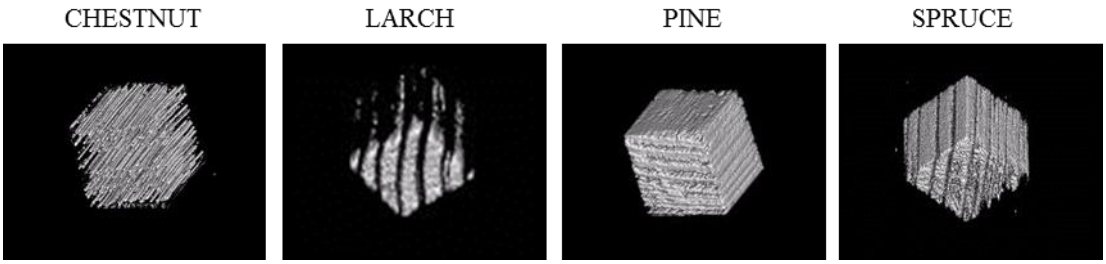

Figure 1 –Oil distribution in wood samples after impregnation of wood with tung oil.

The efficacy of wax emulsion against the moisture uptake was also checked and compared with the moisture uptake of untreated samples. The samples were soaked in water for 1 h and the moisture distribution in the samples was determined from MRI signal intensity. The moisture distribution during sample drying was monitored for 24 h. The amount and distribution of the moisture in the samples and the drying kinetics among different wood species and treatments were compared.

Results of the two studies demonstrated the efficiency of MR microscopy in analysis of responses of live trees to different stress conditions (first study) as well as its efficiency in analysis of wood preservation (second study). All the studies have in common the role of water in the samples that is used as a MRI sensor for the ongoing process in tree / wood. There are several additional wood products the production of which could be followed and possibly optimized by MRI. One such example is cross-laminated wood panel in which the effect of glue layers on migration of water across the panel is not yet fully understood.

References

[1] J.F. Siau, Wood: Influence of moisture on physical properties. New York, Polytechnic Institute and State University, New York,1995.
[2] J. G. Haygreen, J. L. Bowyer, Forest Production and Science, Iowa State university Press, Ames, iowa, 1996.
[3] P. Oven, M. Merela, U. Mikac, I. Serša, Holzforschung 62 (2008) 322-328.

O10

In situ visualization of Flow and Fouling layer formation during alginate filtration

F. Arndt[a], S. Schuhmann[a,b], G. Guthausen[b], S. Schütz[c], H. Nirschl[a]

[a]Karlsruhe Institute of Technology (KIT), Institute of Mechanical Process Engineering (MVM), Straße am Forum 8, 76131 Karlsruhe, Germany; [b]Pro^{2}NMR Karlsruhe Institute of Technology (KIT), MVM and IBG-4, Adenauerring 20b, 76131 Karlsruhe, Germany; [c]MANN+HUMMEL GmbH, Schlieffenstraße 42, 71636 Ludwigsburg, Germany

In membrane processes, fouling is one of the critical issues affecting the productivity, plant operation and maintenance costs [1]. This is true not just for membrane applications in wastewater and water treatment processes with high organic load, but also for membrane processes in dairy and beverage applications [2]. Operating conditions, feed composition and membrane material have a major influence on filtration performance and fouling behavior of the membranes. Ceramic hollow fiber membranes used in this study are characterized by a high chemical, thermal and mechanical stability as well as a high specific membrane filter surface.

Focusing on wastewater treatment processes, it has been reported that extracellular polymeric substances (EPS) are one of the main causes of membrane fouling [3]. In membrane filtration research, sodium alginate often serves as a model compound for EPS [1, 3]. Sodium alginate is a hydrophilic unbranched binary copolymer. In the presence of divalent cations, e.g. Ca^{2+}, alginates form complexes, which lead to a significant change in filtration mechanisms in dead-end filtration and also to a change in filtration performance during cross-flow filtration experiments.

In addition to the description of filtration data using conventional cake filtration model, nuclear magnetic resonance imaging was used to elucidate the influence of Ca^{2+} on the fouling layer structure for alginate filtration with ceramic hollow fibre membranes. In order to visualize the alginate layers inside opaque ceramic hollow fibre membranes by means of MRI, magnetic iron oxide nanocrystallites (MIONs) were applied as contrast agents due to low image contrast between alginate fouling layer and surrounding water. The *in situ* filtration set up allowed not only spatially and time resolved imaging of fouling layer build up using the multi slice multi echo (MSME) pulse sequence, also flow velocity measurements were performed in order to gain more insight into the hydrodynamics in the fouled membranes (Fig. 1).

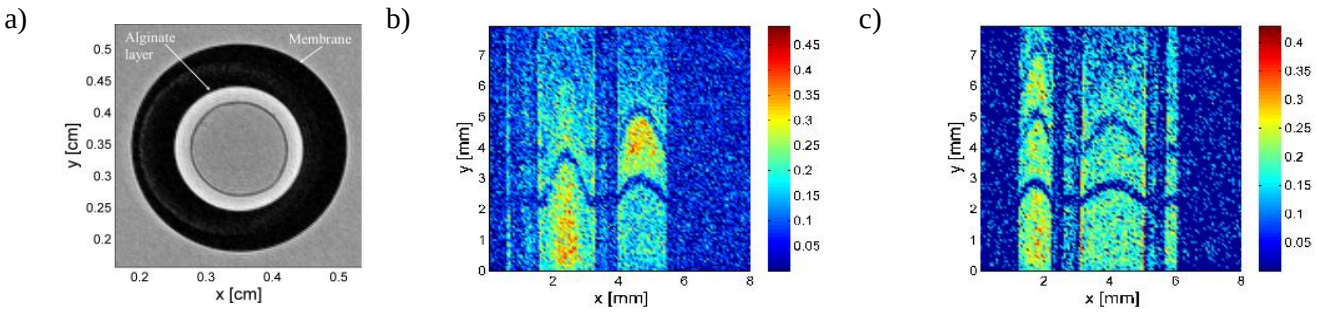

Figure 1 – Axial MSME Image of a fouled membrane after filtration of 200 mg/l sodium alginate solution with addition of 2 mmol/l Ca^{2+} at 100 kPa (a)); sagittal MSME images with saturation stripes in order to illustrate of flow in the ceramic hollow fiber membranes during dead-end filtration of 200 mg/l sodium alginate without (b)) and with (c)) addition of 2 mmol/l Ca^{2+}.

On the one hand MRI reveals the structure of the alginate layers and confirms the conclusion from the evaluation of filtration data, that the addition of Ca^{2+} is leading to the formation of an alginate gel layer on the membrane, whereas in the absence of Ca^{2+}, the structure of the alginate layer is better described by means of concentration polarization, hence more fluid and hydrodynamically better controllable. On the other hand, MRI allows additionally the measurement of flow profiles and hence provide a deeper understanding regarding the role of operating conditions and feed composition on hydrodynamics in the membrane lumen and thereby in the deeper understanding of factors leading to fouling layer formation [4]

References

[1] K. Katsoufidou, S.G. Yiantsios, A.J. Karabelas, An experimental study of UF membrane fouling by humic acid and sodium alginate solutions: the effect of backwashing on flux recovery, Desalination, 220 (2008) 214-227.
[2] Membrane processing dairy and beverage applications, in: A.Y. Tamime (Ed.), Wiley-Blackwell, Chichester, West Sussex ;, 2013.
[3] Y. Ye, P. Le Clech, V. Chen, A.G. Fane, B. Jefferson, Fouling mechanisms of alginate solutions as model extracellular polymeric substances, Desalination, 175 (2005) 7-20.
[4] F. Arndt, U. Roth, H. Nirschl, S. Schütz, G. Guthausen, New insights into sodium alginate fouling of ceramic hollow fiber membranes by NMR imaging, AIChE Journal, (2016) n/a-n/a.

Mass transport in microfluidics: How Flow-MRI can help understand flow phenomena

S. Benders[a], M. Wiese[b], M. Küppers[a], M. Wessling[b,c], B. Blümich[a]

[a]RWTH Aachen University, Institut für Technische und Makromolekulare Chemie, Worringerweg 2, 52074 Aachen, Germany;[b]RWTH Aachen University, Aachener Verfahrenstechnik, Turmstraße 46, 52064 Aachen, Germany;[c]RWTH Aachen University, DWI Leibniz-Institut für interaktive Materialien, Forckenbeckstrasse 50, 52074 Aachen, Germany;

With the help of 3D-printing, reaction vessels with channel dimension from a few to a few hundred micrometers are feasible to manufacture [1,2]. While these systems are characterized by a good surface-to-volume ratio favorable for liquid-wall interaction, mass transport in these vessels is limited by the laminar flow pattern typical for these reactors. By introducing dedicated geometries, flow patterns can be tailored to the needs of the reaction. Characterizing these patterns in an experiment is challenging due to the small channel dimensions and the necessity to determine the three dimensional vector field for full characterization. Magnetic resonance imaging velocimetry (MRI velocimetry) acquires three-dimensional vector fields without requiring special tracer particles which could block the channel. In case of stationary flow, MRI velocimetry can reveal flow patterns in good spatial resolution and accuracy.

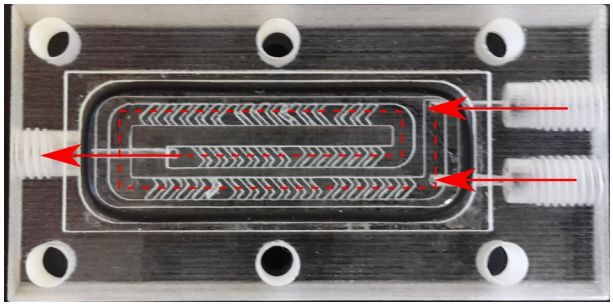

Figure 1 – Microreactor with herringbone structure used in this study

In this study a microfluidic reactor with herringbone structure was examined (Figure 1). It was designed to fit to a 30 mm Bruker Birdcage resonator, which was utilized on an Avance III 300 with a Micro 2.5 gradient system (max. gradient strength 1.5 T/m). The channels were 2 mm wide and 0.5 mm deep with two fluid inlets and one outlet, from which only one inlet was used with water. In the grooves of the herringbones, the channel deepens to 1 mm. This induces movement to the fluid favorable for fluid mixing and liquid-wall interactions. The channels are sealed with a glass plate, which can act as a carrier for solid-state catalysts[3].

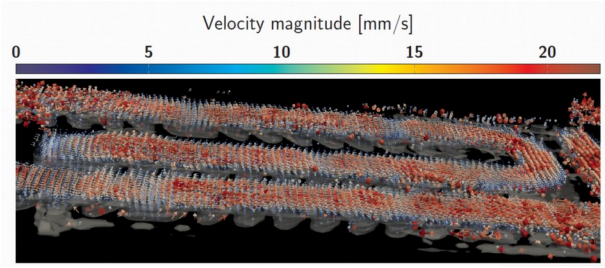

Figure 2 – Three-dimensional velocity vector map

An extension of the Flow Imaging Employing Single Shot Encoding (FLIESSEN) pulse sequence to the third dimension was employed to determine the 3D flow pattern [3,4]. A three-dimensional velocity vector field plot (Figure 2) emphasizes the ability of the herringbone structure to break up the laminar flow pattern. A measure for the interactions of the liquid with the glass plate is the surface shear rate. It can be calculated from three dimensional velocity data using finite differences [3]. For a slice near the glass plate, the induced patterns are clearly visible (Figure 3). This yields an improved liquid-wall interaction favorable for solid-liquid reactions at these positions.

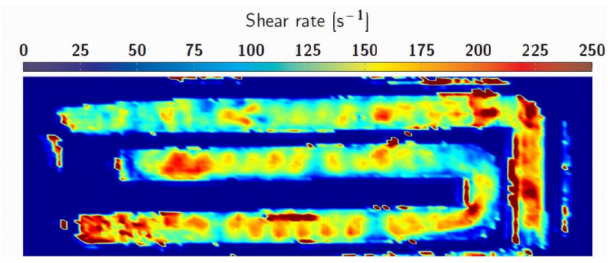

Figure 3 – Surface shear map (near glass plate)

References

[1] J. Kobayashi, Y. Mori, K. Okamoto, R. Akiyama, M. Ueno, T. Kitamori, S. Kobayashi, Science 304 (2004) 1305–1308.
[2] A. Stroock, S. Dertinger, A. Ajdari, I. Mezic, H. Stone, G. Whitesides, Science 295 (2002) 647-651.
[3] M. Wiese, S. Benders, B. Blümich, M. Wessling, *in prep.*
[4] A. Amar, B. Blümich, F. Casanova, ChemPhysChem 11 (2010) 2630-2638

O12

Influence of Fluid Dynamics on Polymerization Kinetics measured by Rheo-NMR

E. Laryea[a], G. Guthausen[b], T. Oerther[c], N. Schuhardt[a], M. Kind[a]

[a]Institute of Thermal Process Engineering, Karlsruher Institute of Technology, 76131 Karlsruhe, Germany; [b] Pro^{2}NMR Institute for Mechanical Process Engineering and Mechanics, Karlsruher Institute of Technology, 76131 Karlsruhe, Germany; [c] Bruker BioSpin GmbH 76287 Rheinstetten, Germany.

Rheo-NMR combines nuclear magnetic resonance (NMR) and magnetic resonance imaging (MRI) respectively velocimetry. On the one hand rheo-NMR offers the possibility to gain information about a fluid on a molecular level, for example about its chemical composition. On the other hand it enables the determination of the fluid flow and deformation – the rheology. Because of that dualism it is possible to figure out relations and dependencies between the fluid dynamics and the chemical composition. The present work introduces a method based on Rheo-NMR, which allows investigations of the influence of fluid dynamics on the kinetics of a polymerization. Such a dependency has already been reported in some manuscripts [1, 2]. However, there is no detailed explanation nor description for the phenomena observed.

For this work, a heatable NMR measuring cell was constructed which corresponds to a Taylor-Couette reactor (TCR). It mainly consists of two concentric cylinders. The inner cylinder rotates and the fluid is placed in the gap between those cylinders. The fluid dynamics inside a TCR can be controlled by its geometry (diameter, gap width, length) and its operational parameters (rotational speed, viscosity of the fluid). It is well-known in literature and can be characterized theoretically by the use of dimensionless numbers. Figure 1 shows the measuring cell. The heating is realised by hot nitrogen gas flowing through small axial channels in the wall of the outer cylinder. For the laboratory experiments, the free radical polymerization of methyl methacrylate (MMA) in xylole initiated by AIBN was used as model system. Rheo-NMR measurements are of particular interest because the rise of the viscosity of the reaction mixture during polymerization causes different flow regimes.

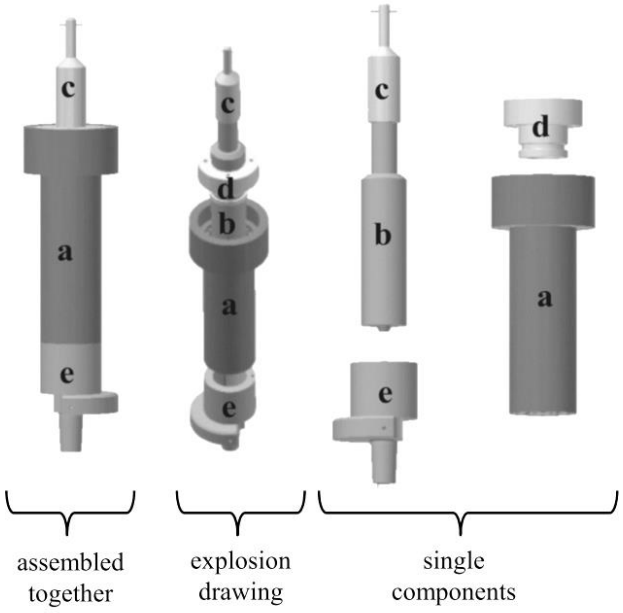

Figure 1 – Design drawing of the Rheo-NMR measuring cell, a) outer cylinder, b) inner cylinder, c) coupling, d) bearing, e) heating adapter

With NMR spectroscopy the evolution of the monomer concentration was determined during polymerization at different rotational speeds. The monomer conversion depends on the rotational speeds for the same reaction time. From these results the rate constants for a global kinetic modeling approach are deduced. Furthermore, velocity profiles of the reactor cross section were measured by MRI. This allows for a determination of the flow regimes and for a comparison respectively validation with data calculated from literature [3]. It is conceivable that the fluid dynamics change the polymer conformation and, thus, the polymerization kinetics. A similar hypothesis is corroborated by Boodhoo et al. [4]. Further experiments are necessary to understand the reason of the dependency shown.

References

[1] M. Vicevic, K. Novakovic, K.V.K. Boodhoo, A.J. Morris, Chemical Engineering Journal 135 (2008) 78–82
[2] A.H. Navarchian, F. Picchioni, L.P.B.M. Janssen, Polymer Engineering & Science 45, (2005) 279–287
[3] Racina and M. Kind Experiments in fluids, 41(3):513–522, 2006
[4] K. Boodhoo, W. Dunk, and R. Jachuck Journal of applied polymer science 85,(2002) 2283–2286

Lithium Ion Diffusion in a Solid Conductor of Amorphous $(Li_2S)_8(P_2S_5)_2$ studied by Pulsed-Gradient Spin-Echo ^{7}Li NMR Spectroscopy

Kikuko Hayamizu[a], **Seitaro Ito**[b],**Yuichi Aihara**[b]

[a]Institute of Applied Physics, University of Tsukuba, Tsukuba 305-8573, Japan; [b]Samsung R&D Institute Japan, Senba-nishi, Minoshi, Osaka 562-0036 Japan;

A sulfide-based solid lithium electrolyte, amorphous $(Li_2S)_8(P_2S_5)_2$ (named 8020A) has large ionic conductivity (σ) and is one of important candidates to use for all-solid lithium rechargeable batteries. A number of lithium ion solid conductors have been proposed, and the origin of the large σ values is supposed to be induced by fast migration of lithium ions. We have measured lithium ion diffusion in the solid electrolytes by pulsed-field spin-echo (PGSE) ^{7}Li NMR [1-4]. It is known that the σ can become larger by crystallization procedure, although the amorphous samples are softer and better to make lithium batteries. The present 8020A has largest σ values at room temperature in the series of amorphous conductors. The ^{7}Li spectra consist of broad and narrow components and were fitted by overlapped two Lorentzian curves. The ratio of the narrow component increased as the temperature increased. The ^{7}Li PGSE NMR method was applied to observe the ^{7}Li ion migration for the narrow component.

With the PGSE NMR experiments, the diffusion coefficient *D* in homogeneous systems can be expressed by

$$E = \exp(-\gamma^2 g^2 \delta^2 D(\Delta - \delta/3)) = \exp(-bD),$$

where *g* is the strength of pulsed-field gradient (PFG) and δ is the duration time of the PFG. Δ is the time interval of the two PFG and determine the observation time. It is known in the porous matters, *D* is dependent on Δ (anomalous diffusion). Previously, we found that the lithium diffusion in the solid conductors depends on the measuring parameters not only Δ but also *g*. As an example, Figure 1 shows the *g*-dependent diffusion of the 8020A at 80 ºC with Δ = 50 ms.

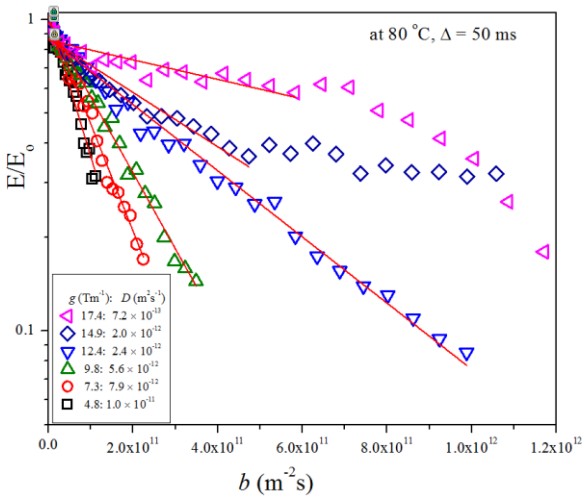

Figure 1. *g*-Dependent diffusion plots at 80 ºC with a fixed Δ = 50 ms for *g* = 4.8 to 17.4 Tm^{-1} (6 points). The plots were measured at a constant *g* with varying δ = 0.2 to 4 ms. The PFG has a good rectangular shape.

The plots with Δ = 50 ms were linear from *g* = 4.8 to 12.4 Tm^{-1} and the apparent diffusion constants ($D_{apparent}$) decreased as the *g*-values became larger (10 to 2.4 × 10^{-12} m^{2}s^{-1} for *g* = 4.8 to 12.4 Tm^{-1}). For the larger *g*-values, only the initial echo decays were linear. Then, we observed diffusion phenomena in most cases at or below *g* = 9.8 Tm^{-1}. The slowly migrating lithium ions were observed by the larger *g* on the same Δ. We observed similar *g*-dependent phenomena between 30 and 120 ºC for Δ = 10 to 100 ms.

For the short Δ, the echo attenuation plots showed diffracted patterns. Generally, the diffusive diffraction can be interpreted by restricted diffusion for particles in a confined space. In the present observations, the diffraction behaviors are irregular, depending on Δ and *g*, and not sensitive to temperature. The present sample contains standing P_2S_5 (anion) and immobile Li_2S. The ^{31}P spectrum showed the co-existence of vibrating and rigid anions. It is not certain how much lithium ions are mobile at every temperature. On the other hand, at any temperature, one definite value of σ can be observed. The apparent diffusion constant observed by the PGSE ^{7}Li NMR method gives us variety of values at a certain temperature. The lithium migration behaviors suggest polydispersities of diffusion depending on observation time and *g*. The ionic conductivity is reflected by the lithium migration in rather long time and distance at equilibrium state. We would like suggest that the quick migration observed in short Δ by the PGSE NMR contributes the efficiency of all-solid lithium batteries.

References

[1] Hayamizu, K.; Aihara, Y. *Solid State Ionics* **2013**, *238*, 1-7.
[2] Hayamizu, K.; Aihara, Y.; Machida, *Solid State Ionics* **2014**, *259*, 59–64.
[3] Hayamizu, K.; Aihara, Y.; Watanabe, T.; Yamada, T.; Ito, S.; Machida, N. *Solid State Ionics* **2016**, *285,* 51-58.
[4] Hayamizu, K; Matsuda, Y.; Matsui, M.; Imanishi, N. *Solid State Nucl. Magn. Reson*. **2015**, *70*, 21-27.

NMR imaging of hydrogenation in micro-scale porous catalyst layers

Vladimir V. Zhivonitko[a,b], Ville-Veikko Telkki[c], Igor V. Koptyug[a,b]

[a]International Tomography Center SB RAS, Institutskaya St. 3A, 630090 Novosibirsk, Russia; [b]Novosibirsk State University, Department of Natural Sciences, Pirogova St. 2, 630090 Novosibirsk, Russia; [c]University of Oulu, NMR Research Unit, Oulu, Finland.

NMR imaging is one of the rare candidates for *in situ* monitoring of physico-chemical processes, since it has versatile and rich toolkit for mass transport visualization. Conventional NMR imaging techniques often suffer from low sensitivity. This is especially crucial for imaging of fluids in small voids like in the case of chemical reactions occuring in a porous catalyst. We show that a substantial sensitivity boost can be achieved by combining remote-detection (RD) NMR and parahydrogen-induced polarization (PHIP), allowing one to visualize mass transport and hydrogenation reaction inside microfluidic packed-bed reactors.[1] This technique provided information about reaction product distribution, mass transport and adsorption effects.

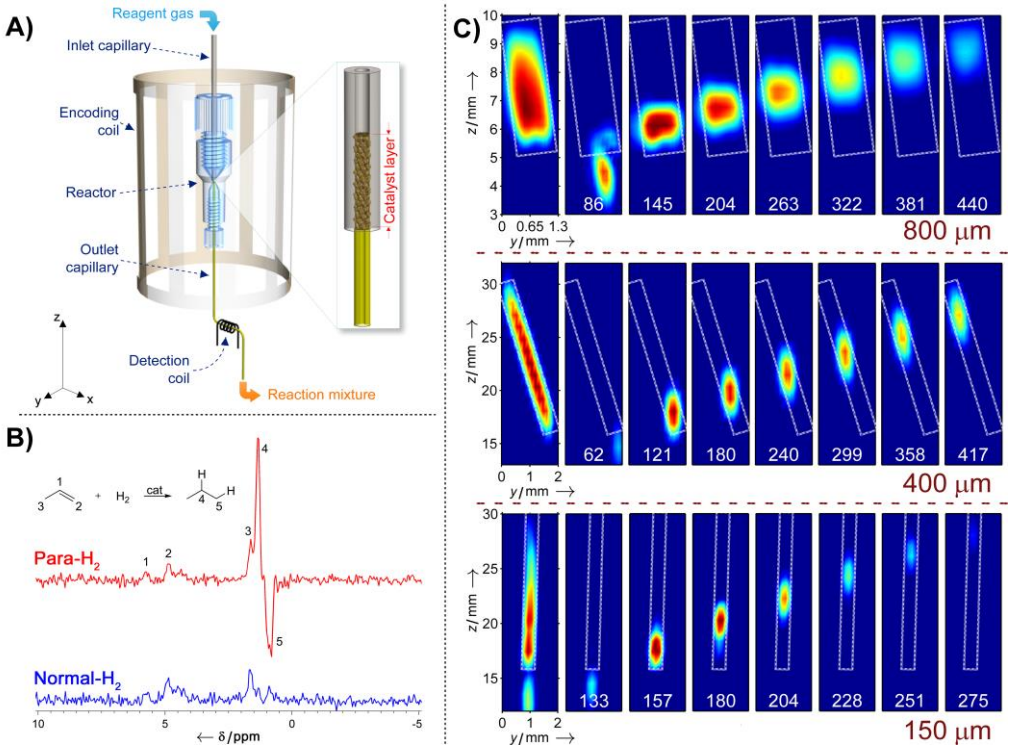

Figure 1 – A) RD NMR setup. A gas mixture of propene and parahydrogen flows through a model reactor with Rh/SiO_2 hydrogenation catalyst layer located inside the encoding coil. The spatial encoding is performed, and the fluid gas flows to the microsolenoid coil. B) ^1H NMR spectra measured with the detection coil for para- and normal hydrogens. C) 2D RD TOF NMR images of hyperpolarized propane flowing inside the reactors. The first image is the time projection. Travel times are indicated in the images in ms.

The reactors were made by using 800, 400 or 150 µm ID tubes (inlet capillaries) connected to outlet 150 µm ID capillary inside a large birdcage encoding RF-coil, Figure 1A. The inlet capillaries were packed with solid porous Rh/SiO_2 catalyst to perform propene hydrogenation with parahydrogen. A small, ultrasensitive solenoid coil wound around the outlet capillary was used for detecting the signal in RD MRI experiments. The comparison of the spectra for produced hyperpolarized and thermally polarized propane in Figure 1B reveals significant signal enhancement (~ 60 times), implying that the use of parahydrogen is crucial in our experiments. Given that the detection coil was 820 times more sensitive than the encoding coil, the overall sensitivity boost provided by PHIP and RD was $60 \times 820 \approx 50\,000$. Such a significant improvement was used in experiments with spatial encoding in one an two dimentions. The 1D experiments were used to extract reaction product distribution along reactor lengths. The RD scheme natuarally provided the time-of-flight (TOF) information about fluid gases in the catalyst layers, allowing mass-transport quantification. The reaction kinetic constants were determined by using measured fluid residence times. Moreover, it was demonstrated that comparison of the flow velocities in the catalyst layers and in the empty outlet capillary can be used to calculate the amount of dynamically adsorbed gases on the catalyst surface. The 2D experiments were used to resolve hyperpolarized propane distribution and fluid gas velocities in the transverse dimension of the reactors, Figure 1C. These data confirmed that, to a good approximation, the fluid flow in the given reactors was plug-like, and all the conclusions made in this assumpltion using 1D RD TOF images are relevant.

The grants 16-33-60198-mol_a_dk, 14-03-93183-MCX-a (RFBR) and 14-13-00445 (RSF) are acknowledged.

References

[1] V. V. Zhivonitko, V.-V. Telkki, I. V. Koptyug, Angew. Chem. Int. Ed. 51 (2012) 8054-8058.

Solid-state and field-cycling NMR relaxometry studies on the dynamics of glass forming liquids and polymers in nanoprous systems

M. Hofmann, Th. Körber, S. Gradmann, B. Hartmann-Azanza,* M. Steinhart,* E.A. Rössler

Experimentalphysik II, Universität Bayreuth, Germany; *) Institut für Chemie, Universität Osnabrück

We present ^{2}H and ^{31}P solid-state as well as ^{1}H field-cycling (FC) NMR investigations of glass forming liquids and polymers in porous media. While solid-state NMR techniques like line-shape analysis and measuring stimulated echo decays provide information on the primary (α-) relaxation determined by the glass transition phenomenon [1], FC NMR probes the slow, polymer-specific relaxation processes [2,3]. In Figure 1(a) the stimulated echo decays of the glass forming liquid tricresyl phosphate in MCM-41 matrices of different pore sizes are shown. Pronounced stretching is observed when the pore radius becomes smaller than 10 nm. The results are explained via a geometrical model which describes the observed broad distribution of correlation times by assuming a radial gradient $\tau(r)$ within the cylindrical pore (cf. Figure 1(b)). As $\tau(r)$ changes with temperature, we were able to introduce the idea of a dynamic correlation length.

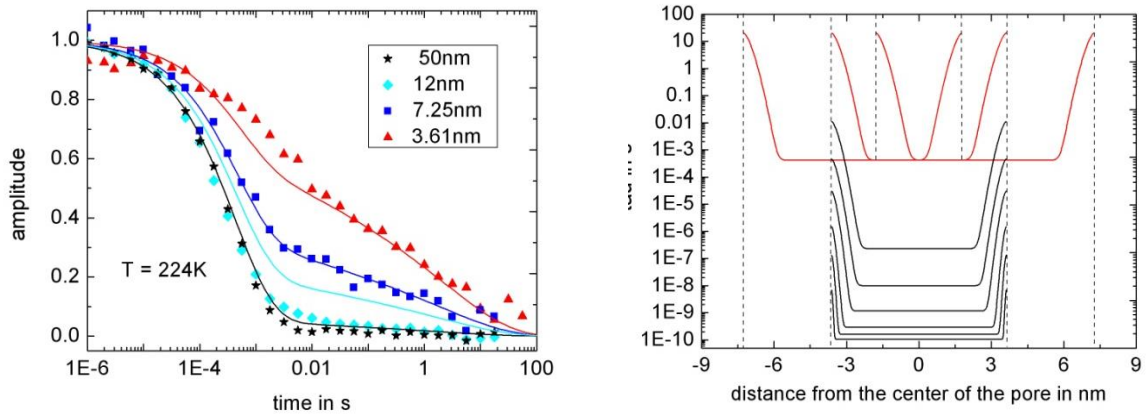

Figure 1 – (a) ^{31}P Stimulated echo decay of tricresyl phosphate in porous material MCM-41; pore radius as indicated (b) Derived correlation time as a function of radius $\tau(r)$ for different pore radii (top) and for different temperatures (bottom).

Next we consider the polymers poly(propylene-alt-ethylene) (PEP, 29 kD)) and polybutadiene [4] which are embedded in anodic Al_2O_3 (AAO) matrices. Collective polymer as well as "local" glassy dynamics are probed by ^{1}H FC NMR relaxometry. Exploiting frequency-temperature superposition master curves can be constructed from experiments done at different temperatures and susceptibility spectra result, which extend over eight decades in frequency (Figure 2a). The corresponding dipolar correlation function for PEP in 15nm pores (with the strongest confinment effect) in comparison to that of bulk PEP are shown in Figure 2(b). While in the "local" (0) and in the Rouse relaxation regime (I) no effects are found, the entanglement (II) and terminal relaxation regime (III,IV) are significantly changed in the pores. Thus, subtle changes are observed for confinment sizes larger even than R_F which estimated as R_F = 15nm.

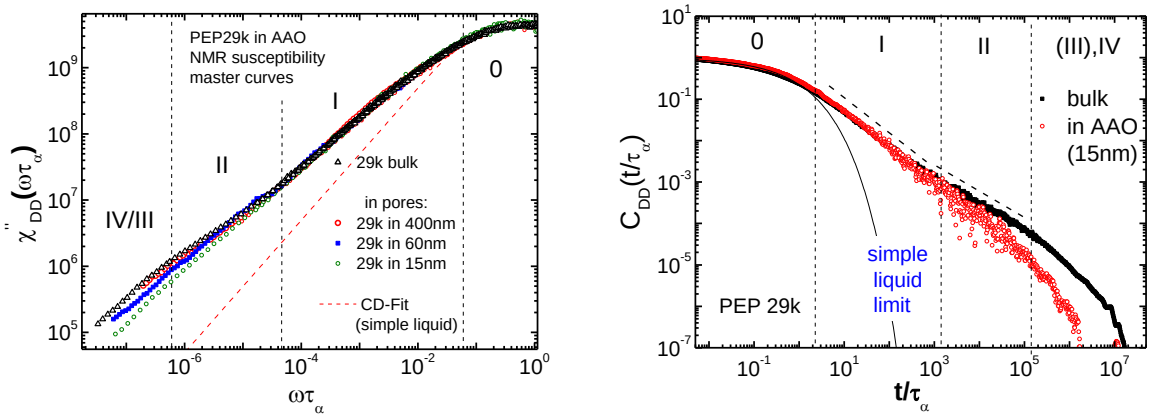

Figure 2 – (a) Susceptibility master curves for PEP in AAO matrices obtained from ^{1}H FC NMR. (b) Corresponding dipolar correlation function.

References

[1] S. Gradmann, P. Medick, E.A. Rössler, J. Phys. Chem. 113 (2009) 8443
[2] D. Kruk, A. Herrmann, E.A. Rössler, Progress in NMR Spectroscopy 63 (2012) 334
[3] R. Meier, D. Kruk, E.A. Rössler, ChemPhysChem 14 (2013) 3071
[4] M. Hofmann, A. Herrmann, S. Ok, C. Franz, D. Kruk, K. Saalwächter, M. Steinhart, E. A. Rössler, Macromolecules 44 (2011) 4017

Ultrafast Laplace NMR of hyperpolarized xenon in CPG materials

O. Mankinen[a], J. Hollenbach[b], S. Ahola[a], J. Matysik[b], V.-V. Telkki[a]

[a]NMR Research Group, P.O. Box 3000, FIN-90014 University of Oulu, Finland; [b]Universität Leipzig, Institut für Analytische Chemie, Leipzig, Germany.

NMR relaxation and diffusion measurements provide detailed information about dynamics and structures of substances such as porous materials. Since relaxation and diffusion data comprise exponentially decaying components, the processing requires a Laplace inversion in order to extract the diffusion coefficient and relaxation time distributions. Thus, these methods are referred to as Laplace NMR (LNMR). [1]

As in traditional NMR, multidimensional approach increases the information content and resolution of LNMR experiments [1]. However, experimental time becomes much longer as compared to one dimensional counterparts, restricting the applicability of these methods in monitoring fast processes. To address this issue, spatial encoding is applied to multidimensional LNMR. This approach enables single-scan acquisition of full multidimensional data, reducing experimental time by orders of magnitude [2, 3]. The price to pay is slightly reduced sensitivity. However, the single-scan approach enables one to use hyperpolarization techniques, improving the sensitivity of experiment by orders of magnitude, and hence opening new horizons in the investigation of dilute samples.

Hyperpolarized ^{129}Xe-NMR is a very powerful tool for the characterization of porous materials and surfaces. Chemical shift of xenon is very sensitive to its local environment and, thus, it can reveal interaction between gas and the sample material [4]. One can also characterize pore size distribution and interconnectivity as well as dynamics of porous systems. Porous media are extremely important in many biological systems and technological applications. Silica based materials such as CPG (Controlled Porous Glasses) can be synthesized so that geometry and pore structure can be well-modelled. Therefore, they are attractive construction materials in various fields of science and technology such as biotechnology and micro-reaction engineering [5].

In this work, we will to combine ultrafast multidimensional Laplace NMR method and hyperpolarization of xenon for the first time in characterization of porous media. With hyperpolarization one is able to increase the sensitivity of the experiment significantly. We will show that the sensitivity boost allows us to investigate dynamics of gases absorbed in porous structures. When successfully completed, the method will open new area of interesting applications such as xenon-biosensors.

References

[1] Y.-Q. Song, J. Magn. Reson. 229, (2013), 12-24.
[2] S. Ahola, V.-V. Telkki, ChemPhysChem, 15, (2014), 1687-1692
[3] S. Ahola, V.V. Zhivonitko, O. Mankinen, G. Zhang, A. M. Kantola, H.-Y. Chen, C. Hilty, I. V. Koptyug, V.-V. Telkki, Nature. Comm. 6, (2015), 8363.
[4] T. Meersmann and E. Brunner, eds., Hyperpolarized Xenon-129 Magnetic Resonance: Concepts, Production, Techniques and Applications, The Royal Society of Chemistry, 2015.
[5] D. Enke, F. Janowski, W. Schwieger, Micropor. Mesopor. Mater. 60, (2003), 19-30.

Noninvasive Relaxometry Evidence of Linear Pore Size Dependence of Water Diffusion in Nanoconfinement

H. Chemmi[a], D. Petit[a,b], P. Levitz[c], R. Denoyel[d], A. Galarneau[e], J.-P. Korb[a]

[a]Physique de la Matière Condensée, Ecole Polytechnique, CNRS-UMR 7643, 91128 Palaiseau, France; [b]Laboratoire Charles Coulomb, Université de Montpellier, CNRS-UMR 5221, Place Eugène Bataillon, 34095 Montpellier Cedex 5, France; [c]Physicochimie des Electrolytes et Nanosystèmes Interfaciaux, Université Pierre et Marie Curie, CNRS-UMR 8234, 4 place Jussieu, 72522 Paris Cedex 5, France; [d]MADIREL, Université Aix-Marseille, CNRS-UMR 7246, Centre de St Jérôme, 13397 Marseille Cedex 20, France; [e]Institut Charles Gerhardt Montpellier, UMR 5253 CNRS-UM-ENSCM, ENSCM, 8 rue de l'Ecole Normale, 34296, Montpellier Cedex 05, France.

We propose an original experimental method based on NMR at variable magnetic fields experiments (NMRD) and a theoretical analysis of the data that allows probing the spatial dependence of the diffusion coefficient of liquids specifically at proximity to pore surfaces. One of the key results found from these experiments is the linear relationship between average parallel diffusion coefficients and pore radii [1]. Another result is the robustness of the frequency scaling [1, 2, 3, 4] of the master curve approach able to take into account the complexity of the water dynamics at pore surface for samples of different geometries. This approach has proven useful for evaluating the efficiency of the coupling between liquid layers within nanopore by extracting gradients of diffusion coefficients.

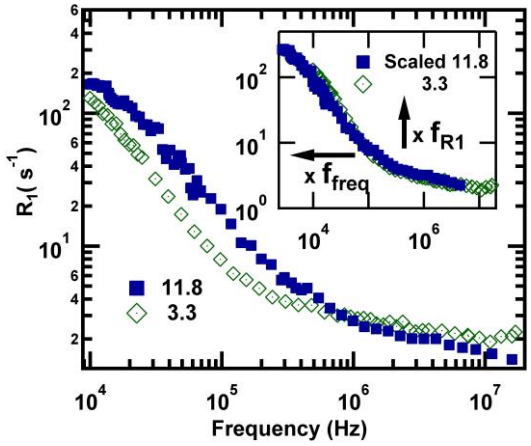

Figure 1 ^{1}H NMRD profiles of MCM-41 saturated samples with 3.3 nm (diamond) and 11.8 nm (square) pore diameters (main figure). In inset, the master curve obtained by scaling both relaxation rate and frequency by the factors f_{R1} = 1.6 and f_{freq} = 3.3/11.8, respectively is superposed to the MCM-41 of 11.8 nm pore diameter.

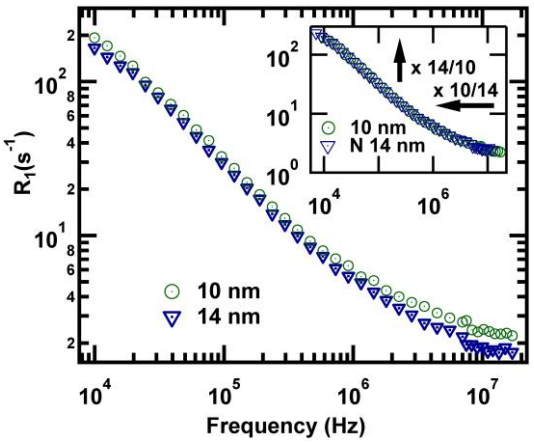

Figure 2 ^{1}H NMRD profiles of SEOS saturated samples with 10 nm (circle) and 14 nm (triangle) cavities diameters (main figure). In inset, the master curve obtained by scaling both relaxation rate and frequency by the factors f_{R1} = 14/10 and f_{freq} = 1/f_{R1}, respectively, is superposed to the SEOS of 14 nm cavity diameter.

The application of this method to water confined in synthesized calibrated nanopores like MCM-41 for cylindrical geometry [5] and SEOS for spherical geometry [6] has been successful to deal with several dynamical processes on pore surface for different materials. This shows the ability of the proposed method to discriminate between the influence of the geometrical confinement on intrapore dynamics and the chemistry of the interface induced by different synthesis of the materials. For instance, the frequency selectivity of NMRD profiles has been able to separate the different couplings coming from the spatial heterogeneities on the pore surfaces [1, 2]. This frequency selectivity of NMRD has also allowed discriminating several steps of a complex dynamics process composed by both loops in water and surface diffusion during adsorption events [7, 8, 9]. Based on our experimental and theoretical results, we believe that the proposed noninvasive method allows exploring the interplay between molecular and continuous description of fluid dynamics relevant in physical and biological confinements.

References

[1] H. Chemmi, D. Petit, P. Levitz, R. Denoyel, A. Galarneau, J.-P. Korb, J. Phys. Chem. Lett. 7 (2016) 393−398.
[2] H. Chemmi, Diffusion Multi-Echelle et Sorption Hydrique dans les Matériaux Cimentaires. PhD thesis, Ecole Polytechnique, Palaiseau, Fr., 2011.
[3] H. Chemmi, D. Petit, J.-P. Korb, R. Denoyel, P. Levitz, Micro. and Meso. Mater. 178 (2013) 104-107.
[4] H. Chemmi, D. Petit, V. Tariel, J.-P. Korb, R. Denoyel, R. Bouchet, P. Levitz, Eur. Phys. J. Special Topics 224 (2015) 1749-1768.
[5] B. Coasne, A. Galarneau, F. Di Renzo, R. J. M. Pellenq, Langmuir 22 (2006) 11097-11105.
[6] E. Bloch, T. Phan, D. Bertin, P. Llewellyn, V. Hornebecq, Micro. and Meso. Mater. 112 (2008) 612-620.
[7] P. Levitz, J.-P. Korb, D. Petit, Eur. Phys. J. E 12, 1 (2003) 29-33.
[8] P. Levitz, J.-P. Korb, Europhys. Lett. 70, 5 (2005) 684-689.
[9] J.-P. Korb, P.E. Levitz, AIP Conf. Proc. 1081 (2008) 55-58.

Diffusion MRI/NMR at high gradients: challenges and perspectives

D. S. Grebenkov[a]

[a]Laboratoire de Physique de la Matière Condensée, CNRS – Ecole Polytechnique, F-91128 Palaiseau, France ; Email : denis.grebenkov@polytechnique.edu

Diffusion magnetic resonance imaging (dMRI) is a broadly applied non-invasive technique to study structural properties of porous media such as sedimentary rocks or cements, as well as anatomical, physiological, and functional properties of biological tissues such as brain, skin, lungs, and bones [1-4]. A reliable interpretation of dMRI signals in biomedical applications requires accounting for water exchange across semi-permeable membranes that separate cells from the extra-cellular space. Although numerous works have been devoted to water exchange across membranes [5,6], estimation of permeability by NMR methods remains a challenging and controversial topic. Conventionally, the dMRI signal is measured at relatively small diffusion-encoding gradients (or b-values), from which an apparent diffusion coefficient can be extracted and then related to the permeability. This perturbative approach is known to fail at high gradients, so that many phenomenological models have been proposed to partly remedy this failure and to get simple fitting formulas for the dMRI signal. While these models are often successful in fitting experimental data on a broad range of gradients, none of them has addressed the theoretical question how the dMRI signal is indeed modified at high gradients.

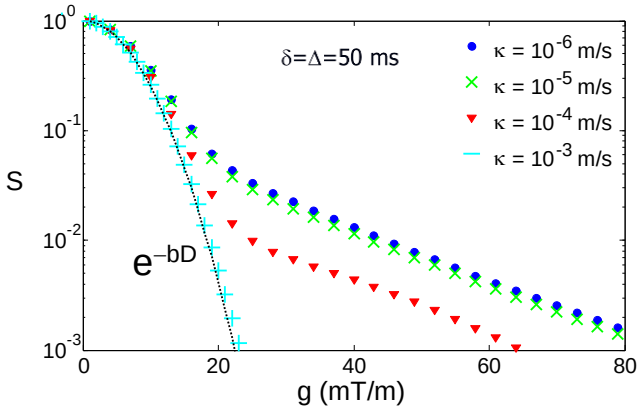

Figure 1 – PGSE signal as a function of the gradient g for an isolated slab of width 200 μm containing a semi-permeable membrane in the middle. The water diffusion coefficient is $D=2.3\cdot10^{-9}$ m^2/s, and four values of permeability κ are used. The contribution of exterior borders is removed by computing the signal in the middle of the slab. Black dotted line shows the PGSE signal for unrestricted diffusion.

In order to understand the physical mechanism of the dMRI signal formation at high gradients, we developed a non-perturbative approach to solve the Bloch-Torrey equation describing the evolution of the transverse magnetization for one-dimensional diffusion across multiple semi-permeable barriers [7]. The obtained analytical solution generalizes the seminal work by Stoller, Happer, and Dyson [8], in which the non-Gaussian stretched-exponential behavior of the pulsed-gradient spin-echo (PGSE) signal was predicted at high gradients in the so-called localization regime. Based on this solution, we investigate how the diffusive exchange across a semi-permeable barrier modifies this asymptotic behavior, and explore the transition between the localization regime at low permeability and the Gaussian regime at high permeability. High gradients are suitable to spatially localize the contribution of the nuclei near the barrier and to enhance the sensitivity of the PGSE signal to the permeability κ. For instance, the ratio between two PGSE signals formed by the nuclei diffusing near weakly-permeable (κ>0) and impermeable (κ=0) membranes is shown to be $\exp(-1.7\,\kappa\,(\gamma g/D)^{1/3}\,\delta)$, where γ is the gyromagnetic ratio, g the gradient, D the diffusion coefficient, and δ the gradient pulse duration. New physical features and potential perspectives of the non-Gaussian behavior are explored. The emergence of the localization regime in two- and three-dimensional domains is discussed and illustrated through numerical simulations.

References

[1] D. Le Bihan, H. Johansen-Berg, NeuroImage **61** (2012) 324-341.
[2] S. B. Fain, F. R. Korosec, J. H. Holmes, R. O'Halloran, R. L. Sorkness, T. M. Grist, J. Magn. Reson. Imag. **25** (2007) 910-923.
[3] F. W. Wehrli, H. K. Song, P. K. Saha, A. C. Wright, NMR Biomed. **19** (2006) 731-764.
[4] D. S. Grebenkov, Rev. Mod. Phys. **79** (2007) 1077-1161.
[5] C. R. House, *Water Transport in Cells and Tissues* (Edward Arnold, Ltd., London, UK, 1974).
[6] D. S. Grebenkov, D. V. Nguyen, J.-R. Li, J. Magn. Reson. **248** (2014) 153-163.
[7] D. S. Grebenkov, J. Mang. Reson. **248** (2014) 164-176.
[8] S. D. Stoller, W. Happer, and F. J. Dyson, Phys. Rev. A **44** (1991) 7459.

Multidimensional correlation of nuclear relaxation and diffusion tensor size, shape, and orientation

J. P. de Almeida Martins[a], D. Topgaard[a]
[a]Division of Physical Chemistry, Department of Chemistry, Lund University, Lund, Sweden.

Despite their usefulness in the study of porous materials, classical diffusion NMR techniques yield ambiguous results when the sample comprises multiple regions with different pore sizes, shapes, and orientations. Such ambiguities stem from the fact that those experiments are based on the Stejskal-Tanner sequence, a method where the effects of the aforementioned properties are intrinsically entangled. The separation of contributions from the various types of water environments have thus been made by fitting mathematical models of increasing complexity to the acquired data. However, selection of a single model from all the ones that are able to reproduce the data is typically challenging [1].

Here, we present a novel experimental protocol designed to resolve distinct microscopic water populations. In our approach, the heterogeneity of a given material is characterized via the individual values of isotropic diffusivity D_{iso}, diffusion anisotropy D_Δ, orientation of the diffusion tensor (θ,ϕ), and relaxation rates R_1 and R_2, of different microscopic environments. Fig. 1(a) displays a pulse sequence that encodes the NMR signal for both diffusion and nuclear relaxation. Said sequence gives access to a 6D sampling space defined by the echo τ_e, and repetition τ_R, times, and the magnitude b, anisotropy b_Δ [2], and orientation (Θ,Φ), of the diffusion-encoding tensor. In the suggested NMR method, the full 6D space (τ_R,τ_e,b,b_Δ,Θ,Φ) is pseudo-randomly sampled (See Fig. 1(b)), thus enabling the estimation of 6D correlations between the diffusion tensor parameters (D_{iso},D_Δ,θ,ϕ) and the relaxation rates R_1 and R_2. Within the diffusion tensor formalism, such acquisition scheme allows us to write the measured signal amplitude as

$$S(\tau_R,\tau_e,b,b_\Delta,\Theta,\Phi) = S_0 \int_0^\infty\int_0^\infty\int_0^\infty\int_{-1/2}^{1}\int_0^{\pi}\int_0^{2\pi} K(\tau_R,\tau_e,b,b_\Delta,\Theta,\Phi,R_1,R_2,D_{iso},D_\Delta,\theta,\phi) \times P(R_1,R_2,D_{iso},D_\Delta,\theta,\phi)\,\mathrm{d}\phi\sin\theta\,\mathrm{d}\theta\,\mathrm{d}D_\Delta\mathrm{d}D_{iso}\,\mathrm{d}R_2\mathrm{d}R_1,$$

where $P(R_1,R_2,D_{iso},D_\Delta,\theta,\phi)$ is the 6D probability distribution that characterizes the material's heterogeneity, and $K(\ldots)$ denotes a twelve-dimensional kernel that weights the effects of each one of the experimental parameters on the signal-decay, thus mapping $P(R_1,R_2,D_{iso},D_\Delta,\theta,\phi)$ into $S(\tau_R,\tau_e,b,b_\Delta,\Theta,\Phi)$. Making use of a data inversion algorithm based on the one used in ref. [3], the distribution $P(R_1,R_2,D_{iso},D_\Delta,\theta,\phi)$ is retrieved in a model-free fashion, and the different values of R_1 and R_2, as well as the parameters (D_{iso},D_Δ,θ,ϕ) of the assumedly axisymmetric microscopic diffusion tensors, are determined and reported as correlation maps. All the presented methods are experimentally validated on materials with known diffusion properties.

Since the typical MRI voxel comprises multiple microscopic domains with varying chemical and diffusion properties, the presented method shows great potential for *in vivo* studies of the human brain. In particular, through the imposition of physiologically reasonable constraints, we expect that our protocol can serve as a basis for experiments capable of determining the composition of a voxel in terms of tissue and cell types.

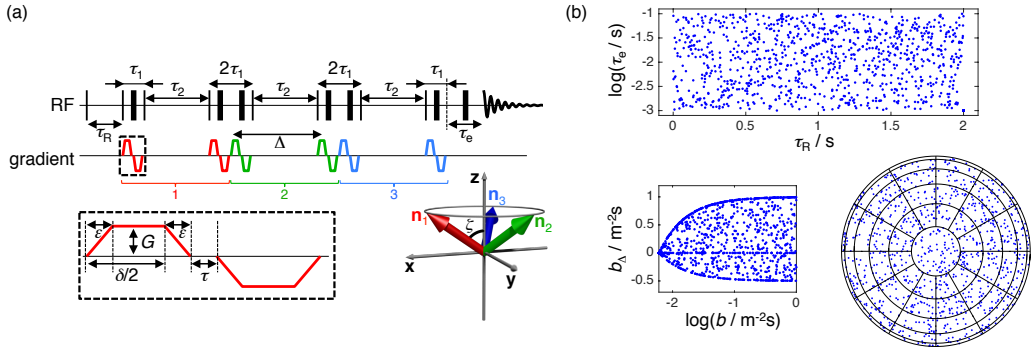

Figure 1 – (a) NMR pulse sequence for encoding diffusion and nuclear relaxation effects. The thin vertical lines denote $90°_x$ RF pulse while the thick vertical lines represent $180°_y$ pulses. The bottom right panel illustrates the unit vectors (n_1,n_2,n_3) of the three sets of gradient pulses which allow for isotropic and anisotropic diffusion encoding. The dashed box shows a magnification of the first bipolar gradient pulse. (Adapted from ref. [4]). **(b)** Pseudo-random data sampling strategy for 6D correlation of (R_1,R_2,D_{iso},D_Δ,θ,ϕ). The bottom right panel displays the orientation distribution (Θ,Φ) of the b-values as an azimuthal projection of a sphere.

References

[1] M. Nilsson, D. van Westen, F. Ståhlberg, P. C. Sundgren, and J. Lätt, Magnetic Resonance Materials in Physics, Biology, and Medicine 26, 345 (2013).

[2] S. Eriksson, S. Lasic, M. Nilsson, C.-F. Westin, and D. Topgaard, J. Chem. Phys. 142, 104201 (2015).

[3] J. P. de Almeida Martins, D. Topgaard, Phys. Rev. Lett. 116, 087601 (2016).

[4] D. Topgaard, Microporous Mesoporous Mater. 205, 48 (2015).

Single-file diffusion of gas mixtures by high field diffusion NMR

A. R. Dutta,[a] P. Sekar,[a] M. Dvoyashkin,[b] C. R. Bowers,[b] K. J. Ziegler,[a] S. Vasenkov [a]

[a]Univ. of Florida, Dept. of Chem. Engineering, Gainesville, FL 32611, USA; [b]Univ. of Florida, Dept. of Chemistry, Gainesville, FL 32611, USA.

Single-file diffusion (SFD) is diffusion in one dimension inside non-intersecting channels so narrow that they forbid mutual passage of molecules. While normal diffusion shows a linear dependence of mean square displacement (MSD) on diffusion time, for sufficiently long channels with negligible boundary effects at their edges, SFD can be distinguished by its MSD growth with the square root of time

$$\left\langle z^2(t)\right\rangle = 2Ft^{0.5}, \qquad (1)$$

where F is the SFD mobility. This distinctive difference is manifested in the reduced growth of MSD over time for SFD relative to normal diffusion. The potential use of this property in highly-selective separations and controlled catalysis provides motivation for studies of SFD in mixtures containing different types of molecules. We had recently reported experimental observation of SFD of a molecular mixture for the first time [1]. In the present work, SFD of CO/CH_4 and CO/CO_2 mixtures as well as of the corresponding pure gases in L-Ala-L-Val (AV) channels was investigated by pulsed field gradient (PFG) NMR technique using the combined advantages of high magnetic field (17.6 T) and large magnetic field gradients (up to 30 T/m). The diffusion studies were performed at 298 K for a broad range of diffusion times, which allowed for verification of the time scaling of the MSD for single-file diffusion (Figure 1).

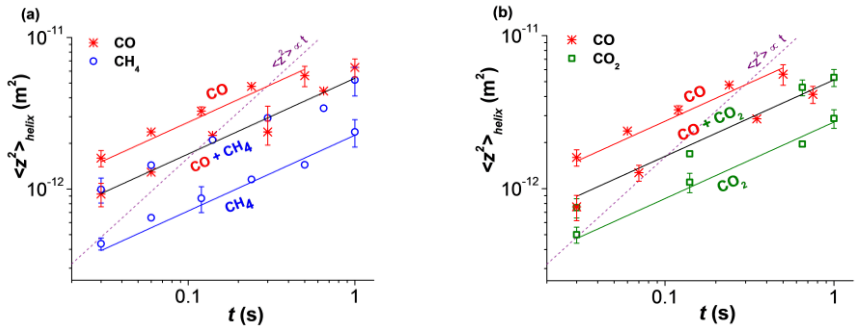

Figure 1 – Time dependence of the MSD for two-component gas mixtures and the coresponding pure gases in AV channels at 298 K. The MSD reported here accounts for the helical topology of the channels. Solid lines are best-fits to the measured time dependences of the MSD to Eq. 1.

In agreement with the expectation of the exclusion of mutual molecular passages, the SFD mobilities of the individual gas components in the gas mixture samples were found to be identical. These mixture SFD mobilities were observed to be larger than the smallest SFD mobilities of the corresponding slowest individual components at comparable total molecular concentrations in the channels and identical temperature (Table 1). This finding deviates from the observation often made for normal diffusion where the addition of a faster-diffusing component does not significantly change the diffusivity of a slower-diffusing component in microporous channels.

Table 1. SFD mobilities in AV channels at 298 K obtained from the measured PFG NMR data.

	Mixtures		Single-Sorbate Samples		
	$CO + CH_4$	$CO + CO_2$	CO	CH_4	CO_2
$F\times10^{14}$ ($m^2\ s^{-1/2}$)	3.1 ± 0.2	2.5 ± 0.2	4.6 ± 0.4	0.8 ± 0.06	1.5 ± 0.1

Molecular clustering in the studied single-file channels is proposed to reconcile the experimental SFD data with the random walk model, which predicts a transition from the SFD mechanism to the mechanism of the center-of-mass diffusion (COM) at sufficiently large diffusion times [2,3]. COM is characterized by concerted movements of all molecules in each channel, resulting in a linear growth of the MSD with time. Although predicted by the model to occur within our experimental conditions, the transition from SFD to COM was not observed experimentally, and its absence can be attributed to clustering. Molecular clustering may also contribute to the observed relationship between the SFD mobilities for the mixtures and the corresponding one-component sorbates. Our data suggest that pure CO forms larger clusters than the CO/CH_4 and CO/CO_2 mixtures in AV nanochannels. This is consistent with the stronger dipole-dipole interactions in pure CO and weaker dipole-induced dipole interactions that are introduced in mixtures of CO with CH_4 or CO_2.

References

[1] A. R. Dutta, P. Sekar, M. Dvoyashkin, C. R. Bowers, K.J. Ziegler, S. Vasenkov, Chem. Commun. 51 (2015) 13346-13349.
[2] K. Hahn, J. Kärger, J. Phys. Chem. 102 (1998) 5766-5771.
[3] P. H. Nelson, S. M. Auerbach. Chem. Eng. J. 74 (1999) 43-56.

Understanding Deactivation in Porous Catalysts Using NMR Diffusion Techniques

C. D'Agostino[a], Y. Ryabenkova[b], G. J. Hutchings[b], M. D. Mantle[a], L. F. Gladden[a]

[a]Dept of Chemical Engineering and Biotechnology, University of Cambridge, Cambridge, CB2 3RA, United Kingdom; [b]Cardiff Catalysis Institute, Cardiff University, Cardiff, CF10 3AT, United Kingdom.

Catalyst deactivation is an issue of paramount importance in order to make a catalytic process viable. This is particularly the case for highly porous heterogeneous catalysts. The loss of activity in such materials may be due to a number of different reasons, for example, the active sites of the catalyst within the pore space may be covered by coke or organic material. Moreover, the pores and channels of the catalyst may become partially or completely blocked due to changes in catalyst porosity, sintering of crystallites and/or deposition of other external material [1]. These changes in structural properties may also prevent the diffusing reactants from reaching the active sites with a consequent decrease of reaction rate [2].

In the current work we have investigated the deactivation of a highly porous bimetallic AuPt/C catalyst for the aerobic liquid-phase oxidation of 1,2-propanediol to lactic acid under mild conditions, an important reaction in sustainable chemistry. The catalyst showed good activity and selectivity but exhibited significant deactivation, thereby limiting its reusability. Therefore, we have investigated the deactivation process of this catalyst with several techniques including N_2 adsorption, temperature-programmed oxidation (TPO) and Pulsed-Field Gradient (PFG) NMR diffusion measurements.

Figure 1 shows a typical PFG NMR log attenuation plot of the system under investigation, which indicates the presence of three diffusion components: one is assigned to the free diffusion of the bulk liquid surrounding the catalyst particles; a second component is due to guest molecules diffusing inside the mesopores of the catalyst; a third component, with much lower values of diffusivity, is assigned to molecules diffusing in the micropores. In such pores the size of the diffusing species becomes comparable with the pore size, hence a very slow diffusion is observed.

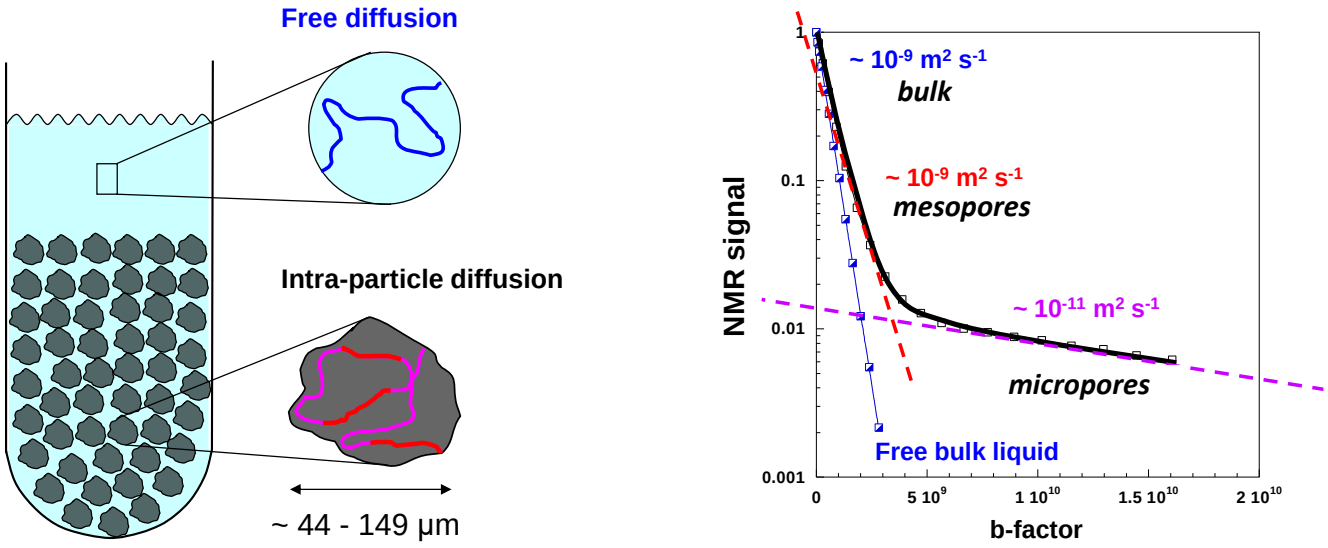

Figure 1 – Typical sample (left) and corresponding PFG NMR diffusion plot (right). Three diffusion components are observed (non-linear plot) within the system, one due to the free liquid and two associated to the intra-particle space of the catalyst (meso and micropores). The experimental plot of the free bulk liquid is shown as a reference.

Table 1 shows the results from N_2 adsorption analysis together with data on conversion and diffusivity in the micropores. It is clear that a dramatic decrease of surface area and pore volume is observed after each cycle of reaction.

Table 1. Surface area, pore volume, conversion and micropore diffusivity in fresh and reused catalyst samples.

Sample	Surface area [$m^2\ g^{-1}$]	Pore volume [$cm^3\ g^{-1}$]	Conversion [%]	Diffusivity [$m^2\ s^{-1}$]
AuPt/C fresh	1305	0.95	97	5.63×10^{-11}
AuPt/C 1st run	910	0.56	83	3.40×10^{-11}
AuPt/C 4th run	628	0.38	31	2.30×10^{-11}

The results reveal that a decrease in catalyst porosity affects the diffusion within the microporous region, hence some catalyst sites become inaccessible. Using the values of diffusivity for the reagent we have also estimated the Weiz-Prater number, which revealed the presence of diffusion limitations within the microporous space. This work shows that combining NMR diffusion techniques with more traditional methods can yield new insights into catalyst deactivation mechanisms.

References

[1] M. H. Haider, C. D'Agostino, N. F. Dummer, M. D. Mantle, L. F. Gladden, D. W. Knight, D. J. Willock, D. J. Morgan, S. H. Taylor, G. J. Hutchings, Chemistry - A European Journal. 20 (2014) 1743–1752.
[2] J. Wood, L. F. Gladden, Applied Catalysis A: General. 249 (2003) 241–253.

Marginal distributions constrained optimization (MADCO) used to accelerate 2D MRI relaxometry

D. Benjamini, P. J. Basser
Quantitative Imaging and Tissue Sciences, NICHD, National Institutes of Health, Bethesda, MD 20892, USA

Introduction: Multidimensional NMR experiments allow us to study correlations between relaxation properties, such as T_1 and T_2 and physical parameters, such as the diffusivity (D). In the 2D case, when the kernels have an exponential form, application of a 2D inverse Laplace transform (ILT), which is a classic ill-conditioned problem, is required. The most common and efficient 2D-ILT algorithm [1] is typically used in 2D relaxometry experiments that involve a CPMG acquisition, which results in high-density sampling of the signal decay. Although multidimensional diffusion/relaxation experiments have been of great interest in recent years, preclinical and clinical applications remain infeasible. In high-field MRI scanners, specific absorption rate limits the use of multi-echo or CPMG pulse trains, and the large amounts of data required cannot be collected in *in vivo* experiments due to long scan times. The goal of this work is to vastly reduce the number of acquisitions required for an accurate 2D diffusion/relaxation spectrum reconstruction. Recently, a strategy was introduced that used the marginal 1D distributions of the desired 2D function as equality constraints [2] to stabilize and reduce the number of acquisitions. Here we apply the concept of marginal distributions constrained optimization (MADCO) to multidimensional NMR experiments.
Methods: Although the method is equally applicable to other types of multidimensional experiments, we chose to demonstrate it on a *D-T₁* polyvinylpyrrolidone (PVP) water solution phantom. Doped water and PVP were used to create a 3-peaks MRI phantom. Two purified water samples with 0.18 mM and 0.5 mM gadopentetate dimeglumine were prepared, along with a 20% w/v PVP water solution sample. The corresponding relaxation times and diffusivities (T_1,D), as measured separately for each sample (referred to as ground truth, Fig. 1A). MRI data were acquired on a 7 T Bruker wide-bore vertical magnet with an inversion recovery DW EPI sequence. The full 2D experimental set had 40 diffusion gradient linear steps, and 37 inversion times (τ) with logarithmic spacing. A single 5 mm axial slice with a matrix size and resolution of 64x64 and 0.2x0.2 mm, respectively, acquired with 2 averages and 4 segments. For *D-T₁* measurements, for a given recovery time the fully recovered data are subtracted from the data, and the signal attenuation can be expressed as:

$$M(\tau, b) = \sum_{n=1}^{N_{T1}} \sum_{m=1}^{N_D} \mathbf{F}(T_{1,n}, D_m) \exp(-\frac{\tau}{T_{1,n}}) \exp(-bD_m) \qquad (1)$$

In this work we suggest a simple way to stabilize the estimation of $F(T_1,D)$ in Eq. 1, while significantly reducing the number of required acquisitions and improving accuracy, by constraining the solution according to the following relations:

$$\sum_{n=1}^{N_D} \mathbf{F}(T_1, D_n) = F(T_1) \quad and \quad \sum_{n=1}^{N_{T1}} \mathbf{F}(T_{1,n}, D) = F(D) \qquad (2)$$

These marginal distributions can be separately estimated from 1D experiments, which require an order of magnitude less data than a conventional 2D acquisition.
Results and Discussion: The performance of MADCO was determined and compared with the conventional method by estimating the *D-T₁* distribution by using 500 random subsamples from the full data at 19 logarithmically distributed acquisitions, from 7 to 1480. 2D distributions and their 1D projections obtained from MADCO and conventional analyses of the signal using 7 and 1480 acquisitions, respectively, are shown in Figs. 1 B and C. Purposely oversampled, the full acquisition scan time in the 2D experiment was ~37 h. As shown, the *D-T₁* distribution estimated with the conventional method was far from accurate, even when the full data set was used (Fig. 2C). Conversely, applying the proposed method led to very good agreement with the ground truth distribution, even when only 7 randomly sampled data points were used (Fig. 2B). This immense improvement in accuracy and efficiency translates to a reduction in the required 2D scan time from 37 h to 10 min.

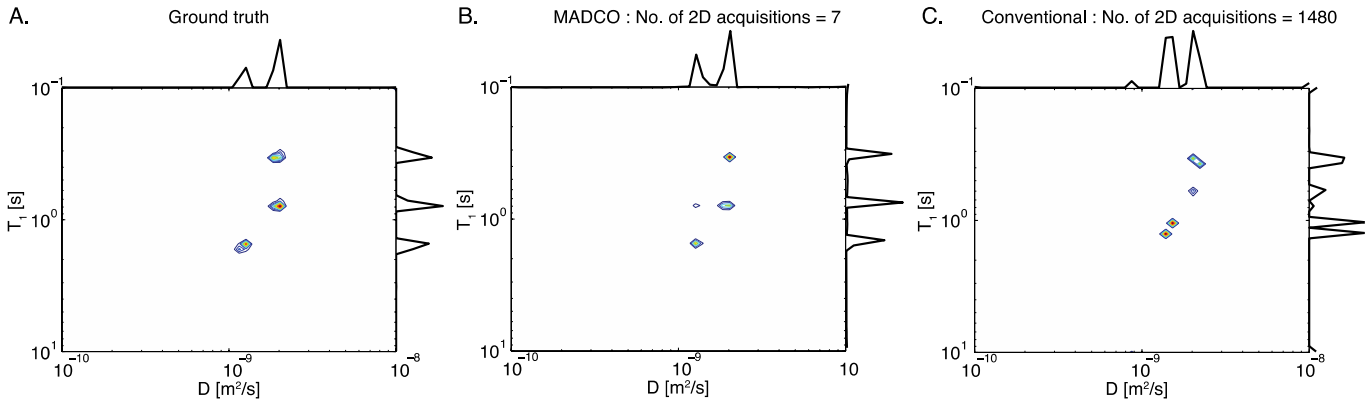

Figure 1 – *D-T₁* distributions. (A) Ground truth, estimated using (B) MADCO with 7 acquisitions, and (C) conventional using 1480 acquisitions.

Conclusion: The potential impact of this work is directed towards preclinical and clinical applications, where it would allow a comprehensive investigation in a reasonable time frame by using the MADCO method in conjunction with a variety of 2D MRI experiments. Furthermore, our work may be extended beyond 2D, since application of the marginal distributions constrained optimization principle in higher dimensions enables the main limitation of experimental time to be lifted.

References

[1] Y.-Q. Song et al., J. Mag. Res. 154 (2002) 261–268.
[2] D. Benjamini and P. J. Basser, J. Chem. Phys. 141 (2014) 214202.

Magnetic Resonance Imaging with a Variable Field Superconducting Magnet that can be rotated for Vertical or Horizontal Operation

B. Balcom[a]

[a]Department of Physics, University of New Brunswick. 8 Bailey Drive, Fredericton, New Brunswick, Canada.

We have recently installed a horizontal bore superconducting magnet that is maintained in a superconducting state by active cooling, rather than through conventional cryogens. The magnet is permanently connected to its power supply which means it is facile to change the static magnetic field to suit a particular sample or experimental study. It is not however a field cycling magnet. The magnet is dramatiaclly smaller and lighter than conventional superconducting magnets given the lack of cryogens. This means it is feasible to rotate the magnet on a cradle for vertical or horizontal sample access and sample orientation.

Our initial experience with this magnet, including heteronuclear studies with varaible field but constant frequency RF probe will be described, as will our experience with rotating the magnet for vertical and horizontal bore operation. Variable field operation is very advantageous for samples with susceptibility driven inhomogenous broadening since one can readily control the experimental line width [1].

References

[1] Chen, Q., Marble, A.E., Colpitts, B.G. and Balcom, B.J. *Journal of Magnetic Resonance* (2005) 175, 300-308.

A new downhole MRI tool

W. Liu[a], L. Xiao[a], X. Li[b], S. Luo[a]

[a]State Key Laboratory of Petroleum Resources and Prospecting, China University of Petroleum, Beijing, China; [b]Sinopec Research Institute of Petroleum Engineering, Beijing, China.

Traditional NMR logging instruments can not distinguish the formation pore fliud properties of the circumferential borehole. This paper describes a new downhole circumferential partitional MRI tool to measurement formation pore fliud properties of the vertical apertures and circumferential apertures. The principle of circumferential partitional MRI changes original model that detection area is single in azimuthal aperture into circumferential partitional measurement.

The new MRI tool includes sensor, electronics and capacitor cartridge. The magnetic field distribution of different direction is shown in Fig.1, and array antenna can respectively excite one-eighth of its aperture. 40 sensitive volumes from 8 circumferential partitions and 5 radial depths can be obtained in this way.

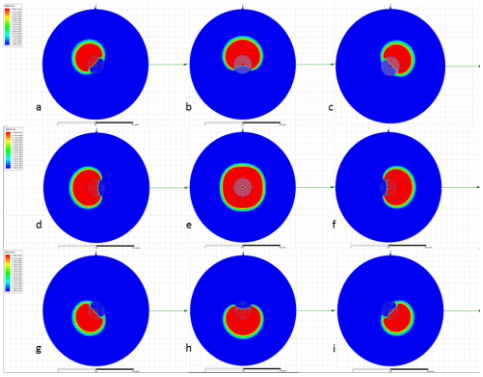

Figure 1 – The magnetic field distribution of different direction

For the sensor characteristics of downhole circumferential partitional MRI tool, electronic cartridge control array antenna to transmit high power pulse sequence and receive echo signal. In the case of narrow borehole environment, transmit-receive circuit can't increase with the change of antenna number. In order to save the electronic cartridge space, instrument use time-sharing multiplexing technology to achieve the measure of arry antenna in different circumferential partitions and radial depths. Fig.2 shows the schematic circuit diagram of downhole MRI tool. Electronic cartridge includes antenna interface circuit, transmit-receive circuit and main control circuit. With the increase of antenna number, the antenna interface circuit become particularly complex. In order to realize the impedance matching of each part, an active MOS tube control technology is used to design the option switch of interface circuit. Adopting multistage discharge mode to shorten the antenna recovery time. The function of transmit-receive circuit is high power pluse emission and weak signal acquisition.

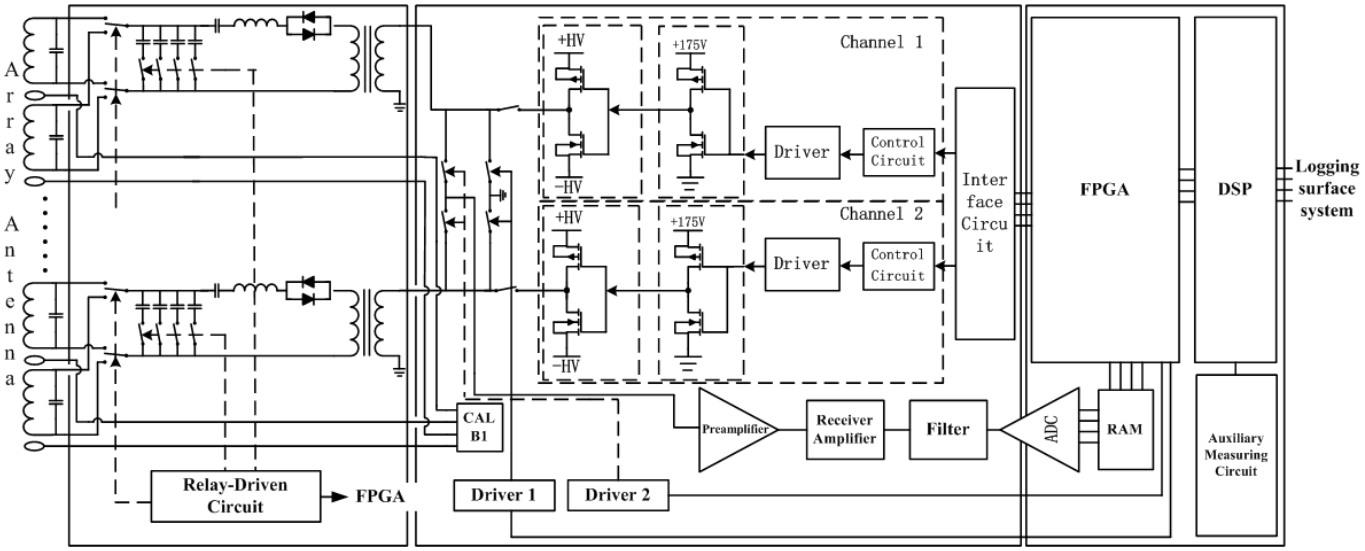

Figure 2 – the schematic circuit diagram of downhole MRI tool.

This new downhole circumferential partitional MRI tool can be used for wireline logging or LWD. Facing the high heterogeneity of Complex reservoir, pore structure and fluid properties can be obtained By collecting echo signal from different azimuthal formation. Instrument can truly realize the 3D MRI of the reservoir.

Acknowledgements

This work was supported by “863 program (Grant No. 2013AA064605)”.

References

[1] M. Prammer, S. Menger, S. Knizhnik, G. Goodman, E. Harris, E. Drack, Directional Resonance: New Applications for MRIL. SPE 84479.
[2] G.R. Coates, L.Z. Xiao, M. Prammer, NMR Logging Principles and Applications, 1999.

O25

A compact X-Band resonator for DNP-enhanced Fast-Field-Cycling NMR at 340 mT

O. Neudert[a], C. Mattea[a], S. Stapf[a]

[a]Ilmenau University of Technology, Institute of Physics, PO Box 100565, 98684 Ilmenau, Germany.

Dynamic Nuclear Polarization (DNP) is a versatile technique that can be used to hyperpolarize nuclear spins that are coupled to unpaired electron spins. Previous studies [1,2] have demonstrated that DNP-enhanced Fast-Field-Cycling (FFC) relaxometry at 73 mT can provide an increased sensitivity over standard FFC techniques using liquid-state DNP effects. DNP measurements of polymer melts at 340 mT[3], however, have shown that in such systems hyperpolarization is created via solid-state DNP effects. Those effects appeared to be much less effective at 73 mT [2], providing only small DNP enhancements.

A new probehead was developed for DNP-enhanced FFC relaxometry at 340 mT polarization field strength [4]. It is based on a dielectric-filled microwave cavity resonator operating in the TM_{110} mode at 9.5 GHz and is suitable for axial magnet geometries with a bore access of at least 20 mm. The probehead includes a single-resonant planar radio freqeuncy coil for NMR detection at 16.7 MHz and is compatible with standard 3 mm NMR tubes. The microwave resonator was assessed in terms of the microwave conversion factor and microwave-induced sample heating effects.

A comparison of three exemplary viscous samples shows that for such systems DNP at 340 mT provides a more than 5-fold improved enhancements over DNP at 73 mT. Furthermore, the 4.7-fold increase of the polarization field causes a gain of both electron and nuclear spin Boltzmann polarization. Hence, an overall 23-fold improvement of nuclear spin hyperpolarization is obtained from DNP-enhanced FFC relaxometry of viscous systems at 340 mT. This development significantly widens the range of potential application for this technique.

References

[1] O. Neudert, H.-P. Raich, C. Mattea, S. Stapf, K. Münnemann, J. Magn. Reson. 242 (2014) 79-85.
[2] O. Neudert, C. Mattea, S. Stapf, M. Reh, H.W. Spiess, K. Münnemann, Micropor. Mesopor. Mat. 205 (2015) 70-74.
[3] O. Neudert, M. Reh, H.W. Spiess, K. Münnemann, Macromol. Rapid. Commuin. 36 (2015) 885-889.
[4] O. Neudert, C. Mattea, S. Stapf, J. Magn. Reson. (2016) *(under review)*

A Robust NMR Method to Measure Porosity of Low Porosity Rocks

J.M. Sun[a], W.C. Yan[a], T. Li[b]

[a]China University of Petroleum (East China), China; [b]Suzhou NIUMAG Analytical Instrument Corporation, China.

Nuclear magnetic resonance (NMR) is wildly used in petrophysical analysis, such as porosity, irreducible water saturation and wettability. Accurate rock porosity measurements are critical for oil and gas reservoir evaluation, especially for complex reservoirs with low porosity. When rocks are saturated with water, the NMR signals reflex total volume of fluid in the pores. Typical laboratory NMR porosity measurements are divided two parts: preparing the standard samples and establishing the standard equation, and testing water saturated rock samples [1]. Four factors mainly affect the accuracy of NMR total porosity measurement of a rock sample, including the waiting time (TW), the echo time (TE), hydrogen index (HI) and rock temperature. By choosing the properly parameters and exciting a series of RF pulses, the rock porosity is calculated directly by the integral area of the T_2 spectrum or initial amplitude of the echo signal. However, due to the insufficiently short echo time, NMR porosity measurements of low porosity rocks are usually underestimated. Magic-sandwich echo is famous for its capability of providing a reasonably long final delay that covers the dead time [2], which has not yet found its way into application for NMR porosity measurement, and we think it is a robust method to detect fluid in micro pores of low porosity rocks.

In order to compare the accuracy of porosity measurements between magic-sandwich echo (MSE) and Carr – Purcell – Meiboom – Gill (CPMG) train, we selected both conventional oil reservoir rock samples and low porosity reservoir rock samples, including relative high porosity sandstones (samples A1, A2) , tight sandstones (samples B1, B2) and shale stones (samples C1, C2) respectively. Laboratory water porosity analyses were also needed to verify results of different NMR porosity measurement methods. Both MSE initial amplitude and CPMG train initial amplitude were measured to calculate total porosity of a sample. **Figure 1** shows the comparison between MSE signal and CPMG train signal of water saturated sample B1, and the initial amplitude of MSE (5707.209 a.u.) is larger than the latter one (5057.418 a.u). In our research, the echo time of CPMG train we used was 0.1ms, and the initial amplitude would be lower (3451.795a.u) if the echo time was 0.3ms.

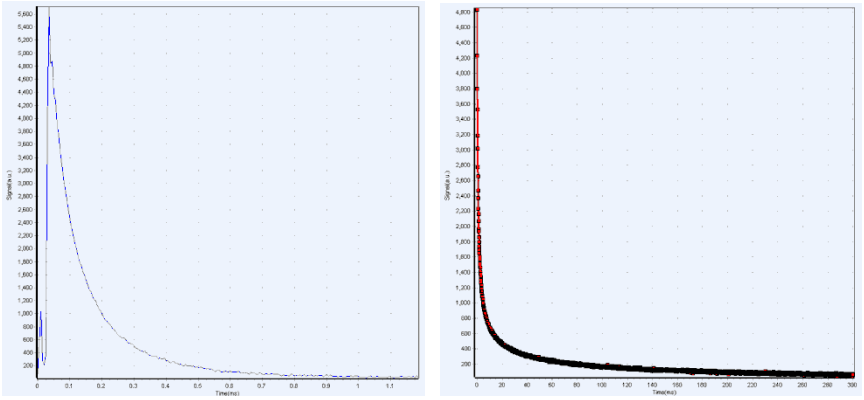

(a) MSE (b) CPMG train

Figure 1 – NMR signals of sample B1. (a) MSE measured signal, (b) CPMG train measured signal.

By using the standard equation of standard samples, we could calculate porosity of different rock samples. It should be noticed that the initial amplitudes of shale samples cannot be used directly to calculate porosity, because dry shale samples have strong NMR signals, and the signals come from the clay minerals which contain crystalized water. After measured water saturated samples signals, these samples were dried for 24 hours and measured NMR signals again. The values we used as equivalent initial signals were calculated by subtracted dry signals from water saturated signals. The porosity results of different rocks with different NMR measurement methods are shown in **Table 1**.

Table 1. Porosity results of different rocks with different NMR measurement methods.

	A1 (%)	A2 (%)	B1 (%)	B2 (%)	C1 (%)	C2 (%)
MSE	18.63	13.10	4.25	6.44	3.39	2.19
CPMG train	18.40	12.96	3.87	6.05	3.01	1.93
Water porosities	18.76	13.37	4.48	6.62	3.52	2.41

Comparing MSE and CPMG train porosity results, we can make a conclusion that the MSE detects more fluid volume, which is a better way to measure porosities of rock samples. MSE is a robust NMR Method to measure porosity more accurately in low porosity rocks, and the experimental time is also faster than traditional methods.

References

[1] Hao X, et al. Fuel 2015; 143:47-54.
[2] Maus A, et al. Macromolecular Chemistry & Physics, 2006; 207(13):1150 – 1158.

Emerging NMR approaches for characterizing rock heterogeneity

Huabing. Liu[a,b], Lizhi. Xiao[a], Petrik. Galvosas[b]

[a]State Key Laboratory of Petroleum Resources and Prospecting, China University of Petroleum, Beijing, China; [b]Victoria University of Wellington, School of Chemical and Physical Sciences, MacDiarmid Institute for Advanced Materials and Nanotechnology, Wellington, New Zealand.

Rock heterogeneity provides clues about the processes of sediments deposition and subsequent compaction, cementation or dissolution during geological evolution period [1]. Some heterogeneity features, for instance variations of pore structure and mineral compositions over microscopic scale, may largely influence the permeable and mechanical characteristics of rocks. In common, NMR techniques unravel the morphology features and the hierarchy of interactions with fluids confined in its pore space, therefore can readily evaluate the structural and compositional heterogeneity of rocks [2-4].

In this context, we introduce two 2D-NMR methods to probe the hetergeneity degree of rock cores. The first presented framework is eigenmode correlation experiment. It relies on the correlation of ground and high relaxation eigenmodes in spin-bearing molecular diffusion equation in successive time domains of 2D-NMR experiments [5]. This approach allows one to obtain pore length scales correlated to NMR relaxation times, and to intrinsically extract surface relaxivity values from 2D eigenmode correlation maps. This experiment utilizes a shorter effective encoding period in the first domain as compared to diffusion-relaxation correlation method, thus, the additional signal attenuation caused by relaxation effect is much weaker [5, 6]. By this means, the information of pores with comparably small size and significant internal gradients can be preserved, which provides more detailed insights of structural and pore surface heterogeneity of rocks. The experimental results of two rock samples with different lithology (Figure 1.a-b) reveals a wider relaxation time distribution but narrower pore length scale in sandstone, implying more sophisticated surface mechanism and lower structural heterogeneity. Moreover, the stronger deviation of 2D distribution in shorter relaxation time in sandstone (Figure 1.a) indicates larger surface relaxivities occurred in smaller pore regions, which may be due to the existence of strong paramagnetic materials.

The second approach is designed to investigate the solid composition heterogeneity of rocks [7]. By coupling the aforementioned high eigenmode contribution and T_2^* attenuation along FID decay in a 2D experiment, the determination of pore length scales can be easily correlated with solid-liquid magneitc susceptibility contrast $\Delta\chi$. Since the variation of $\Delta\chi$ in different pore regimes is associated with the local variation of solid matrix compositions, it provides a straightforward indication of compositional heterogeneity from the obtained 2D correlation maps. A relevant factor can be defined from the inverse correlation line of 2D map and utilized to quantitatively evaluate this rock heterogeneity. As shown in Figure 1. c-d, the susceptibility contrast value is larger in sandstone than that in limestone, which infers more paramagnetic components in sandstone. Furthermore, the 2D distribution of limestone extends more along both directions, indicating diverse solid compositions over differnt pore regimes and therefore a higher compositional heterogeneity degree.

Since these two proposed 2D techniques offer alternative ways of investigating rock heterogeniety, it enables one to study the permeability and elastography behaviors in rocks [8]. Moreover, both methods do not require sophisticated NMR hardware as compared to MRI techniques, which facilitates their implementation in NMR systems during porous materials research.

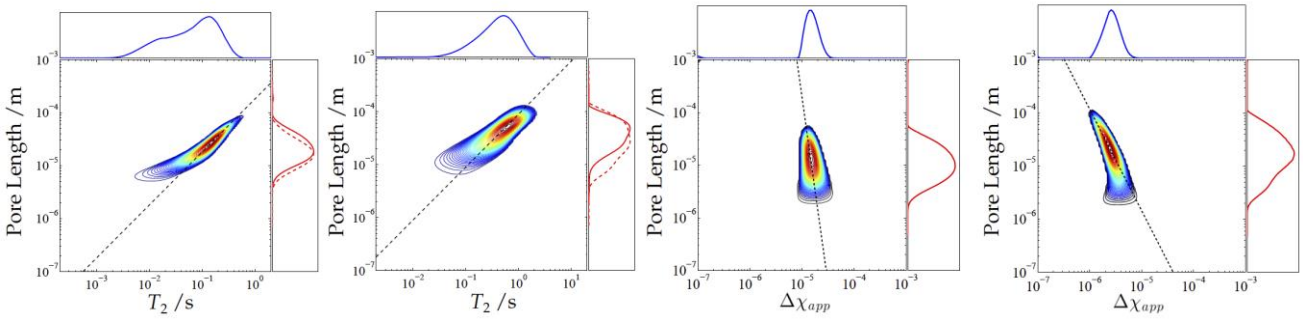

Figure 1 –Eigenmode correlation experimental results in sandstone (a) and limestone (b) at 2 MHz. Correlation experimental results of pore length with susceptibility difference in sandstone (c) and limestone (d) at 64 MHz.

References

[1] D. Tiab, E. C. Donaldson, Petrophysics: theory and practice of measuring reservoir rock and fluid transport properties. Gulf professional publishing, 2011.
[2] Y.-Q. Song, S. Ryu, P. Sen, Nature, 407 (2000) 178–181.
[3] D. J. Holland, J. Mitchell, A. Blake, L. Gladden, Phy. Rev. Lett, 110 (2013) 018001.
[4] C. H. Arns, K. E.Washburn, P. T. Callaghan, Petrophysics, 48 (2007) 380-392.
[5] H. Liu, M. Nogueira d'Eurydice, S. Obruchkov, P. Galvosas, J. Magn. Reson, 246 (2014) 110–118.
[6] L. Zielinski, R. Ramamoorthy, C. Minh, K. Daghar, R. Sayed, SPE Annual Conference, (2010) 1–8.
[7] J. Mitchell, J. Magn. Reson, 240 (2014) 52–60.
[8] D. S. Grebenkov, pmc.polytechnique.fr, (2015) 1–65.

Low field NMR surface relaxivity studies of chalk and argillaceous sandstones

K. Katika[a], H. Fordsmand[b], I.L. Fabricius[a]

[a]Technical University of Denmark, Civil Engineering Department, Brovej, Building 119, 2800 Kongens Lyngby, Denmark; [b]Haldor Topsøe, Haldor Topsøes Allé 1, 2800 Kongens Lyngby, Denmark.

This paper provides an insight into how the surface relaxivity of minerals constituting rocks are affected by changes in temperature and Larmor frequency. This is relevant for connecting conventional rock core testing data to reservoir logging data.

In the present study, we perform laboratory NMR T_2 measurements on Gorm field chalk, Stevns Chalk, Solsort field greensand and Berea sandstone so as to determine the surface relaxivity, ρ, of the rock forming minerals. Transverse relaxation rate, $1/T_2$ is proportional to ρ and the surface-to-volume ratio (S/V) of the pore space [1]:

$$\frac{1}{T_2} = \rho_2 \frac{S}{V} \quad (1)$$

Paramagnetic minerals in contact with the water accelerate the surface transverse relaxation (equation 1) at higher frequencies, so T_2 distributions at Lamor frequency 2 and 20 MHz at 40ºC were used to identify the presence of paramagnetic minerals in water saturated rocks. Therefore, the surface relaxivity of the respectively purely calcitic and purely quartzitic Stevns chalk and Berea sandstone proved not to be affected by the changes in frequency. By contrast, paramagnetic minerals in the Gorm field chalk and Solsort field greensand resulted in higher values of ρ when the NMR measurements were performed at higher Larmor frequency (Figure 1).

T_2 distributions at temperatures ranging from 10 to 70ºC provide a valuable connection between lab and field transverse relaxation measurements. The T_2 distributions illustrate that ρ for calcite tends to decrease with temperature whereas ρ for quartz tends to increase with temperature. These changes may be used to describe changes in the porosity and pore size distribution obtained in the lab, compared to those in the logs.

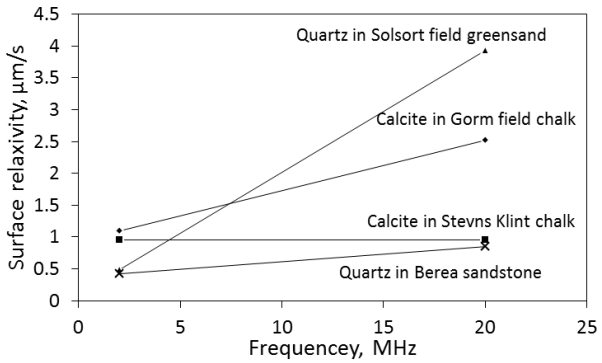

Figure 1 – Changes in the surface relaxivity of the main minerals constituting the rocks under investigation versus the Larmor frequency of the measurements. The T_2 value was acquired at 2 and 20 MHz at 40ºC.

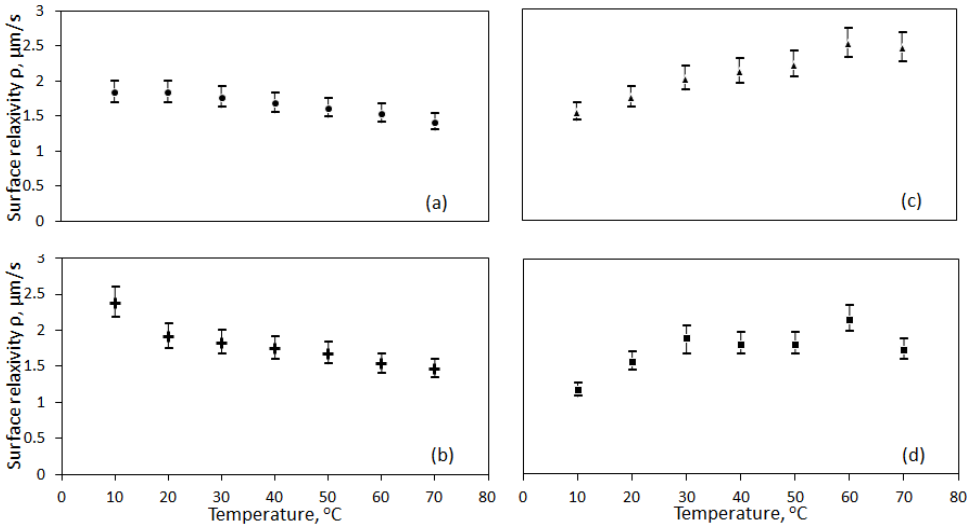

Figure 2 – The surface relaxivity of calcite in (a) Gorm field chalk and (b) Stevns Klint chalk, quartz in (c) Solsort field greensand and (d) Berea sandstone at 20 MHz obtained at temperatures ranging from 10 to 70ºC.

References

[1] Dunn, K., Bergman, D.J., and LaTorraca, G.A., 2002, Nuclear Magnetic Resonance-Petrophysical and Logging Applications. New York: Handbook of Geophysical Exploration: Seismic Exploration, Pergamon Press.

Measurement of interfacial area from NMR time dependent diffusion and relaxation measurements

M. Fleury

IFP Energies nouvelles, 1 avenue de Bois-Préau, 92852 Rueil-Malmaison, France.

During forced displacement of water by oil in a water-wet porous media, a fraction of the energy injected into the system is dissipated due to the multiple restrictions in the pore network system. The other fraction, reversible, is used to create an interfacial area between the two phases. These thermodynamical aspects have been considered as early as 1970; today, based on recent high resolution 3D tomography, it is estimated that about 40% of the energy is reversible [1]. Taking into account the interfacial area may be a new way of understanding and predicting two-phase flow in porous media, especially in the context of enhanced oil recovery where predicting the behavior of trapped phases is crucial.

The measurement of interfacial area is not an easy task. Indeed, conventionnal techniques such as gas adsorption require non saturated samples. In liquid saturated samples, tracer techniques can be used [2] but they require no interaction of the tracer with the solid surface. For a porous media saturated with only phase, it is well known that T_1 or T_2 relaxation gives quantitative information about the solid-liquid surface providing the surface relaxivity is known. Alternatively, short-time diffusion measurements [3] provide, without calibration coefficient, a specific surface area similar to gas adsorption technique providing the surface is small enough (typically $<1 m^2/g$). We show first on a reference material that the surface determined by NMR is the same the one determined by gas adsorption. On different grain packs, the measured surface is also proprotionnal to the grain size as expected. Then, we extended the short time diffusion technique in two phase situation to determine the interfacial area in porous media saturated with oil and water in drainage and imbibition. It requires in general the detection or separation of the oil from the water signal, and this is performed by doping water with paramagnetic manganese chloride. An example is shown in Figure 1. In this case, we record the effective diffusion time of dodecane in a synthetic model porous media saturated with oil and water. The oil was forced into the sample by centrifuge. The sequence used is a bipolar PGSTE in which the shortest diffusion time available is 8 ms (23 MHz resonance frequency). With a T_2 reaxation time below 1 ms, the doped water diffusion is therefore filtered. However, diffusion lengths of dodecane below about 5 µm are not available and the data were fitted with a 3 parameter model allowing the determination of the slope, proportionnal to S/V, at $L_d=0$. In the case of Figure 1, we measured a surface area of 0.20 m^2 after centrifuging, the volume of dodecane being 1.10 ml. After spontaneous imbibition, the surface area increased to 0.27 m^2. The solid surface area is 0.47 m^2.

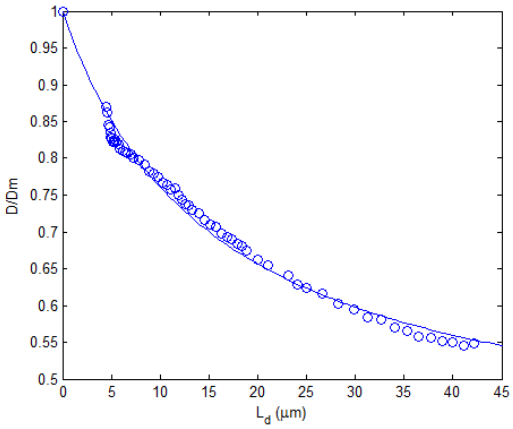

Figure 1 – Effective diffusion coefficient D of dodecane vs. the one dimensionnal diffusion length $L_d=(2Dmt)^{1/2}$, D_m diffusion coefficient of dodecane, t diffusion time of the NMR sequence.

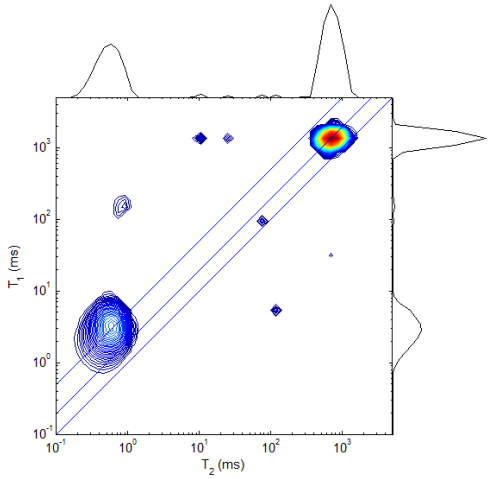

Figure 2 – T_1-T_2 map of dodecane (T_2~600ms) and doped water (T_2~0.8ms) in a porous media saturated with both fluids.

Diffusion measurements are however sensitive to internal gradients, especially close to interfaces where they are the strongest. An alternative simple technique exist: although the relaxation of dodecane at the oil-water interface is too weak to be exploited, we observed that the presence of paramagnetics in the water strongly enhanced its relaxation (Figure 2). A T_1/T_2 ratio of about 2 is a convincing evidence of the interfacial relaxation of dodecane. Using the above mentionned surface area, we determined a surface relaxivity of about 4 µm/s. We used this effect to measure interfacial area by NMR relaxation while performing flooding experiments.

References

[1] S. Berg *et al.*, Proceedings of the National Academy of Sciences of the United States of America **110**, 3755 (2013).
[2] L. Chen and T. C. Kibbey, Langmuir, 6874 (2006).
[3] P. P. Mitra, P. N. Sen, L. M. Schwartz, and P. Le Doussal, Physical review letters **68**, 3555 (1992).

Permeability from time dependent methane saturation monitoring in shales

A. Valori[a], S. Van den Berg[a], F. Ali, R. Taherian[a], W. Abdallah[a]

[a]Schlumberger Dhahran Carbonate Research, Dhahran Techno Valley, Saudi Arabia.

Measurement of permeability of very tight rocks is difficult, uncertain, and no clear industry standard has yet been agreed. This paper will investigate a novel technique to determine the permeability in shales, by using NMR to monitor saturation and de-saturation of gas shale plugs as a function of time.

In our approach, the raw NMR signal of the sample is measured before and during methane injection. During the injection of methane, the raw NMR signal increases, and subtraction of the base signal returns purely the response from the injected methane. This difference is used to obtain the T_2 distributions and T_1–T_2 correlations related solely to the injected methane in the shales. Figure 1 illustrates one example of time lapse T_2 distributions for the methane acquired during de-saturation.

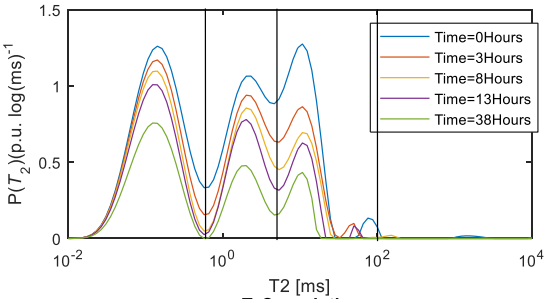

Figure 1 – Methane T_2 distribution during de-saturation.

The T_2 distributions of conventional rocks are typically used as source of information on the pore size distribution and fluid viscosity. In the case of gas in unconventional reservoirs, the interpretation may be more complex. However, it can be confidently stated that the different T_2 values refer to gas in different "environments" with different dynamic processes. The T_2 cutoffs can still be used to partition the T_2 distributions into components of the signal arising from gas whether the environments refer to pores of different sizes or gas at different conditions.

Our approach uses the rate of change for different T_2 components during the production of gas (Figure 2) and the signal amplitude of each component at maximum saturation pressure to calculate the permeability related to the individual environment modifying the approach of Sutherland et al. [2].

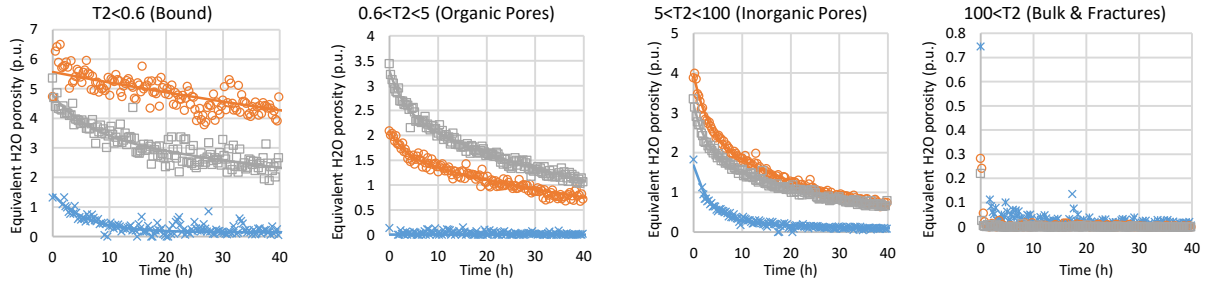

Figure 2 – decay for diffenret T_2 components and three different samples as a function of de-saturation time, corresponding to the T_2 windows identified in Figure 1

In the majority of shale gas formations, there are two types of pore systems: kerogen-hosted organic pores(OP) and inorganic pores (IP). By fully saturating 1.5-inch shale cores with methane and by continuously measuring the NMR signal it is possible to determine the individual porosity and permeabilities of thesesystems. T_1–T_2 correlation measurements are also incuded to confirm the individual zones and the mobility of the fluid in the zones. It was determined that a single exponential decay is unable to account for the heterogeneity in the pore structures of shales, leading to errors in reservoir simulations using ECLIPSE*.

This work demonstrates that a multi-exponential system is required for proper description of the depletion from shales, and their storage and release mechansisms. Also, it proposes an approach to extract permeability information for each T_2 component.

References

[1] Kausik, R., Minh, C. C., Zielinski, L., Vissapragada, B., Akkurt, R., Song, Y.,… Blair, E. SPE 14718-PP (2011) 1–16.
[2] Sutherland, H. J., & Cave, S. P. International Journal of Rock Mechanics and Mining Sciences & Geomechanics Abstracts, 17(5), (1980) 281–288.

O31

Accurate phase-shift velocimetry in porous media: the importance of propagator asymmetry

A. Vallatos[a], M.N. Shukla[a,b], V.R. Phoenix[b], W.M. Holmes[a]

[a] University of Glasgow, Glasgow Experimental MRI Centre, Institute of Neuroscience and Psychology, Glasgow, United Kingdom, [b] University of Glasgow, Department of Geographical and Earth Sciences, Glasgow, United Kingdom

For producing velocity maps in porous media, where voxel size is greater than the typical pore size, it has been generally advised to use the more time consuming propagator method [1], as numerous issues have been reported with the use of phase-shift velocimetry. These issues can be broadly categorised as:

1. Measured average velocity values do not agree with values calculated from the known flow rate and porosity. Lower values than expected are reported at higher flow rates [2] making the relationship of measured velocity to the imposed flow rate non-linear [3, 4].
2. Standard deviation of voxel velocities exceeds the expected values. This effect becomes stronger at lower flow rates [5] with a large proportion of the voxels unexpectedly indicating negative velocities [4].
3. Measured velocity can vary with experimental PFG parameters. Several authors have shown that at fixed flow rate, different velocity values are measured when different gradient strengths (G) [1] or observation times (Δ) [4] are used.

Such issues have not been reported when using the propagator imaging approaches in porous media [1], however propagator imaging comes with an enormous time penalty, as multiple $\boldsymbol{q}$-space values (or gradient encoding steps) need to be acquired ($n_{\boldsymbol{q}} \geq 8$). Despite the fact that phase shift velocimetry is much faster, requiring only two gradient encoding steps, the above-mentioned problems tend to make it unreliable for use with porous media like rocks.

In this work we investigated the effect of several parameters on the accuracy of phase-shift velocimetry, by performing spatially-resolved phase-shift and propagator velocity measurements in Benthheimer sandstone samples and pipe flow using a bipolar Alternating Pulsed Gradient Stimulated Echo (APGSTE) pulse sequence in a 7T Bruker Instrument.

Our measurements in rock show that the relation of phase-shift to gradient becomes increasingly non-linear at higher gradient values and longer observation times (Δ) (Fig. 1a). We show that this deviation depends on the product of the flow rate to the observation time, $Q \times \Delta$, that is proportional to the average molecular displacement. Combining experimental data with simulations (Fig. 1b), we demonstrate that asymmetries in the propagator (i.e. the probability distribution of displacements) within each voxel are the main source of these phase-shift velocimetry errors. In addition, we theoretically relate these errors to the variance, skewness and kurtosis of the propagator. These results allow us to explain the issues described in the literature, and propose a methodology for avoiding such errors when using phase-shift velocimetry in porous media. We successfully applied this general approach to flow through Bentheimer sandstone and produced accurate and noise-less velocity maps for a range of flow rates[6] (Fig 1c).

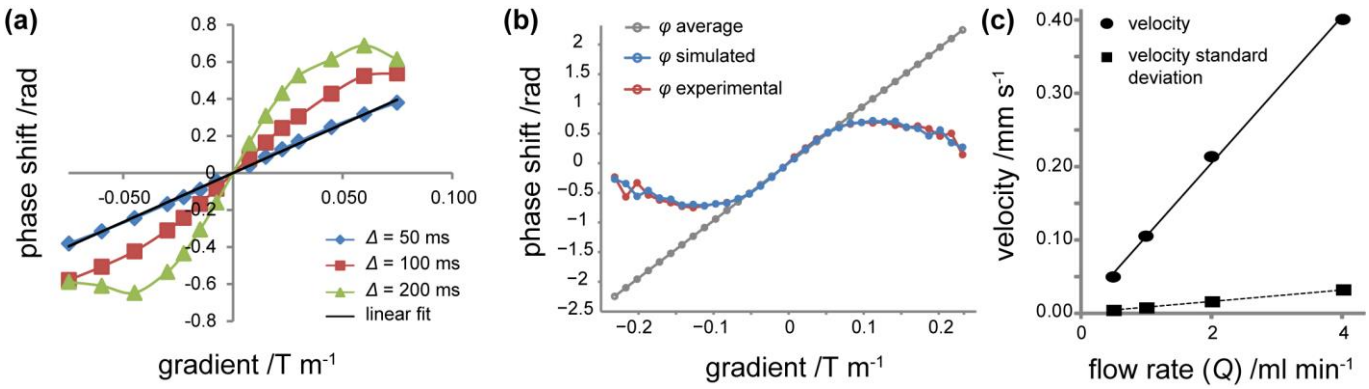

Figure 1 – (a) Measured phase-shift against applied gradient for different and observation times Δ (Q = *2* ml min^{-1}). (b) Average and measured phase-shift obtained by simulations using the propagator data and experimental phase-shift extracted from the same data (Q = *2* ml min^{-1} / Δ = 100 ms) (c) Average velocity and standard deviation of velocity against flow rate.

References

[1] C.T.P. Chang, A.T. Watson, NMR imaging of flow velocity in porous media, Aiche J., 45 (1999) 437-444.
[2] M.R. Merrill, Local Velocity and Porosity Measurements inside Casper Sandstone Using Mri, Aiche J., 40 (1994) 1262-1267.
[3] R.A. Waggoner, E. Fukushima, Velocity distribution of slow fluid flows in Bentheimer sandstone: An NMRI and propagator study, Magn. Reson. Imaging, 14 (1996) 1085-1091.
[4] N. Spindler, P. Galvosas, A. Pohlmeier, H. Vereecken, NMR velocimetry with 13-interval stimulated echo multi-slice imaging in natural porous media under low flow rates, J. Magn. Reson., 212 (2011) 216-223.
[5] Q. Chen, W. Kinzelbach, S. Oswald, Nuclear magnetic resonance imaging for studies of flow and transport in porous media, J Environ Qual, 31 (2002) 477-486.
[6] M.N. Shukla, A. Vallatos, V.R. Phoenix, W.M. Holmes, Accurate phase-shift velocimetry in rock, J. Magn. Reson., 267 (2016) 43-53.

Water spray measurements with Magnetic Resonance Imaging: the near-nozzle region

I.V. Mastikhin[a], S.Ahmadi[a], K.M. Bade[b]

[a]MRI Centre, Dept of Physics, University of New Brunswick, Fredericton, NB Canada; Spraying Systems Co., Spray Analysis and Research Services, Wheaton, IL, USA.

Sprays are dynamic collections of droplets dispersed in a gas, with many industrial and agricultural applications. Quantitative characterization is essential for understanding processes of droplet formation (atomization) and dynamics. There exists a wide range of measurement techniques to characterize sprays, from direct imaging to phase Doppler interferometry to X-rays, which provide detailed information on spray characteristics in the "far-nozzle" region (>> 10 diameters of the nozzle). However, traditional methods are limited in their ability to characterize the "near-nozzle" region where the fluid may be inside the nozzle, optically dense, or incompletely atomized. In the near-nozzle region, the liquid transitions from a continuous flow to a disperse flow to the spray: first, it quickly accelerates to very high speeds (supersonic in some cases, e.g., diesel injectors), it interacts with the surrounding gas, undergoing violent vibrations, and then gets fragmented into droplets of ever-decreasing size (typically sub-µm-µm).

Magnetic Resonance Imaging (MRI) presents potential as a non-invasive technique that is capable of measuring optically inaccessible fluid in a quantitative fashion. Challenges in measuring sprays with MRI are those typical for a disperse flow, with its very high mechanical dispersion and interphase-susceptibility differences, but they are compounded by extreme transition rates.

In this work, MRI measurements of the water spray generated by ceramic flat-fan nozzles were performed [1]. A wide range of flow speeds in the system (0.2 - >25 m/s) required short encoding times. Imaging parameters had to be carefully chosen to reduce the smear artefact and provide an accurate geometric depiction of water inside the nozzle. The 3D Conical SPRITE and motion-sensitized 3D conical SPRITE sequence [2,3] were employed. The strong NMR signal from water inside the nozzle permitted well-resolved (0.47x0.3x0.3m voxel size) proton and velocity mapping measurements. The signal outside the nozzle, in the near-nozzle region, even though considerably weaker, was reliably detected. It corresponded to the expected flat-fan spray pattern up to 3 mm away, and then steadily decayed with distance in the area of the droplet formation (atomization). To better identify possible causes of the signal loss, measurements on a variety of paramagnetic solutions were performed.

The results present challenges of using MRI to study sprays and demonstrate the potential of MRI for measuring spray characteristics in areas inaccessible by other methods.

References

[1] I.V. Mastikhin, A. Arbabi, K.M. Bade. J. Magn.Reson. 266 (2016) 8-15.
[2] M. Halse, D.J. Goodyear, B. MacMillan, P. Szomolanyi, D. Matheson, B.J. Balcom, J. Magn. Reson. 165 (2003) 219–229.
[3] O. Adegbite, L. Kadem, B. Newling, MAGMA. 27 (2014) 227–35.

O33

An On-line NMR for Drilling Fluid Analysis System

S. Li[a,b], L. Xiao[a], X. Li[b], Z. Wang[b]

[a]China University of Petroleum Beijing, 18 Fuxue Road, Changping, Beijing China 102249 ; [b]Sinopec Research Institute of Petroleum Engineering, Room 707, North Star Times Tower, No.8 Beichendong Road, Chaoyang District, Beijing China, 100101.

The most economical and optimal method to find oil and gas formations is analysis of oil and gas released into the drilling fluid and returned to surface while drilling, commonly accomplished by mud logging. Practice shows the quantitative detection of the oil and gas contents in drilling fluid is beneficial to identify characterization of reservoirs and evaluate the reservoirs' productivity. Presently gas content and composition in drilling fluid are able to be detected continuously in gas analysis of mud logging [1], but the same is not true for detection of oil content in real time. Through drilling fluid NMR logging it is able to quantitatively detect the oil content in drilling fluid base on the difference in transverse relaxation time(T_2) of drilling fluid and crude oil even under conditions of weak oil showing and fluid mixed with organic additives [2], the use of laboratory NMR measuring instruments is cumbersome and therefore limits its use at well site. On the other hand, the analysis of a single sample data source does not represent the actual reservoir oil data for it is subject to a length of time to obtain the analysis result following collection of the drilling fluid samples.

To enable continuous and quantitative analysis of oil content in drilling fluid in real time, and to solve the difficulties in discovery and identification of oil reservoirs base on cuttings and gas analysis in mud logging under the conditions of drilling with PDC bit and fluorescence fluid and weak gas showing, an on-line NMR Surface Logging System is developed to operate at well sites (Fig. 1). The integrated system comprises five subsystems: auto-sampling, miniaturized NMR sensor, spectrometer, main controller and wireless data communication. Auto-sampling device takes samples of drilling fluid continuously and quantitatively from the flowline returning from the well and removes cuttings in diameter greater than 1mm. Miniaturized NMR sensors are implemented based on halbach magnets, which weigh 20 kg and achieve larmor frequency up to 20 MHz. An approach for customized temperature control is employed to maintain stable magnetic field. NMR spectrometer's amplifier is capable of emitting 300W RF pulses on antenna coil. The integrated device utilizes TCP/IP protocol for remote data acquisition, transmission and control. The software interfaces with NMR auto-tuning, fast inversion and measurements control.

The On-line NMR Surface Logging System, installed close to buffer tanks of the outlet of drilling fluid, is tested at a number of wells(Fig. 2) and is successful in the discovery of oil-bearing formations.

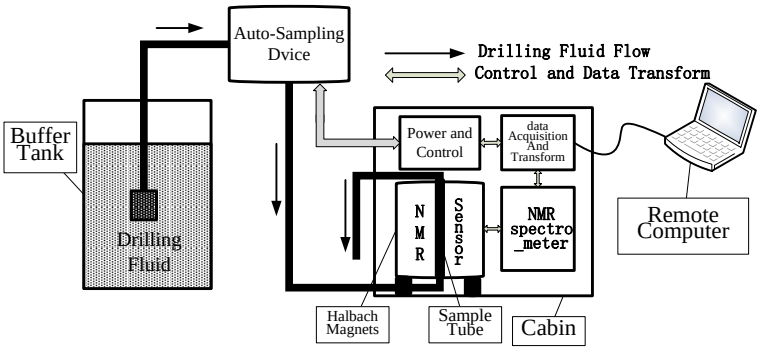

Fig. 1 On-line NMR for drilling fluid analysis System

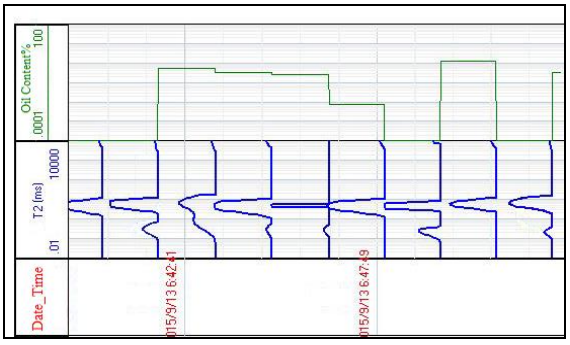

Fig. 2 Application at well X37X60

References:

[1] P. Blanc, J. Brevière, F. Laran ect.. Reducing Uncertainties In Formation Evaluation Through Innovative Mud Logging Techniques. SPE-84383-MS, SPE Annual Technical Conference and Exhibition, 5-8 October, Denver, Colorado,2003

[2] Zhizhan Wang, Xinhua Zhang, Wei Zhang, Huangsheng Lu. Origin and Applications of Drilling Fluid NMR Technology. the 11th international conference on magnetic resonance microscope, paper 2011-32.

A novel spatially resolved 2D Laplace NMR method for porous materials at low magnetic field

Y. Zhang, L. Xiao

State Key Laboratory of Petroleum Resources and Prospecting, China University of Petroleum, Beijing, 102249, China

Heterogeneity is an important property of porous media such as biological materials and rock samples. Spatially resolved NMR is a suitable method to extract heterogeneous information and structure information from porous materials. Recently 1D and 2D Laplace NMR were combined with spatially resolved NMR to examine the detailed structure of heterogeneous samples. For example, spatially resolved D-T_2 and G_{int}^2D-T_2 correlation maps were measured using back-projection method to retrieve the abundant structure information of porous media [1-4].

Here we present a novel method which yields spatially resolved pore size (a) - relaxation (T_2) distributions correlation maps of porous samples. The experiments were implemented at low field NMR to reduce the distortion of T_2 measurements arising from internal gradients. The pore size distributions were obtained by the method of Decay due to Diffusion in the Internal Field (DDIF) [5]. The delay t_d was varied logarithmically from 1 ms to 2 s in 40 steps. The echo time t_{E1} was 1.5 ms and 200 ms for the experiments carried on at 2 MHz and at 23 MHz, respectively, to satisfy the weak encoding limit. The relaxation information was measured by CPMG method. In order to obtain accurate T_2 distributions the echo time t_{E2} was 100 μs to minimize the internal gradients effect [6]. The frequency encoding method was applied to acquire the spatially resolved information about porous samples. Two kinds of samples were measured. One kind is glass-bead model samples. Model sample A consists of glass beads with different diameters filled with water and model sample B is glass-bead packs saturated with oil and water. Another kind is water-saturated sandstone sample with unknown structure. The a-T_2 correlation maps from the model samples provide right information about structure and fluids contents, which shows the validity of this method. Localized information such as pore size distributions and surface relaxivities were extracted from the spatially resolved a-T_2 correlation maps. The heterogeneity of the samples was characterized at both microscopic (correlation maps) and macroscopic (MRI) scales. This method was first applied on 2 MHz Rock core analyzer (Oxford, UK) which was used to measure one-dimensional spatially resolved a-T_2 correlation maps. Then a 23 MHz MRI spectrometer (Niumag, China) was used to obtain two-dimensional spatially resolved a-T_2 correlation maps. The back-projection and compressed sensing method will be implemented to save the measurement time. This method is expected to benefit many areas such as food industry and oil industry.

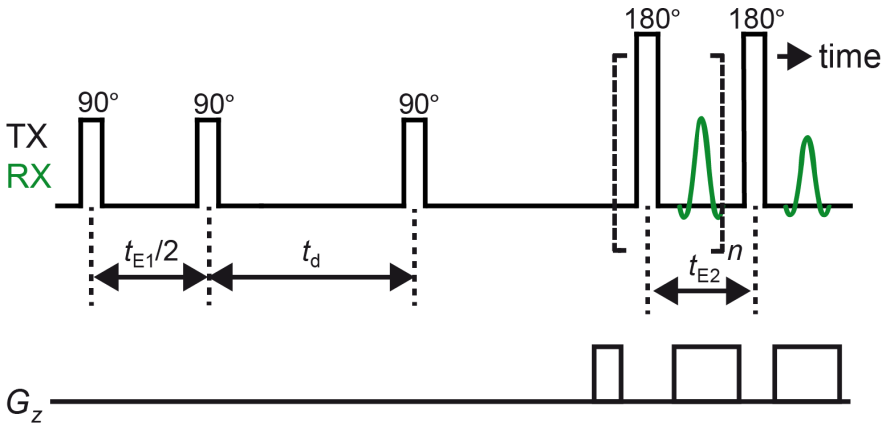

Figure 1 Pulse sequence for spatially resolved a-T_2 correlation experiments.

References

[1] D. Xiao, B. J. Balcom, Two-dimensional T_2 distribution mapping in rock core plugs with optimal k-space sampling, J. Magn. Reson. 220 (2012) 70-78.
[2] Y. Zhang, B. Blümich, Spatially resolved D-T_2 correlation NMR of porous media, J. Magn. Reson. 242 (2014) 41-48.
[3] Y. Zhang, B. Blümich, G_{int}^2D - T_2 correlation NMR of Porous Media, J. Magn. Reson. 252 (2015) 176-186.
[4] Y. Zhang, L. Xiao, G. Liao, B. Blümich, Direct correlation of internal gradients and pore size distributions with low field NMR, J. Magn. Reson. 267 (2016) 37-42.
[5] Y. Song, S. Ryu and P. N. Sen, Determining multiple length scales in rocks, Nature 406 (2000) 178-181.
[6] H. Liu, M. d' Eurydice, S. Obruchkov, P. Galvosas, Determining pore length scales and pore surface relaxivity of rock cores by internal magnetic fields modulation at 2 MHz NMR, J. Magn. Reson. 246 (2014) 110-118.

Remote Detection NMR Gas Adsorption Meter

A. Selent[a], V. V. Zhivonitko[b], V.-V. Telkki[a]

[a]NMR Research Group, University of Oulu, P.O.Box 3000, FIN-90014 University of Oulu, Finland; [b]International Tomography Center, 3A Institutskaya Street, Novosibirsk 630090, Russia.

The development of efficient methods for gas adsorption studies is extremely important for a broad range of key technologies of modern society relying, e.g., on the large storage capacity of porous materials, heterogeneous catalysis and separation as well as purification of low-relative-volatility mixtures. Standard adsorption measurement techniques are slow and require an additional compositional analysis of non-adsorbed components of the gas mixture. The aim of this study is to develop a new, fast method for the quantitative measurement of competing adsorption of gas mixtures in porous media, based on spatially resolved remote detection time-of-flight nuclear magnetic resonance (RD TOF NMR).

In the experiment gas flows through a sample packed inside a capillary (called inlet capillary) close to the connection between the inlet and the outlet capillaries (see Figure 1a). Adsorption makes the average concentration of gas significantly higher in the sample area than in the outlet tubing, and therefore the average flow velocity in the sample region (u_{cat}) becomes lower than in the outlet tubing (u_{out}).This can be clearly seen in z-encoded TOF image as the slope in the sample region is much smaller than in the outlet capillary region (see Figure 1b).

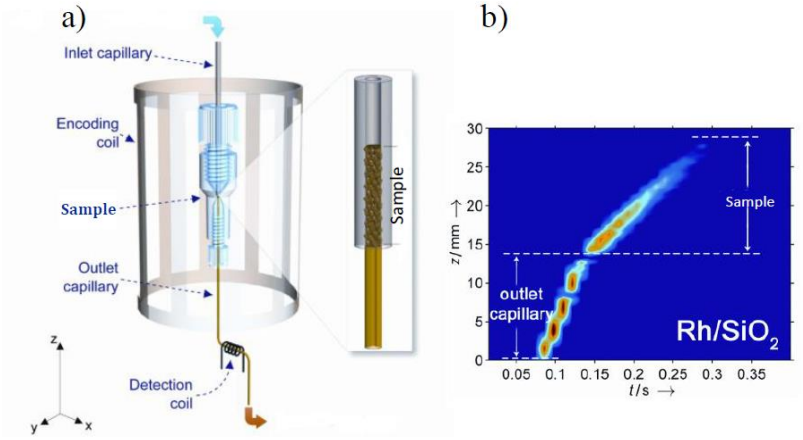

Figure 1 – a) Experimental setup. Gas mixture flows through the sample packed inside the inlet capillary close to the connection between the inlet and the outlet capillaries. b) z-encoded RD TOF images measured for Rh/SiO_2. The sample and the outlet capillary regions are shown with white dashed lines in the image.

The novel adsorption measurement technique introduced here uses the flow velocities, obtained from the slopes by linear least-squares fit, to calculate the amount of adsorbed gas (n_{ua}) using the initial analysis done by V. V. Zhivonitko et. al [1].The model states that the amount of absorbed gas per unit of the surface area is directly proportional to the ratio of the observed velocities:

$$n_{ua} \propto \frac{u_{out}}{u_{cat}} \quad (1)$$

A preliminary application of the model to analyze the amount of adsorbed propane when a mixture of propane, propene and hydrogen gas flowed through a microfluidic packed-bed reactor generating parahydrogen-induced polarization (PHIP) resulted in reasonable values, implying that TOF RD NMR is a very promising method for adsorption analysis. [1] However the conditions, such as amount of gases in the mixture, temperature of the system, pressure, sample dimensions, sample preparation, etc., were not optimized for these preliminary measurements, resulting in very large uncertainty in the calculated values. Consequently, new set of experiments with optimized conditions are required in order to prove the true potential of the method. An optimal experimental framework and theoretical model required for the investigations of single and multicomponent gases is developed by comparing the obtained quantitative information with standard measurements of gas adsorption isotherms. The latest results will be presented.

References

[1] V. V. Zhivonitko, V.-V. Telkki, I. V. Koptyug, Angew. Chem. Int. Ed. 51 (2012) 8054-8058

NMR Cryoporometry: What have we overlooked?

D. Kondrashova, R. Valiullin

University of Leipzig, Faculty of Physics and Earth Sciences, Linne Str. 5, 04103 Leipzig, Germany.

NMR cryoporometry [1] belongs to a family of the thermoporometry methods developed for structural characterization of porous solids. It exploits the occurrence of the pore size-dependent solid-liquid and/or liquid-solid transitions temperatures. Despite an extremely high resolution in the determination of the pore sizes which it may provide [2], this method has not found widespread applications. In part this is caused by the fact that an in-depth quantitative analysis of the thermoporometry data is often impeded by the lack of the appropriate theoretical models allowing for an assumption-free description of the solid-liquid equilibria in confined spaces. Thus, any analysis shall be based on the predictions of macroscopic thermodynamics with critical postualtes needed to be made. This especially has dramatic consequences for material possessing structural disorder, which have promoted many controversial discussions in the literature on the occurrence of phase transitions under confinements.

Recently, we have developed a microscopic lattice model which has allowed to gain deeper insight into the physics of the freezing and melting transitions for fluids confined in mesoporous materials with arbitrary pore geometries [3]. The model was based on the one of the earliest lattice models developed by Kosel and Stranski [4] for description of bulk crystal growth processes and which has greatly contributed to understanding of the diverse accompanying phenomena, including, most importantly, prediction of the roughnening transition. In our work, we have adapted this model to capture all essential physics of the solid-liquid equilbria in confined spaces. Starting with the configurational probabilty

$$P(\Psi_j) = Q^{-1} exp\left\{-\left[\sum_i \beta(-N_{ii}\phi_{ii} - N_{is}\phi_{is} + N_i F_i) + \sum_{i\neq k}\left(-\frac{1}{2}N_{ik}\phi_{ik}\right)\right]\right\} \quad (1)$$

for the occurrence of a certain crystal configuration as a function of all interactions involved, including the solid-lqiuid and solid-crystal ones, we have been able to re-derive on the microscopic basis the analogue of the Gibbs-Thomson law for both melting and freezing transitions. As the most important point, we have established that, depending on a parameter referred to as the Jackson's α-factor, which quantifies the entropic contribution to the overal free energy, the occurrences of the melting transition and, under certain conditions, of the freezing transition, can be dramatically different. The effect of the α-factor is exemplified in Figure 1 showing the relative change of the free energy upon crystal shape fluctuations for substances with the different α-factors. This finding warns that any comparison of the freezing and melting behaviors for different liquids should be done with care and not reporting on their α-factors can be a source for controversies. In this way, taking account of this parameter allowed us to explain uniformly the majority of the experimental observations reported so far.

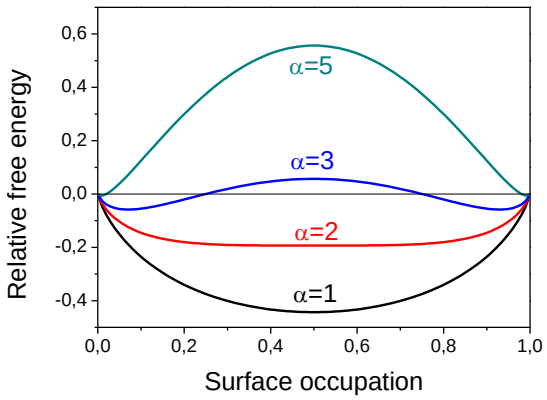

Figure 1 – Relative change of the free energy upon fluctuation of a crystal surface for materials with different Jackson factors.

The microscopic theory was complemented by the Monte Carlo studies, which delivered further imporant information on thermodynamics of the solid-liquid and liquid-solid equilibria in ideal and disordered pore structures. By comparing the thus obtained data to the experimental results obtained for mesoporous solids with ideal pore structures, we show that the model reproduces the key findings obtained in the thermoporometry experiments, including the shifted transition temperatures, irreversibility between freezing and melting, and strong impact of the pore structure. On considering disordered materials, we identify conditions and provide recipes for the most reliable characterization of disordered porous solids using the thermoporometry methods.

References

[1] Strange, J. H., Rahman, M. & Smith, E. G. Characterization of Porous Solids by Nmr. Phys. Rev. Lett. 71 (1993) 3589-3591.
[2] Schulz, P. S. Ionic Liquids as Solvent Probes for NMR Cryoporometry. ChemPhysChem 11 (2010) 87-89.
[3] Kondrashova, D. & Valiullin, R. Freezing and Melting Transitions under Mesoscalic Confinement: Application of the Kossel–Stranski Crystal-Growth Model. J. Phys. Chem. C 119 (2015) 4312-4323.
[4] Jackson, K. A. Kinetic Processes: Crystal Growth, Diffusion, and Phase Transitions in Materials. (Wiley-VCH, 2004).

Effects of Coherence Pathways on the Performance of the Modulated Gradient Spin Echo Sequence

I. Serša[a,b], F. Bajd[a,b], A. Mohorič[a,b]

[a]Jožef Stefan Institute, Jamova 39, 1000 Ljubljana, Slovenia, [b]Faculty of Mathematics and Physics, University of Ljubljana, Jadranska 19, 1000 Ljubljana, Slovenia.

Translational dynamics of liquids in various materials can also be characterized by a diffusion spectrum. In theory, a diffusion spectrum $D(\nu)$ is equal to a Fourier transform of molecular velocity autocorrelation function [1]. The diffusion spectrum can be measured by NMR using a sequence that uses a real or creates an effective oscillating gradient. As it is quite challenging to create a rapidly oscillating gradient of a high amplitude, we proposed another approach in which the gradient is static, however, the corresponding effective gradient is oscillating due to a simultaneous application of the CPMG RF pulse train. In the train each refocusing RF pulse changes the sign of the effective gradient thus making the effective gradient oscillating (Fig. 1). The sequence is therefore called modulated gradient spin echo (MGSE) sequence. By the MGSE sequence it is relatively easy to reach high frequency of a diffusion measurement and the sequence is seemingly easy to implement. However, MGSE measurements of unrestricted diffusion in simple liquids often gives unexpected results (red curve in Fig. 2) which indicates that there are important weaknesses in the experimental design of the MGSE sequence that need clarification.

In the MGSE sequence (Fig. 1), consecutive echoes are attenuated by a factor $\exp(-\gamma^2 G_N^2 TE^3 D/12)$ for a liquid sample with unrestricted diffusion. The attenuation at the end of the sequence that has N echoes and is T_{MGSE} long in therefore equal to $\exp(-\gamma^2 G_N^2 T_{MGSE}^3 D/12N^2)$. To attain a constant attenuation of the echo train at all measured MGSE frequencies $\nu_{MGSE} = N/2T_{MGSE}$ gradient amplitude must be increased proportionally with the MGSE frequency, i.e. $G_N = NG_2/2$. This has as a consequence different spread of precession frequencies over the sample with each measured MGSE frequency. For a cylindrical sample with a diameter d that is oriented with its axis perpendicularly to the gradient direction the frequencies are spread over the range $-\gamma G_N d/2 \le \Delta\omega_0 \le \gamma G_N d/2$. As the angular frequency of the RF pulses ω_1 is constant the condition $\omega_1 \gg |\Delta\omega_0|$ that guaranties prevalence of the direct coherence pathway of the MGSE sequence can no longer be met for the entire sample with an increasing MGSE frequency and therefore increasing G_N. However, the condition can still be met in a central slice across the sample perpendicular to the gradient direction. In the slice the diffusion attenuation obeys the above given diffusion attenuation formula, while in other parts of the sample where $\omega_1 \approx |\Delta\omega_0|$ signal attenuation due to diffusion is higher. This is because in these parts contributions of more complicated coherence pathways, which decay due to diffusion faster than the direct pathway, becomes significant [2,3]. The contribution of the pathways results also in a faster decaying signals of the entire sample that can be incorrectly attributed to a faster diffusion at higher MGSE frequencies. An example of such misinterpretation is shown in Fig. 2, red curve that corresponds to the calculated diffusion spectrum of water from signals measured from the entire sample. The sample was a 5 mm water filled tube and MGSE parameters were: T_{MGSE} = 100 ms, N = 10, 20 … 600, G_{600} = 4.4 T/m, $|\Delta\omega_{0,\max}|/2\pi$ = 466 kHz, $\omega_1/2\pi$ = 135 kHz. The unusual frequency dependency of the diffusion spectrum was not observed when signals were analyzed only from an 8 kHz 'thick' central slice so that the condition $\omega_1 \gg |\Delta\omega_0|$ was met quite well (Fig. 2, black curve). Signals from the slice were obtained as a central frequency point of the Fourier transformed acquired echo signals in a time domain; echoes were acquired in 128 points with a dwell time of 1 µs.

The presented improvements in the MGSE sequence implementation enable relatively reliable application of the sequence for measurements of diffusion spectra of various materials in the frequency range of up to 3 kHz.

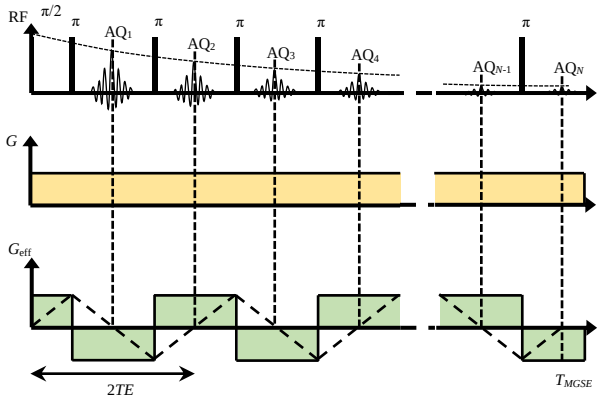

Figure 1 – MGSE pulse sequence.

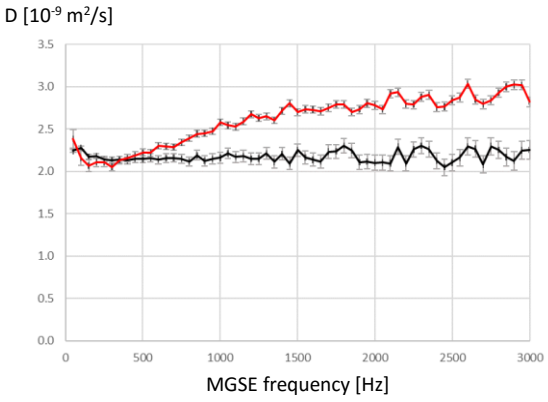

Figure 2 – Diffusion spectrum of water measured at $\omega_1 \gg |\Delta\omega_0|$ (black) and $\omega_1 \approx |\Delta\omega_0|$ (red).

References

[1] J. Stepisnik, S. Lasic, A. Mohoric, I. Sersa, A. Sepe, J Magn Reson 182(2) (2006): 195-199.
[2] M. D. Hurlimann, J Magn Reson 148(2) (2001): 367-378.
[3] Y. Q. Song, J Magn Reson 157(1) (2002): 82-91.

Development of continuous flow Xenon-129 for gas phase NMR flow and velocimetry studies in porous media

Fraser Hill-Casey[a,b], Sean P. Rigby[b], Thomas Meersmann[a] and Galina E. Pavlovskaya[a]

[a]Sir Peter Mansfield Imaging Centre, University of Nottingham, Nottingham, NG7 2RD, United Kingdom; [b] Department of Chemical and Environmental Engineering, University of Nottingham, Nottingham NG7 2RD, United Kingdom

Flow within porous media is an important factor in many aspects of science and technology and thus requires suitable probe to integrate the behaviour of liquids and gases within the porous structures. Traditionally used measurement techniques, such as the optical laser doppler anemometry and particle imaging velocimetry, tend to require either transparent or translucent samples and necessitate the use of "scatterers" present within the fluid. In turn typical gas velocimetry measurements normally utilises either hot wire anemometry or pressure differences as a probe of the flow however these measurements are in turn a single point and a bulk measurement, further both require invasive sensors [1]. With careful selection of a probe nuclei Nuclear Magnetic Resonance (NMR) provides a non-invasive method to directly interrogate the flow properties of the nuclei within a flow regime. NMR techniques show further promise by the ability to probe opaque samples.

Gas flow in particular is extremely important in a wide range of industrial processes and the ability to examine operational conditions of a variety of these processes is extremely valuable. Moreover with the ability to use gas as a probe of opaque samples, such as foams, and rocks. Further, gases are able to provide information not typically available from liquid phase NMR such as pressure dependence, gas dispersion, molecular self-diffusion and sheer rates. Nevertheless, gas phase flow monitoring provides a particular challenge for NMR due to the far lower density's hence, lower signal density with dry air density being only 1.197 kg/m^3 compared to 998.2 kg/m^3 for that of water. Common gas phase probes include sulphur hexafluoride (SF6) and alkenes, however such molecular probe suffer from short T_1 and T_2 relaxation times making imaging problematic and impacting on the timescales accessible [2].

Utilising continuous flow spin exchange optical pumping (SEOP) for production of hyperpolarised (hp) ^{129}Xe we are able to circumvent a number of the challenges found by thermally polarized gas probes such as the low signal intensity and short T_1 and T_2 relaxation times. Further the signal produced by the system is such that it was possible to perform both 2D and 3D imaging. With this we present a robust methodology for measurements of gas dispersion throughout model porous media foams with heterogeneous permeability profiles. Utilising the same production methodology it was further possible to perform rapid acquisition of temporally resolved velocimetry experiments. These developments show great promise for the use of hp ^{129}Xe as a non-invasive probe for the determination of properties within porous structures.

References

[1] Newling, Benedict. "Gas Flow Measurements By NMR". Progress in Nuclear Magnetic Resonance Spectroscopy 52.1 (2008): 31-8.
[2] Koptyug, Igor V et al. "Thermally Polarized 1H NMR Microimaging Studies Of Liquid And Gas Flow In Monolithic Catalysts". Journal of Magnetic Resonance 147.1 (2000): 36-42.

Recent progress in Magnetic Resonance Imaging of hard and soft solids

S. Barrett[a]

[a]Yale University, Department of Physics, Sloane Physics Lab, 217 Prospect Street, New Haven, CT, USA.

Magnetic resonance imaging (MRI) of solids is rarely attempted. A principal reason is that solids have broader NMR linewidths, compared to that of ^{1}H in free water, which severely limits both the spatial resolution and the signal-to-noise ratio. Basic physics research, stimulated by the quest to build a quantum computer, unexpectedly led to a novel NMR pulse sequence that helps with this long-standing problem [1]. Applying field gradients in synch with this 'quadratic echo' line-narrowing pulse sequence opens a fresh approach to the MRI of hard and soft solids with high spatial resolution, and with a range of potential uses. For example, this technique can be used for three-dimensional MRI of ^{31}P in ex vivo bone and soft tissue samples [2]. Recent progress using this approach, including strategies to accelerate the imaging of solid samples (as well as nD NMR experiments) [3], will be reported. Future applications (for example, to geology, and to the physics of granular matter) will be discussed.

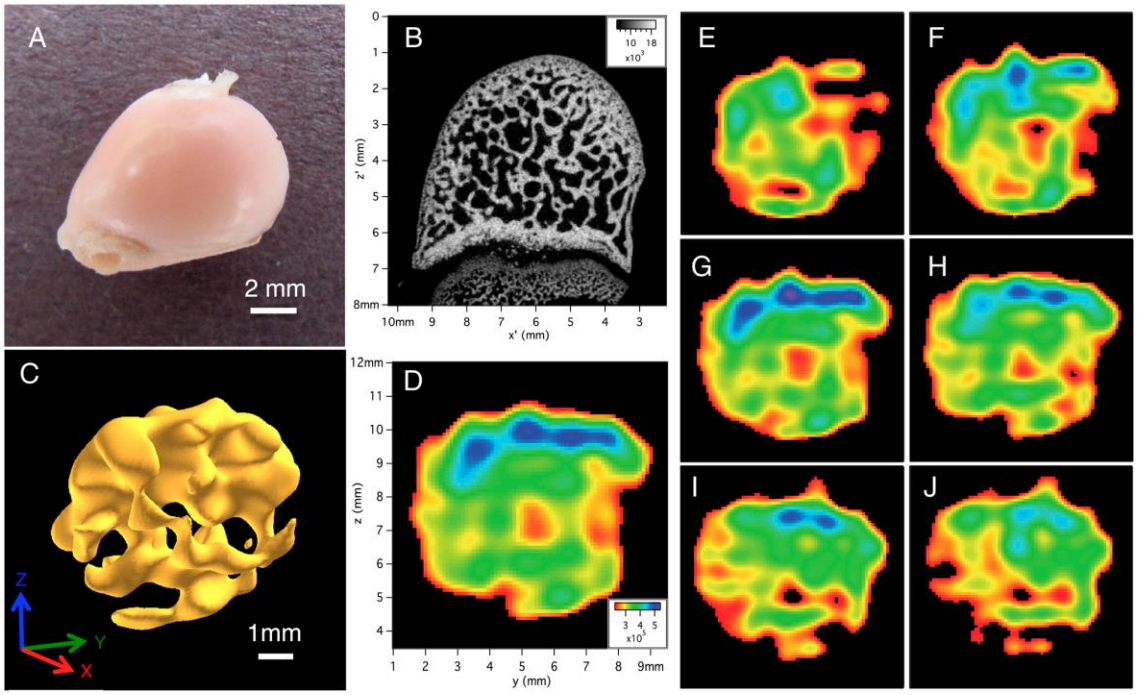

Figure 1 – Images of an ex vivo rabbit femoral head sample. (A) Photo of sample. (B) Two-dimensional slice of micro-CT data. The 2D resolution is $(0.0185\ mm)^2$ and the slice thickness is 0.0185 mm. (C) Isosurface rendering of the 3D image of ^{31}P in rabbit femoral head. The isosurface value is 60% of the maximum signal value and shows trabecular bone. The spatial resolution is 0.458 x 0.458 x 0.422 mm^3 and the imaging time was 70.4 h. (D) A 2D slice of the 3D data shown in Fig. 1C (zero-filled by a factor of four) with thickness of 0.115 mm. Note that these axes are different from those used in Fig. 1B and the orientation of the bone is different than in both Fig. 1 A and B. Here the "flat end" of the bone is on the right edge. (E–J) Multiple 2D slices (each 0.115 mm thick) cutting along the x axis going in the positive x direction (with a 0.458-mm step size) through the 3D dataset shown in Fig. 1C, using the same color scale and FOV as in Fig. 1D. The 2D slice shown in Fig. 1D is between slices shown in Fig. 1G and Fig. 1H. Adapted from reference [2].

References

[1] Y. Dong et al., Phys Rev Lett **100**, 247601 (2008).
[2] M.A. Frey et al., Proc. Natl. Acad. Sci. U.S.A. **109**, 5190 (2012).
[3] M.A. Frey et al., J. of Magn. Reson. **237**, 100 (2013).

Load-dependent low-field profiling and relaxometry of osteoarthritic articular cartilage

E.Rössler[1], C. Mattea[1], M. T. Nieminen[2,3], S. Karhula[2,3], S. Saarakkala[2,3], S. Stapf[1]

[1]Dept. of Technical Physics II, TU Ilmenau, 98584 Ilmenau, Germany; [2]Research Unit of Medical Imaging, Physics and Technology, University of Oulu, P.O. 5000, 90014 Oulu, Finland; [3]Medical Research Center, University of Oulu and Oulu University Hospital, P.O. 50, 90029 Oulu, Finland

At low magnetic fields, T_1 variation within cartilage represents a robust parameter that is employed to quantify the layered structure in the tissue and is sensitive to factors such as enzymatic degradation, external load, and diseases such as osteoarthritis. Variable-field relaxometry provides access to the quadrupolar dips that probe proton-nitrogen interaction and thus the content and local order of glycosaminoglycans and collagen. In this study on 20 human cartilage samples, low-field and variable-field techniques were combined for the first time to correlate NMR parameters and response to load with the severity of osteoarthritis.

While low-field MRI significantly enhances the T_1 contrast in cartilage tissue, variable-field relaxometry identifies the properties of cartilage and glycosaminoglycan (GAG) as well as overall molecular mobility. In particular, the ^{14}N content of both collagen and GAG give rise to so-called quadrupolar dips, i.e. enhanced relaxation rates of ^1H particularly at field strengths between 50 and 70 mT. In this study, both methods are combined for the first time with the purpose of quantifying correlations with the degree of osteoarthritic degeneration in human cartilage, and to establish cross-correlations between low-field and variable-field NMR.

The dependence of magnetic resonance relaxation times T_2 and T_1 in bovine and human articular cartilage is investigated by portable, single-sided scanners at magnetic field strengths of 0.27 T and 0.44 T, respectively. One-dimensional, depth-dependent scans (profiles) were carried out with spatial resolutions between 20 and 50 μm. The well-known triple layer structure of cartilage was assigned with the relaxation weighted profiles for bovine as well as human samples. Bovine samples were measured before and after soaking for 24 h in either trypsin or collagenase. Twenty human samples with different degrees of osteoarthritis, covering Mankin grades 0-12, were compared with respect to their average and maximum vs. minimum values of relaxation times. In addition, the variation of these values under unidirectional compression at 0.6 MPa were recorded.

Employing field-cycling relaxometry, the dispersion of T_1 in the ^1H Larmor frequency range of 10 kHz to 30 MHz was monitored, and results were analysed in terms of power-law relations $T_1 \sim \omega^\gamma$ and total area of the ^1H-^{14}N cross-relaxation quadrupolar dips for the set of human samples.

The layered structure of mammalian articular cartilage, which is a consequence of different degrees of order of the collagen fibers but also of a gradient of water and glycosaminoglycan (GAG) concentration, results in a pronounced T_2 variation at all magnetic field strengths [1]. A similar variation of T_1, typically covering a ratio of 3-5 between maximum and minimum values inside the tissue, was identified at a field strength of 0.27 T, while it has been reported as minimal at high magnetic field strengths [2]. T_1 thus has thus been identified as a suitable parameter to follow changes in cartilage properties by low-field NMR. While previously the T_1 relaxation rate at 400 MHz has been associated with water content of articular cartilage [3], T_1 at lower field strength is anticipated to relate more directly to cartilage constituents.

Average T_1, as well as cartilage thickness obtained from T_1 measurements of human samples, is found to correlate negatively with Mankin grade. At the same time, a significant correlation was identified for relaxation time reduction before and after uniaxial compression at 0.6 MPa, a typical value for forces appearing in the human knee and hip joint. This finding is of importance since the spatial resolution of 50 μm obtained with the single-sided scanner is about one order of magnitude better than the one in clinical high-field or low-field scanners [4], thus allowing a much more reliable definition of thickness change which even includes resolution of the three main cartilage layers.

At ^1H Larmor frequencies of 2-3 MHz, the so-called quadrupolar dips are superimposed onto a frequency-dependent signature of T_1 that can be approximated by power-laws. Varying the composition, water content or structural integrity of cartilage affects both the general frequency dependence of T_1 and the shape of the quadrupolar dips, providing a possible diagnostic access to arthropathies such as osteoarthritis (OA) [5]. In this study, a statistically significant correlation of the area of the quadrupolar dips with Mankin grade is demonstrated: diseased tissue contains less GAG but more water. This observation is confirmed by artificially altered tissue using trypsin or collagenase [6]. Furthermore, the exponent γ in the relation $T_1 \sim \omega^\gamma$ correlates with the thickness of the tissue, providing a further approach to relating the molecular mobility to the macroscopic properties of cartilage. These results allow for an improved diagnostic interpretation of low-resolution clinical MRI particularly at dedicated extremity scanners.

References

[1] Y. Xia, Invest. Radiol. 35 (2000) 602-621.
[2] E. Rössler, C. Mattea, A. Mollova, S. Stapf, 213 (2011) 112-118.
[3] J.E. Berberat, M.J. Nissi, J.S. Jurvelin, M.T. Nieminen, Magn Reson Imaging. 27 (2009) 727-32.
[4] E. Rössler, C. Mattea, S. Stapf, J. Magn. Reson. 251 (2015) 43-51.
[5] L.M. Broche, G.P. Ashcroft, D.J. Lurie, Magn. Reson. Med. 68 (2012) 358-362.
[6] E. Rössler, C. Mattea, S. Stapf, Magn. Reson. Med. 73 (2015) 2005-2014.

Single-sided NMR on a quasi-real model of bone for the diagnosis of osteoporosis

M. Barbieri[a], L. Brizi[a,b], M. Nogueira d'Eurydice[c], S. Obruchkov[c], H. Liu[c], V.Bortolotti[d], P. Fantazzini [a,b], P. Galvosas[c]

[a]Department of Physics and Astronomy, University of Bologna, Italy; [b]Museo della Fisica e Centro Studi e Ricerche Enrico Fermi, Roma, Italy; [c]MacDiarmid Institute for Advanced Materials and Nanotechnology, School of Chemical and Physical Sciences, Victoria University of Wellington, PO Box 600, Wellington 6140, New Zealand ; [d]Department DICAM, University of Bologna, Italy.

Osteoporosis is a disease characterized by a reduction of bone mineral density (BMD) and alterations of trabecular architecture, leading to high risk of bone fractures [1]. Dual X-rays Absorptiometry (DXA) is the gold standard technique, although it does not measure microarchitecture parameters, which are important in addition to BMD for a correct diagnosis [1]. MRI is able to assess bone microarchitecture parameters [2] and applications have been reported for trabecular bone porosity assessment by NMR Relaxometry [3]. A new application of NMR to assess Bone-Volume to Total-Volume (BV/TV) of trabecular bone structure has been proposed by using different single sided devices [4], including the NMR-MOUSE (Magritek) [5] and the NMR MOLE [6]. The signal detected comes from ^{1}H nuclei of the marrow filling the inter-trabecular space. Good agreement between NMR and micro-CT determinations of BV/TV was found [4]. The procedure is based on the evaluation of the ratio between the signals detected by the single sided device from the sensitive volume inside the bone and inside a sample of bulk marrow.

In [4], measurements were performed on cylindrical bone samples cored from pig shoulders. In order to extend this novel procedure to an in-vivo scenario, a deeper study is needed on samples more realistic than simple samples of bone. Methods have been tested to physically suppress the signal of tissues other than bone marrow, as muscle and cartilage, but preserving the signal from the marrow of the inter-trabecular space. First of all, the characterization of the different tissues was performed by T_1-T_2 and D-T_2 correlation maps acquired with the NMR-MOLE and the NMR-MOUSE, respectively. While the NMR MOUSE provides a better-localized magnetic field, the sensitive volume of the NMR-MOLE is larger and an increase of the SNR is expected. These measurements have shown that the self-diffusion coefficient of the fat in the marrow is an order of magnitude smaller than those of the water in muscle and cartilage (Fig. 1a). On the basis of this observation, a customize pulse sequence was edited, to weight the signal by diffusion (DW- T_1-T_2). As shown in Fig. 1b, this sequence allowed us to suppress, in a quasi-real model of bone made of muscle, cartilage and bone, the signals of muscle and cartilage, leaving only the signal from intertrabecular marrow.

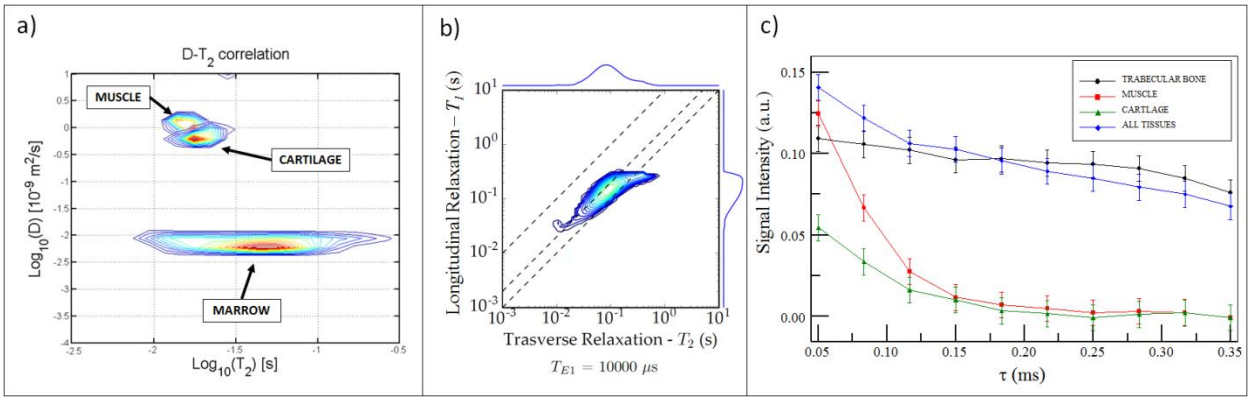

Figure 1 – a) D-T_2 correlation maps of cartilage, muscle and marrow; b) DW- T_1-T_2 correlation map for a sample containing trabecular bone (with marrow), muscle and cartilage. Inversions were performed by an algorithm based on [7]. c) Stimulated Spin Echo: Signal intensities weighted by diffusion for different tissues. Error bars correspond to two STD. Scanned volumes of MUSCLE and CARTILAGE are bigger than those of muscle and cartilage in the sample ALL TISSUES.

Finally, the application of a Stimulated Echo sequence by NMR-MOUSE with the choice of a suitable time for diffusion, allowed us to suppress the cartilage and muscle signals (Fig. 1c), and to determine BV/TV on the quasi-real model of bone, opening to the way for the application in-vivo. The NMR-MOUSE was chosen because it has a strong constant field gradient within the sensitive volume, that allows one to set the optimal time for diffusion, independently by the position of the tissues within the sensitive volume, and thus it is easy to weight the signal by diffusion. Moreover, it allows one to select the signal from thin slices in selected regions of the analyzed sample. The whole of the experiments performed assures that single-sided NMR scanners can be used to assess the value of BV/TV in trabecular bone, with the advantage of being portable, low-cost and non-invasive devices, so allowing one to easily perform wide campaigns of screening of the population at risk of osteoporosis.

References

[1] H.K. Genant, G. Guglielmi, M. Jergas, M. EDITORS, Bone Densitometry and Osteoporosis, Springer Berlin, 1998.
[2] K. Roland , A.J. Burghardt, S.Majumdar , T.M.Link, High-resolution Imaging Techniques for the Assessment of Osteoporosis, Radiol Clin North Am, 48 (2010) 601–621; A.J. Burghardt, T.M. Link, S.Majumdar, Clin Orthop Relat Res, 469 (2011) 2179-2193.
[3] P. Fantazzini, V. Bortolotti, R. J. S. Brown, M. Camaiti, C. Garavaglia, R. Viola, G. Giavaresi, Two 1H-NMR Methods to Measure Internal Porosity of Bone Trabeculae: by Solid-Liquid Signal Separation and by Longitudinal Relaxation, J Appl Phys 95 (2004) 339-343.
[4] M. Barbieri, The use of mobile single-sided NMR for the diagnosis of osteoporosis: a preliminary study, Master Degree thesis, Univ. Bologna, April 2016.
[5] B. Blümich, F.Casanova, J.Perlo, Single-Sided NMR, Springer, 2010.
[6] B. Manz, A. Coy, R. Dykstra, C.D. Eccles, M.W. Hunter, B.J. Parkinson, P.T. Callaghan, A mobile one-sided NMR sensor with a homogeneous magnetic field: The NMR-MOLE, J Magn Res, 183 (2006) 25-31.
[7] L. Venkataramanan, Y. Q. Song, M. D. Hürlimann, Solving Fredholm integrals of the first kind with tensor product structure in 2 and 2.5 dimensions, IEEE Transactions on Signal Processing, 50(5) (2002) 1017–1026.

Application of Earth's Field Nuclear Magnetic Resonance to Multiphase Flow Metering

M.L. Johns[a], K.T. O'Neill[a], P.L. Stanwix[a] and E.O. Fridjonsson[a]

[a] School of Mechanical and Chemical Engineering M050, University of Western Australia, 35 Stirling Highway, Crawley 6009, Western Australia, Australia.

(Near) instantaneous multiphase flow metering has significant potential in a number of industries, including the oil and gas industry [1]. Multiphase flow meters (MPFMs) provide several benefits with respect to both process safety and reducing operational costs. The exploitation of nuclear magnetic resonance (NMR) in MPFMs is now a commerical reality [2]; by comparison with alternative methods, NMR is non-invasive, does not require any nuclear source material, provides a number of mechanisms to differentiate phases and is able to measure both velocity and phase fraction. Here we present the use of the Earths's magnetic field (NMR) for detection in a multiphase flow meter.

This NMR MPFM system (shown in Figure 1), constructed at minimal cost and fully operational at the University of Western Australia (UWA) [3], consists of a pre-polarising permanent magnet (Halbach array) located upstream of an Earth's field NMR detection coil (resonance frequency of ~2KHz). By appropriate analysis using Tikonov Regularisation techniques of the simple free induction decay (FID)) acquired for a flowing stream, we are able to determine the velocity probability distributions. This is in effect a 'time-of-flight' measurement. The accuracy of the system (for such single phase flow) is verified over a wide parameter space by direct comparison of the mean values of the velocity distributions to the velocities measured from an in-line rotameter as well as with the theoretically expected velocity distributions.

In two phase gas/liquid flow, NMR FID signal analysis is used to track both the liquid holdup and liquid velocity over time (at 1-3 Hz). This readily enables various two phase flow regimes (e.g. stratified or slug flow) to be instantaneously identified, which is useful in its own right and critical to the subsequent NMR data analysis. The NMR liquid holdup measurement show a good correlation to video analysis of a transparent section of the flowing stream and matches well with the expected superficial system liquid velocity. Sample liquid hold-up data is shown in Figure 2 for stratefied and slugging flow. Finally a proposed extension of the apparatus to three-phase flow and high pressure/temperature conditions will be outlined.

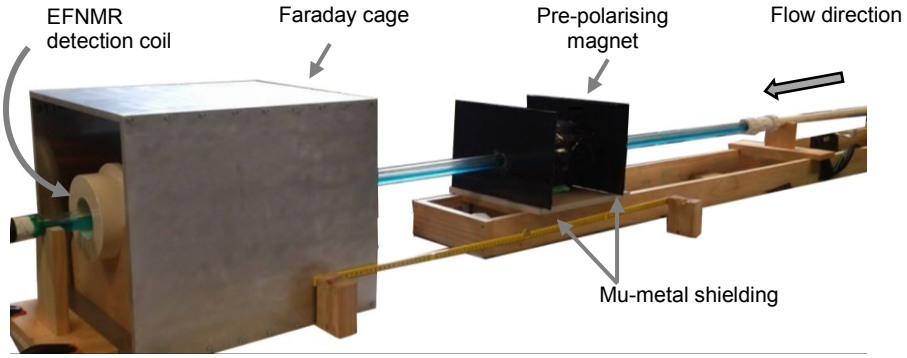

Figure 1 – UWA 'simple' NMR MPFM with detection in the Earth's magnetic field.

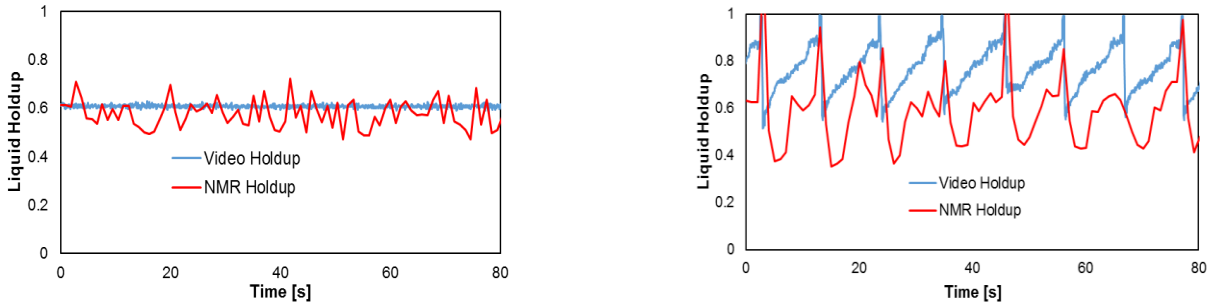

Figure 2 – Sample liquid holdup measurements for (a) stratefied and (b) slugging two-phase flow as determined by both NMR and video-analysis. NMR measurements were performed at 2 Hz. The slugs are clearly evident in (b).

References

[1] Thorn, R., Johansen G.A and Hjertaker, B.T., Three-phase flow measurement in the petroleum industry, *Meas. Sci. Technol.*, 24(2013) 012003.
[2] http://krohne.com/en/products/flow-measurement/magnetic-resonance-flowmeters/m-phase-5000/
[3] Fridjonsson E.O., Stanwix P.L., Johns M.L., Earth's field NMR flow meter: Preliminary quantitative measurements, *J. Magn. Reson.*, 245 (2014) 110-115.
[4] O'Neill, K.T., Fridjonsson, E.O., Stanwix, P.L. and Johns, M.L, Quantitative Velocity Distributions via Nuclear Magnetic Resonance Flow Metering, *submitted to J. Magn. Reson.*

A modular single-sided NMR sensor design with multifunction

Z. Sun, L. Xiao, G. Liao, Y. Zhang

State Key Laboratory of Petroleum Resources and Prospecting; China University of Petroleum, Beijing 102249, Beijing, China.

In this research, the NMR sensor is designed with both gradient and uniform magnetic field detection modes, and it also has the advantage of both portability of mobile instrument and precision of medium-sized instrument. It can not only do the mobile detection but also do accurate detection with the whole sample or different slices at multiple frequencies in different magnetic fields.

The sensor designed in this research has three work modes. Each mode's magnet model and the corresponding B_0 field distribution are simulated as shown in the figure 1. Mode 1 is designed as mobile detection mode. In this mode only 1 set magnets module is used. So its weight and size are small. Mode 2 is based on mode 1. An outer magnet module is combined with mode 1's magnet module in this mode. Both mode 1 and 2 are inhomogeneous magnetic field detection modes, but mode 2 has higher precision, higher working frequency and larger sensitive volume. Mode 3 is uniform magnetic field detection mode. The outer magnet module is combined with a bar magnet to generate uniform magnetic field.

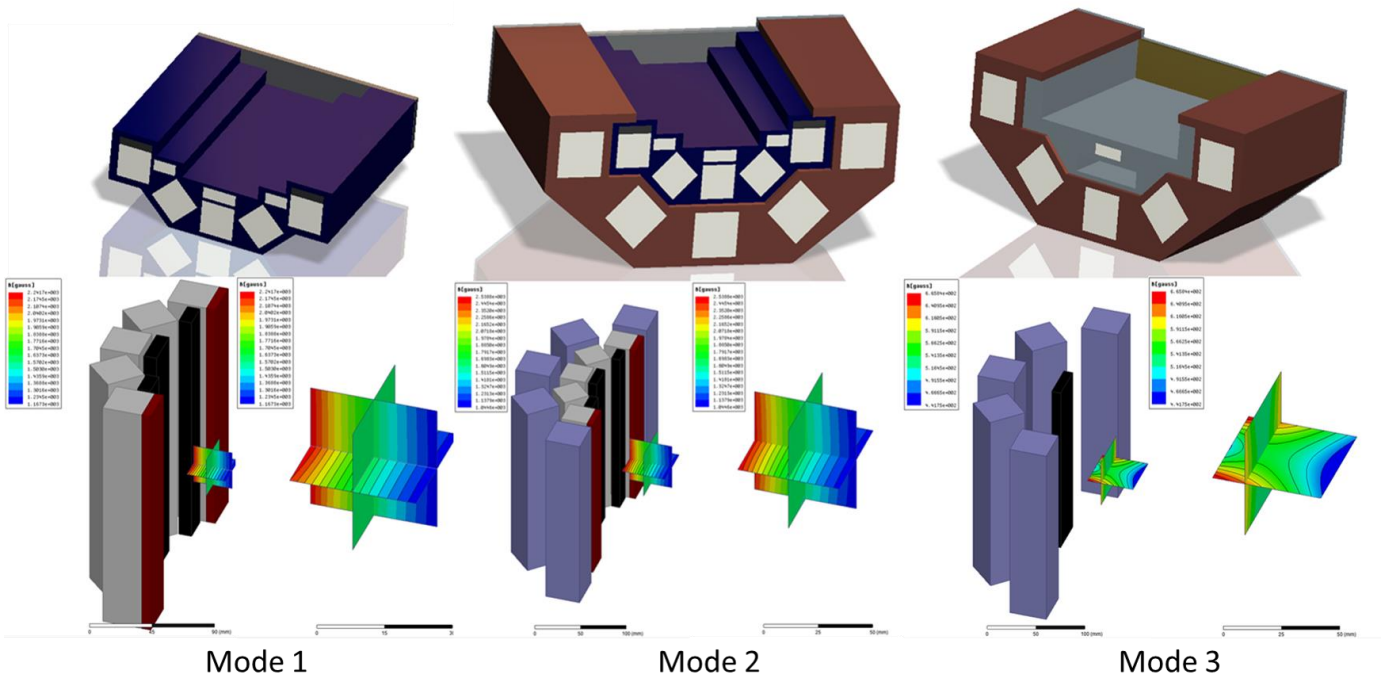

Figure 1 – Magnet model and magnetic field distribution of each detection mode.

In each target area the B_0 field of mode 1 and 2 has a constant vertical gradient and distribute uniformly in horizontal direction. The target area of mode 1 is 30*30*30mm^3 whose center is located at 40mm above the surface of the magnet. In this area B_0 field has a constant gradient of 3.54T/m. And the uniformity of mode 1's B_0 field magnitude can reach 197ppm in a 10*10 mm^2 lateral plane at the center of the area. The center of mode 2's target area is located at 50mm above the surface of the magnet, and the area of it is 50*50*50mm^3. In this area the gradient of B_0 field is 3.94T/m. And the uniformity of mode 2's B_0 field can reach 49ppm in a 10*10mm^2 lateral plane at the center of the area. The B_0 field of mode 3 distributes uniformly in an X shape area, and the strength of B_0 in this area is about 53.2 mT.

The corresponding RF magnetic field B_1 can be calculated out from each B_0 field generated by these 3 modes. And with the information of RF magnetic fields the antenna could be designed out. Then with B_0 and B_1 the SNR could be calculated out with the following equation.

$$(S/N) = \left\{\frac{\sqrt{2}N\emptyset\gamma^3h^2I(I+1)}{6(\mathrm{k}T)^{3/2}}\right\}\frac{B_0^2VB_1}{(I_1^2Z_0/2)^{1/2}(\Delta\omega)^{1/2}} \quad (1)$$

References

[1] F. Casanova, J. Perlo, B. Blümich (Eds.), Single-Sided NMR, Springer, Manheim, 2011.
[2] Baoxin. Guo, Lizhi. Xiao, The design and applications of unilateral NMR probe, China University of Petroleum, Beijing, 2012.
[3] Andrew. E. Marble，Igor. V. Mastikin, et al. An analytical methodology for megnetic field control in unilateral NMR, Jounal of Magnetic Resonance, 2005, 1784(1):78-87.
[4] Xu Zheng, Guo Pan, He Xiaolong, et al. Based on the principles of NMR study of the aging of composite insulators, High-Voltage Electrical. 2012, 48(3):21-25.

NMR and X-ray µCT study of plasticizer (Hexamoll® DINCH®) in PVC

N.Nestle[a], A. Šandor[a] M. Pfeiffer[b]

[a]BASF Materials Physics and Analytics, GMC/R, B007, D-67056 Ludwigshafen, Germany; [b]BASF Industrial Petrochemicals Europe E-CPI/MB, H201, D-67056 Ludwigshafen, Germany

Hexamoll® DINCH® (1,2-cyclohexane dicarboxylic acid di-isononylester) is BASF's non-phthalate plasticizer which has been available for more than 10 years now as a substitute for traditional phthalate plasticizers. Due to its excellent toxicological profile it meets the demanding regulatory requirements for highly sensitive applications, e.g. toys, food packaging and medical devices. Until very recently [1], there was no non-destructive NMR method available for the study of plasticizer content in PVC. In [1], the potential of unilateral NMR profiling for non-destructive studies of plasticizer content in PVC materials was demonstrated for diisononyl phthalate and 1,2-cyclohexane dicarboxylic acid diisononyl ester.

We have performed similar experiments on PVC plasticized with Hexamoll® DINCH®. In addition to the NMR profiling experiment, we have also applied conventional NMR relaxation time measurements and field gradient diffusion NMR on the same system. Furthermore, we also studied the potential of X-ray mictrotomography for studies of the plasticizer content in PVC. The rationale behind the X-ray experiments is the fact that PVC due to its chlorine content exhibits a higher X-ray absorption than simple aliphatic hydrocarbons. With the introduction of increasingly large plasticizer quantities into the PVC, the volume density of PVC and thus of chlorine is reduced and lower X-ray absorption is observed. It can be seen from figure 1 (A) that this is indeed the case. However, the achieved contrast is not very strong and like that only plasticizer concentration differences in the range of 10% phr can be safely discerned.

A 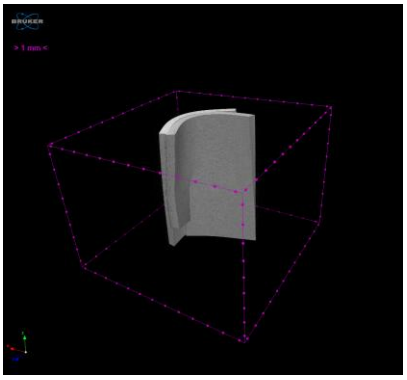

B 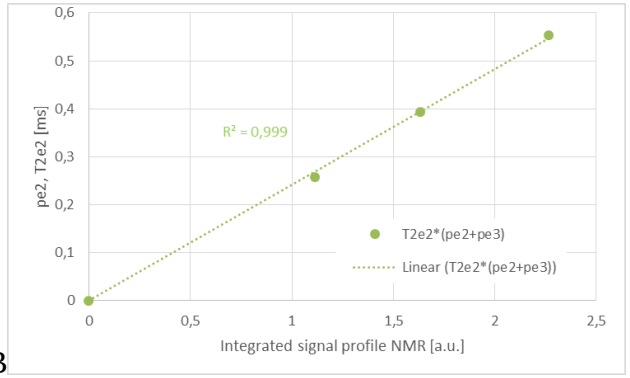

Figure 1 – (A) X-ray micro CT image of two pieces of PVC containing 50 % phr (outer) and 70% (inner) phr Hexamoll® DINCH® (B) correlation between measured signal intensity in NMR profiling and expected intensity on the basis of the conventional TD-NMR experiments.

In conventional time domain NMR studies, we observed a signal decay with several clearly distinguishable componentens that can be attributed to (A) still crystalline PVC, (B) mobilized PVC, and two further components that come from the plasticizer. Relaxation times are less than 20 µs for (A), about 100 µs for (B), about 500 µs for the main signal component from the plasticizer and about 20 ms for a more mobile plasticizer population that only makes up 10 % or less of the overall plasticizer signal. The relaxation times of the mobilized PVC and of the majority plasticizer component show an excellent correlation with the plasticizer content. Similarly, there is a very good correlation between the fraction of non-mobilized PVC and the plasticizer content. The correlations are good enough to observe significant differences for plasticizer concentrations about 1% phr different from each other.

Based on the relaxation times observed in conventional NMR, we can expect the plasticizer signal to dominate the signal in the profiling NMR experiment. As can be seen from figure 1 (B), this is indeed the case. The best correlation between the profiling data and the data from the TD-NMR is found for the computed signal integral.

Furthermore, we studied the diffusion behaviour of the plasticizer both by PFG NMR in the high field and by profiling NMR. In PFG NMR multiexponential self-diffusion behaviour was observed with self-diffusion coefficients in the range between 10^{-11} m^2/s and 10^{-14} m^2/s. In the profile NMR experiment transport diffusion of plasticizer between polymer layers with different plasticizer content and different chemistry can be visualized.

References

[1] A.Adams., R. Kwamen, B. Woldt, M. Graß Macromol. Rapid Commun., 36 (2015): 2171–2175. doi: 10.1002/marc.201500409 .

Visualizing the Sensitive Volume of a Unilateral NMR Sensor

C. Rehorn[a], R. Höhner[a], B. Blümich[a]

[a]Institut für Technische und Makromolekulare Chemie, RWTH-Aachen University, Germany.

Stray-field magnets such as the NMR-MOUSE (MObile Universal Surface Explorer) [1, 2] or the Surface GARField (Gradient At Right angles to the Field) [3] are known for performing well in a magnetic field that is tuned to be homogeneous within a small spot located a few millimeters away the surface of a sensor, thus enabling measurements on samples of arbitrary size. The size and shape of the sensitive volume is governed by the interaction of the magnetic field (B_0) produced by the permanent magnets and the rf-field (B_1) produced by a coil.

The high axial gradient in the MOUSE causes the sensitive volume to be a very thin slice, in most cases between 100 µm and 250 µm thin. Because the thickness of the slice determines the minimum axial resolution in depth profiling this value has often been measured and reported [4]. The lateral shape and dimensions of the excited volume, however, were previously only measured in a time consuming process, by moving a very small block of sample in a two dimensional grid. [5] Here we present a faster and simpler way that utilizes the inverse Radon transformation to reconstruct the two dimensional image of the sensitive volume.

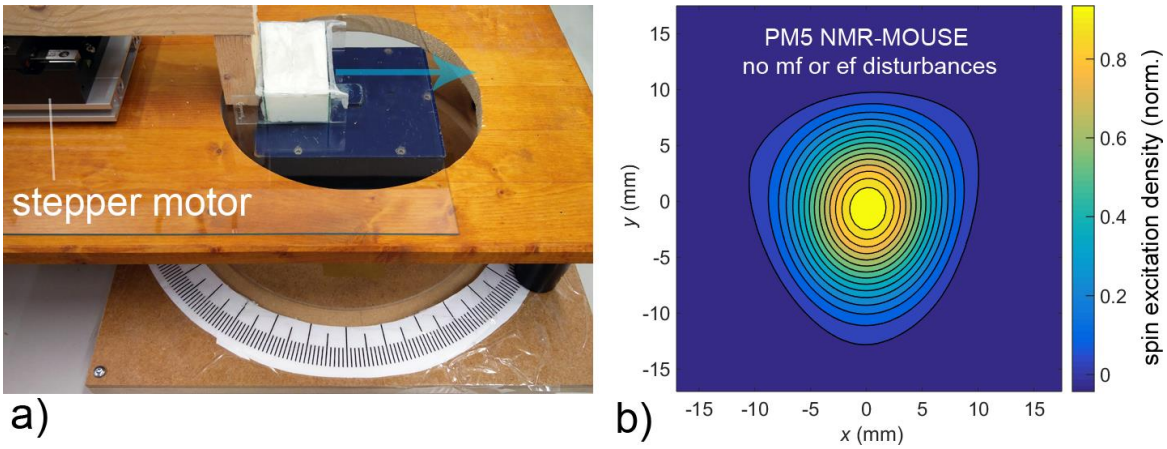

Figure 1 – The sensitive slice of a PM5 NMR-MOUSE is measured by moving a block of sample through the spot (a). The resulting reconstruction of the excited volume (b) shows an oval shape with an unexpected asymmetry likley due to the inhomogeneity of the permanent magnets.

While step-wise pushing a block of homogeneous sample over the surface of a PM5 MOUSE, CPMG sequences were measured in order to obtain contrast similar to an NMR depth profile (Fig. 1a). This process was repeated while increasing the angle spanned by the magnetic field irection and the stepping direction. By differenciating the resulting profiles, projections of the sensitive volume are created for each angle. These projections are then subjected to inverse Radon transformation to obtain a reconstruction of the plane (Fig 1b).

With this method we show the shape and also the density of excited spins for the case of disturbances in both in the radio frequency field and in the magnetic field. These disturbances are a common occurence when measuring samples that include metal that can interact with either one or both, B_0 and B_1. Furthermore, by correlating spin excitation densities of different experiments we display spatially resolved signal loss for cases where field disturbances occur.

To show how the shape of the B_1 coil can change the sensitive volume, we constructed a rectangular coil with dimensions similar to the ones used in the commercially available version of the PM5 NMR-MOUSE. The resonant circuit was tuned and matched to the same frequency, and the parameters pulse length and dwell time were kept constant in each new experiment. We hope that the simplified measurement along with a better understanding of the shape of the excited volume will aid in constructing and characterizing future sensors.

References

[1] G. Eidmann, R. Savelsberg, P. Blümler, B. Blümich, , J. Magn. Reson. A 122 (1996) 104–109.
[2] B. Blümich, J. Perlo, F. Casanova, Prog. Nucl. Magn. Reson. Spectrosc. 52 (2008) 197–169.
[3] P.J. McDonald, P.S. Aptaker, J. Mitchell, M. Mulheron, J. Magn. Reson. 185 (2007) 1–11.
[4] J. Perlo, F. Casanova, B. Blümich, J. Magn. Reson. 176 (2005) 64–70.
[5] S. Anferova, V. Anferov, M. Adams, P. Blümler, N. Routley, K. Hailu, K. Kupferschläger, M.J.D Mallett, G. Schroeder, S. Sharma, B. Blümich, Concepts Magn. Reson. 15 (2002) 15–25.

Multi ion transport in concrete as studied by multi-nuclei NMR

L.Pel[a], P.A.J. Donkers[a]

[a]Eindhoven University of Technology, 5600 MB Eindhoven, The Netherlands.

One of the most used and most versatile building materials is concrete. It is cheap, can maintain high loads and as a result it is one of the most used material in civil engineering constructions. It is well known that the main reason for the durability limit of concrete is caused by ion interactions. Chloride-induced corrosion is one of the main degradation mechanisms in civil structures based on reinforced concrete [1]. The corrosion starts as soon as the chloride comes in contact with reinforcement steel bars. The source of chloride can be natural, i.e., sea water, or from de-icing salts. In general the chloride will enter a concrete by advection with moisture or diffusion within the moisture present in concrete. Another important effect is the deterioration of the concrete structures due to Alkali-Silica Reaction (ASR) [2]. Alkali-silica reaction is a chemical reaction between the hydroxyl ions present in the pore solution and reactive silica. An efficient method to prevent ASR is by introducing Li ions into the system which will form a non-expansive gel. The most effective way to drive Li into a sample is by electro-migration. In general there is a complex interaction between the ions and the cement matrix in these deterioration mechanisms. Gaining insight into these deterioration phenomena can not only improve the assessment of durability aspects of existing structures, but might lead to improved design for new reinforced concrete structures that are to be used in aggressive environments.

At the moment there is lack of experimental data on this topic that can be used to validate or discard the wide range of models of ion interaction available in the literature. Whereas such models might be correct, erroneous input is bound to lead to false predictions (i.e., the garbage in, garbage out principle). Modelling with faulty input parameters might have catastrophic consequences. There are various methods available to measure ionic chloride content in porous building materials. The most common method is to drill a specimen out of a concrete structure and analyze it chemically in the laboratory. Traditionally this is done by pulverizing the sample and chemically analysis. The most obvious drawback of this method is its destructiveness, but there are more shortcomings, such as its poor spatial resolution and irreproducibility.

Despite the low sensitivity for ^{35}Cl (see Table 1) NMR is still be preferred as it allows us, in contrast to other methods, to measure different nuclei, like ^{1}H, ^{7}Li, ^{23}Na and ^{35}Cl simultaneously with a high spatial resolution and give a full insight into dynamic interactions between the ions and cement matrix taking place. In addition, NMR can not only provide information on the pore-size distribution, but also on the pore ion distribution over the pores.

Various studies have shown that it is possible to quantitatively study chloride in cementitious materials using NMR imaging techniques. However, the reported studies on Cl transport are limited often to white cements, whereas ordinary cements always contain magnetic impurities (e.g., Fe), which can influence the relaxation behaviour. Since the time scale of our experiments covers the region from a few seconds to a few days, our original aim was to build an insert designed for semi-simultaneous measurements of ^{1}H, ^{7}Li, ^{23}Na and ^{35}Cl in ordinary cementitious materials. As the gyromagnetic ratios and hence the resonance frequencies of the selected nuclei are too far apart to be covered by one insert without seriously compromising the sensitivity, we have chosen to use the main field of a 4.7T wide bore magnet. The large space within this system allows us to combine various inserts.. Within the magnet we have opted for our own anti Helmholtz gradient system allowing a max gradient of 0.6 T/m. The insert consists of 4 separate birdcages, each for a specific nuclei stacked on top of each other. With the help of a stepper motor the selected birdcage can be moved into the center of the gradient coils. Hence we are able to measure quasi- simultaneously ^{1}H, ^{7}Li, ^{23}Na and ^{35}Cl. Special attention was given to making the measurements quantitative.

In order to test the set-up we have looked at the hydration of ordinary cement, i.e., Portland CEM I and blast furnace CEM III, with a 4 m salt solution, where we have focused on the relation between the ^{23}Na and ^{35}Cl content/concentration as a function of time, which could not be studied up to now. Moreover we have looked at the multi ion transport in the electro-migration both for ^{35}Cl, as well as ^{7}Li penetration, where there is a complex interaction/exchange with the cement matrix and other ions like ^{23}Na.

Table 1. Various properties of the nuclei studied by NMR.

Nucleus	spin	Natural abundance	$\gamma/2\pi$ (MHz/T)	Relative sensitivity
^{1}H	1/2	99.985	42.57	1.0000
^{7}Li	3/2	92.58	16.54	0.29
^{23}Na	3/2	100	11.26	0.0925
^{35}Cl	3/2	75.78	4.17	0.0047

References

[1] A. Neville, Mater. Struct. 28 (1995) 63.
[2] McCoy, E.J., and Caldwell, A.G., . Journal of the American Concrete Institute 22 (1951), 693-706.

Probing into the porous structure of hydrated cement paste with the NMR relaxometry of cyclohexane and ethanol molecules under partially saturated conditions

I. Ardelean, A. Bede, A. Scurtu

Technical University of Cluj-Napoca, Department of Physics and Chemistry, 400114, Cluj-Napoca, Romania.

Nuclear magnetic resonance (NMR) relaxometry techniques are widely used for the characterization of cement based materials. They rely on the proportionality between the relaxation rate and the surface to volume ratio of the investigated pores [1, 2]. The proportionality constant, also called the relaxivity, is settled by the adsorption properties of the molecules on the surface, the magnetic impurity content, their protic character and the magnitude of the external magnetic field [2].Note however that the NMR relaxation studies of cement materials mostly refer to water molecules and saturated pores. Here we extend these studies to the ethanol and cyclohexane molecules partially saturating a white cement paste. The two filling liquids were selected as representatives of polar (protic) and nonpolar (aprotic) molecules which should experience different interactions with the surface containing OH groups [2]. The cement paste was prepared using white cement and a water-to-cement ratio of 0.5. The white cement was chosen in order to reduce the internal gradient effects on relaxation measurements [4]. The transverse relaxation measurements were performed using the well-known CPMG pulse sequence with an echo time interval of 0.1 ms [4, 5].

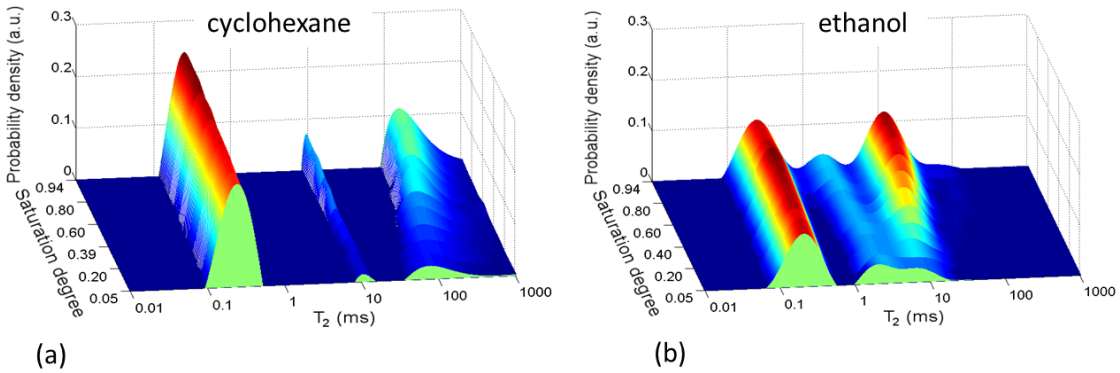

Figure 1 – Relaxation time distribution of liquid molecules inside a hydrated cement paste partially filled with cyclohexane (a) or ethanol (b). The first peak corresponds to the intra-C-S-H pores, the second to the inter-C-S-H pores and the third to the capillary pores. The intra-C-S-H pores are filled with water while the inter-C-S-H and capillary pores with the two solvents.

Figure 1 shows the relaxation time distributions of cyclohexane and ethanol molecules at different saturation degrees inside cement paste. The data revealed three pore reservoirs: intra-C-S-H sheet pores, inter-C-S-H gel pores and capillary pores respectively [1]. It is observed that the intra-C-S-H pores remain filled with water originating in the preparation approach while the inter-C-S-H and capillary pores are filled by the solvent molecules. Moreover, a different dependence on filling degree of the relaxation time of molecules confined inside inter-C-S-H pores was observed as compared with the capillary pores. To explain such dependence a two-phase exchange model, describing the effective relaxation rate under partially saturated conditions was considered [5]. In the frame of such a model the relaxation rate is given by the formula [5];

$$\frac{1}{T_2} = \frac{1}{T_{2l}} + \rho \frac{S}{V_0} \frac{1}{f^k}. \qquad (1)$$

In the above equation T_{2l} represents the relaxation time of the bulk like molecules, ρ is the relaxivity constant, S/V_0 the surface to volume ratio and f the filling factor of the pores. The empiric coefficient k accounts for the liquid distribution on the pore surface. Thus, for $k = 1$ the uniform coverage is described while $k = 0$ corresponds to a plug-like distribution.

In the case of cement paste the fitting approach for the empiric coefficient of molecules confined inside capillary pores provided a value $k = 0.5$ for cyclohexane and $k = 0.4$ for ethanol. In the case of inter-C-S-H pores, the best fit of the data was obtained for $k = 0$ both in the case of cyclohexane and ethanol molecules. This demonstrates a different distribution of molecules inside inter-C-S-H pores as compared with the capillary pores at lower filling degrees. Thus, while the molecules inside the inter-C-S-H pores satisfy a plug-like distribution, the molecules inside the capillary pores depict a non-uniform coverage on the surface.

References

[1] P.F. Faure, S. Rodts, Magn. Reson. Imaging. 26 (2008) 1183–1196
[2] J.-P. Korb, Curr. Opin. Colloid Interface Sci. 14 (2009) 192–202
[3] P. McDonald, V. Rodin, A. Valori, Cem. Concr. Res. 40 (2010) 1656–1663.
[4] A. Pop, I. Ardelean, Cem. Concr. Res. 77 (2015) 76–81.
[5] M. Simina, R. Nechifor, I. Ardelean, Magn. Reson. Chem. 49 (2011) 314–319

One and Two-dimensional NMR studies for Cultural Heritage: evaluation of consolidants performance

L. Brizi[a,b], M. Camaiti[b,c], V. Bortolotti[d], P. Fantazzini[a,b], B. Blümich[e], S. Haber-Pohlmeier[e]

[a]University of Bologna, Dept. of Physics and Astronomy, Viale Berti Pichat 6/2, 40127 Bologna, Italy; [b]Museo Storico della Fisica e Centro Studi e Ricerche "Enrico Fermi", Piazza del Viminale 1, 00184 Roma, Italy; [c]Institute for Geosciences and Earth Resources, National Research Council, Via G. La Pira 4, 50121 Florence, Italy; [d]University of Bologna, Department of Civil, Chemical, Environmental, and Materials Engineering, Via Terracini 28, 40131 Bologna, Italy; [e]RWTH Aachen University, Institute for Technical Chemistry and Macromolecular Chemistry, Worringerweg 1, 52074 Aachen, Germany.

The preservation of historical buildings and outdoor cultural assets is a necessity for the humankind because the artworks are the testimony of our past, as well as an economic resource for the present and future times. One of the main causes of degradation of stone artifacts are linked to chemical-physical processes that influence the ingress and diffusion of water (liquid or vapour) into the porous structure [1]. NMR has been proved to be a suitable tool to study porous materials of interest to Cultural Heritage [2]. In this study, the Maastricht stone was chosen as the material under investigation as its high porosity (P=48-50%) well simulates a high-deteriorate carbonate rock. The analyses investigate the behavior of commonly used consolidants like ethyl silicate (ESTEL 1000) and nanosilica particles (both supplied by CTS s.r.l., Vicenza, Italy) at two different Relative Humidities (RH). In consequence of the known hydrophilic properties of these consolidants, a commercial hydrophobic product used as protective agent, the fluoroelastomer N215, was also tested to be combined with the above consolidants and so to reduce their hydrophilic property. By mixing nanosilica and the fluoroelastomer, a new formulate was obtained. Figure 1a summarizes the products used.

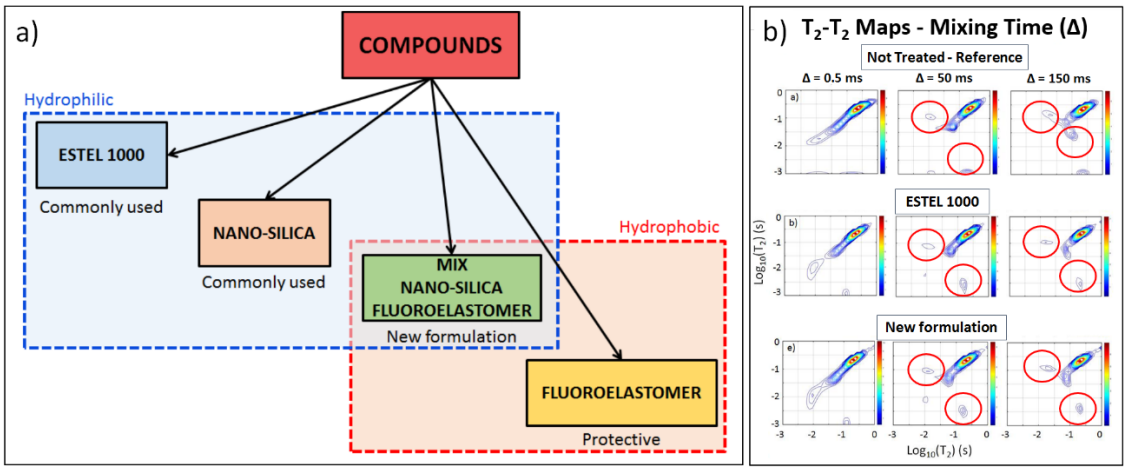

Figure 1 – a) Compounds used in this study. b) Examples of T_2-T_2 relaxation-exchange maps for different samples, varying the mixing time Δ. The circles indicate the crosspeaks caused by exchange of water.

The single-sided NMR MOUSE was used for one-dimensional NMR analyses and the Benchtop MRI Tomograph (both manufactured by Magritek) for the two-dimensional ones. *One-dimensional: samples in controlled RH conditions (dry and RH of 75% at 25°C).* The transverse relaxation time distributions for the stones treated with ESTEL 1000 and the fluoroelastomer showed that most of the signal, characterized by a peak in the range between 0.1 and 1 ms, was proportional to the amount of applied product. This effect did not appear for a not treated (reference) sample and the other two treatments, the nanosilica and the new formulate. This suggests that ESTEL 1000 and fluoroelastomer had trapped water during the treatment. However, the hydrophobic nature of the fluoroelastomer was proved by the absence of further water absorption in the RH of 75%. On the contrary, the ESTEL treated sample absorbed a considerable amount of water vapor, revealed by the increased area under the peak respect to the dry condition. The best performance of the new formulation with respect to the nanosilica was confirmed, as expected, by the less amount of water vapor absorbed. In summary, the mix nanosilica and fluoroelastomer seems to have the best behavior, because it absorbs less water vapor than nanosilica and does not absorb water during the treatment. *Two-dimensional: samples in full saturation conditions.* Two-dimensional NMR relaxometry measurements were performed as T_2-T_2 relaxation-exchange experiment [3] and evaluated in terms of correlation maps (Fig. 1b). For each sample it was possible to observe the occurrence of peaks that showed an exchange of water between domaines characterised by T_2 peaks centered at about 10 ms and 100 ms, respectively. The presence of these peaks in each map, with a mixing time $\Delta \geq 10$ ms, tells us that consolidation treatments did not change the connectivity properties of the stone material, assuring that compounds entered in the stone without a blockage of the pore structure. This is one of the most important characteristic that a conservative treatment must have to be used as a restoration compound for Cultural Heritage. In conclusion, we successfully exploited low-field NMR techniques in order to evaluate performance of consolidants, commonly used and new formulated ones, of interest to Cultural Heritage purposes.

References

[1] S. Siegesmund, T. Weiss, A. Vollbrecht, Natural stone, weathering phenomena, conservation strategies and case studies, Geological Society Special Publications No. 205 2002. The Geological Society, London.
[2] M. Camaiti,V. Bortolotti, P. Fantazzini, Stone Porosity, wettability changes and other features detected by MRI and NMR relaxometry: a more than 15-year study, Magn Reson Chem, 53 (2015) 34-47.
[3] A. Haber, S. Haber-Pohlmeier, F. Casanova, B. Blumich, Relaxation-Relaxation Experiments in Natural Porous Media with Portable Halbach Magnets. Vadose Zone Journal, 9 (2010) 893–897.

Recovering 2-dimensional T_1-T_2 distribution functions from 1-dimensional T_1 and T_2 measurements

N.H. Williamson[a], M. Röding[b,c], S.J. Miklavcic[d], M. Nydén[a,c]

[a]Future Industries Institute, University of South Australia, Mawson Lakes, SA 5095, Australia; [b]SP Food and Bioscience, Frans Perssons väg 6, 402 29 Göteborg, Sweden; [c]School of Energy and Resources, UCL Australia, University College London, Torrens Building, 220 Victoria Square, Adelaide, SA, 5000, Australia.; [d]Phenomics and Bioinformatics Research Centre, School of Information Technology and Mathematical Sciences, University of South Australia, Mawson Lakes, SA 5095, Australia.

The two dimensional inverse Laplace transform (2-D ILT) of T_1-T_2 correlation data allowed for the possibility of obtaining a functional relationship between T_1 and T_2 of fluid in a porous material [1]. The functional relationship provides information about surface interactions [2], which is unobtainable from a 1-D distribution alone. However, the observed relaxation rates generally follow the Brownstein-Tarr [3] equations for the fast-diffusion limit, i.e., a sum of surface and bulk contributions, with the sum controlled by the surface-to-volume ratio:

$$\frac{1}{T_{1,2}} = \frac{1}{T_{1,2\ bulk}} + \frac{S}{V}\frac{1}{T_{1,2\ surface}}; \qquad (1)$$

from this pair a functional relationship between T_1 and T_2 can be described by a single monotonic equation. Therefore, to recover the 2-D distribution function does not necessarily require a full correlation experiment, a fact which opens up the possibility of adopting alternative means, which could save experimental time. Kleinberg, et al. [4] obtained $T_1:T_2$ ratios by applying a cross-correlation function to the 1-D T_1 and T_2 distributions, assuming that the entire rock core could be described with a single value of $T_1:T_2$. More recently, the Driven-Equilibrium Carr-Purcell-Meiboom-Gill (DECPMG) pulse sequence opened for rapid assessment of the average ratio of $T_1:T_2$ as a function of T_2 [5]. We present a method by which a functional relationship between measurement parameters, T_1 and T_2, can be estimated through a process of fitting parametric models to 1-D T_1 and T_2 measurement data sets. From this *pseudo 2-D relaxation model (P2DRM)*, based on completely independent 1-D information, a joint 2-D probability distribution trace in T_1-T_2 space is derived, in the sense of establishing a mapping of two orthogonal and independent 1-D probability distributions to 2-D space using the assumed functional relationship. The advantage of the P2DRM over the full T_1-T_2 correlation experiment is clear; experimental time can be reduced when rapid 1-D measurements of T_1 and T_2 are utilized. We test this on experimental as well as simulated data, extracting 1-D T_1 and T_2 data from T_1-T_2 data so that the results can be compared to those of the 2-D ILT of the full 2-D dataset. In its estimation of the dominant behaviour, the P2DRM displayed a high degree of accuracy in relation to the known functional relationship of the simulation, as well as consistency with the functional relationships obtained from the 2-D ILT.

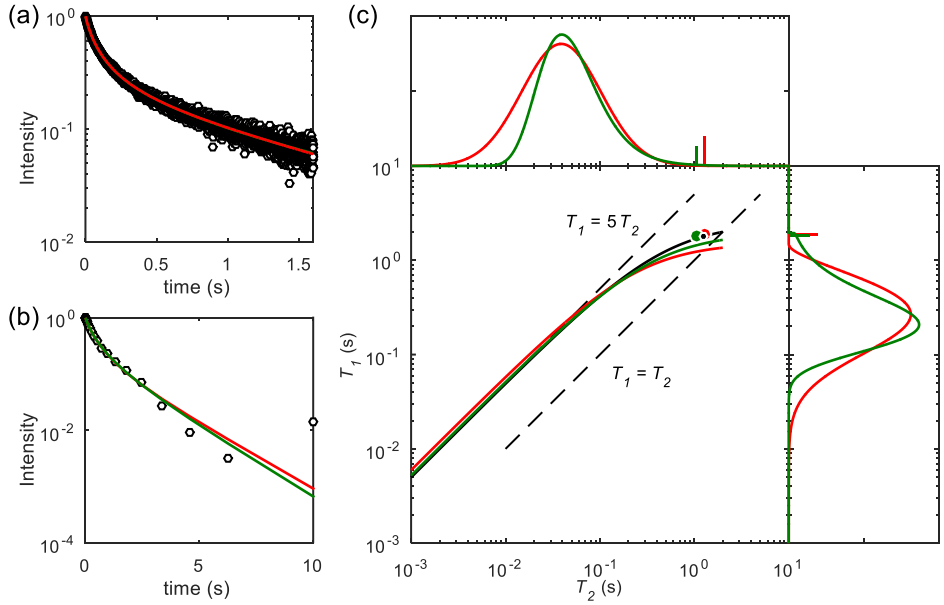

Figure 1 –The P2DRM applied to simulated (a) 1-D T_2 and (b) 1-D T_1 relaxation data from fluid in pores (black circles) resulting in (c) estimated T_2 distributions, T_1 distributions, and functional relationships between T_1 and T_2. By Eqs. (1), the T_2 distribution models (lognormal plus delta function (red) and inverse gamma plus delta function (green)) define T_1 distribution models from which the fit parameters give the estimated functional relationships, coincident with the known (solid black) functional relationship. The delta function components incorporated into the simulation as well as the distribution models are associated with fluid in large, connected pores for which bulk relaxation behaviour is expected.

References

[1] Y.Q. Song, L. Venkataramanan, M.D. Hürlimann, M. Flaum, P. Frulla, C. Straley, T1–T2 Correlation Spectra Obtained Using a Fast Two-Dimensional Laplace Inversion, J Magn. Reson., 154 (2002) 261-268.

[2] P. McDonald, J.P. Korb, J. Mitchell, L. Monteilhet, Surface relaxation and chemical exchange in hydrating cement pastes: a two-dimensional NMR relaxation study, Phys. Rev. E, 72 (2005) 011409.

[3] K.R. Brownstein, C.E. Tarr, Importance of Classical Diffusion in Nmr-Studies of Water in Biological Cells, Phys. Rev. A, 19 (1979) 2446-2453.

[4] R.L. Kleinberg, S.A. Farooqui, M.A. Horsfield, T1/ T2 Ratio and Frequency Dependence of NMR Relaxation in Porous Sedimentary Rocks, J. Colloid Interface Sci., 158 (1993) 195-198.

[5] J. Mitchell, M. Hürlimann, E. Fordham, A rapid measurement of T1/T2: the DECPMG sequence, J. Magn. Reson., 200 (2009) 198-206.

O50

Memory Efficient Multidimensional NMR Inversion without Kronecker Products

David Medellin, Vivek R. Ravi, Carlos Torres-Verdín

[a] The University of Texas at Austin, Department of Petroleum and Geosystems Engineering, 200 E. Dean Keeton, Mail Stop C0300, Austin, Texas, 78721, USA.

State of the art two-dimensional linear NMR inversion is usually accomplished in three steps [1-2]. First, the data is binned. Then, the kernel matrices are compressed using singular value decomposition (SVD). Finally, the Kronecker product of the compressed kernels is used to transform the two-dimensional inversion problem into an equivalent one-dimensional inversion problem, to which methods such as the Lawson-Hanson (LH) or the Butler-Reeds-Dawson (BRD) can be applied. The previous scheme has several issues. First, kernel compression is only possible when the kernel matrices are separable, and in recent years, there has been an increasing interest in NMR sequences with non-separable kernels. Second, in three or more dimensions, the SVD is not unique, therefore kernel compression is not well-defined for higher dimensions. Without kernel compression, the Kronecker product yields matrices that require large amounts of memory, making the inversion intractable for common computers. Finally, incorporating arbitrary regularization terms is not possible with the LH or BRD method.

We use multilinear forms to perform multidimensional NMR inversion by minimizing cost functions using a generalized multidimensional version of steepest descent that uses gradients in tensor form. This new method solves the three previously mentioned issues present in current methods: it is memory efficient, requiring less than 0.1 % of the memory required by the LH or BRD method; it is flexible, as it can be extended to arbitrary dimensions and adapted to include non-separable kernels, linear constraints, and arbitrary regularization terms; and it is easy to implement, because just the cost function and its first derivative are required. Tensor gradients allow us to generalize inversion methods to higher dimensions, avoiding memory expensive Kronecker products. Figure 1 shows a comparison between the memory required to perform 2D NMR inversion using kronecker products and multilinear forms. Note that 2D NMR inversion using kronecker products can require over 3 orders of magnitude more memory than using multilinear forms.

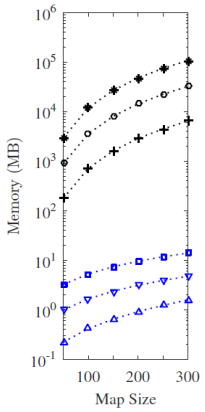

Figure 1 – Memory required to perform 2D NMR inversion using kronecker products (three topmost curves) and multilinear forms (three bottommost curves) for a T1-T2 inversion with 30 polarization steps and a symmetric map size. From top to bottom: 5000 echoes, 1500 echoes, 300 echoes, 5000 echoes, 1500 echoes, and 300 echoes.

The reason for this can be understood considering a 2D NMR cost function of the form

$$C = \left\| \mathbf{K}_2 \mathbf{F} \mathbf{K}_1^T - \mathbf{D} \right\|^2, \tag{1}$$

where K1 and K2 are kernel matrices, F is a 2D NMR distribution map, and D is the 2D NMR data. For square matrices, the memory required to compute the tensor gradient:

$$\nabla C = 2\mathbf{K}_2^{\mathbf{T}} (\mathbf{K}_2 \mathbf{F} \mathbf{K}_1^T - \mathbf{D}) \mathbf{K}_1 \tag{2}$$

is of the order of N^2, while for the gradient obtained by using the kronecker product,

$$\nabla \mathbf{C} = 2(\mathbf{K}_1 \otimes \mathbf{K}_2)^{\mathbf{T}} \left((\mathbf{K}_1 \otimes \mathbf{K}_2) \mathbf{f} - \mathbf{d} \right) \tag{3}$$

where **f** and **d** are the vectorized representations of **F** and **D**, the required memory is of order N^4

References

[1] L. Venkataramanan, Y.-Q. Song, M. D. Hürlimann, IEEE Transactions on Signal Processing, 50 (5), 1017-1026, 2002.
[2] C. H. Arns, K. E. Washburn, P. T. Callaghan, Petrophysics 48 (5), 380-392, 2007

O51

Improved inversion of two-dimensional NMR Relaxation data with the UPEN principle

V. Bortolotti[a], R. J. S. Brown[b], P. Fantazzini[c, e], G. Landi[d], F. Zama[d]

[a]Department of Civil, Chemical, Environmental, and Materials Engineering, University of Bologna; [b]900 E Harrison Ave, Apt B-9 Pomona CA 91767-2024, USA; [c]Department of Physics and Astronomy, University of Bologna, Italy; [d]Department of Mathematics, University of Bologna; [e]Museo Storico della Fisica e Centro Studi e Ricerche Enrico Fermi, Roma. Italy.

The inversion of two-dimensional NMR relaxation data requires the solution of a first-kind Fredholm integral equation with separable exponential kernel, typical of two dimensional inverse Laplace transforms. In this paper we present the I2DUPEN algorithm that extends the Uniform Penalty (UPEN) algorithm [1] to two-dimensional data. The discrete model for recovering the unknown discrete distribution $F \in R^{N_x \times N_y}$ from 2D NMR relaxation data, can be obtained by the following linear model:

$$K f + e = s \tag{1}$$

where $K \in R^{M \times N}$ is the discretized exponential kernel, $s \in R^M$ is the discrete vector of the measured noisy signal, $f \in R^N$ is the vector reordering of the distribution F and $e \in R^M$ is the vector with the discretized additive Gaussian noise.

The ill-conditioning of (1) is well known and Tikhonov regularization is commonly applied to the inversion of NMR data. It is well known that the main difficulty of the Tikhonov method is the estimation of the regularization parameter. Furthermore a single regularization parameter does not allow one to reconstruct peaks and flat regions with the same accuracy. We show that the UPEN principle is a suitable criterion for choosing the regularization parameters in multiple parameter Tikhonov regularization. The local values of the regularization parameters are related to the curvature in each point of the distribution by means of an iterative algorithm [2]. At each iteration, the locally adapted regularization parameters are automatically updated and the approximate solution is obtained by solving a regularized least squares problem:

$$\min_f \left\{ \| B K f - B s \|^2 + \sum_{i=1}^{N} \lambda_i \cdot (L f)_i^2 \right\} \tag{2}$$

where the matrix $L \in R^{N \times N}$ is the discrete Laplacian operator, $B \in R^{M \times M}$ is a diagonal matrix of weights related to the statistics of the data and λ_i are the local regularization parameters defined by the UPEN principle. Moreover, the data can be compressed using Singular Value Decomposition (SVD) of the kernel to reduce the computation cost. Results of numerical experiments on simulated and real data are presented in order to illustrate the potential of the proposed method in reconstructing peaks and flat regions with the same accuracy.

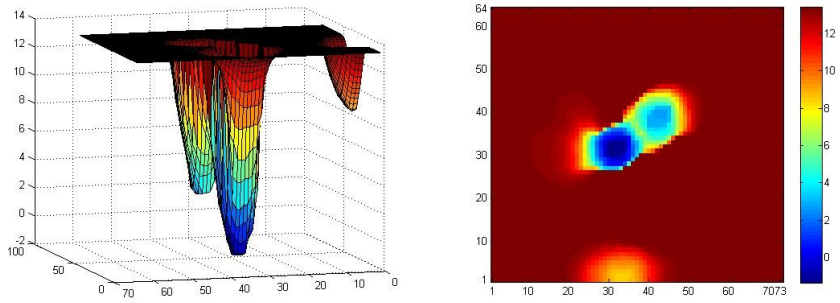

Figure 1 – Surface (left) and map (right) of the local regularization parameters λ_i in log-scale.

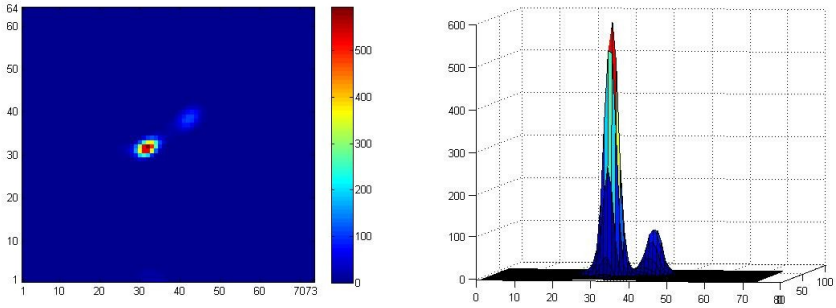

Figure 2 – $T_1 - T_2$ maps (left) and 3D distributions (right), obtained by the I2DUPEN.

Figure 1 shows the spatially adapted regularization parameter which is locally adapted to the inverse of the curvature of the distribution. Figure 2 shows the distribution obtained from the inversion of real NMR data where an SVD filter has been applied with threshold equal to 10^{-10}. Preserving the quality of the reconstruction, the computational cost was approximately halved.

References

[1] G.C. Borgia, R.J.S. Brown, and P. Fantazzini, Journal of Magnetic Resonance, 147(2): 273–285, 2000.
[2] V. Bortolotti, R.J.S. Brown, P. Fantazzini, G. Landi, F. Zama, submitted, 2016.

POSTER

P01

Ultrafast multidimensional Laplace NMR for a rapid and sensitive chemical analysis

S. Ahola[a], V.-V. Telkki[a]

[a]NMR Research Group, P.O. Box 3000, FIN-90014 University of Oulu, Finland. email: susanna.ahola@oulu.fi.

Laplace NMR (LNMR) consists of relaxation and diffusion measurements which provide detailed information about molecular rotation and diffusion, explore interactions of nuclei with their microscopic environments, and can ultimately provide complementary chemical resolution. [1]

As with traditional NMR, the resolution and information content of Laplace NMR can be significantly improved by the use of a multidimensional approach [1]. However, the duration of such experiments becomes very long, because it requires a repetition of the experiment with varying evolution times. Typically, the experiment time ranges from minutes to hours, which restricts the applicability of the method. In ultrafast, multidimensional Laplace NMR [2, 3] the encoding in the second dimension is done in a spatially depended manner, also known from conventional ultrafast NMR spectroscopy [4], and thereby experimental time is reduced by orders of magnitude. Such a dramatic speedup of measurement technique enables the investigation of transient phenomena previously out of reach of multidimensional NMR. Such systems could include, for example, gel formation, phase changes of ionic liquids and liquid crystals. Furthermore, it is possible to collect the entire data space after a single excitation pulse, and apply the method even to hyperpolarized spin systems otherwise out of reach of multidimensional NMR. Hyperpolarization techniques improve the sensitivity of NMR up to 10^5 orders of magnitude, and thus enable NMR experiments even from very dilute concentrations

In this presentation we explain the principles of ultrafast multidimensional LNMR and present several different measurement schemes together with experimental demonstrations and simulations. We show that multidimensional Laplace NMR experiments are capable of bringing chemical resolution to systems, which may lack it in traditional NMR spectra: For example, it is possible to resolve signals arising from different physical environments of a fluid inside a porous medium. In addition, it is possible to resolve hydrocarbons of different size, which have completely overlapping NMR spectrum. We also demonstrate that the method is applicable to hyperpolarized substances, and that we can carry out ultrafast relaxation correlation experiments even with portable, single-sided low field instruments [5].

References

[1] Y. Q. Song, *J. Magn. Reson.*, **229**, 12-24 (2013).
[2] S. Ahola, V.-V. Telkki, *Chem Phys Chem*, **15**, 1687-1692 (2014).
[3] S. Ahola, V. V. Zhivonitko, O. Mankinen, G. Zhang, A. M. Kantola, H-Y Chen, C. Hilty, I. V. Koptyug and V.-V. Telkki, *Nature Comm*., **6**, 8363, (2015).
[4] A. Tal, L. Frydman, *Prog. Nucl. Mag. Res. Sp.*, **57**, 241-292 (2010).
[5] J.N. King, V. J. Lee, S. Ahola, V.-V. Telkki, and T. Meldrum, *Angew. Chem. Int. Ed. Engl.* **55**, 5040-5043 (2016).

Accurate T2 distribution of fluids in porous media measured with Phase Incremented Echo Train Acquisition

D. J. Srivastava[a], A. G. de Araujo-Ferreira[b], D. R. Cole[c], J. H. Baltisberger[d], T. J. Bonagamba[b], P. J. Grandinetti[a]

[a]Department of Chemistry, The Ohio State University, Columbus, OH, USA; [b]São Carlos Institute of Physics, University of São Paulo, PO Box 369, 13560-970, São Carlos, SP, Brazil; [c]School of Earth Sciences, The Ohio State University Columbus, OH, USA; [d]Division of Natural Science, Mathematics, and Nursing, Berea College, Berea, Kentucky 40403, USA

One of the oldest magnetic resonance experiments used in the sciences and medicine is the Carr-Purcell-Meiboom-Gill (CPMG) sequence. A well-understood problem with CPMG is that its signal contains a number of artifacts [1] arising from undesired stimulated echoes. Since stimulated echoes decay on a timescale associated with T1, the T2 distributions measured with CPMG are often contaminated with artifact intensities associated with higher decay constants that are not representative of the true T2 values within the sample. These artifacts vary in intensity with the number of pi pulses and time to echo (TE). With changing TE one also expects changes in the measured decay constant distribution due to diminishing contributions from diffusion at shorter TE values. These diffusion contributions, however, can be obscured by the undesired stimulated echo artifacts.

Recently, we developed the Phase Incremented Echo Train Acquisition (PIETA) method [2] which eliminates all artifacts from stimulated echo contributions. Using PIETA we have performed a series of measurements comparing the T2 distributions obtained by the CPMG versus PIETA for a variety of porous rock cores at different externals magnetic fields that cover a range of proton NMR frequencies from 2MHz to 400MHz. This comparison can be seen in the figure below. As expected the CPMG-derived decay constant distribution has consistently more intensity associated with longer decay constants. Additionally, we see that the shape of the decay constant distributions obtained with CPMG has greater variations with changing TE than PIETA. Again these variations arise from the changing amount of stimulated echo artifacts. With the elimination of stimulated echo artifacts the changes in the PIETA decay constant distribution with decreasing TE is a more accurate reflection of the decreasing diffusion contribution with decreasing TE.

The PIETA data also provides additional information on the amount of coherence lost to undesired pathways. This information could be useful in predicting the T2 distributions that would be obtained with ideal pulses.

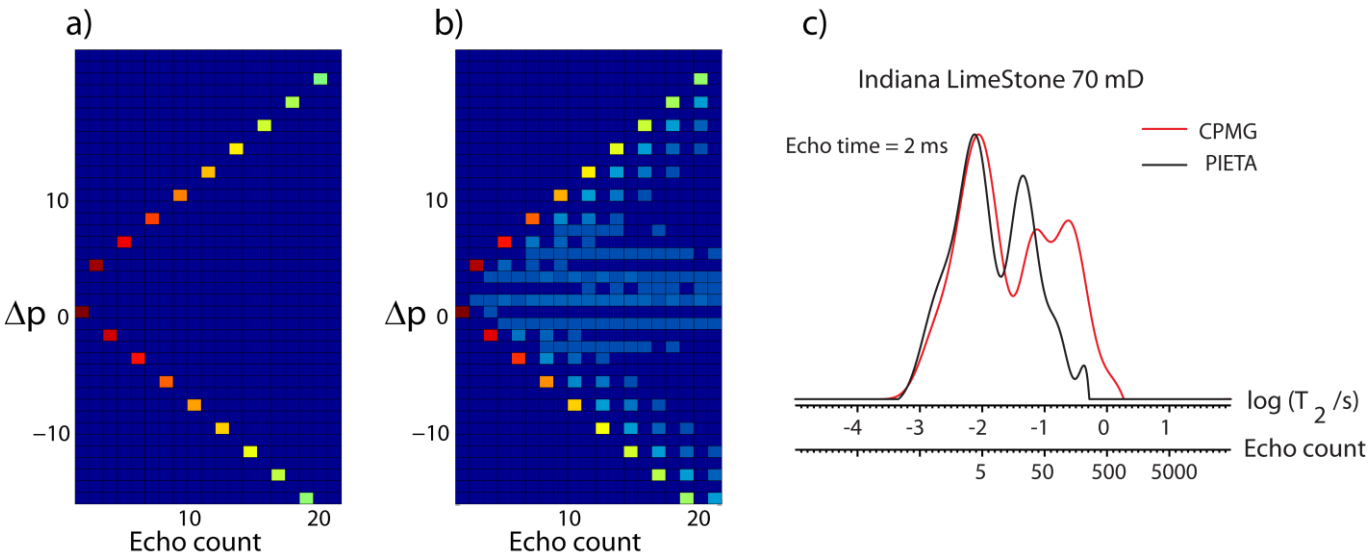

Figure 1 a) 2D PIETA simulated map showing the pathway produced by ideal pulses; b) Experimental PIETA map. Pulses are not ideal and part of the magnetization can be seen following different pathways; c) Comparison of CPMG and PIETA T_2 distributions.

References

[1] Y.-Q. Song, Journal of Magnetic Resonance 157 (2002) 82–91
[2] Jay H. Baltisberger, Brennan J. Walder, Eric G. Keeler, Derrick C. Kaseman, Kevin J. Sanders, Philip J. Grandinetti, J. Chem. Phys. 136 (2012) 211104

TOPOLOGICAL STUDY OF POROUS MEDIA THROUGH µCT IMAGING AND COMPLEX NETWORKS

M. B. Andreeta[a], R. S. Polli[a], E. Lucas-Oliveira[a], F. A. Rodrigues[b], T. J. Bonagamba[a]

[a]São Carlos Institute of Physics, University of São Paulo, PO Box 369, 13560-970, São Carlos, SP, Brazil, [b]São Carlos Institute of Mathematics and Computer Science, University of São Paulo, PO Box 668, 13560-970, São Carlos, SP, Brazil.

The interconnecting system of pores and throats in porous materials is a high complexity system. The development of methods that allow quantifying its topological properties is of vital importance to understand the structure of the material. The application of µCT imaging to this media has opened a new branch of research which uses image processing algorithms to quantify the pore-throat interconnection network and assess properties such as pore size distribution and throat size distributions [1,2]. In order to extract this information, the 3D porous matrix is characterized by assessing the total void volume, pore surface and fractal dimension amongst other properties. Furthermore, the media can be segmented into pores and throats, forming a large network in which the pores are the nodes and the throats are the edges. This segmentation allows a new form of visualization of the porous structure and the possibility of applying network theory to analyze its topology. In this work, we propose the extraction of the pore network to characterize the topology of the system by measurements of degree distribution, node/edge centralities and molecular diffusion (through random walk). We show that this information provides a powerful tool to analyze the media's morphology. A direct application is the identification preferential paths of molecular diffusion, an important quantity measured by the NMR techniques.

The analysis of the topology was first applied to characterize the morphology of *wormhole*s in carbonates. Wormhole is the denomination of a pathway formed after the application of an acid treatment as a stimulation procedure for the reservoir. Acid treatment is one of the most commonly stimulation treatment used in carbonate reservoirs (such as the *pre-salt*), since it accounts for the heterogeneity of the carbonate rocks to maintain a continuous fluid output. It consists of a reactive fluid flow injected in the inner rock of the reservoir. This procedure creates a preferential path (*wormhole*) that optimizes the extraction of the hydrocarbon fluids [3,4]. Therefore, the characterization of the wormhole's topology is of vital importance to assess the efficiency of the stimulation procedure.

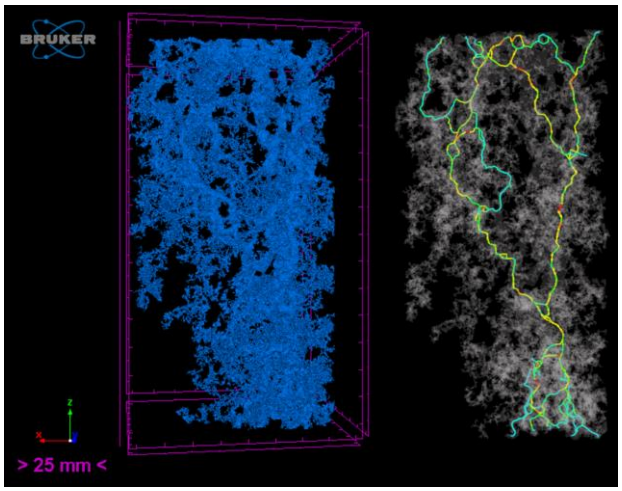

Figure 1 – Topology of a wormhole on an Indiana Limestone. Left: the whole body of the wormhole (Bruker SkyScan "CT-analyser"). Right: the main paths of fluid flow identified by network analysis (developed software).

This project used the µCT images to reconstruct the 3D porous matrix of the rock cores after acidification. A percolation algorithm was used to identify the wormhole, having any other pores excluded from the measurements. Then, a modified Max Ball Algorithm [5], developed on this project, was applied to construct the pore interconnection network. This network presented not the free scale characteristic as it is found in most networks in nature, but instead an exponential decay behavior on the connection of nodes. In addition, the network presented the "small world" property, which shows that the typical pore is easily accessible with a small number of steps. Through measurements of node closeness centralities and edge betweenness centralities, the method allowed to identify the main paths of molecular diffusion and fluid flow that had the largest hydraulic radius (Figure 1). We have found that the lengths and number of connecting preferential paths correlates with the acid flow used. We intend to apply the method to identify the ramifications lengths, and use it as a complementary technique on the choice of the acidification procedure that can provide the best results in carbonates. For further work, the network extracted will be used to simulate NMR 1D and 2D experiments in order to find the correlations of the network's topology to the NMR relaxation times distributions.

References

[1] R. I. Al-Raoush and C. S. Willson, Extraction of physically realistic pore network properties from three-dimensional synchrotron X-ray microtomography images of unconsolidated porous media systems, J. Hydrol. 300 (2005), 44–64.
[2] O. Talabi, S. AlSayari, S. Iglauer, and M. J. Blunt, Pore-scale simulation of NMR response, J. Pet. Sci. Eng. 67 (2009), 168–178.
[3] L. Kalfayan, Production Enhancement with Acid Stimulation. PennWell, 2008.
[4] M. Krebs, B. Lungwitz, A. Souza, A. Pepin, S. Montoya, P. Schlicht, A. Boyd, E. Vidoto, R. Polli, and T. Bonagamba, The First Visualization of Acid Treatments on Carbonates With 3D Nuclear Magnetic Resonance Imaging (NMRI), In SPE Conference, Society of Petroleum Engineers (2014).
[5] Silin, D. B., Jin, G., & Patzek, T. W. Robust determination of the pore space morphology in sedimentary rocks. In SPE Conference , Society of Petroleum Engineers (2004).

P04

Parameterization of multi-exponential NMR relaxation in terms of logarithmic moments of an underlying relaxation time distribution

O. V. Petrov[a], S. Stapf[a]

[a]Technische Universität Ilmenau, Institut für Physik, D-98684, Ilmenau, Germany

There are two common approaches to the mathematical description of multi-exponential relaxation. One is to fit an empirical function whose parameters relate to a characteristic time of relaxation and its deviation from exponential. Kohlrausch-William-Watson, Cole-Cole, Cole-Davidson and log-normal fit functions are but some of the examples. This approach requires specifying a functional form of relaxation, or in other words, *a priori* knowledge of underlying relaxation time distribution $g(\tau)$, which makes it difficult to compare samples with dissimilar relaxation behavior using this method. The other approach is calculation of $g(\tau)$ by resolving an experimental relaxation function into a number of exponentials by means of the inverse Laplace transform (ILT). It provides an ultimate description of the multi-exponential relaxation and allows a direct comparison of different samples. However, since ILT of a noisy data is a numerical approximation and relies strongly on the regularization algorithm used, one may consider thus obtained $g(\tau)$ and derived moments ambiguous.

R. Zorn [1] has proposed to characterize multi-exponential relaxation in terms of logarithmic moments (LMs) of $g(\tau)$ which can be calculated without inversion of data by using only integral (and optionally differential) calculus. The first logarithmic moment, $<\ln\tau>$, represents the geometric mean relaxation time, wihle the second, $\sigma^2_{\ln\tau}$, and the third, $\mu_{3\ln\tau}$, moments relate to the width and the asymmetry of $g(\tau)$, respectively. The calculation of the LMs is based on the moment rules for convolution (see *e.g.* [2]) and requires that a relaxation function is sampled at logarithmically spaced delays and normalized to unity.

Ref. [1] contains all necessary equations for the LMs calculation and provides examples for a number of empirical fit functions used in dielectric relaxometry. Here we have applied the method to experimental data acquired under various conditions from NMR T_1 relaxation and stimulated echo experiments as well as to simulated data. In particular, we tested the effects of a signal-to-noise ratio (SNR), the number of acquisition points, the onset of acquisition, and a sampling rate on the calculated LMs. It was possible to exclude a numerical differentiation from the working equations in [1], which left numerical integration and normalization of the data the only intrinsic sources of error. To normalize the data, we used the total amplitude of the best-fit triple-exponential function as a normalization factor. The same fit function was utilized to extrapolate the relaxation function to short relaxation delays if necessary.

The LMs calculated from the experimental datasets were found in a good agreement with those from ILT and multi-exponential analysis. The geometric mean $<\ln\tau>$ is robust with respect to the presence of noise, including outliers, to a moderate shift of the acquisition onset to longer delays, and to its early truncation. The variance $\sigma^2_{\ln\tau}$ and the asymmety parameter $\mu_{3\ln\tau}$ were found to be much more sensitive to those factors. For example, it was important for a good accuracy that the relaxation decay be sampled starting above a 90% level of the relaxation function, otherwise extrapolation to short delays was necessary.

The objective of this work was to obtain a compact representation of relaxation curves with possible applications to tissues, polymer melts and heterogeneous porous media such as solids and rocks. As future work, it would be also of interest to study the sensitivity of different LMs to the factors of relaxivity in those systems.

References

[1] R. Zorn, J. Chem. Phys. 116 (2002) 3204-3209.
[2] C. A. Laury-Micoulaut, Astron. & Astrophys. 51 (1976) 343-346.

Application of Principal Component Analysis in NMR Relaxometry

O. V. Petrov[a,b], M. Vogel[a]

[a]Technische Universität Darmstadt, Festköperphysik, 64289 Darmstadt, Germany; [b]Technische Universität Ilmenau, Institut für Physik, D-98684, Ilmenau, Germany (present address)

A host of NMR techniques rely on the measurement of magnetization versus a variable parameter. Among them are T_1/T_2 relaxometry, diffusometry, NOE and chemical exchange monitoring, as well as more specific stimulated-echo measurements of high-order correlation functions and multiple coherence buildups. The experiments often result in an NMR signal of low signal-to-noise ratio (SNR), making an optimum data quantification a matter of great concern. Commonly, one quantifies individual signals successively as they are generated in response to a variable parameter's update. The measurements consist of direct integration of spectral peaks or taking the initial part of a time signal or points at the spin-echo top as the estimation of the total magnetization.

As an alternative, methods of NMR quantification that are based on statistical approaches which encompass simultaneous analysis of an entire set of signals have recently been arisen [1]. In particular, principal component analysis (PCA) has gained popularity among the biomedical NMR community for the quantification of metabolite concentrations in tissues [2]. The technique was initially introduced for estimating the peak areas in an array of NMR spectra [1] and then was extended to include estimation of variations in peak positions and phases [3]. As a method of multivariate analysis, PCA has the advantage over the direct measurements of utilizing "the collective power of the data" [3] to reveal signal-related factors of data variance.

The subject of our work was to exploit this potential of PCA in NMR relaxometry, both conventional and field-cycling (FC), and to demonstrate the advantage of the method over direct measurements on individual signals.

In the case when the change in the signal's amplitude is the only factor of the data variance, the total magnetization is measured straightforwardly as a sum of properly scaled principal components' (PCs') scores, with the scaling factors being the sums of respective PCs' elements. If, however, there are other factors such as variations in frequency and phase, as in case of FC relaxometry, then one first applies an iterative PCA-based procedure [3] for estimating and correction for those unwanted signal variations. From the tests taken, comparison of PCA with direct measurements of total magnetizaton is mostly in favor of PCA as it produces less scattered points along build-up curves (Fig. 1). PCA was found to perform equally well in both the frequency and time domains, in contrast to direct integration of time signals which underestimates faster-decaying components in general. PCA is a 'black-box' method, meaning that user interaction is minimal and all signal parameters are estimated in one step. As such, it can be readily implemented as an automatic processing routine within the NMR software used. Yet the user has to determine the number of PCs to deal with, *e.g.*, when measuring a multi-component relaxation.

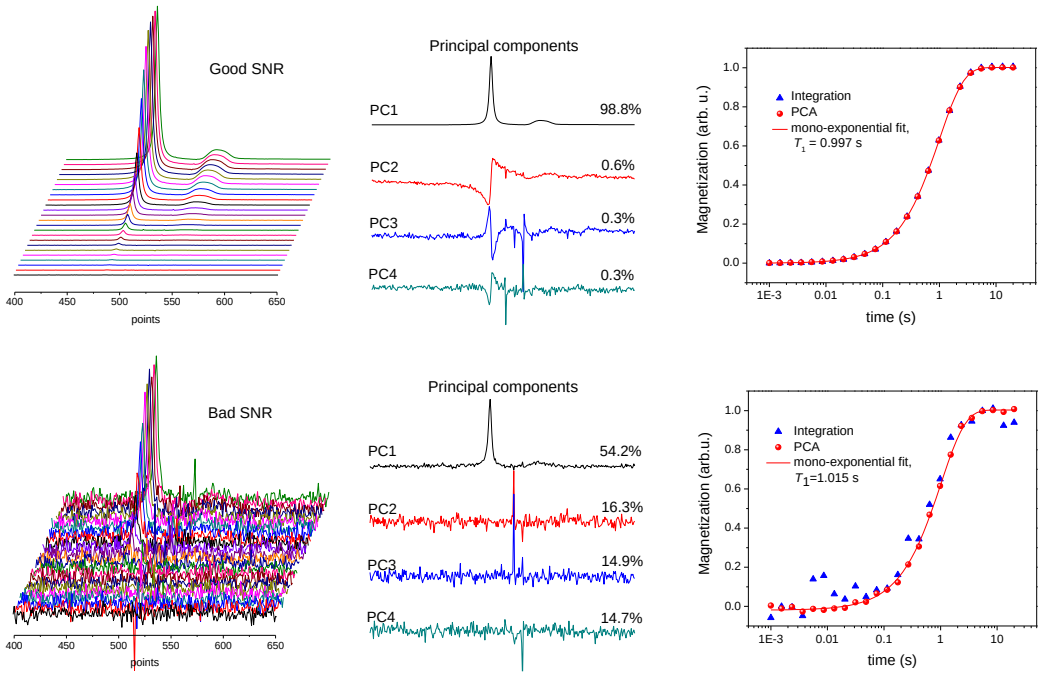

Figure 1 – Principal component analysis of ^{19}F T_1-relaxation in a LaF_3 crystal as compared to direct integration.

References

[1] NMR Biomed. 14 (2001) 223-283, issue dedicated to NMR spectroscopy quantitation.
[2] R. Stoyanova, A. C. Kuesel, T. R. Brown, J. Magn. Reson. A 115 (1995) 265-269
[3] R. Stoyanova, T. R. Brown, J. Magn. Reson. 154 (2002) 163–175

Real-time NMR data processing and management

Y. Shi[a], L.Z. Xiao[a], G.Z. Liao[a] , Y. Zhang[a] , S.J. Jiang[a] , L. Gao[a]

[a]State Key Laboratory of Petroleum Resources and Prospecting, China University of Petroleum, Beijing, China

NMR logging can provide many parameters of formation fluid properties such as T1、T2、D for formation evaluation. We can obtain porosity、permeability、identify fluid types through NMR logging, which causing NMR method to be one of the important tool for oil resources exploration. As the fast development of NMR technology in wireline and drilling logging, NMR is playing a more and more important and effective role in fluid identification and quantitative evaluation.

Nowadays, data processing and interpretation in the software of NMR logging are all preformed after data being collected. But due to the great development of NMR technology in wireline and drilling logging, the characterization of real-time, continuity and accuracy for NMR data processing has become more and more important. Since the establishment of a sophisticated NMR laboratory for identification and analysis of fluid has gained increasing attention, real-time NMR data processing turns into a new trend in NMR logging data processing and development of technology in the field of oil exploration. Therefore, this work is aimed at realizing real-time NMR data processing, and trying to achieve the target of analyzing the feasibility and necessity of data management by information technology in the field of NMR logging which is based on NMR real-time data processing system. This work is based on the NMR identification and analysis of fluid device designed by China University of Petroleum Beijing NMR laboratory. And figure 1 shows the interface of the software. For the real-time data processing and management, we use specific database skill to take the data into two parts—'head' and 'rear'. When the tool is working and transmitting sig -nals, the software can identify which information is not in the database by the 'head' and put the useful information of the new signal (the rear) in the database, causing the real-time data processing.

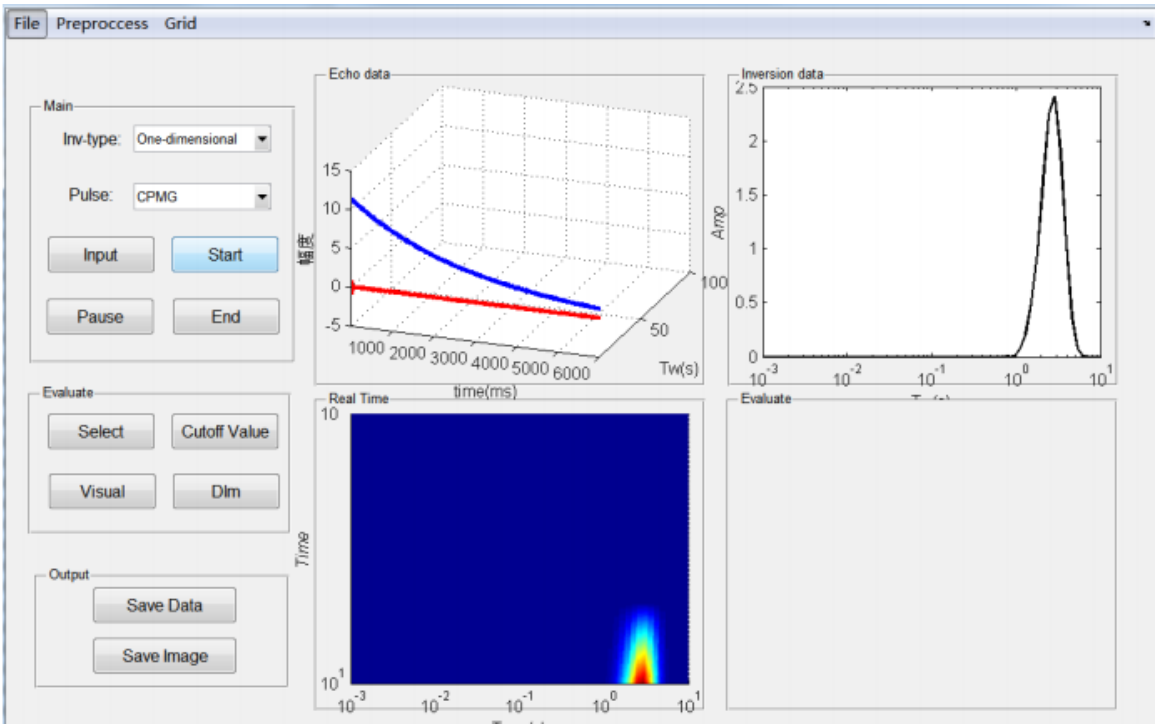

Figure 1 –Interface of real-time NMR data processing software

The main contents include: (1)Using numerical simulation and experimental verification to realizing the real-time NMR data processing in two dimensional.(2)Using four different methods to do the quantitative identification of downhole fluid in two dimensional; (3)Combined with the quantitative characterization of measurement results to improve the accuracy of oil exploration and production efficiency; (4)Try to build a databases to realize the real-time data reading and the information management of data.

References

[1] G.R. Coates,L.Z. Xiao L,M.G . Prammer. NMR Logging Principles and Applications. Texas:

[2] S.Q. Fu, L.Z. Xiao, T. An et al. Optimization of Nuclear Magnetic Resonance Logging Data Processing Speed. Computational and Information Sciences (ICCIS), 2012 Fourth International Conference on. IEEE, 2012: 151-154.

[3] J.Mitchell, T.C. Chandrasekera, L.F. Gladden. Numerical Estimation of Relaxation and Diffusion Distributions in Two Dimensions, Progress in Nuclear Magnetic Resonance Spectroscopy. 2012, 62:34-50.

P07

Proper coherence pathways selection in echo train acquisition for T_2 measurements

R. Shakhovoy[a], V. Sarou-Kanian[a], M. Yon[a], F. Fayon[a]

[a]CNRS, CEMHTI UPR3079, Univ. Orléans, F-45071 Orléans, France

Nuclear Magnetic Resonance relaxation time constants are relevant parameters to characterize porous media. Indeed, the nuclear spin transverse relaxtion time of confined molecular species, T_2, is well-known to correlate with the pore size distribution. The NMR methodology for the T_2 measurements is based on the the commonly used CPMG sequence [1,2] which employs the acquistion of a train of echoes to overcome the effects of molecular diffusion. In theory [1,2], CPMG decay should provide correct T_2 value; however, non-ideal refocusing pulses produce experimentally undesired signals, particularly stimulated echoes, which were found to be responsible for significant elongation of the CPMG decay. This unwanted contribution is mainly caused by the radio frequency field inhomogeneities, and by the absence of proper coherence pathway selection by phase cycling in the conventionnal CPMG sequence.

The very large number of steps (i.e.scans) needed to select precisely the coherence pathways makes prohibive the use of nested phase cyling for CPMG acquisiton. For instance, a CPMG sequence with N π pulses requires at least 2^N steps with nested phase cycling [3,4]. Recently, Baltisberger et al. [5] proposed an elegant approach to select the desired spin echo pathway in a CPMG-type experiment called “Phase Incremented Echo Train Acquisition” (PIETA). By introducing an indirect phase incremented dimension in combination with an adapted data post-processing, PIETA also succeeds in reducing the number of steps such that it requires only 2N scans for N π pulses.

Here we present an alternative way to achieve a proper coherence pathway selection in CPMG echo train acquisition, which is based on the “cogwhell phase cycling” introduced by M. Levitt et al. [6]. With respect to PIETA, the number of steps remains the same, but data post-processing related to the introduction of an additionnal dimension is no longer needed. We apply this new methodology on porous materials with well-defined pore size distributions, and propose a critical discussion with respect to the standard CPMG sequence in terms of T_2 measurements.

References

[1] H.Y. Carr and E.M. Purcell, Phys. Rev. 94 (1954) 630-638.
[2] S. Meiboom and D. Gill, Rev. Sci. Instr. 29 (1958) 688-691.
[3] A.D. Bain, J. Magn. Reson., 56 (1984) 418-427.
[4] G. Bodenhausen, H. Kogler and R.R. Ernst, J. of Magn. Reson. 58 (1984) 370-388.
[5] J.H. Baltisberger, B.J. Walder, E.G. Keeler, D.C. Kaseman, K.J. Sanders and P.J. Grandinetti, J. Chem. Phys. 136 (2012) 211104.
[6] M.H. Levitt, P.K. Madhu and C.E. Hughes, J. Magn. Reson. 155 (2002) 300-306.

Ring Dynamics in Functionalized UiO66(Zr) MOFs via SLF Solid-State NMR

J. Damron[a], J. Ma[a], K. Saalwächter[b], A. Matzger[a], A. Ramamoorthy[a]

[a] Uni. Of Michigan, Dept. of Chemistry, 930 N. University. Ann Arbor, Mi 48109, USA; [b]Martin-Luther-Universität Halle-Wittenberg, Inst. Für Physik, Friedemann-Bach-Platz 6, D-06120 Halle, Germany.

Control of molecular dynamics has been a crucial requirement in the design and development of molecular machines and devices for end-use applications. Rotational ring flipping events of benzilic moieties are, for instance, an influencing factor for guest-host interactions or structural transitions such as "breathing" events in porous media. Towards the goal of truly *a priori* synthesis of tailored materials, systematic modification of substituent groups on the rotor dramatically influences flipping frequencies serving as a viable strategy for molecular control. Metal coordination polymer (MCPs) (also known as Metal Organic Frameworks) are an ideal porous architecture to explore dynamics features for rotational frequencies in crystalline solids. To probe ring dynamics in MCPs, solid-state NMR has proven to be a powerful tool as a non-invasive means of exploring a wide dynamic range. Here, we employ dipolar chemical shift correlation (DIPSHIFT) [1], a separated local field experiment, measuring the CH heteronuclear dipolar coupling as a proxy for ring dynamics. The recent extension of the methodological approach detects a unique T2 like relaxation during the DIPSHIFT curve which provides a unique marker for dynamics in the "intermediate" motional regimes (100us). The ring events were measured as a function of chemical modification and temperature in a series of UiO66(Zr)[2] MOFs. The results show dramatic differences in dipolar coupling constants (see Figure 1.), demonstrating a wide range of dynamic timescales. By carefully designing the interaction between the substituent and the cluster, the energy potential for rotational barrier is dictated by the interaction strength and thus affects the rotational dynamics. Results were supported by DFT calculations where the activation energy for a full ring flip matched the experimental trends.

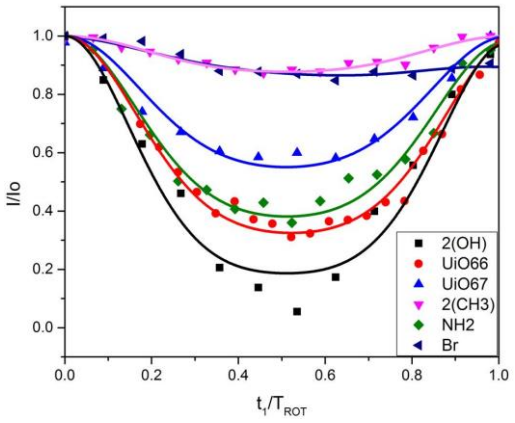

Figure 1 – Dipolar chemical shift (DIPSHIFT) correlation experiment curves on chemically modified UiO66 at 23C. The depths of the curve is roughly proportional to the strength of the heteronuclear dipolar coupling constant.

References

[1] E.R. deAzevedo, K. Saalwachter, O. Pascui, A.A. de Souza, T.J. Bonagamba, D. Reichert. J. Chem. Phys. 128 (2008) 104505.
[2] J. H. Cavka, S. Jakobsen U. Olsbye, N. Guillou, C. Lamberti, S. Bordiga, K. P. Lillerud. J. Am. Chem. Soc, 130 (2008), 13850-13851.

Homodyne Relaxation Analysis

S. Huber, A. Joos, B. Gleich, A. Haase

Institute of Medical Engineering, TU Munich, Boltzmannstrasse 11, 85748 Garching, Germany.

Many NMR relaxation and diffusion experiments can be modeled by a multi-exponential decay where each decay rate describes a distinct component in the sample. Through an inverse Laplace transform of the decay curve one passes from the time domain over to the relaxation domain which gives new physical insight. To perform an inverse Laplace transform numerically we developed a new algorithm which is adopted to the homodyne detection principle well-known from signal analysis in the Fourier domain. We applied our homodyne algorithm to experimental data and compared its results with the outcome of the Tikhonov regularization method, of a multi-exponential NNLS fit and of the Laplace-Padé approximation [1].

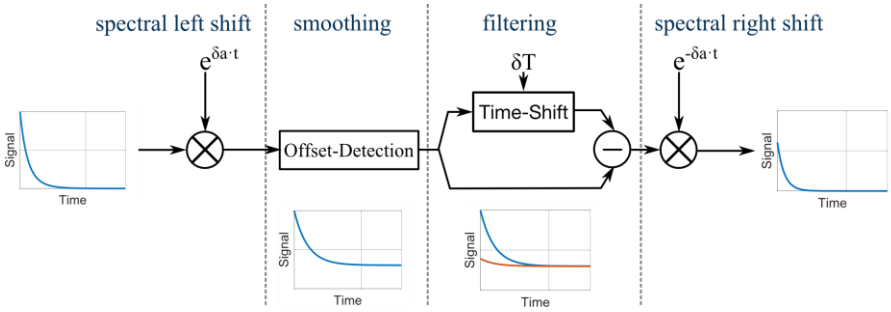

Figure 1 – Schematic of a single iteration step for a double exponential signal when δa equals the smallest relaxation component in the spectrum.

Our algorithm is an iterative approach. Fig. 1 shows a single iteration step applied to a double exponential signal. We interpret the decay signal as the result of a two-sided Laplace transform of a relaxation spectrum. This allows us to shift the relaxation spectrum by δa to the left through a multiplication of the decaying signal in the time domain. With each iterative step δa is incremented. As soon as δa equals the smallest relaxation rate in the spectrum an offset will appear in the time domain. When such an offset is detected the smallest relaxation rate in the spectrum is zero. That means by subtracting the signal from a copy of itself shifted in time by δT this component can be filtered away completely. Relaxation rates close to it get damped. After that the remaining signal undergoes a spectral back shift before the next iteration step begins.

To evaluate our algorithm with experimental data we investigated the T2-decay of four different 1.5 ml samples each with different $CuSO_4$ concentrations (0 g/l, 0.1 g/l, 0.5 g/l and 1 g/l) with a CPMG sequence at 1 T. At first a T2-decay curve of each single sample was individually recorded in a single configuration. Then a T2-decay curve of all four samples together in a quattro configuration was measured. The results are given in Fig. 2a). The outcome of the single configuration experiments were analyzed with a mono-exponential NNLS fit. The quattro configuration decay was analyzed with a quattro-exponential NNLS fit, with the Laplace-Padé method, with the Tikhonov regularization method and with our homodyne detection algorithm. For the application of the quattro-exponential NNLS fit and for the Laplace-Padé approximation the knowledge about 4 components was employed in the input settings.

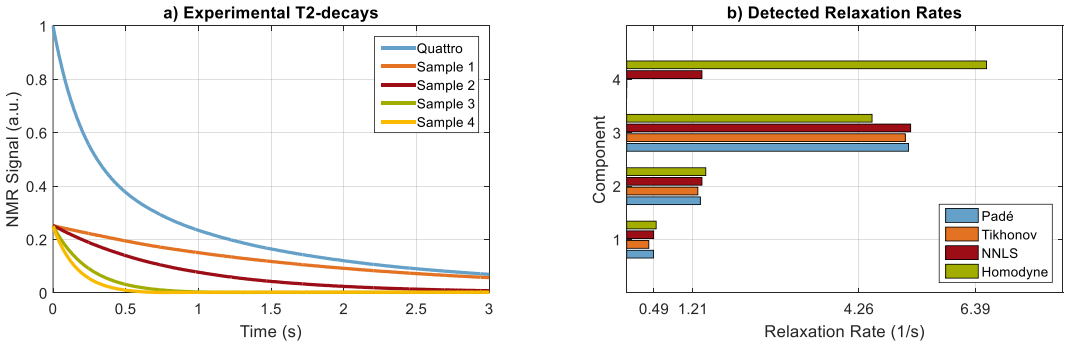

Figure 2 – a) Experimental T2-decays b) Detected relaxation components with the four methods investigated

Fig. 2b) shows the relaxation rates detected by the four investigated numerical Laplace inversion methods when applied to the quattro configuration decay signal. The labeled x-coordinates give the relaxation rates determined by a mono-exponential NNLS analysis of the four samples measured in the single configuration and can be regarded as the benchmark for the multi-exponential analysis. The y-axes lists the relaxation components. Clearly none of the three established methods was able to detect four distinct relaxation components. Although we employed the knowledge of four relaxation components. For our method the number of components in the sample is irrelevant since the algorithm can stop at any time when going to higher relaxation rates. Additionally, the resolution of our homodyne approach can be increased by decreasing the increment step of δa. However, this would increase the computational time due to the increasing number of iteration steps.

References

[1] A. Istratov, O. Vyvenko, Rev. Sci. Instrum. 70, 1233 (1999) 1233–1257.

P10

^{129}Xe NMR Methodology for Complex Porous Matter

J. Hollenbach[a], V. Kotolup[b], R. Valiullin[b], D. Enke[c], J. Matysik[a]

[a]Universität Leipzig, Insitut für Analytische Chemie, Linnéstr. 3, 04103 Leipzig, Germany; [b]Universität Leipzig, Abteilung für Grenzflächenphysik, Linnéstr. 5, 04103 Leipzig, Germany; [c]Universität Leipzig, Insitut für Technische Chemie, Linnéstr. 3, 04103 Leipzig, Germany.

Porous media exist ubiquitous in nature and industry, e.g., as rocks, biological foams, lung tissue as well as silica and metal oxide based catalytic materials, molecular sieves and porous membranes in sensors. Hence, the determination of structural and transport properties of those materials is of great importance in a broad range of scientific, technological and medical fields. There are several "classical" methods, such as X-ray diffraction, gas adsorption and Pulsed Field Gradient (PFG)-NMR allowing to characterize either structural parameters or dynamics inside the voids. Each method, however, has its own limitations in dimensions and resolution. Additionally, it is demanding to obtain full information of all properties.

The application of ^{129}Xe-NMR offers an alternative insight, as it can be used to probe both structure and transport in porous media. During the last decades, it has become a well-established technique to study different classes of porous materials and surfaces.[1–4] In general, the NMR parameters are correlated to the interactions of the gas, the symmetry of the voids and also the motion of the gas inside the material. Using hyperpolarized (HP) ^{129}Xe gas, the sensitivity, i.e., the signal strength can be enhanced by several orders of magnitude allowing to work with very low Xe concentrations in the sample. In this range, effects of Xe-Xe interactions can be neglected, thus, the spectroscopic information exclusively reflects the gas-sample interaction. Thus, it is possible to extract structural properties, such as the number of different adsorptions sites, their size and geometric shape. At the same time, transport properties can be observed, e.g., by ^{129}Xe-Exchange Spectroscopy (EXSY) experiments and the extension of PFG-diffusion measurements to ^{129}Xe-NMR. Compared to "classical" PFG-NMR, the latter approach allows investigating much greater length scales and thus, making the extraction of long-range transport properties achievable.[5]

Here, we present the application of HP ^{129}Xe-NMR for the characterization of structure and dynamics in different classes of mesoporous materials such as Controlled Pore Glasses (CPG) and MCM-type materials providing a broad range of pore sizes and structural order. The ^{129}Xe chemical shift and the linewidth are the main parameter to derive information about the pore structure but can be influenced by exchange and transport effects. These processes are investigated in greater detail by selective EXSY experiments and diffusion measurements. Combining the information about structure and dynamics, the influence of local (structural) properties on long-range (transport) properties is investigated.

References

[1] J.P. Butler, R.W. Mair, D. Hoffmann, M.I. Hrovat, R.A. Rogers, G.P. Topulus, R.L. Walsworth, S. Patz, J. Phys.: Condens. Matter 14 (2002) 297–304.

[2] I.L. Moudrakovski, A. Nossov, S. Lang, S.R. Breeze, C.I. Ratcliffe, B. Simard, G. Santyr, J. Ripmeester, Chem. Mater. 12 (2000) 1999–2001.

[3] M.-A. Springuel-Huet, J.-L. Bonardet, J. Fraissard, Appl. Magn. Reson. 8 (1995) 427–456.

[4] S.M. Lee, S.C. Lee, V. Mehrotra, H.J. Kim, H.C. Lee, A. Nano, Bull. Korean Chem. Soc. 33 (2012) 511–514.

[5] R.W. Mair, M.S. Rosen, R. Wang, D.G. Cory, R.L. Walsworth, Mag. Res. Chem. 40 (2002) 29-39.

Confined fluids: Nanotechnology-driven quest for new physics

S. Mascotto[a], R. Valiullin[b]

[a]University of Hamburg, Institute of Inorganic and Applied Chemistry,Martin-Luther-King Platz 6, 20146 Hamburg, Germany. [b]University of Leipzig, Faculty of Physics and Earth Sciences, Linnestr. 5, 04103 Leipzig, Germany.

The art of chemical synthesis of nanoporous materials with well-defined structural properties has substantially progressed over the last decades. It has now become possible to produce porous materials, which allow for the most accurate explorations of different properties of confined condensed matter, which may dramatically deviate from those known for their bulk counterparts. By using the structure-templating precursors, the structural properties, such as pore size, pore geometry, and long-range pore ordering can be independently tuned to address different aspects of quite diverse phenomena. In this contribution, by considering one selected family of nanoporous silica material with a well-organized pore structure, we demonstrate the new potentials opened by these materials for fundamental research.

The two materials used in this work, referred to as PIB-IL and FDU-12 have very similar pore structures. It is composed of body-centered and face-centered cubic close-packing of spherical cages with the pore diameters of 16 nm and 12 nm, respectively (see, e.g., Figure 1a). The spherical cages are interconnected with one another with worm-like cylindrical channels with a diameter below 2 nm. Further details on the synthesis principle can be found in, e.g., Refs. [1,2]. This particular organization of the pore space, namely the nanometer-scale cavities separated in space and weakly coupled to one another, makes it ideal to address various physical phenomena. Here we focus on two long-standing problems concerning (i) mass transfer under condition of inhomogeneous density distribution and (ii) nucleation phenomena in deeply supercooled liquids.

By exploiting the large pore size difference between the spherical cages and the worm-like channels, giving rise to a notable difference in their capillary-condensation and capillary-evaporation pressures, the pore space in this materials can easily be prepared to contain the capillary-condensed liquid in the small channels and the gaseous phase in the big cages. The spatial ordering of the thus created domains with the different fluid densities serves an ideal model system to address transport under conditions of imhomogeneous density distributions. According to the classical diffusion theory, the effective transport rates in these situations, namely when the phase with the highest diffusion rate forms closed regions, are dictated by the phase with the lowest transport resistance. In contrast, the experiments performed using pulsed field gradient NMR revealed an almost three-fold transport enhancement (Figure 1b) [3]. By taking a closer look into transport mechanisms, the occurrence of this puzzling observation could be traced to a peculiar statistics of the molecular propagations in the gas-filled spherical cages. It has been shown that, depending on the thermodynamic conditions deciding on the gas-liquid equilibrium, the emerging memory effects in the molecular propagation directions can indeed either lead to the situations predicted by the classical diffusion approaches or to a transport acceleration if the memory effects become negligible. Exactly the latter conditions were shown to be applicable for the experiments performed. The respective theory developed has lead to perfect agreement between experiment and theory.

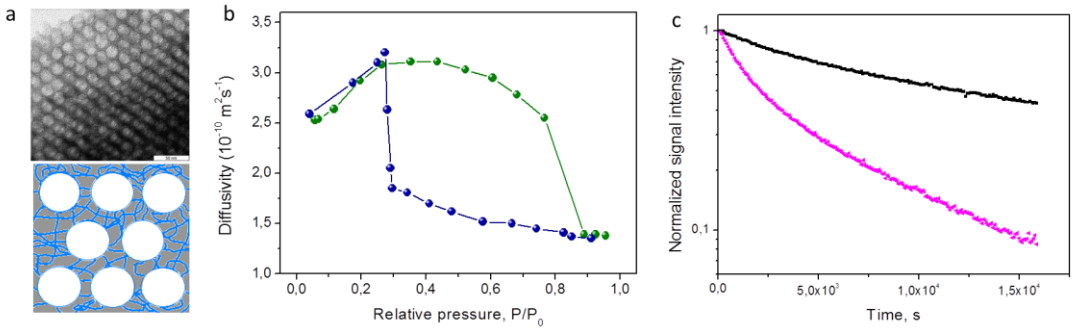

Figure 1 – (a) Electron micrography image and schematic structure of the PIB-IL material. (b) Diffusion behavior of cyclohexane in PIB-IL for different gas-liquid equilibria. (c) Frezing kinetics of water in FDU-12 following temperature quenches from -35°C to -39°C and from -35°C to -41°C.

Another interesting potential application of this type of material concerns physics of the nucleation processes close to the spinodal points. Their advantage in this respect is that the nucleation process can be followed in tiny volumes of the spherical cages. In the bulk substances any single nucleation event leads to a phase transition over the whole sample, precluding accurate determination of the nucleation rates. In contrast, in PIB-IL or FDU-12 the transitions are limited to occur in the single cages. Figure 1c demonstrates typical freezing kinetics measured for water after temperature quenches to temperatures close to the spinodal temperature. We demonstrate that their analysis allows for a very accurate determination of the nucleation rates not accessible by other techniques. In addition, we show that the experimental data signal the emergence of the inter-pore coupling phenomena for the phase transitions, which have never been reported before and which are presumably associated with the alterations of the density fluctuations in the course of the transition.

References

[1] Yu, T. et al. Pore structures of ordered large cage-type mesoporous silica FDU-12s. J. Phys. Chem. B 110 (2006) 21467-21472.
[2] Sel, O., Kuang, D., Thommes, M. & Smarsly, B. Principles of Hierarchical Meso- and Macropore Architectures by Liquid Crystalline and Polymer Colloid Templating. Langmuir 22 (2006) 2311-2322.
[3] Zeigermann, P., Naumov, S., Mascotto, S., Kärger, J., Smarsly, B. M., & Valiullin, R. Diffusion in Hierarchical Mesoporous Materials: Applicability and Generalization of the Fast-Exchange Diffusion Model. Langmuir 28 (2012) 3621-3632.

Online NMR measurements and parameter optimization by fluid analysis system

W.L. Chen[a], L.Z. Xiao[a], Y. zhang[a], G.Z. Liao[a]

[a]State Key Laboratory of Petroleum Resources and Prospecting, China University of Petroleum, Beijing, China

NMR measurements can provide fluid type, content and many fluid properties, through which we can instruct activities on oil drilling, mining, refining and transportation.

When fluid flows, NMR responses will be more complicated. Not only does flow rate affect the echo amplitude, but the presence of local inhomogeneous magnetic field can also cause additional signal attenuation, which would lead to deviation in identification and quantitative calculation of flowing fluids. Therefore, we need to: 1. correct the offset by flow rate. It notes that the influence of flow rate on acquired signal is also related to fluid type. Thus, to flow fluids, the spectrum shift is related to V*T_2, where V is flow rate and T_2 is the transverse relaxation time of measured sample. 2. minimize the impacts of inhomogeneous magnetic field. At the beginning, we should consider the effects of different factors (eg, B_1 intensity, echo spacing, flow rate, polarization time et al) on signal amplitude in inhomogeneous field. By doing so, optimized parameters can be set when measurements are going on.

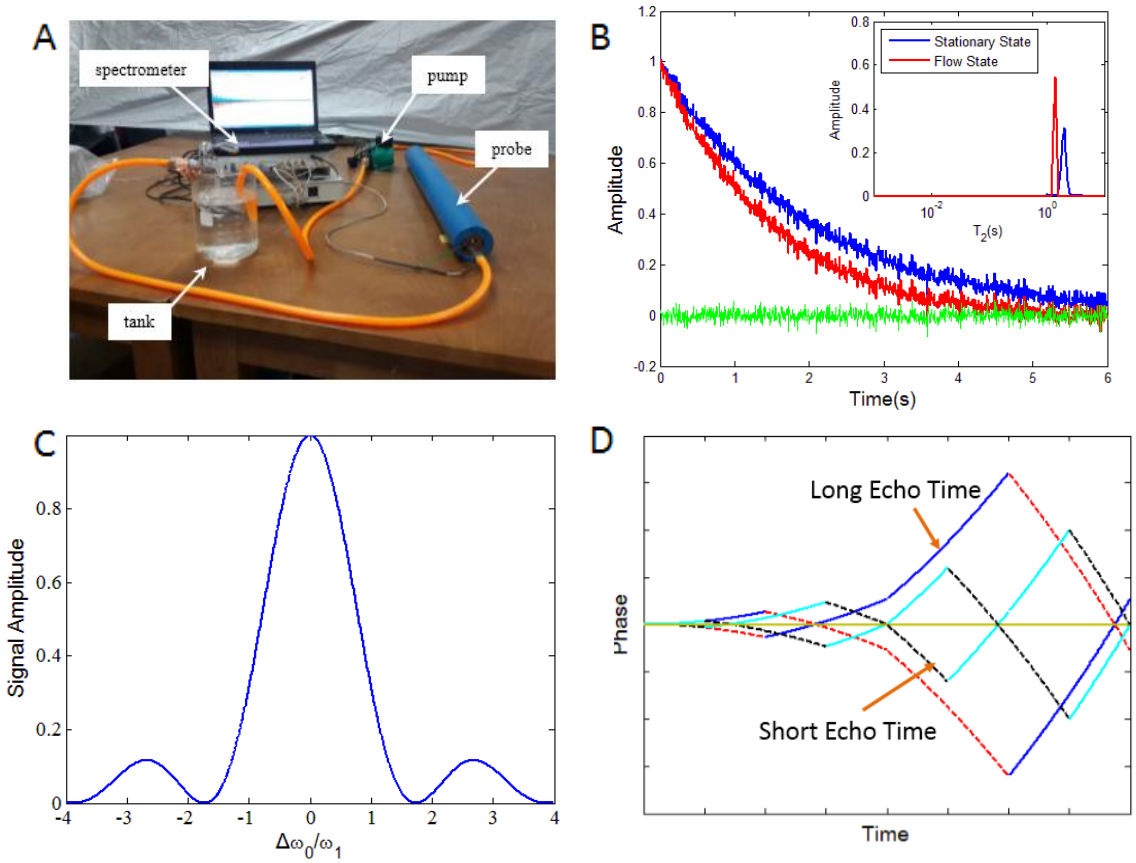

Figure A is the online fluid analysis system which consists of probe, spectrometer, upper computer, et al; Figure B tells us the response differences between stationary fluid and flow fluid; Figure C presents the relationship between B_1 intensity and signal amplitude. From the figure, it is seen that when B_1 gets larger, the influence by field inhomogeneity on acquired signals will be smaller. Figure D shows the signal intensity of different echo time. In the figure, long echo time contributes to more serious dispersed phase. In addition, as the fluid flows forward, the dispersed phase will be accumulated.

Reference

[1] F. Deng, L.Z. Xiao, W.L. Chen, et al. *J. Magn. Reson*, 2014, 247:1-8.

[2]A Caprihan, E Fukushima. *Phys. Rep*, 1990, 198(4): 195-235.

[3] F. Casanova, J. Perlo, B. Blümich. *Springer Berlin Heidelberg*, 2011.

A home-built NMR Core Analytic system based on the OPENCORE Spectrometer

Guang Yang, Lizhi Xiao, Wei Liu

China University of Petroleum Beijing, 18 Fuxue Road, Changping, Beijing China 102249

Oil and gas production is highly dependent on understanding key properties of reservoir rock, such as porosity, permeability and wettability[1]. Geoscientists have developed a variety of approaches to measure these properties, including log and core analysis techniques.[1] To visualize the fluids in small pores, the measurement parameter known as TE (Time to Echo) must be as short as possible. We describe the design of a home-built 2MHz NMR core analytic system (figure 1) which is based on the OPENCORE spectrometer[2] (Thank Professor Takeda).

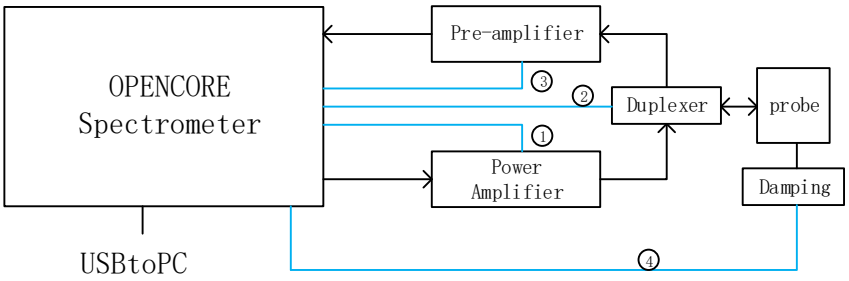

Figure 1 -A block diagram of the core analytic core system

The spectrometer contains the console software which was developed by Qt, the whole program for the FPGA chip and several peripheral circuits. We reproduced the spectrometer and did little modification in order to add some other necessary parts, like the power amplifier, pre-amplifier, duplexer and damping circuit. This system has two new characters: the active broadband duplexer (1-25MHz) and the active damping circuit. In previous work, for the duplexer part, like the based-on cross diode pairs and quarter-wave length line, π network equal to quarter-wave length line. But the former is not suitable for the low frequency system and the latter one is a passive circuit and it will increase the ring down time. We designed the broadband duplexer which is consist of two FET switches connected back to back that isolate the receiver when the transmitter is ON, and a pair of cross-coupled diodes that isolate the transmitter from the coil when it is OFF. For the recovery time, A.S. Peshkovsky used a transformer to absorb the energy from the antenna after the transmitter pulse [3]. Based on it, here we optimized the circuit, during the damping “on”, the damping circuit work and dissipate the energy from the antenna through two resisters. The time sequence is showed in figure2. The active way (including the duplexer and damping circuit) introduce to the noise to the FID signal, but phase cycle of the receiver in the FPGA can eliminate this affection.

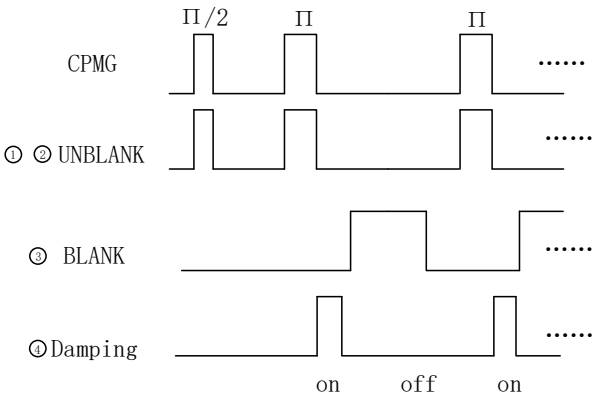

Figure 2 –The time sequence for each part of the system

This can substantially decrease acquisition times while simultaneously increasing signal to noise ratio. The shorter the echo time provided by the NMR instrument, the shorter T2 that can be resolved, enabling smaller pore sizes to be detected. This is especially important in unconventional reservoirs, more specifically, shale oil, gas and heavy oil reservoirs.

References

[1] C. Straley, D. Rossini Log Analyst. 38(1997)84-93

[2] Kazuyuki Takeda. Journal of Magnetic Resonance. 192 (2008) 218–229

[3] A.S. Peshkovsky a,*, J. Forguez b, L. Cerioni a. Journal of Magnetic Resonance 177 (2005) 67–73

Machine Learning for Magnetic Resonance

Yiqiao Song[a], Martin D. Hurlimann[a], David Cory[b]

[a]Schlumberger-Doll Research, Cambridge MA USA; [b] University of Waterloo, Canada.

As is common in MR experiments, the measurement typically includes a long wait time to allow nuclear magnetization to substantially recover to its equilibrium. As a result, most MR experiments are time consuming. In particular, for a multiple dimensional experiment, many scans are needed for all dimensions and signal averaging. Thus methods to reduce the number of scans are highly desirable, e.g. the use of compress sensing. Furthermore, different samples exhibit different T1, T2, diffusion coefficient, J-coupling and dipole coupling, etc. Thus a particular pulse sequence with fixed timings won't be optimized for all samples.

Take T1 measurement as an example. Assuming using inversion-recovery sequence to measure Sample 1 with T1 in the range of 1 s. The optimal recovery time list would be, for example, 0.1 s to a few seconds. However, this time list won't be appropriate for different samples with a T1 in the range of 0.01 s. In practice, NMR laboratory often uses protocols to cover the recovery time from 0.001s to 10 s. As such, the conventional approach is always sub-optimum for every sample.

In this paper, we propose a new method to dynamically optimize the measurement program so that it is always optimized for the specific sample under investigation. This method utilizes the concept of machine learning to analyze the acquired data during the measurement to dynamically determine the experimental parameters for the subsequent sequences. As a result, the NMR measurement will always focus on the appropriate parameters to obtain the most effective data to determine the properties of the individual sample. The concept is shown as a flow chart in Figure 1.

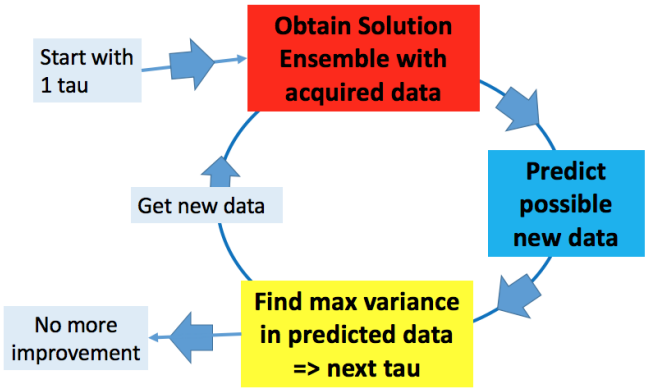

Figure 1. An example flow chart of the machine learning algorithm for optimizing NMR pulse sequence**.**

The key step in the above algorithm is to obtain the solution ensemble for a given data. We have used Monte Carlo method to sample the solution space and some example algorithms have been reported [1,2]. We will show numerically that optimization of the pulse sequence parameters can be achieved for T1, T2, diffusion coefficient, and J-coupling measurements.

References

[1] Prange, Michael D and Song, Yi-Qiao, Understanding NMR T2 Spectral Uncertainty, Journal of Magnetic Resonance 204, 118-123(2010).
[2] Michael D Prange and Yi-Qiao Song, Quantifying uncertainty in NMR T2 spectra using Monte Carlo inversion. J Magn Reson 196, 54-60(2009).

A New Side-looking Design For Downhole NMR Probe

S. Luo, L.Xiao, G. Liao, Y.Zhang

State Key Laboratory of Petroleum Resources and Prospecting; China University of Petroleum, Beijing 102249, Beijing, China.

Downhole NMR probe is one of the main components of NMR well logging tool, which is used to polarize underground formation fluids and receive NMR signals[1]. Centralized probe has its advantages for high signal-to-noise ratio, but it will be affected by borehole fluids which can attenuate the RF power and received signal amplitude, And it sometimes does not work well in deviated and horizontal wells. A new side-looking downhole NMR probe is designed for 45cm vertical formation resolution and investigation of depth (from the surface of the probe to the target) is ranged from 9.5 cm to 12.5 cm. The diameter of the probe is 127cm (5 inch) that can be applied in small borehole whose diameter is 6 inch in general. Because of the side-looing design, 80 degree azimuthal sensitive region is detected by the probe for the purpose of using low transmitter power and getting high signal-to-noise ratio.

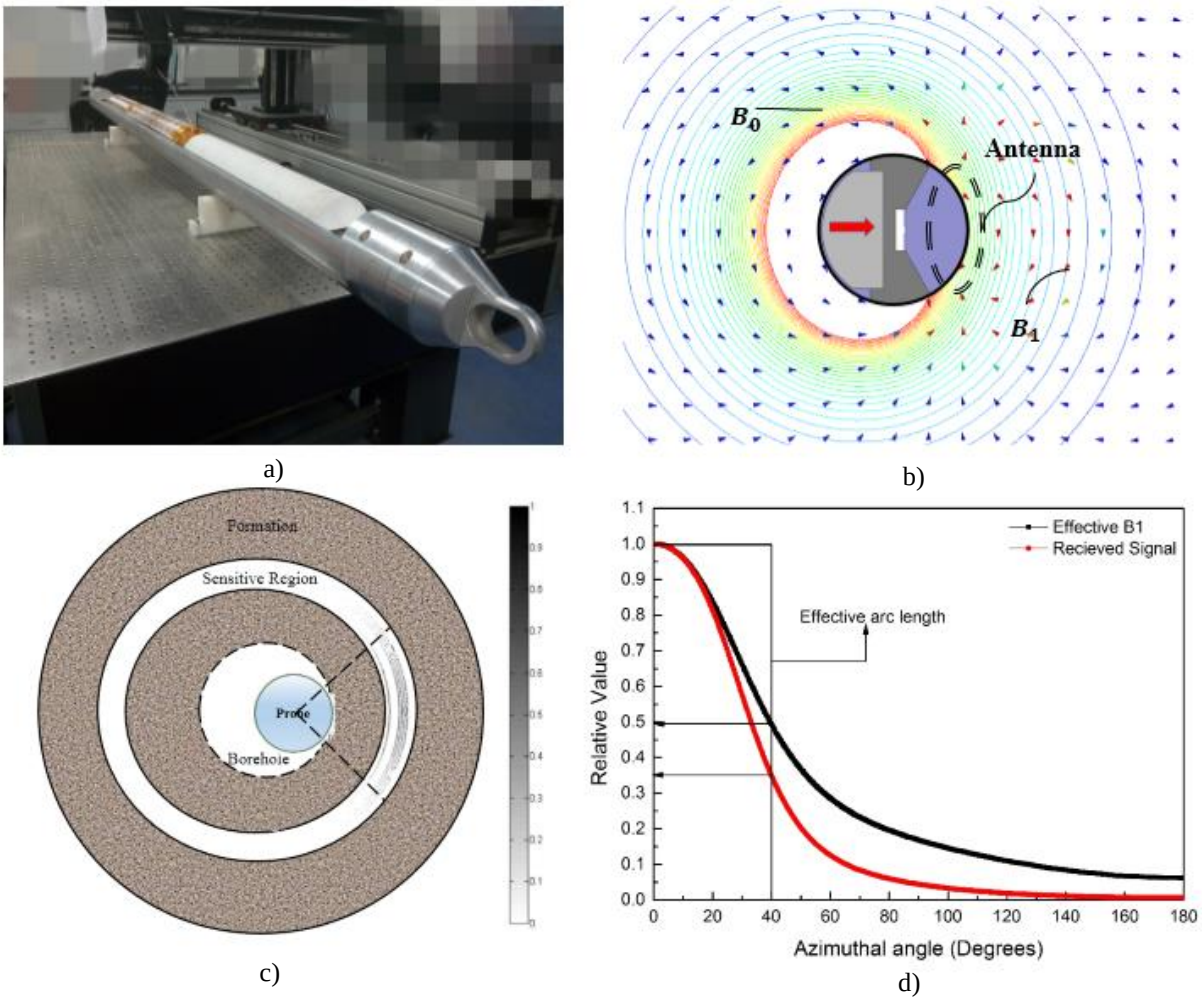

Figure 1. Illustration of porbe for field distribution, sensitive region and received signal distribution.

As shown in Figure 1, a) is the probe without fiberglass sleeve. b) is the illustration of the cross section of B_0 and B_1 distribution from the probe, the isolines represent the B_0 distribution and the arrows represent the B_1 distribution. c） is the illustration of sensitive volume, each slice corresponding to different operating frequency is shown, signals[2] calculated are contributed from this part at an arc length approximate 80°. d) is the calculated effective B_1 and received signal in front of the probe, for simplifying the illustration[3], only one half of the azimuthal angel is shown.

References

[1]Coates G R, Xiao L Z, Prammer M G. NMR Logging Principles and Applications: Gulf Professional Publishing, 1999.
[2]Hürlimann M D, Griffin D D. Journal of Magnetic Resonance, 2000.S
[3]Reiderman A, Beard D R. U.S. 6580273, 2003.

A new proof and applications in NMR inversions of the Tikhonov method

Y. GAO [a,b], L. XIAO [a*], B. Wu [a,c]

[a]State Key Laboratory of Petroleum Resources and Prospecting, China University of Petroleum, Beijing 102249, China; [b]College of Science, China University of Petroleum, Beijing 102249, China; [c]ABQMR, Albuquerque, NM 87106, USA

The nuclear magnetic resonance (NMR) relaxation time inversion is crucial. However, the inversion is ill-posed. So, the inversion is often found much less accurate and bear little resemblance to the true solution. The regularization methods are employed to overcome the ill-posedness, while Tikhonov is a classical and effective method among those regularization methods [1]. Given an operator equation $Kf=g$, where f and g are in Hilbert spaces X and Y, respectively, and K is a compact linear operator from X to Y. The solution of the Tikhonov method satisfies the minimum optimization: $\min\|Kf-g\|^2+\alpha\|f\|^2$, where $\alpha>0$ is a regularization parameter. Using the Euler formulas, the Tikhonov solution is $f=(K^*K+\alpha I)^{-1}K^*g$, where K^* is the conjugated operator of K and I is the identity operator.

First, we prove that Tikhonov method is well-posed, i.e.,

Theorem 1: for each $\alpha\in(0,+\infty)$, the inversion operator of $K^*K+\alpha I$ exists and is continuous.

Proof. Since K^*K is compact, all the spectra of K^*K except for 0 are eigenvalues [2] and all the eigenvalues of K^*K are non-negative real numbers. Hence, for each $\alpha\in(0,+\infty)$, $-\alpha$ is a regular value of K^*K. This means $-\alpha I-K^*K$ has a continuous inversion, so does $K^*K+\alpha I$.

By Theorem 1, the solution is well defined and the Tikhonov method is well-posed. The existence and uniqueness of the Tikhonov solution account for the existence of the inversion of the operator $K^*K+\alpha I$. While the stableness thanks to the continuity of the inversion operator of $K^*K+\alpha I$.

Next, we show:

Theorem 2: the operator value function $m(\alpha)=(K^*K+\alpha I)^{-1}$ is differentiable on $(0,+\infty)$ with the variable α.

Proof. It can be deduced that $m(\beta)-m(\alpha)=-(\beta-\alpha)m(\beta)m(\alpha)$ and $m(\alpha)=(I+(\beta-\alpha)m(\alpha))m(\beta)$. Since $I+(\beta-\alpha)(K^*K+\alpha I)^{-1}$ has a continuous inversion and $\|(I+(\beta-\alpha)(K^*K+\alpha I)^{-1})^{-1}\|<2$ when β approximates α [1], $\|m(\beta)\|=\|(I+(\beta-\alpha)m(\alpha))^{-1}m(\alpha)\|\le 2\|m(\alpha)\|$. Hence, $\|m(\beta)-m(\alpha)\|=\|(\beta-\alpha)m(\beta)m(\alpha)\|\le 2|\beta-\alpha|\|m(\alpha)\|^2$. This means $\lim_{\beta\to\alpha}m(\beta)=m(\alpha)$, i.e., $m(\alpha)$ is continuous. $m(\alpha)$ is differentiable since $\lim_{\beta\to\alpha}\frac{m(\beta)-m(\alpha)}{\beta-\alpha}=\lim_{\beta\to\alpha}-m(\beta)m(\alpha)=-m^2(\alpha)$.

Based on Theorem 2, estimation, which is not so close to the optimal regularization parameter is sufficient to get a satisfactory solution. Thus it greatly decreases the calculation when one determines the regularization parameter.

Finally, two numerical simulations and a core analysis arising from NMR transverse relaxation time inversion are conducted to show the effectiveness of the Tikhonov method. Figure 1 shows the inversions with different signal-to-noise ratio (SNR). SIRT method is used to enforce the nonnegative constraint. It can be seen from the figure that the inversions coincide with the model well when SNR≥5. Even when SNR=2, the shape of the inversion is the same as that of the model. And the peak of the inversion shifts to right and is thinner than that of the model. Figure 2 is the inversions with different regular parameter α. To illustrate how the regular parameter affects the results, gradient projection method is employed to enforce the nonnegative constraint, though the results are worse than those using SIRT method. The figure shows that the inversions are almost similar, though α varies from 0.05 to 2. This agrees with our theory. The NMR shale core analysis is shown in Figure 3. The curve titled by Tikhonov is inversed by Tikhonov method while the curve titled by LNMR is inversed by LapNMR using SVD method. The figure shows that they are in good agreement.

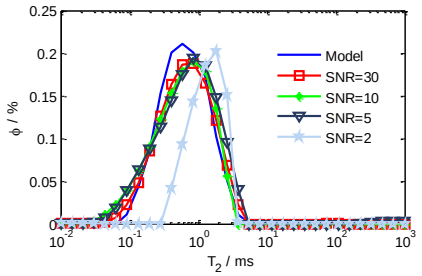

Figure 1 Inversion results with different SNR

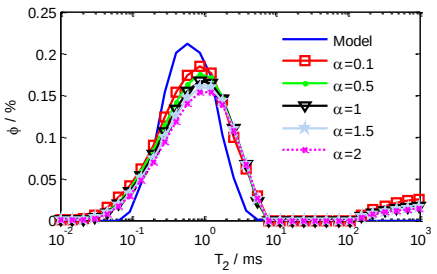

Figure 2 Inversion results with different α

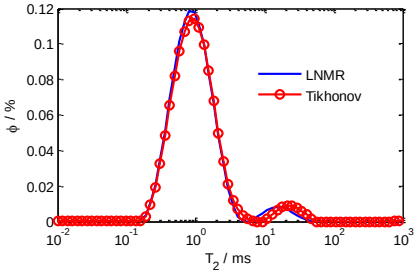

Figure 3 NMR core analysis

Statistics of the solutions of the first simulation are shown in Table 1.

Table 1: Comparison of the inversions and model of the first simulation

SNR	Error of total porosities	Mean of residuals	Std of residuals	Max of residuals
30	0.0358	0.0011	0.0111	0.0371
10	-0.0022	-0.0001	0.0152	0.0464
5	-0.0856	-0.0027	0.0199	0.0565

References

[1] A. Tikhonov, Soviet math.Dok1.4, 1624, 1963.
[2] W. Rudin, Functional Analysis (Second Edition) [M]. Beijing: China Machine Press, 2004.
[3] G. Coates, L. Xiao, M. Prammer. NMR Logging Principles and Applications [M]. Texas: Gulf Publishing Company, 1999.

Biocompatible silicon nanoparticles as MRI contrast agents for cancer diagnosis

Yu.V. Kargina[a,d], M.B. Gongalsky[a], L.A. Osminkina[a], A.M. Perepukhov[b], M.V. Gulyaev[c], Yu.A. Pirogov[c], A.V. Maximychev[b], V.Yu. Timoshenko[a,d].

[a]Lomonosov Moscow State University, Department of Physics, 1, Leninskie gory, 119991, Moscow, Russia; [b]Moscow Institute of Physics and Technology, 9, Institutsky per., 141700, Dolgoprudny, Moscow Region, Russia; [c]Research Center for MRI and MRS, Lomonosov Moscow State University,1, Leninskie gory, 119991, Moscow, Russia; [d]National Research Nuclear University "MEPhI", 115409 Moscow, Russia.

Scientists are paying special attention to the study of nanoparticles nowadays. Nanometer dimensions allow nanoparticles penetrate into cells, allowing use them as agents for therapy and diagnosis. Promising for this purpose are silicon nanoparticles (SiNPs). It has been shown that they have low toxicity and dissolve in biological environment, they transforms into orthosilicic acid $Si(OH)_4$, which is naturally excreted from the body with the urine (biodegradable) [1,2]. SiNPs were used as a basis for the development of new effective methods of cancer therapy. They can sensitize hyperthermia, i.e. local heating of a tumor tissues leading to an efficient destruction of cancer cells, under their irradiation by infrared radiation, ultrasound and radio-frequency waves [3,4]. The proposed methods of cancer treatment can be combined with simultaneous diagnostics. SiNPs can act as contrast agents (CA) for magnetic resonance imaging (MRI).

MRI is one of the most informative diagnostic method to obtain detailed images of the studied areas. CA are often used to improve the quality of images. Currently, the most common CA based on gadolinium and iron oxide. They provide good contrast, but can be highly toxic [5].

Aqueous suspensions of PSiNPs were prepared and the study was devoted to measurements of proton relaxation time. Magnetization relaxation dependencies showed strong shortening of transversal relaxation time T2 in PSiNPs suspensions by comparison with DI water from 2700 to 240 ms, while longitudinal relaxation time T1 was changed moderately from 4000 to 2450 ms

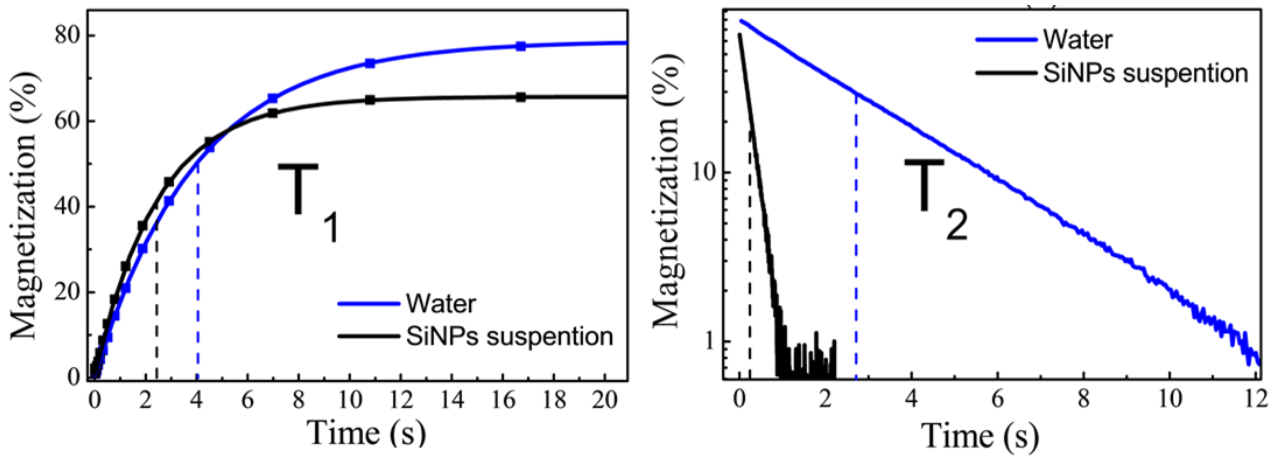

Figure 1 Longitudinal and ransversal magnetization of PSiNPs and water

We assume that the shortening of relaxation times is based on magnetic dipole-dipole interaction between protons in water molecules and paramagnetic dangling bonds on the surface of nanoparticles. Experimental observation of such effects opens the way to the use SiNPs as safe CA for MRI

References

[1] S. Park et al., Mater. Chem. B 3 (2015) 198-206
[2] A.D Durnev et al.,Int. J. Biomed. Nanosci. Nanotechnol. 1 (2010) 70-86
[3] K.P. Tamarov et al., Sci. Rep., 4 (2014) 7034
[4] A.P. Sviridov et al., Microporous and Mesoporous Materials. 210 (2015) 169-175
[5] T. Grobner et al., Nephrol. Dial. Transplant 21 (2006) 1104-1108

Diffusion quantifications in MR-mammography by threshold isocontouring

F. Zong[a], S. Bickelhaupt[b], T. A. Kuder[c], W. Lederer[d], H. Daniel[e], A. Stieber[f], H.-P. Schlemmer[b], P. Galvosas[a], F. B. Laun[c]

[a]School of Physical and Chemical Sciences, MacDiarmid Institute for Advanced Materials and Nanotechnology, Victoria University of Wellington, Wellington, New Zealand; [b]Department of Radiology, German Cancer Research Center (DKFZ), Heidelberg, Germany; [c]Medical Physics in Radiology, German Cancer Research Center (DKFZ), Heidelberg, Germany; [d]Radiological Practice at the ATOS Clinic Heidelberg, Heidelberg, Germany; [e]Radiology Center Mannheim (RZM), Manheim, Germany; [c]Germany University Hospital Heidelberg, Department of Clinical and Interventional Radiology, Heidelberg, Germany

Breast cancer is the leading disease in women and can be detected by various medical imaging methods, among which non-invasive magnetic resonance imaging (MRI) is of high sensitivity [1]. Diffusion weighted imaging (DWI) has been suggested as an adjunct diagnostic protocol in MR-mammography because of its high specificity and low cost [2]. It allows measuring the mobility of water molecules which can be quantified by the values of apparent diffusion coefficients (ADC) [3]. Other quantifications, such as perfusion factor (*f*), diffusivity (*D*) and kurtosis (*K*) [4,5], also describe different behaviours of water movements. However, breast tissue is a complex porous medium, leading to a heterogenous structural compositions. Large variations of DWI quantifications on different tissue compositions and regions were reported [6]. Furthermore, the DWI results calculated from a defined region of interests (ROI) depends on its volume and according method used for processing. These emphasise the importance of a correct definition of ROI and a proper data processing method to discriminate breast tumour types more effectively and accurately.

Here we propose a threshold isocontouring strategy for reducing the variability caused by different observers. This retrospective subgroup analysis was performed within an ongoing study which was approved by an institutional and governmental ethical review board. Written informed consent was obtained. Twenty female participants with suspicious findings on screening X-ray mammograms and indication for biopsy were included. All patients were imaged on a 1.5T Siemens MRI scanner (Munich, Germany) prior to biopsy. DWI data was acquired with four different *b*-values 0, 100, 750, and 1500 s/mm². Two ROIs were quantified by independent readers, and utilized to test their influences on the final ADC, *f*, *D* and *K* values. Subsequently a threshold was imposed relative to the maximal signal intensity in the region of the DW image with b = 1500 s/mm^2. Pixels with signal intensity larger than the threshold were selected and used for calculating the mean ADC, *f*, *D* and *K* values. These calculations were implemented by fitting the data with the intravoxel incoherent motion (IVIM) and kurtosis models [4, 5].

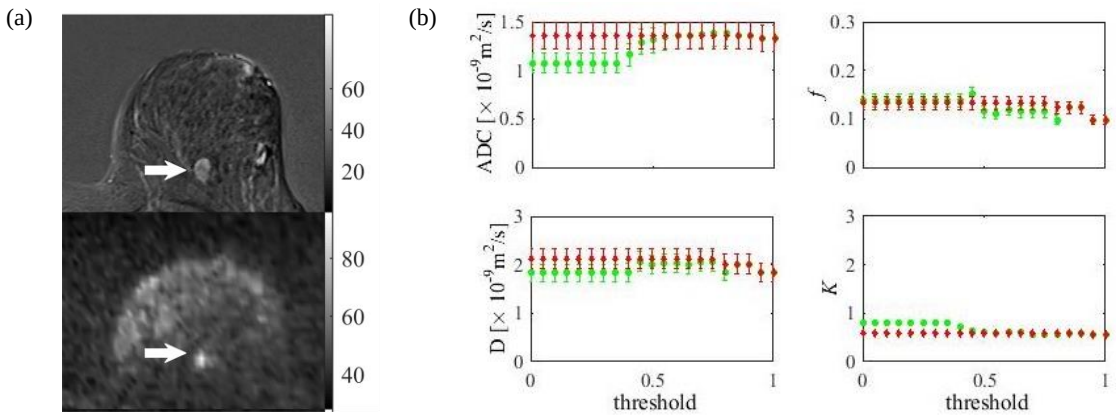

Figure 1 – (a) Dynamic contrast enhanced T_1 weighted (upper) and DW (b=1500 s/mm^2, lower) images of a 50-year-old female patient with fibroadenoma; (b) Mean ADC, *f*, *D* and *K* values of the lesion in (a) as a function of thresholds based on two ROIs (green and red) defined by independent readers.

The mean ADC, *f*, *D* and *K* values of a 50-year-old female patient with fibroadenoma were compared with different thresholds (Figure 1). The mean ADC, *f*, *D* and *K* values for two ROIs were diverse at the beginning, but converged at specific thresholds. These two ROI readings eventually returned the same value for each parameter when threshold arrived at 0.8, which is surprisingly similar to a threshold value used in positron emission tomography for obtaining the correct tumor boundaries [7]. After processing all available patients' datasets and comparing them using the histopathological information from the biopsy as a reference, the statistical analysis showed that the mean ADC value was significantly different in malignant lesions than in benign lesions (p<0.01) when the threshold was 0.85. More detailed results will be presented at the conference.

In conclusion, the threshold isocontouring strategy on the selected ROI can largely reduce the inter-observer variability, thus we suggest applying it prior to the quantitative evaluation and statistical analysis of DWI data. ADC was found to be the most promising quantification parameter in providing the highest specificity in this study.

References

[1] Boetes C, Mus RD, Holland R, et. al. Radiology, 1995;197(3):743-747.
[2] EI Khouli RH, Jacobs M, Mezban SD, et. al. Radiology, 2010;256(1):64-73.
[3] Englander SA, Uluğ AM, Brem R, et. al. NMR Biomed, 1997;10(7):348-352.
[4] Le Bihan D, Breton E, Lallemand D, et. al. Radiology, 1986;161(2):401-407.
[5] Jensen JH, Helpern JA, Ramani A, et. al. Magn. Reson. Med., 2005;53(6):1432-1440.
[6] Arponent O, Sudah M, Masarwah A, et. al. PloS one, 2015;10(10):1-17.
[7] Foster B, Bagci U, Mansoor A, et. al. Comput. Biol. Med., 2014;50:76-96.

Monitoring the animals' health status during vivisection by low-field NMR

J. Viess[a], J. Flohr[a], D. Weidener[a], P. Keschenau[b], H. Simons[b], H. Klingel[b], M. Küppers[a], J. Kalder[b], B. Blümich[a]

[a]RWTH Aachen University, Institut für Technische und Makromolekulare Chemie, Worringerweg 2, 52074 Aachen, Germany; [b]Uniklinikum RWTH Aachen, Clinic for vascular surgery, Pauwelsstraße 30, 52074 Aachen, Germany.

Cardiovascular diseases (CVDs) are the number one cause of death globally. In industrialized countries 25-30 % of all people die because of CVD. Often the cure of CVDs requires surgery accompanied by the use of a cardiopulmonary bypass (CPB). Such surgeries are associated with the highest level of complications, including paraplegia (up to 32 %), renal failure (16-26 %) or mortality (13-42 %) [1]. A small fraction of patients (0.3-3 %) shows complications of the gastrointestinal tract, but the mortality rates for patients with these complications are high with 12-67 % [2, 3]. An explanation for such a high risk of severe complications can be found in a suboptimal efficiency of cardiopulmonary bypasses, whose use in surgeries, leads to insufficient blood supply in different organs of the body and is called ischemia. If not cured immediately ischemia causes expiration of cells. A subsequent regain of blood flow due to the reconnection of the human heart to the vascular system results in a reperfusion injury. During ischemic periods poisons and inflammatory mediators accumulate in the tissue and spread across the whole body, inducing multi organ failure [4]. This study focuses on using the NMR-MOUSE® to monitor the health status of the small intestine during vivisection by determining the self-diffusion coefficients within the intestinal wall. Thus, the efficiency of newly developed and optimized CPBs may be determined and compared to curently operating ones.

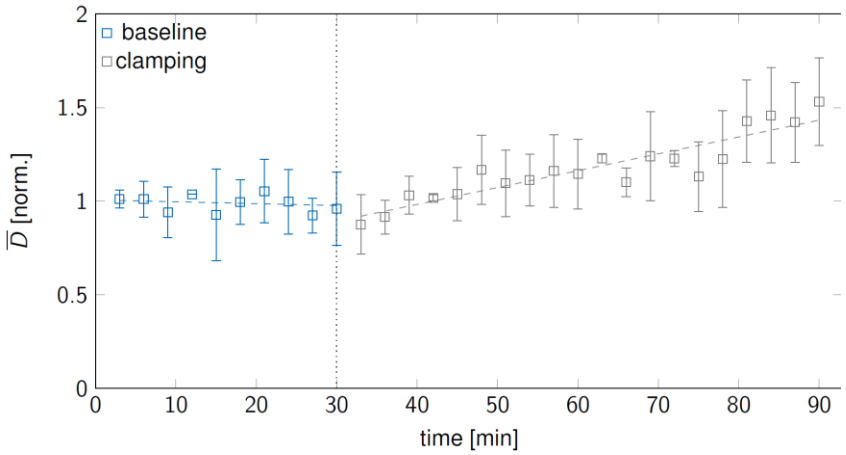

Figure 1 – Averaged, normalized diffusion coefficient as a function of time for intestinal loops, whose afferent blood vessels were clamped for 60 minutes after determination of 10 baseline diffusion profiles.

The intracellular diffusion coefficient was measured with the Fourier-MOUSE [5] using the steady gradient stimulated echo sequence [6]. In the initial stage of this study six different experiments were conducted according to Table 1 to simulate differently efficient CPBs. The result of experiment 3 is shown in Figure 1. During the baseline determination period (blue) the diffusion coefficient does not change, while after closure of the afferent blood vessels (clamping) an ischemic period is initiated. In this period the tissue dies in an autolytic process, leading to a higher mean squared displacement of the intracellular water with time (gray).

Table 1. Experiments conducted during surgical operation with their corresponding number (no.) of measurements per intestinal loop and total experiment duration. Each experiment contained ten diffusion profiles prior to manipulations at the small intestine (baseline).

no.	experiment (no. of measurements)	measurements (total)	duration [min]
1	clamping (10)	20	60
2	clamping (20)	30	90
3	flow reduction (10)	20	60
4	glucose (10) & clamping (10)	30	90
5	glucose (20) & clamping (10)	40	120
6	glucose (10) & flow reduction (10)	30	90

References

[1] J.S. Coselli et al., The Annals of Thoracic Surgery 73 (4) (2002) 1107–1116.
[2] J.T. Christenson, M. Schmuziger, J. Maurice, Cardiovascular Surgery (1994).
[3] A.E. Baue, The Annals of Thoracic Surgery 55 (4) (1993) 822–829.
[4] D.L. Carden, D.N. Granger, The Journal of Pathology 190 (3) (2000) 255–266.
[5] M. Van Landeghem et al., Journal of Magnetic Resonance 215 (0) (2012) 74–84.
[6] D.G. Rata et al., Journal of Magnetic Resonance 180 (2) (2006) 229–235.

Intra-aneurysmal flow and thrombosis

J. Flohr[a], J. Viess[a], J. Clauser[b], G. Cattaneo[c], M. Küppers[a], B. Blümich[a]

[a]RWTH Aachen University, Institut für Technische und Makromolekulare Chemie, Worringerweg 2, 52074 Aachen, Germany, [b]RWTH Aachen University, Helmholtz-Institute for Biomedical Engineering, Pauwelsstraße 20, 52074 Aachen, Germany, [c]Acandis GmbH & Co. KG, Theodor-Fahrner-Str. 6, 75177 Pforzheim, Germany.

An often occurring disease pattern of blood vessels is an aneurysm, a spatially limited enlargement of an artery. With growing size of the aneurysm the danger of a rupture increases. In addition to this health threat blood clots can develop in the damaged blood vessel. These thrombi can wander through the bloodstream and lead to an embolism [1, 2]. To prevent the rupture of an aneurysm, a stent can be inserted into the vessel to cut the aneurysm from the bloodstream. A stent is usually a metallic lattice, which may trigger the formation of a blood clot in the lumen of the aneurysm [3].

For determining the relaxation times of thrombi with varying amounts of blood cells and plasma a 0.22 T tomograph was used [4]. The clotting of pig blood was induced by using tissue factors such as Innovin or Thrombin. The thrombi were grown in three different liquids: pure blood (PB), platelet poor plasma (PPP) and platelet rich plasma (PRP). Pure blood reveals the shortest T_1 and T_2 times, compared to platelet poor and rich plasma. Furthermore, mixtures of pure blood and platelet poor plasma were prepared. A higher amount of platelets leads to a denser sample with a lower iron content and increasing relaxation times [5, 6]. The highest T_1 and T_2 times are obtained from the sample with the highest amount of Innovin, so that more platelets are activated for the clotting mechanism (Fig. 1).

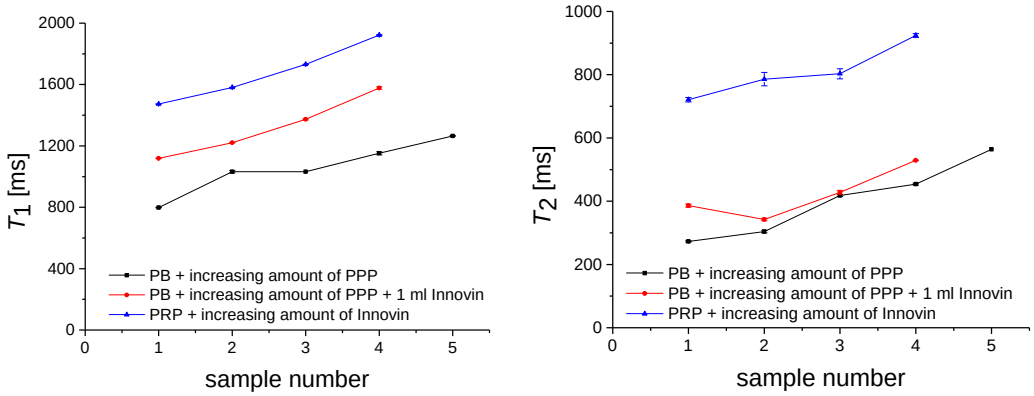

Figure 1 – T_1 and T_2 relaxation times of PB mixed with constantly increasing amount of PPP (black). In order to induce the clotting, Innovin was added to the samples (red). The highest relaxation times were obtained by adding an increasing amount of Innovin to PRP (blue).

In addition to the relaxation time experiments of thrombi, flow patterns in a silicon phantom of a saccular aneurysm were examined by applying the FLIESSEN [7] pulse sequence in high and low magnetic fields. First measurements were conducted both with water (Fig. 2) and blood as a medium and flow rates ranging from 50 mL/h to 1300 mL/h.

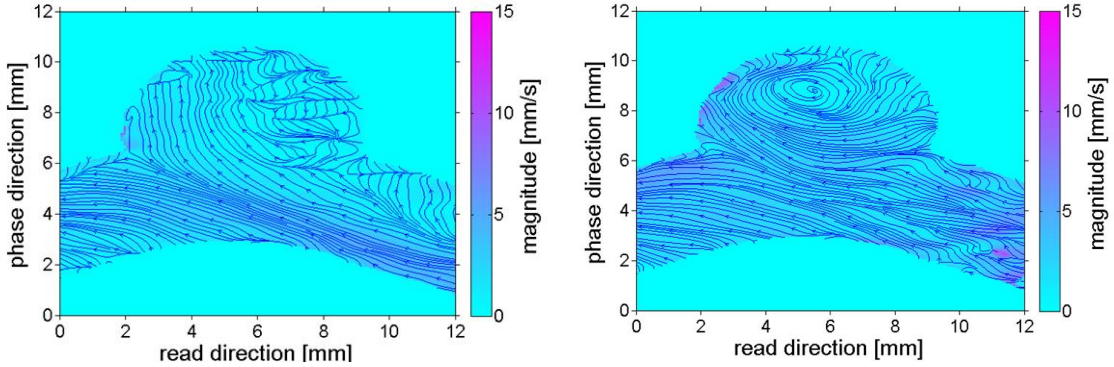

Figure 2 – Magnitude maps of a saccular aneurysm phantom at 500 mL/h (left) and 700 ml/h (right), measured with the low-field tomograph at 0.22 T. The velocity direction is represented by streamlines and arrows. At 700 ml/h a vortex forms in the head of the aneurysm.

References

[1] H. Rieger, G. Küffer, F. A. Spengel, Klinische Angiologie, Spinger-Verlag, Berlin, Heidelberg, 1998.
[2] P. J. Hulcelle, G. C. Dooms, P. Mathurin, G. Cornelis, Neuroradiology 31 (1989) 217-221.
[3] J. R. Cebral, F. Mut, M. Raschi, E. Scrivano, R. Ceratto, P. Lylyk, C. M. Putman, Am. J. Neuroradiol. 32 (2011) 27-33.
[4] E. Danieli, J. Mauler, J. Perlo, B. Blümich, F. Casanova, J. Magn. Reson. 198 (2009) 80-87.
[5] I. Foley, S. A. Farooqui, R. L. Kleinberg, J. Magn. Reson. 123 (1996) 95-104.
[6] J. Vymazal, R. A. Brooks, C. Baumgarner, V. Tran, D. Katz, J. W. M. Bulte, E. Rivka Bauminger, G. Di Chiro, Magn. Reson. Med. 35 (1996) 56-61.
[7] A. Amar, B. Blümich, F. Casanova, ChemPhysChem 11 (2010) 2630-2638.

Fast Field Cycling NMR as a method to study protein dynamics and aggregation of therapeutic proteins

[1]G. Ferrante,[1]R. Steele,[1]M. Pasin,[1]C. Luchinat,[2] M. Fragai, [2]E. Ravera,[2]G. Parigi

[1]Stelar Srl, Via E. Fermi 4, Mede (PV), Italy.
[2]CERM and Department of Chemistry, University of Florence, via Sacconi 6, Sesto Fiorentino, Italy.

Fast Field Cycling NMR relaxometry (FFCR) is a low-field technique which measures the longitudinal (spin-lattice) relaxation rate dependence of the magnetic field strength (NMRD) over a wide range of magnetic fields (from a few kHz upwards), giving important information on the range of molecular motions, such as rotation and diffusion, including slow motions, present in a substance or complex mixture. Herein we will show how FFCR can be used to obtain important information on proteins.

^{1}H NMRD profiles can detect motions occurring on time scales from 10^{-6} to 10^{-9} s, thus allowing the detection of reorientation times of proteins from a few kDa up to MDa. The accessibility of these correlation times can be very useful for monitoring protein aggregation, protein folding, and optimizing protein solution conditions affecting protein tumbling [1,2]. The ^{1}H NMRD profiles show stretched dispersions with respect to the Lorentzian function, possibly due to the combination of fast internal mobility, proton lifetimes shorter than the reorientation time, and aggregation effects. The profiles can be reproduced by a sum of a finite number of Lorentzians, as customarily done in model-free approaches [3]. The largest correlation time obtained in the analysis can provide information of the overall reorientation time of the system, and thus on the presence of aggregation.

The aggregation of therapeutic proteins is an important problem in the bio-pharmaceutical industry. Protein product aggregates are potent inducers of immune responses to therapeutic protein products, thus manufacturers of therapeutic protein products should ensure that their products contain minimal product aggregates. There is a real need for new and improved analytical methods for defining protein aggregates [4,5]. FFCR shows considerable promise for routine assessments of therapeutic protein aggregation. NMRD can be used to characterize very large aggregates because of the very low frequencies achieved and does not suffer from aggregate fractionation or separation as the system is measured [6].

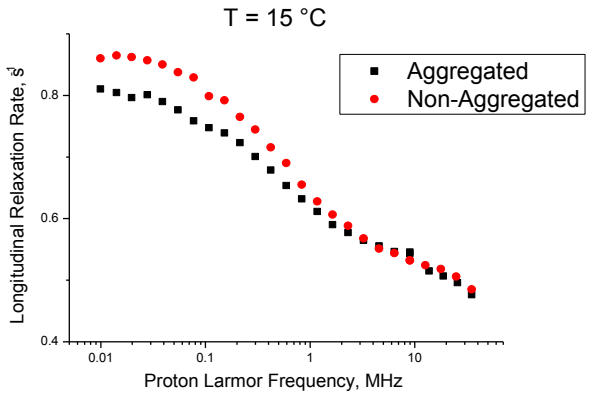

Figure 1 - ^{1}H NMRD profiles of a therapeutic protein in non-aggregated and artificially aggregated states.

References

[1] E. Ravera, G. Parigi, A. Mainz, T.L. Religa, B. Reif, C. Luchinat, *J. Phys. Chem. B* 2013, *117*, 3548;
[2] C. Luchinat, G. Parigi, *J. Am. Chem. Soc.* 2007, *129*, 1055;
[3] I. Bertini, M. Fragai, C. Luchinat, G. Parigi, *Magn. Reson. Chem.* 2000, *38*, 543;
[4] E. Shacter, CHI meeting, April 4 2011, Bethesda, MD, USA;
[5] A.S. Rosenberg, The AAPS journal, 2006, 8(3), article 59;
[6] G. Diakova, Y.A. Goddard, J.-P. Korb, R.G. Bryant, *Biophys. J.* 2010, *98*, 138.

Developing fingerprinting systems to identify fake paintings and assign ancient wall paintings through NMR relaxation studies

C. Rehorn[a], W. Zia[a], T. Meldrum[b], C. Kehlet[c], E. Del Federico[c], G. Zolfo[d], J. Thompson[e], B. Blümich[a]

[a]Institut für Technische und Makromolekulare Chemie, RWTH-Aachen University, Germany; [b]The College of William and Mary, Williamsburg, Virginia; [c]Pratt Institute, New York; [d]Restauration and Conservation, Ercolano, Italy; [e]The Herculaneum ConservationProject, Ercolano, Italy

Non-destructive analysis of arbitrarily sized samples with the NMR-MOUSE [1, 2], a unilateral stray-field NMR sensor, has proven to be a valuable procedure in many branches of cultural heritage as insights into the stratigraphy of intact objects can be gained while information about material properties such as molecular mobility is provided at the same time. As the MOUSE selectively detects signal only from a slice a few millimeters away from the surface, depth profiles are acquired by mounting the device on a stepper-motor controlled sled.

Sub-surface layers of mock-ups and forged paintings (Fig. 1, left) were analyzed *in situ* with unilateral NMR relaxometry. Ongoing work concerns structural changes within the paint layers which are invoked by different methods of cleaning and restoration. Furthermore, a correlation map of T_1 and T_2 relaxation times similar to [3] is presented that can serve as a fingerprinting chart for paints employed by a painter or art forger.

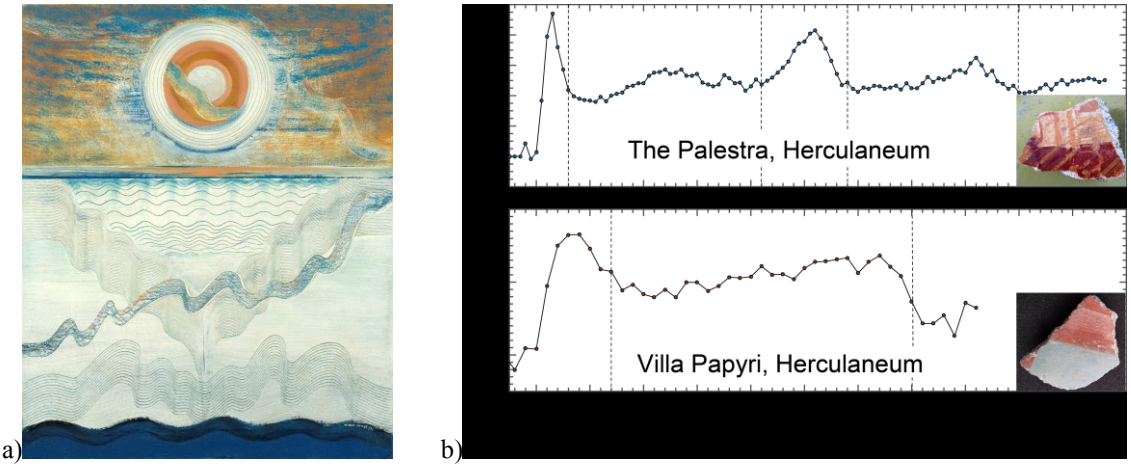

Figure 1 – (a) Fake paintings by Wolfgang Beltracchi in which he copied the original artists style show a remarkable resemblance to originals. (b) Depth profiles of Roman wall paintings from Herculaneum, Italy provide insight in the makings of the mortar-covered wall and can serve to assign fragments.

Wall paintings from the remains of ancient villas in Herculaneum [4] are known to exhibit layered structures of mortar underneath the painted surface (Fig. 1, right) [5]. Due to the high degree of perfection obtained by the master craftsmen it was possible to observe striking similarities in NMR depth profiles of fragments that belong to a room of the same house. The characteristic profiles are independent of the color and pattern of individual pieces and allow identification even when visual assignment fails. Characteristic profiles enable differentiations of different rooms and houses and correlate with the use of the room and the status of the owners. A high number of subsequent mortar layers signal a high quality of the wall painting while a simple structure indicates low quality. Studies on houses that were still in the process of being repaired after the 62 AD earthquake when they were engulfed by the lava of the 79 AD eruption of Vesuvius led us to believe that separation of fragments from before and after the Vesuvius earthquake of 62 is possible just from the structure of the fragments.

References

[1] G. Eidmann, R. Savelsberg, P. Blümler, B. Blümich, , J. Magn. Reson. A 122 (1996) 104–109.
[2] B. Blümich, J. Perlo, F. Casanova, Prog. Nucl. Magn. Reson. Spectrosc. 52 (2008) 197–169.
[3] F. Presciutti et al., Appl. Phys. Lett. 93 (2008) 033505.
[4] A. Wallace-Hadrill, Houses and Society in Pompeii and Herculaneum, Princeton University Press, Princeton (1996).
[5] A. Haber, B. Blümich, D. Souvorova, E. Del Federico, Anal Bioanal Chem 401 (2011) 1441–1452.

Noninvasive examination of an ancient tear bottle

S. Benders[a], B. Blümich[a], I. Bohm, J. Ehling[c], A. Eterović[d], N. Gross-Weege[b], V. Schulz[b], D. Truhn[c], J. Wehner[b]

[a]RWTH Aachen University, Institut für Technische und Makromolekulare Chemie, Worringerweg 2, 52074 Aachen, Germany. [b]RWTH Aachen Universitym Department of Physics of Molecular Imaging Systems, Institute of Experimental Molecular Imaging, Pauwelesstraße 19, 52074 Aachen, Germany. [c]RWTH Aachen University, Universitätsklinikum Aachen, Pauwelesstraße 30, 52074 Aachen, Germany. [d]Museum of Ancient Glass, Poljana zemaljskog odbora 1, HR-23000 Zadar.

Tear bottles (lachrymatory, ungumentarium) are ancient relics used in many cultures, e.g. in ancient Greece, Egypt and Rome [1,2]. As their name suggests, they are suspected to be vessels where mourners dropped their tears in, although this is subject to discussion [3]. Since these bottles are fragile, most of the excavated bottles are broken. Therefore intact bottles are rare and need to be treated with special care since their content can help understand their use in history.

In this study, we measured an intact tear bottle from the collection of Iva Bohm (Figure 1) utilizing nuclear magnetic resonance (NMR), which is well-suited for the analysis due to its noninvasive nature and the ability to access information about the composition of the liquid enclosed in the bottle by spectroscopy. To investigate the wall structure, micro-CT was employed.

Figure 1 – Pictures of the tear bottle.

The pear-shaped tear-bottle is 57.8 mm tall with a weight of 84.85 g (Figure 1). A micro-CT measurement (resolution: $0.14 \times 0.14 \times 0.14$ mm^3) reveals a very thin vessel wall at the top of the bottle (Figure 2). By analysis of a three-dimensional spin density image measured with turbo spin echo [4] (resolution: $0.5 \times 0.5 \times 0.5$ mm^3) the volume of the liquid inside of the tear-bottle can be estimated to 21.8 mL (Figure 2). Spectra from three regions of interest (size: $5 \times 5 \times 5$ mm^3) were measured with Point RESolved Spectroscopy (PRESS) [5] utilizing water suppression. These spectra suggest substances other than water to be present.

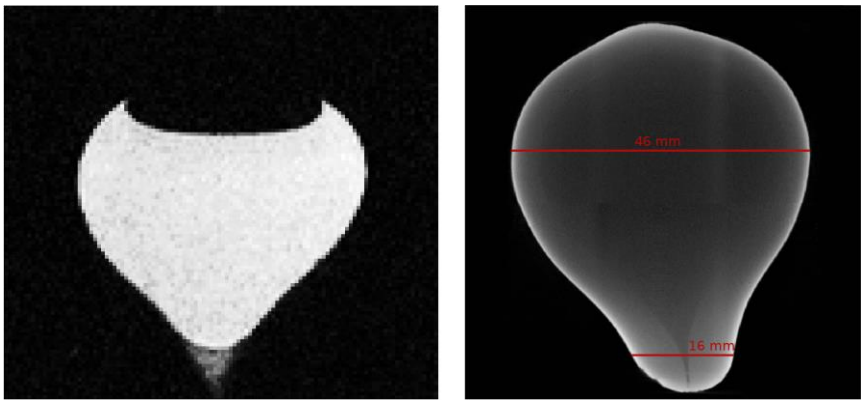

Figure 2 – MRI spin density (left) and micro-CT (right) images of the tear bottle.

References

[1] H. Chisholm, Encyclopedia Britannica, 1911.
[2] C. Spurgeon, The Treasury of David, 1872.
[3] V. Anderson-Stojanovic, AJA 91 (1987) 105-122.
[4] J. Hennig, A. Nauerth, H. Friedburg, Magn. Reson. Med. 3 (1986) 823-833.
[5] P. Bottomley, Ann. N. Y. Acad. Sci. 508 (1987) 333-348.

Cyclic hygro-expansion of oak studied by NMR

T. Arends[a], L. Pel[b]

[a,b] Eindhoven University of Technology, Dept. of Applied Physics, Den Dolech 2, 5612 AZ, Eindhoven, The Netherlands.

Examples of wood products exposed to cyclically fluctuating relative humidity are abundant: furniture, parquet floors, structural elements, or art objects. The moisture content in such conditions changes continuously, which in wood is associated with expansion and shrinkage. This can lead to undesired effects, e.g. when the shape of an object changes, or in case of cracking due to exceeding of the strength of the material by the associated stresses. It is therefore important to study the influence of moisture on the expansion of wood. Several methods exist to assess this relationship, e.g. gravimetrical moisture content measurement in combination with a micro-meter [1], X-ray computed tomography [2], or NMR combined with a Bragg grating sensor [3]. NMR has the advantage that the spatial moisture content can be determined non-destructively and additional information on the system can be obtained in terms of relaxation times.

To study the relation between moisture sorption and expansion of oak, a combination of NMR and an optical fiber displacement sensor is used. Experiments are performed on cylindrical samples contained in a sample holder inside a 0.78 T magnet. The relative humidity in the sample holder is varied sinusoidally with a humidifier, which intermixes a dry and humid air flow to provide a constant air flow with continuously changing relative humidity. The hydrogen signal of the sample is captured by NMR using a CPMG echo train sequence, which not only provides the moisture content, but also the T_2 distribution over time. Meanwhile, the optical sensor measures the distance to a reflective surface on top of the sample. With the simultaneous measurement of moisture content, T_2, and expansion, these parameters can be correlated to each other.

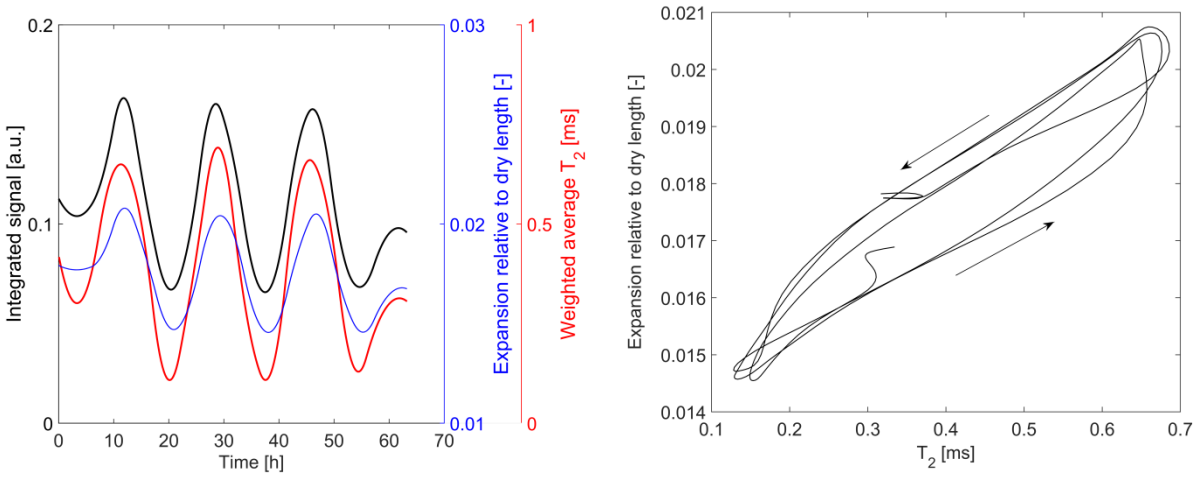

Figure 1 – a) Integrated signal, expansion, and weighted average of T_2 during sinusoidal relative humidity fluctuations between 10 % and 90 % with a period of 17 hours, b) the relation between T_2 and expansion of the sample during the same experiment.

Figure 1a shows the evolution over time of the integrated signal, the expansion, and the weighted average of the T_2 distribution during an experiment with a sinusoidally varying relative humidity. All three parameters are seen to vary sinusoidally as well. In Figure 1b, the expansion of the sample is plotted against T_2. A hysteresis loop is observed, which assumes the form of a sorption curve. More than one expansion state thus exists for a certain T_2 value. In this study, the combination of NMR with an optical fiber displacement sensor enables the simultaneous evaluation of moisture content, T_2, and expansion. It is demonstrated that this provides supplementary information about the processes involved in hygroscopic expansion of oak.

References

[1] A. Chomcharn, C. Skaar, Wood Sci. Technol. 17 (1983) 259-277.
[2] D. Derome, A. Rafsanjani, A. Patera, R. Gruyer, J. Carmeliet, Philisophical Magazine 92 (2012) 3680-3698.
[3] L. Senni, M. Caponero, C. Casieri, F. Felli, F. De Luca, Wood Sci. Technol. 44 (2010) 165-175.

Spatially resolved NMR:
MRI and single-sided profiles on samples treated with environmentally safe fluorinated compounds to preserve Cultural Heritage porous media

V. Bortolotti [a], L. Brizi [b,c], M. Camaiti [d], P. Fantazzini [b,c]

[a]DICAM, Univ. of Bologna, Via Terracini 28, 40131 Bologna, Italy; [b]Dept. Physics and Astronomy, Univ. of Bologna, Viale Berti Pichat 6/2, 40127 Bologna, Italy; [c]Museo Storico della Fisica e Centro Studi e Ricerche Enrico Fermi, P.zza del Viminale 1, Roma, Italy; [d]IGG-CNR Florence, Via G. La Pira 4, 50121 Firenze, Italy

In previous papers [1], it has been shown how MRI allows one to evaluate and compare the performance of products and treatments used to reduce water uptake by porous materials exposed to rain, moisture and air pollutants. Those products were commercial ones, made for different uses than Cultural Heritage items protection. In the middle of the '80s, the group of CNR in Florence started to synthesize mono-bi- and tetra-functionalized perfluoropolyetheric compounds for the specific use in the protection of stone, with the following properties: (i) stable to chemical agents, heating and UV irradiation; (ii) high water-repellency; (iii) ability to perform treatments in such a way that the natural permeability of stone to air and water vapor is not significantly reduced; (iiii) chemically inert with the stone substrate, and therefore completely reversible. Unfortunately, the best products synthesized were soluble in Chlorofluorocarbons (CFCs) [1]. Because CFCs contribute to ozone depletion in the upper atmosphere, the use of these perfluoropolyetheric compounds as protective agents for historical stone artifacts has been abandoned since 1995.

For this reason, new products containing a perfluoropolyetheric block have been synthesized, soluble in alcohols and hydro-alcoholic solvents, but not soluble in water or Chlorofluorocarbons [2]. Their hydrophobic and penetration properties have been investigated by quantitative MRI images and by single-sided NMR profiles on biocalcarenite samples at increasing times during capillary water absorption.

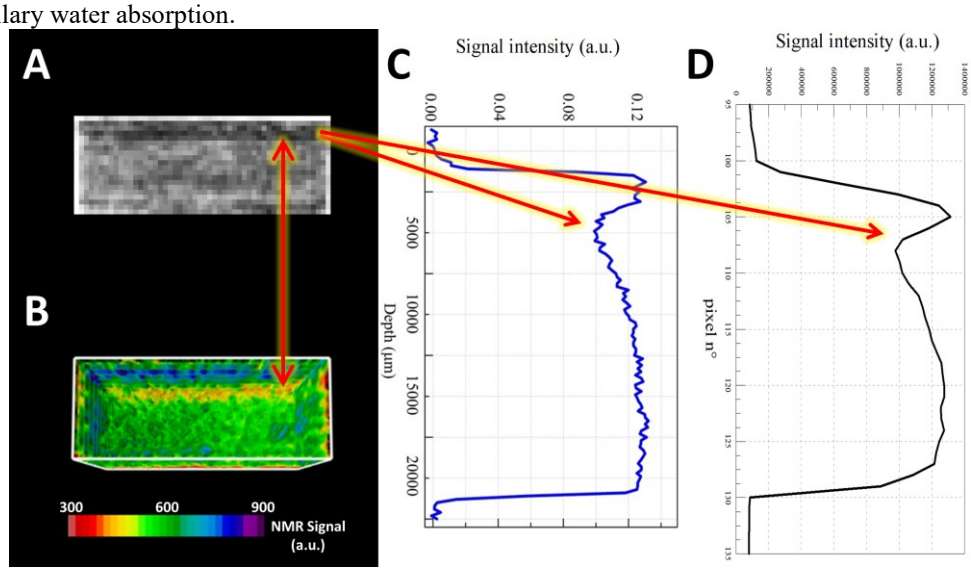

Sample treated with the new compound applied in solution after water uptake from the untreated face. Comparison MRI and MOUSE Profile. (A) MRI of an internal slice by ArtoScan tomograph (Esaote S.p.a., Genova, Italy). (B) MRI - 3D reconstruction of the sample. (C) Proton density profile by NMR single-sided MOUSE PM25 (Magritek, Aachen, Germany). (D) Profile reconstruction from MRI by ARTS, a homemade software to quantitatively process MRI image.

The images showed the different protection efficiency of products and treatments. The qualitative images of internal sections of the samples were compared with the profiles obtained by the quantitative analysis of the images themselves and by the profiles by the single-sided device. A very good agreement was obtained among these three different measurement methods. The same features of the treated samples were visible also in the 3D rendering of the same samples, showing different performance of the treatments. For example, in the case of the sample treated with the new product after water uptake from the untreated face, the low amount of water at the upper face was justified with the high propensity of the product to penetrate inside the porous medium, with an accumulation of the product at the face opposite to the treated one, due to the limited thickness of the specimen (2 cm). The results demonstrate the better performance, as compared with the commercial one, of the new environmentally safe fluorinated compounds, able to preserve the integrity of stones.

Acknowledgments: the authors wish to thank Bernhard Blümich and Sabina Haber-Pohlmeier for the use of MOUSE PM25.

References

[1] M. Camaiti, V. Bortolotti, P. Fantazzini, Stone Porosity, wettability changes and other features detected by MRI and NMR relaxometry: a more than 15-year study, Magn Reson Chemistry, 2015, 53, 34-47.

[2] V. Bortolotti, L. Brizi, R.J.S. Brown, M. Camaiti, P. Fantazzini, M. Mariani, M. Vannini, Quantitative-MRI tests on fluorinated compounds to preserve Cultural Heritage porous media and safe for the environment, Abstract, XII International Conference of Magnetic Resonance in Porous Media (MRPM-12, 9-13 Feb. 2014, Victoria University of Wellington, New Zealand) p. 45-46.

Changes of Water Status in Relation to Strawberry Fruit Development and Ripening

Jizheng Li[1,2], Wensuo Jia[1] , Lizhi Xiao[2]

[1]College of Horticulture, China Agriculture University; [2]China University of Petroleum Beijing, P.R. China.

Water status is one of the most important factors controlling cell division and expansion， thereby controlling plant organ morphogenesis. But limited information about water relationship during fruit growth and development is available. Here, we report the changed profile of the water status, as analyzed by low field nuclear magnetic resonance (NMR)[1-3], in relation to strawberry (*Fragaria ananassa* and *Fragaria vesca*) fruit development and ripening. Both water potential and osmotic potential decreased during fruit development and ripening, and dramatic decreases were observed at the start of veraison, while fruit firmness stared to dropped dramatically at the middle green stage, suggesting that the changes of water status was more closely correlated with fruit ripening. NMR analysis indicated that fruit water tended to change from bound to free status during receptacle along with the fruit development, and in contrast, it tended to change from free to bound status in seeds. The changed profile of the water status is consistent with anatomic observations on fruit structure[4]. The results above have provided valuable information on further probe into the deep mechanisms for the regulation of strawberry fruit development and ripening.

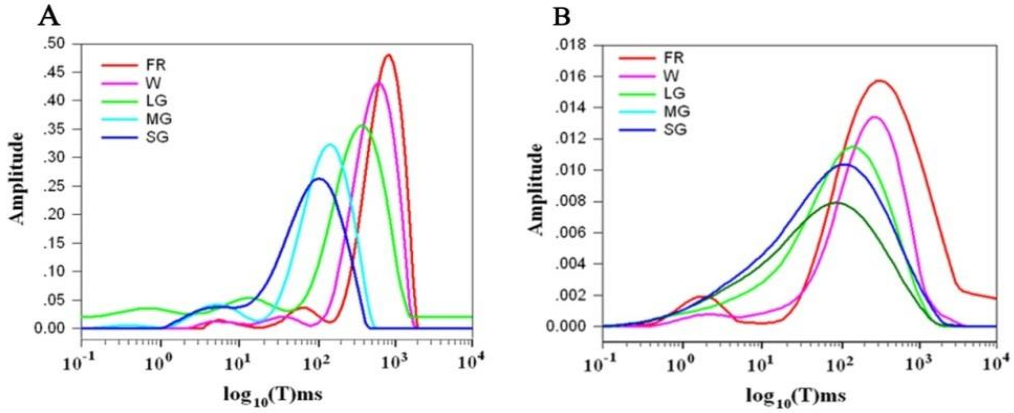

Figure 1—T_2 spectra of moisture modility of octoploid and diploid strawberry fruit with five stages

(A) diploid strawberry fruit with five stages (B) octoploid strawberry fruit with five stages

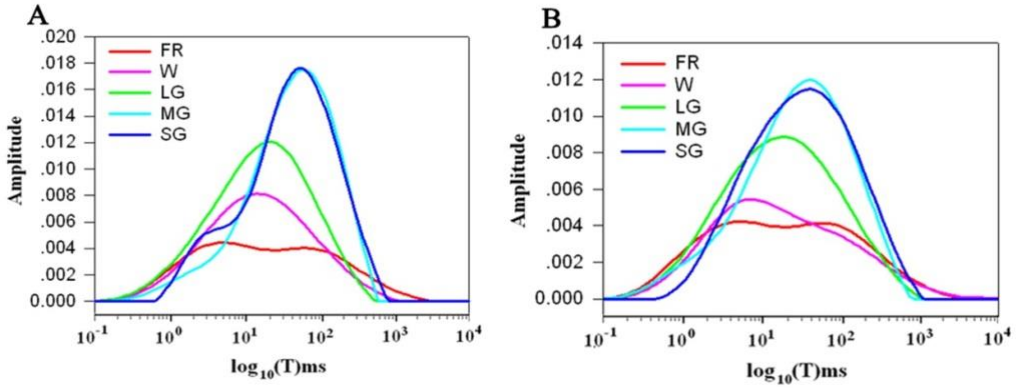

Figure 2 —T_2 spectra of moisture modility of octoploid and diploid strawberry seeds with five stages

(A) diploid strawberry seeds with five stages (B) octoploid strawberry seeds with five stages

References

[1] Song P, Yang T, Wang C, et al. Analysis of moisture changes during rice seed soaking process using low-field NMR. Transactions of the Chinese Society of Agricultural Engineering, 2015,31(15):279~284

[2] Wang X, Gao K, Chen Q, et al. Water diffusion characteristics of apple slices during short and medium-wave infrared drying. Transactions of the Chinese Society of Agricultural Engineering, 2015,31(12):275~281

[3] Wu J, Li L, Wu X, et al. Characterization of Oat (Avena nuda L.) beta-Glucan Cryogelation Process by Low-Field NMR. JOURNAL OF AGRICULTURAL AND FOOD CHEMISTRY, 2016,64(1):310~319

[4] Sebaa H S, Harche M K. Anatomical structure and ultrastructure of the endocarp cell walls of Argania spinosa (L.) Skeels (Sapotaceae). MICRON, 2014,67:100~106

Imaging of ^{23}Na accumulation in the soil-root region due to root water uptake

A. Pohlmeier[a], A. Perelman[b], S. Haber-Pohlmeier[c], J. Vanderborght[a,d], N. Lazarovitch[b]

[a]IBG-3, Research Center Jülich, D-52425 Jülich, Germany;
[b]French Associates Institute for Agriculture and Biotechnology of Drylands, Jacob Blaustein Institutes for Desert Research, Ben-Gurion University of the Negev, Sede Boqer Campus, 84990, Israel;
[c]ITMC, RWTH Aachen University, Worringerweg 1, D-52074 Aachen, Germany;
[d]Division of Soil and Water Management, KU Leuven, Celestijnenlaan 200e - Box 2411, B-3001 Leuven, Belgium

Root water uptake may lead to salt accumulation at the root-soil interface, resulting in rhizophere salt concentrations much higher than in the bulk soil. This salt accumulation is caused by soluble salt transport towards the roots by mass flow through the soil, followed by preferential absorption of specific nutrients by active uptake, thereby excluding most other salts at the root-soil interface or in the root apoplast. The salinity build-up can lead to large osmotic pressure gradients across the roots, thus effectively reducing root water uptake and crop production. The increased salinity also leads to a deterioration of soil quality and, eventually, to the loss of productive crop land. Therefore, an understanding and a description of the processes taking place are required, in terms of parametrizing soil physical models. To start with, reliable measurements of the salt accumulation in the soil and the roots are needed. Therefore, we present ^{23}Na-MRI for the visualization of NaCl distribution in the soil-root region, complementary with ^{1}H-MRI for high resolution imaging of the root system and the water content development for providing synergistic information about the underlying water flow and solute transport processes.

While common in medical research, ^{23}Na-MRI is not very well developed for unsaturated porous media such as soils. The ^{23}Na NMR signal is much weaker than the most common ^{1}H signal due to the lower gyromagnetic ratio and the much lower abundance. This results in a lower resolution and requires longer measuring times, which is facilitated by the relatively short T_1 in the range of about 50 ms.

In this pilot study, we used a fast spin echo method with t_E = 5ms, 16 echoes and a matrix size of 32 x 32 x 32, yielding an FOV of 32 x 32 x 64 mm. For the calibration phantom, we showed that the MRI voxel intensity was proportional to the ^{23}Na concentration down to a concentration of 0.05 mol/L (Fig. 1a). This allowed us to apply this procedure to the accumulation of ^{23}Na in the root systems of tomatoes, which were irrigated in three-day intervals with a 0.06-M NaCl solution. After 10 days, we found considerable salt accumulation in the root region, which could be used in the second step to alculate profiles. New perspectives could be obtained by co-registrating these data with the $^{1}H_2O$-MRI of the root system architecture and soil water content.

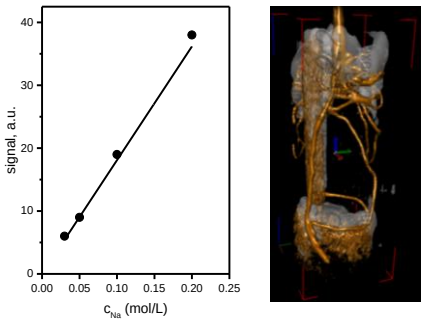

Figure 1 ^{23}Na imaging in natural sand by 3D fast spin echo. Left: voxel intensity at different concentrations. Right: Na accumulation (grey) in the root systems of tomato (brown isosurface) after 10 days irrigation with 0.06 M of NaCl.

P28

Applications of 2D NMR to Soils with Slim-line Logging Tool

B. Guo[a], B. Bluemich[a]

[a]University of RWTH Aachen, Dept. of Technische und Makromolekulare Chemie, Worringerweg 2, 52074 Aachen, Germany.

Soil moisture transport is a key factor to study soil hydrology, plan and optimize crops, and model soil-vegetation-atmosphere processes. Nuclear magnetic resonance (NMR) can quantitatively detect water protons, and thus it is a direct method to measure soil moisture and pore size. Two-dimensional NMR has proven to be an important analytical tool to study porous medium in recently years. After four years developed, the signal-noise-ratio (SNR) of slim-line loging (SLL) tool was increased greatly [1], so it can now be used to measure water moisture in original soil formations in the field, and 2D NMR experiments also could be carried out to study water transport in soil at different saturations in lab.

In laboratory studies, T_2-D and T_2-T_2 experiments were carried out to study water transport during draining scenarios and the water transport between different-size pores. The soil to be studied is filled into a dual-column composed of an external and an internal tube of 20 cm and 7 cm diameter, respectively. The soil contains 95% sand with average grain size of 100 µm and 5% clay. The T_2-D experiments were measured in soils whose water contents were 34%, 29%, 14% and 7%. The results show that the water diffusion coefficient in the smaller pores decreases significantly with decreasing water content. The T_2-T_2 experiments were executed in saturated soil and clear exchange peaks could be observed from the T_2-T_2 correlation maps. The intensities of the exchange peaks vary with the mixing time. This time-dependence served to estimate the exchange rate of water between different pores [2].

References

[1] J. Perlo, E. Danieli, B. Bluemich, J. Magn. Reson.. 406 (2011) 30–38.
[2] M. Landeghem, A. Haber, B. Bluemich, Concepts Magn. Reson.. 36 (2010) 153–169.

Magnetic Resonance Probes as a Tool to Monitor Long Term Clogging In Constructed Wetlands

Robert H. Morris[a], Theodore Hughes-Riley[a], Elizabeth R. Dye[a], Steven Parslow[a], Patrick Hawes[b], Joan García[c], Enrica Uggetti[c], Jaume Puigagut[c] and Michael I. Newton[a]

[a] Nottingham Trent University, School of Science and Technology, Clifton Lane, Nottingham, NG11 8NS, UK; [b] ARM Ltd, Rydal House, Colton Road, Rugeley, Staffordshire, WS15 3HF, UK; [c] Group of Environmental Engineering and Microbiology, Department of Civil and Environmental Engineering, Universitat Politècnica de Catalunya•BarcelonaTech, Barcelona, Spain

Constructed wetlands are an environmentally friendly means of wastewater treatment, which are increasingly used for treatment from source to discharge. They comprise gravel matrices in which plants are grown. They operate in all treatment domains, filtering particulates in the gravel pore space, breaking down pollutants through biological processes and removing heavy metals through the plants. Over time this process decreases in efficiency as the gravel becomes increasingly clogged. The growth of biofilms occlude the pores in the gravel leading to bypass flow of the wastewater and ultimately dysfunctional treatment. These processes can be mediated with the addition of aeration alternative feeding regimes although the efficiency of these is poor if the extent of the clogging can't be measured. Traditional methods require human intervention and are therefore not cost effective. In this work, we present a novel method of monitoring the clog state of constructed wetlands using embeddable magnetic resonance. Inverse Laplace transform of the T_1 decay reveals three distinct components which we have shown, through model experiments, to represent water associated with biofilms, water associated with particulate material and free water.

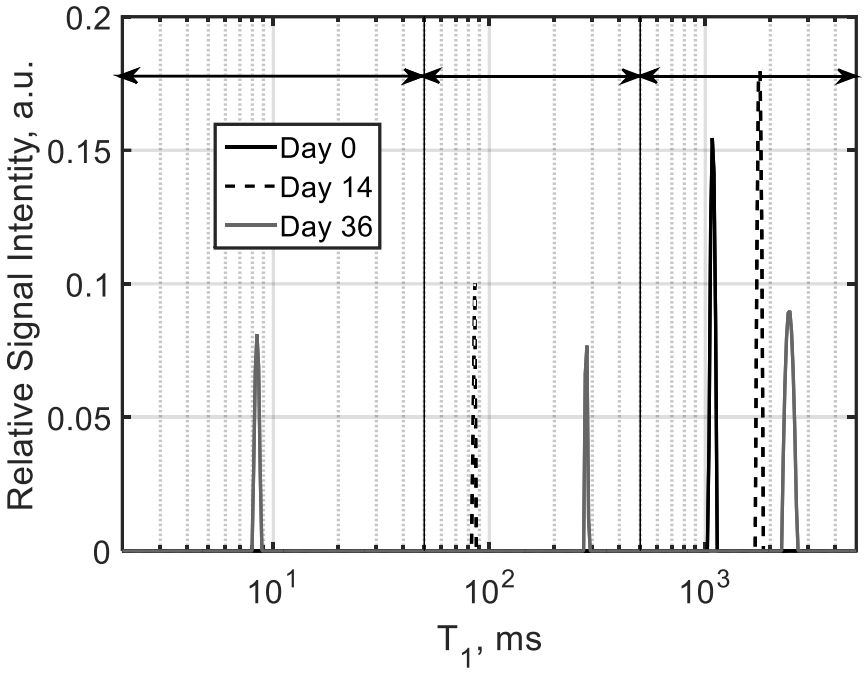

Knowledge of the ratio of these parameters allows the form of the clogging, as well as the extent of the clogging, to be determined which is key to efficient treatment. We go on to validate this technique in a laboratory scale experiment in which a column of gravel undergoes accelerated clogging. The particulate peak increases first as filtration increases with a relative decrease in the free water. Over longer periods, the peak representing the biofilm emerges and grows, with another relative decrease in the free water peak. This represents a major advance in online monitoring of constructed wetlands for the industrial community and will be used as a control element in fully automated wastewater processing modules.

The emerging use of MRI to study River Bed dynamics

Heather Haynes[a], Susithra Lakshmanan[a], A.Ockelford[b], Elisa Vignaga[a], William. M. Holmes[c]

[a]Water Academy, Heriot-Watt University, Edinburgh, UK; [b]Civil Engineering, University of Glasgow, UK; [c]Glasgow Experimental MRI Centre, University of Glasgow, UK.

Introduction. The characterization of surface and sub-surface sedimentology has long been of interest to gravel-bed river researchers. The determination of surface structure is important as it exerts control over bed roughness, near-bed hydraulics and particle entrainment for transport. Similarly, interpretation of the sub-surface structure and flow is critical in the analysis of bed permeability, the fate of pollutants and maintaining healthy hyporheic ecology.

Laboratory experiments of river bed dynamics are conducted using artificial river channels called "flumes". By covering the flume bed with a layer of sediment (e.g. sand or gravel), the effects of water flow on bed "form" can be analysed (see figure 1). Traditionally, extracted core samples, photogrammetry and laser displacement have been used to investigate evolution of bed surface composition and particle arrangement. Increasingly this is coupled with data on the above-bed flow field, via e.g. Acoustic Doppler Velocimetry (ADV) or Particle Image Velocimetry (PIV). However, to truly understand sediment structure inherently requires description of both the surface and sub-surface (and their interaction), hence we demonstrate MRI methods able to advance this science [1-4].

Fine-sediment infiltration into gravel beds using traditional flumes (ex–situ MRI*)*. Using large re-circulating hydraulic flumes (15m long x 0.45m deep x 0.3 - 1.8m width; Figures 2A), a coarse gravel bed was laid of rose-quartz lithology 17 mm grain diameter. Rose-quartz was used due to low heavy metal content, reducing image distortion in the MRI. The channel was inclined to 1/200 gradient with water flowing at 7.7 litres/s; the coarse gravel framework is therefore immobile. Experiments were then conducted by feeding fine gravels (2.4mm diameter) and sands (0.5mm diameter) into the flow for a fixed time period. The flow naturally redistributed the fine sediment fraction, which was mobile under the set flow. At the end of each experiment, sections were frozen with liquid nitrogen and cut for MRI imaging.

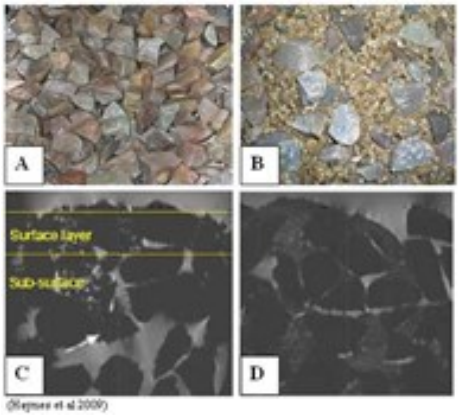

Figures 1 show surface photographs of the initial coarse gravel bed (1A) and the gravel bed after deposition of the fine sediment from the flowing water (1B). Figure 1C and 1D shows a cross-section of a 3D MRI dataset, showing different infiltration behaviour. Sands resulted in deeper infiltration affecting all pore spaces (1C), whereas the fine gravel resulted in infiltration of only upper few layers of the bed (1D).

MRI compatible flume (in-situ MRI). In order to image the sub-surface flows and the infiltration process in-situ, we constructed a miniature flume for serial MRI experiments. The flume had a rectangular cross-section 3m long x 6.2cm deep x 9.3cm width, Figures 2 B,C,D. The flume was constructed in three sections, this allowed it to be dismantled and re-built outside the MRI for Particle Image Velocimetry (PIV) experiments of flow hydraulics over the imaged bed, see Figure 2D.

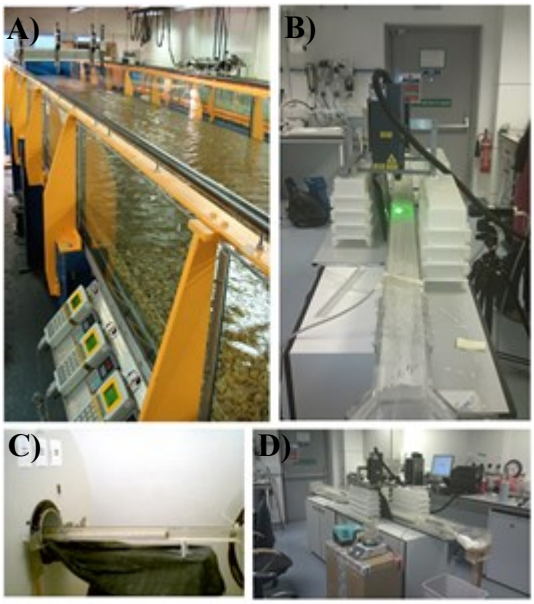

Conclusion. We have demonstrated that MRI can be used for structural analysis of sediments, both ex-situ and in-situ within experimental flumes. The MRI compatible flume allows for serial 3-D high-resolution imaging of the infiltration process and for visualisation of sub-surface flows. In addition, following serial MRI the flume can removed from the MRI scanning and rebuilt, thus allowing for coupling with 'traditional' Particle Imaging Velocimetry and laser surface scanning of the same bed .

Reference.

[1] Lakshmanan S,Pender G, Haynes H, Holmes WM. Int. Journal of Engineering & Technology, 3 (4) (2014) 457-463
[2] Haynes H, Ockelford AM, Vignaga E and Holmes WM. Acta Geophysica. 2012. 60:1589-1606.
[3] Haynes H, Vignaga E and Holmes WM. Sedimentology. 2009. 56. 1961-1975.
[4] Haynes H, and Holmes WM . : Clarke, L.E. (ed.) Geomorphological Techniques. 2012. British Society for Geomorphology: London.

Quo vadis Surface-NMR – adiabatic pulses?

R. Dlugosch[a], M. Müller-Petke[a]

[a]Leibniz Institute for Applied Geophysics, Stilleweg 2, 30655 Hannover, Germany.

Surface-NMR uses large coils of several 10 to 100m and the weak but homogeneous Earth magnetic field to estimate the water content and T_2^* relaxation time distribution down to a depth of >100m into the subsurface. However, the application of surface-NMR is often limited by its low signal to noise ratio (SNR). Up till recently [1], the main strategy to improve SNR was to reduce the electromagnetic noise level, e.g. stacking, filtering or using reference rensors. We target the other part of this fraction and evaluate if adiabatic excitation pulses (adiabatic half passages [2]) can increase the signal amplitudes of the measured free induction decays (FID).

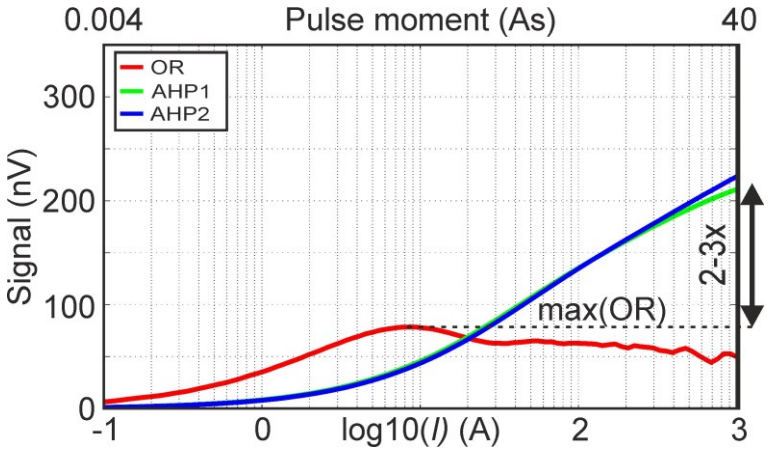

Figure 1 – Surface-NMR sounding curves, i.e. maximum FID signal amplitude vs. maximum pulse current (*I*), for a 20m circular loop using on-resonant (OR) excitation pulses and two adiabatic half passages (AHP1&2).

In contrast to the commonly applied on-resonant excitation at the Larmor frequency (approx. 2kHz), adiabatic excitation pulses use matched frequency and amplitude sweeps. During a surface-NMR experiment, the excitation pulses propagete freely in the subsurface. This leads to a wide range of magnetic field strengths within the huge excited volume (up to 1e6m³), flip angles >180° and therefore a cancellation of NMR-signals originating from different volumes but with opposite phases. The use of adiabatic excitation pulses leads to more homogeneous excitation patterns in the excited volume and therefore a higher measured signal amplitude (Fig. 1). Improving SNR hence increases the range of application for surface-NMR, i.e. to areas with man-made electromagnetic noise sources, or can significantly speed up the measuring progress by reducing the number of stacks. The presented results include modelling of the spin dynamic of adiabatic pulses, an evaluation of pulse parameters and hence calculated sensitivity kernel functions for surface-NMR soundings.

References

[1] E. Grunewald, D. Grombacher, D. Walsh, Geophysics 81/4 (2016).
[2] M. Bendall, D.T. Pegg J. Magn. Reson. 67 (1986) 376-381.

Non-Invasive Magnetic Resonance Imaging of Nanoparticle Migration and Water Velocity Inside Sandstone.

Matsyendra Nath Shukla[a], Antoine.Vallatos[a], Mick Riley[c], John Tellam[c], Vernon Phoenix[b] and William Holmes[a]

[a]Glasgow Experimental MRI Centre, Univeristy of Glasgow, UK ; [b] Dept. of Earth Sciences, Univerisrty of Glasgow, UK.; [c] Dept. ofHydrology, University of Birmingham, UK.

Introduction:- Manufactured nanoparticles (NPs) are already utilized in a diverse array of applications, including cosmetics, optics, medical technology, textiles and catalysts. Problematically, once in the natural environment, NPs can have a wide range of toxic effects. To protect groundwater from detrimental NPs we must be able to predict nanoparticle movement within the aquifer. The often complex transport behavior of nanoparticles ensures the development of NP transport models is not a simple task. To enhance our understanding of NP transport processes, we utilize novel magnetic resonance imaging (MRI) which enables us to look inside the rock and image the movement of nanoparticles within. For this, we use nanoparticles that are paramagnetic, making them visible to the MRI and enabling us to collect spatially resolved data from which we can develop more robust transport models.

Methods:- An epoxy encapsulated Bentheimer sandstone sample was used to make all measurements. The porosity of 0.17 was determined from the weight of the column before and after saturation of water. The MR imaging experiments were carried out on a 7T *Bruker Avance Biospec* system. The rf resonator used for all experiments has a inner diameter 72 mm. A series of T2- weighted images were recorded for the transport of *Carboxyl* NP in sandstone with a time interval of 8 min. In addition, a combination of an Alternating-Pulsed-Gradient Stimulated-Echo (APGSTE) sequence with RARE imaging was used to obtain 3D velocity map. The 3D Images at two different flow rate 1 and 2 ml/min were acquired with a repetition time TR of 5000 ms and measuring time of 16 hours and 32s. The resulting images have a matrix of 60×45×45, a field of view(FOV) of 60×45×45 mm^3, giving a pixel size of 1 mm^3.

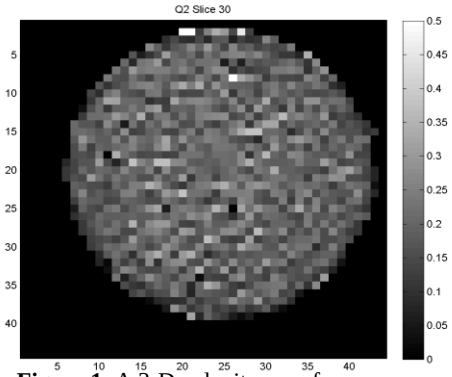

Figure 1. A 3-D velocity map for flowrate 2ml/min.

Results:- Fig1: shows the 3D velocity map with flow rate at 1 and 2 ml/min. The average velocity with flow rate 1 and 2 ml/min of 0.094 ± 0.0384 mm/s and 0.188 ± 0.0747mm/s were calculated from the MRI data. Fig2: shows calibrated image of *Molday ION (Carboxyl Terminated)* Nanoparticle (0.7 mM) Concentration with 24 minutes interval at flow rate 0.2 ml/min.

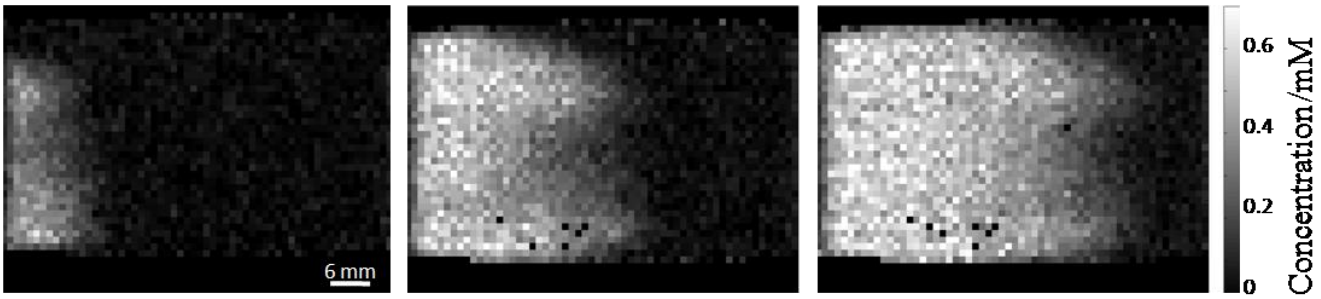

Figure 2. Concentration maps of Molday ION (Carboxyl Terminated) Nanoparticle (0.7 mM) with 24 minutes interval at flow rate 0.2 ml/min.

Conclusion: This work demonstrates we are able to spatially resolve porosity, water velocity and nanoparticle movement, inside rock, using a single technique (MRI). Such quantitative data provides us with a unique and powerful dataset from which we are now developing new models of nanoparticle transport.

References:-

[1] Romanenko, K., Xiao, D. and Balcom, B.J. *Journal of Magnetic Resonance* (2012) 223, 120-128
[2] Matsyendra NS, Vallatos A, Pheonix VR, Holmes WM. *Journal of Magnetic Resonance* (2016) 267, 43-53.

Mobile NMR-Lab for field phenotyping of oilseed rape leaves

Maja Musse[a,c], François Mariette[a,c], William Debrandt[a,b,c], Clément Sorin[a,b,c], Cambert Mireille[a,c], Alain Bouchereau[b,c], Laurent Leport[b,c]

[a]IRSTEA, UR OPAALE, Rennes, France; [b]INRA, UMR 1349 IGEPP, INRA-Agrocampus Ouest-Université Rennes 1, France; [c]Université Bretagne Loire (UBL), France

Low field NMR has been used in several studies for investigation of leaf water status [1-2]. An original interpretation of the multi-exponential transverse relaxation signal of leaf tissue taking into account subcellular compartmentation and heterogeneities at the tissue level has been recently proposed for the oilseed rape leaves [3]. Applied on a wide leaf panel collected from plant grown in controlled conditions, the NMR relaxometry was shown to be able to detect slight variations in senescence associated with structural modifications of leaf tissues. The aims of the present study was to demonstrate the potentiality of NMR to provide robust indicators of the leaf development stage for plant grown directly in field and to illustrate its potential for in situ measurements with a mobile-NMR lab.

Field measurements were performed by a mobile NMR lab specially set up for this purpose. A 20 MHz spectrometer (Minispec PC-120, Bruker, Karlsruhe, Germany) equipped with a temperature control device connected to an optical fiber (Neoptix Inc, Canada) allowing for ±0.1°C temperature regulation was placed inside a van. The electrical power for the experimental devices was provided by a battery. Such equipped van was positioned in the field close to the oilseed rape plants under investigation. Eight discs of 8 mm in diameter were cut from each leaf of the plant studied without derooting the plant. Discs were then placed in NMR tubes which were closed with a cap to avoid water loss during measurements. The temperature of the samples inside NMR probe was set at 18°C. Transverse relaxation was measured using the CPMG sequence with the 90°-180° pulse spacing of 0.1ms. Plants were investigated at different stages of their development cycle (spring regrowth, stem elongation, flowering and seed filling). For each condition, measurements were performed in four replicates.

The pattern of evolution of the transverse relaxation spectra revealing leaf structure changes during senescence observed was very similar to the one that was measured previously under controlled conditions [2-4]. This demonstrated that, despite the great variability of the environmental factors (large temperature and humidity variations, light exposure, etc), the NMR method can provide robust indicators of leaf development stage for plants grown in a field. Furthermore, the results obtained on plants at different development stages showed that the NMR method was also able to discriminate vegetative sequential senescence occurring at regrowth and stem elongation stages from monocarpic senescence occurring during seed filling at the final stage of the plant cycle.

The results of the present study represent an important step toward further field applications of the method for the selection of genotypes with high tolerance to water or Nitrogen depletion.

ACKNOWLEDGEMENTS

We thank the Regional Council of Bretagne for financial support. This work was supported by the program ‘‘Investments for the Future’’ (project ANR-11-BTBR-0004 ‘‘RAPSODYN’’). We also thank Françoise LE CAHEREC[b], Marie-Françoise NIOGRET[b], Carole DELEU[b], Nathalie NESI[b], Anne LAPERCHE[b] et Christine BISSUEL[b] for setting up the field experiment and for cooperation on this study.

References

[1] D. Capitani, F. Brilli,, L. Mannina, N. Proietti, F. Loreto, Plant Physiology 149(4), 1638-1647, (2009)
[2] M. Musse, L. De Franceschi, M. Cambert, C. Sorin, F. Le Caherec, A. Burel, A. Bouchereau, F. Mariette, L. Leport, Plant Physiology 163(1), 392-406, (2013)
[3] C.Sorin C, M. Musse, F. Mariette, A. Bouchereau, L. Leport, Planta 241(2), 333-346, (2015)
[4] C. Sorin, L. Leport, M. Cambert, A. Bouchereau, F. Mariette, M. Musse, Botanical studies, *in press*, (2016)

Soil moisture mapping in the field with a slim-line logging tool

X. Cai[a], B. Guo[a], M. Küppers[a], B. Blümich[a]

[a]Institut für Technische und Makromolekulare Chemie, RWTH Aachen University, 52074, Aachen, Germany.

Investigating water transport in soil plays an important role in improving water inflitration in agriculture and climatology. Nuclear magnetic resonance (NMR) has already become a powerful method in studying the dynamics of fluids in porous media and near-surface geological formation in the last decade due to the rapid improvement of instrumentation [1, 2]. In this study, an improved slim-line logging NMR tool with a cylindrical dumbbell-like permanent magnets was applied to monitor soil moisture content and water transport in the Selhausen field test site of the TR32 collaborative research center. The slim-line logging tool with a four-turn radio-frequency coil surrounding the magnets has a permanent magnetic field strength 3.29 MHz in the measurement region. The lateral view and the size of the dumbbell-like magnet was presented in Fig. 1a. The sensitive volume was at a distance of 2 cm away from the sensor surface. A total of 37 vertical pipes with 1 m depth was installed in the Selhausen field which was already divided into three different soil type regions characterized as silty, sandy and gravelly. Depth dependent 1D profiles were measured with an increment 10 cm for each hole to construct a 3D soil moisture map.

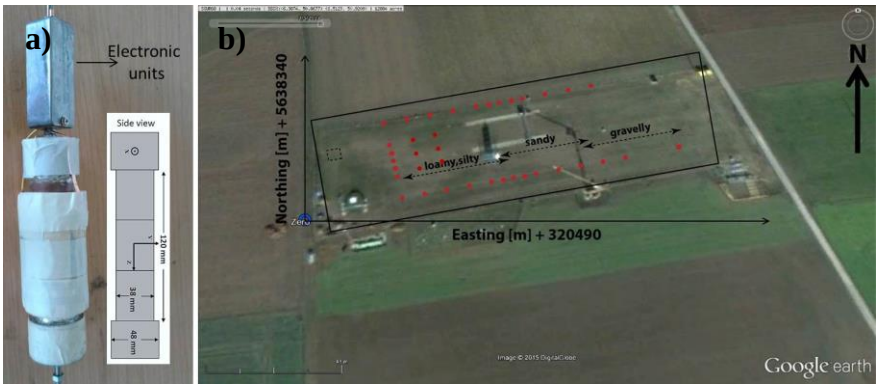

Figure 1 a) The slim-line logging sensor. b) Landscape of the Selhausen site with the positions of 37 tubes indicated by red dots.

Transectional views of the soil moisture map are illustrated in Fig. 2a. The maximum and minimum water contents are 32.8 % and 8.9 %, respectively. It was quite clear that the soil moisture content increased gradually along the soil layer depth, which contains higher water content in deeper layers. Moreover, the soil water content decreased gently towards the East, where the soil type changes from loamy, silty to sandy and then to gravelly. This soil moisture map clearly presents the water content distribution across the whole Selhausen field and indicates that the slim-line logging tool can reliably and easily be applied in the field to obtain the moisture distribution across the field. Two 1D soil moisture profiles are presented in Fig. 2b, c calculated from the data of three tubes in rows 1 and 2 along the East direction. It is obvious that the soil water content drops sharply along towards the Easet due to the soil type changing from silty to gravelly. These profiles also indicate that the water content increases from the surface to deeper soil layers in agreement with the corresponding soil moisture content map. This field experiment demonstrates that the NMR logging tool has promising potential to evaluate and manage ground water sources. We gratefully acknowledge the supporting by DFG as part of the TR32 project.

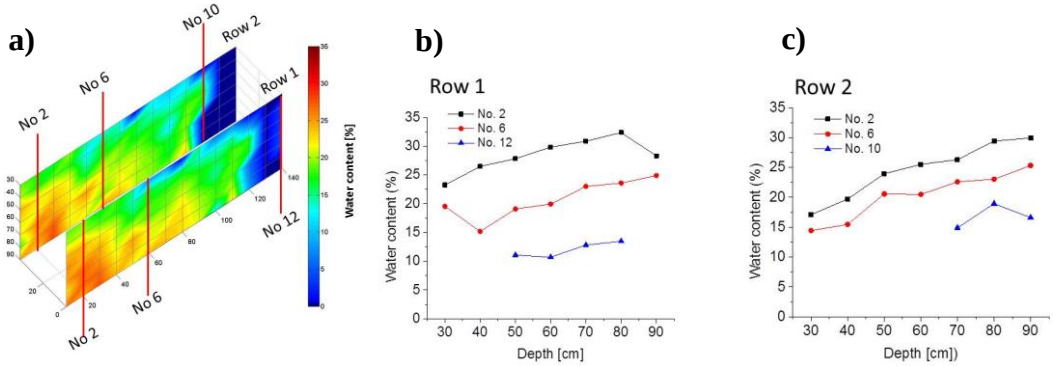

Figure 2 a) Transectional view of the soil moisture content. b) 1D soil moisture content profiles of three tubes from row 1 indicated by the red line. c) 1D soil moisture content profiles from row 2.

References

[1] O. Sucre, A. Pohlmeier, A. Miniere, and B. Blümich, Low-field NMR logging sensor for measuring hydraulic parameters of model soils, J. Hydrol. 406 (2011) 30-38.

[2] J. Perlo, E. Danieli, J. Perlo, B. Blümich, and F. Casanova, Optimized slim-line logging NMR tool to measure soil moisture in situ, J. Magn. Reson. 233 (2013) 74-79.

Effect of water entrapment by a hydrogel on the structural stability of artificial soils

C. Buchmann[a], G. E. Schaumann[a]

[a]Institute for Environmental Sciences Landau, Group of Environmental and Soil Chemistry, University Koblenz-Landau, Germany

Soil organic matter (SOM) or synthetic polymers can form a three-dimensional hydrogel network with the ability to modify soil physico-chemical properties [1, 2]. Besides potential effects of the hydrogel network on soil hydrology (e.g. increased water holding capacity), an improved soil structural stability can be observed [3, 4]. Up to now, the underlying mechanisms of hydrogel-induced structural stabilization of soils are not yet fully understood. In this context, soil texture and the way and degree of water entrapment are expected to contribute to the stabilization potential of hydrogel structures. Hence, the objective of this study was to understand the impact of hydrogel swelling on soil structural stability. For this, artificial soils were prepared with a varying clay:sand ratio and then treated with highly swellable polyacrylic acid (PAA) at different concentrations. One- and two-dimensional ^{1}H proton nuclear magnetic resonance relaxometry (^{1}H-NMR relaxometry) measurements were performed in order to assess the water distribution by transverse relaxation times T_2 and to characterize the degree of water entrapment in terms of rotational mobility (T_1/T_2) and self-diffusion coefficients (D/D_0) in the artificial soils. The information obtained from ^{1}H-NMR relaxometry was combined with the rheological characteristics of each artificial soil sample. Contrary to the untreated artificial soil, the polymer-treated artificial soil revealed significantly higher deformation at the yield point (τ_{YP}) with direct dependence on the swelling of PAA and the degree of water entrapment in the artificial soil matrix. The relationships suggest that, on the one hand, soil structural stabilization is promoted by higher degree of water entrapment as function of hydrogel swelling and mineral composition. On the other hand, clay-polymer interactions such as ab-/ adsorption as well as bridging processes further contributed to the stabilization of the soil structure.

All in all, determining the degree of water entrapment by one- and two-dimensional ^{1}H-NMR relaxometry together with soil rheological measurements seems a promising approach to enlighten the stabilization potential of hydrogel structures in soil.

References

[1] R. A. Hussien, A. M. Donia, A. A. Atia, O. F. El-Sedfy, A. R. A. El-Hamid, R. T. Rashad, CATENA 2012, 92, 172.
[2] F. Jaeger, A. Shchegolikhina, H. van As, G. E. Schaumann, The Open Magnetic Resonance Journal 2010, 3, 27.
[3] G. J. Levy, D. N. Warrington, Functional Polymers in Food Science: From Technology to Biology, Volume 2: Food Processing 2015, 9.
[4] C. Buchmann, J. Bentz, G. E. Schaumann, Soil and Tillage Research 2015.

Hardware and Software for Embedded Compact Broadband Low Field NMR spectrometers (ECBLFNMR).

Alain Louis-Joseph, Alexis Nauton, Denis Coupvent-Desgravier, Jean-Pierre Korb

Physique de la Matière Condensée, CNRS UMR7643, Ecole Polytechnique, Université Paris-Saclay, 91128 Palaiseau, France.

Numerous compact NMR spectrometers have been designed for an easy measure of proton NMR spectra. High sensitivity and resolution can be reached even with low field spectrometers (LFNMR) (i.e.:60MHz), thanks to great improvements in electronic hardware, wich opens up a wide field of analytical quantification and relaxation applications. One specificity of Low field NMR spectrometer is the use of a permanent and cryogen free magnet technology, avoiding the need for weekly and expensive cryogenic services.

Here we present and describe a low field NMR spectrometer fabricated in our laboratory. This spectrometer (ECBLFNMR) operates at frequencies ranging from kilohertz to MHz, with a standard sample diameter (5-10 mm). All the embedded hardware is very compact and requires only a 24V DC power supply, so this spectrometer is portable, easy to install and has a small footprint. This ECBFLNMR is dedicated to education and quantification, and enables low-field NMR research. It may be coupled with scientific experiments not requiring high magnetic fields, for example when nuclear spins are dynamically polarized by coupling with other nuclei or with spin-polarized electrons.

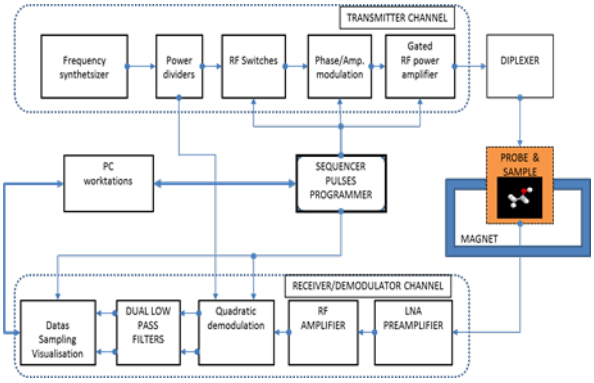

Figure 1 – Block diagram of a low field NMR spectrometer. (shims and lock compensation are not shown).

A basic block diagram of the complete NMR spectrometer is displayed in Figure 1, including all the embedded electronic hardware and software either for the transmission or the receiver channel. It includes a powerful Field Programmable Gate Area (FPGA) for the pulse programmer sequencer [1] and recent ARM microprocessor devices for the general spectrometer control. A Direct Digital Signal processor is used for frequency synthesis. A radio frequency low noise preamplifier and quadrature demodulation design are implemented to get an improved sensitivity. The ECBLFNMR is connected to a PC via only one USB port for the control and processing of experiments. Users can either design their own pulse programming NMR sequences or load/customize ones. A general purpose software interface has been developed and is easy to use, allowing access by different IDE (Interface Development Environment) for processing and development (Matlab, Quartus, ModelSim, Mbed, MestReNova, Eclispe,…).

References

[1] Garay, P. I., Janvier, A., Geerebaert, Y., & Louis-Joseph, A. (2014, Février 6). Pilotage programmable de spectromètre RMN. Rapport d'EA PHY573A, Conception expérimentale micro et nanoélectronique, Département de Physique, X2013. Ecole Polytechnique, Palaiseau, Essonnes, France.

Visualizing the 1-D fluid distribution using FT-NMR in fibrous porous media over time

B. Mohebbi[a,b], J. Claussen[b], B. Blümich[a]

[a] Institut für Technische und Makromolekulare Chemie (ITMC), RWTH Aachen University,Worringer Weg 1, 52074 Aachen, Germany;
[b] Procter & Gamble Service GmbH,Sulzbacher Strasse 40,65824 Schwalbach am Taunus,Germany.

In this study the NMR-MOUSE was used to excite a slice inside a filter paper with a thickness of 200 µm and acquire the signal amplitude using a CPMG sequence. The CPMG echo train was Fourier Transformed along the echo acquisition time to obtain signal intensity over time and position. T_2 contrast was used to visualize the 1D liquid distribution with a resolution of 50 ms and 20 µm over the thickness of the filter paper. Ongoing efforts aim at reducing the gradient strength of the magnetic field generated by single-sided sensors to increase the thickness of the excited sensitive volume without compromising the depth resolution of the sensor [1,2]. However, as the total thickness of the layer of interest in the present study is around 200 µm, the commercially available NMR-MOUSE PM2 with the static gradient of 35 T/m can be used.

In order to address the inhomogeneous magnetic field in z direction a mathematical post processing approach has been established. It uses the signal intensity of fully saturated filter paper as a mask function to normalize the signal amplitude of the filter paper during the fluid injection with a constant flow rate (80 µL/min). Figure 1 shows the signal intensity proportional to the liquid amount over time inside the thin fibrous porous material (filter paper).

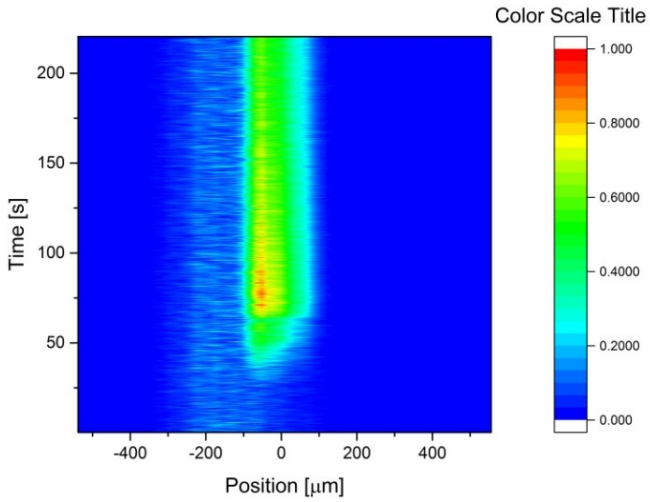

Figure 1 – Fluid distribution as a function of time and position inside a thin fibrous porous medium (filter paper).

This study demonstrates a promising method to non-invasively explore the dynamics of liquid ingress into a thin fibrous porous material. The features of the low-field unilateral NMR measuring device excellently match the geometry of the system of interest, thus allowing a suitable choice of spatial and temporal resolution. This match of geometries also shows that the Fourier transformed NMR signal can be used, rather than physically moving the instrument relative to the sample as is usually done.

References

[1] Maxime Van Landeghem, Ernesto Danieli, Juan Perlo, Bernhard Blümich, Federico Casanova, Low-gradient single-sided NMR sensor for one-shot profiling of human skin, Journal of Magnetic Resonance 215 (2012) 74–84.
[2] S. Rahmatallah, Y. Li, H.C. Seton, I.S. Mackenzie, J.S. Gregory, R.M. Aspden, NMR detection and one-dimensional imaging using the inhomogeneous magnetic field of a portable single-sided magnet, J. Magn. Reson. 173 (2005) 23–28.

Development of a robust mobile plant imager

M. Meixner[a], M. Tomasella[b], P. Först[a], C.W. Windt[c]

[a]Technical University Munich, Chair of process systems engineering, Germany; [b]Technical University Munich, Chair for Ecophysiology of Plants, Germany; [c]Forschungszentrum Jülich, IBG-2: Plant Sciences institute, Jülich, Germany.

Despite its proven utility for monitoring anatomy and physiological processes in plants, the use of MRI in plant research is still limited to a handful of labs worldwide. A major limitation is the cost, bulk and complexity of the equipment; a second limitation is the requirement that the plant has to be brought to the imager, rather than the other way round. In this contribution we demonstrate the construction of a robust small scale MRI imager that is simple and affordable in design, yet allows for acceptable image quality and mobile use.

Although the first applications of MRI to plants date back more than 60 years ago [1], the first successful efforts to bring MRI to the field are fairly recent [2, 3]. Most field work so far has focused on finding ways to adapt full size imagers and large permanent magnets and bring them out of the lab, even though smaller scale magnets and imagers have been developed as well [4]. In the current contribution we present the development of a device that is optimized for mobility and simplicity, yet still provides an acceptable image quality and that allows for the use of CPMG type sequences and (full Q-space) propagator displacement mapping, the latter to measure xylem and phloem sap flow.

We here present a compact 0.25 T C-shaped magnet with a 45 mm air gap, weighing 16 kg. A set of plane parallel gradient coil were made by etching and mounted in on openable probe.The gradient set provided a freely accessible air gap of 25 mm and was not actively shielded. The r.f. probe was made from Teflon and could accept solenoidal coils to suit stems and twigs of 10 to 20 mm Ø. The system was driven by a Kea II spectrometer (Magritek, Wellington, New Zealand), utilizing the built-in 100 W r.f. amplifier and a set of three BAFPA 40 gradient amplifiers (BRUKER, Rheinstetten, Germany). Custom built slice selective CPMG and centered out RARE sequences were written to complement the imager.

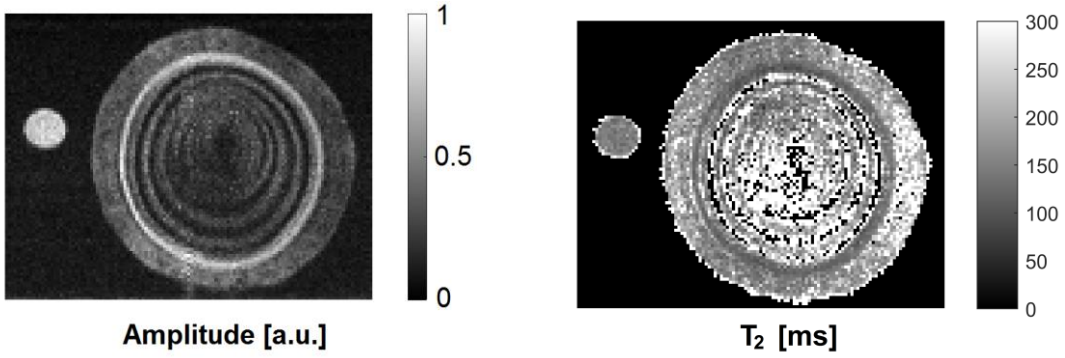

Figure 1 – Amplitude and T_2 map of a 13mm pine twig.

The half open magnet design and openable probe head allowed the system to be mounted onto a living tree in less than 20 minutes. This makes it possible to measure multiple trees per day, even if the a new coil has to be wound onto the tree by hand before mounting the magnet and probehead around it.

For a first test of the instrument a slice selective CPMG sequence was used to image a 13 mm Ø pine twig (Fig. 1), using an echo time of 3.8 ms, a field of view of 30x30 mm, a matrix size of 128x128, a repetition time of 2.5 s, 16 scans, 64 echoes, and a slice thickness of 5 mm. Next to the tree a reference tube filled with doped water and an inner diameter of 1.5 mm was placed. Amplitude and T_2 maps were calculated on the basis of a monoexponential fit. Considering the low field strength of the magnet and the proximity of the non-shielded gradient set to both the object and the polecaps, the image is of a more than acceptable quality. Anatomical features such as bark, phloem and year rings are clearly recognizable.

The robustness and utility of the imager was subsequently proven by its application in a greenhouse experiment. A large number of 4 year old spruce and beech trees were drought stressed for a period of 6 weeks. The imager was used to monitor the onset of drought induced embolism formation in 12 trees, repeating weekly the measurement of a number of trees from the population. The MRI work was used to complement more common plant physiological methods, such as water potential- and percentage loss of conductivity measurements.

References

[1] Shaw, T. M., and R. H. Elsken. Journal of Agricultural and Food Chemistry 4.2 (1956): 162-164.
[2] Umebayashi, Toshihiro, et al. Plant physiology 156.2 (2011): 943-951.
[3] Nagata, Akiyoshi, Katsumi Kose, and Yasuhiko Terada. Journal of Magnetic Resonance 265 (2016): 129-138.
[4] Windt, Carel W., et al. Journal of Magnetic Resonance 208.1 (2011): 27-33.

A COMPACT AND MOBILE NMR PLATFORM

J. Zhen[a], R. Dykstra[a], G. Gouws[a], S. Obruchkov[b]

[a]School of Engineering and Computer Science, VUW, New Zealand; [b]School of Chemical and Physical Sciences, VUW, New Zealand;

A truly mobile NMR system should be able to be carried by the user to any area and operated without much physical effort. The goal of mobile NMR is to bring the system to the sample instead of bringing the sample to the system. A fully integrated mobile NMR platform was developed and tested and can easily be interfaced to several types of NMR MOUSE sensors such as the Mini-MOUSE[1]. The mobile platform was made possible by the successful development of compact and efficient Class-D RF power amplifiers combined with a recently released System On a Chip (SoC) device. The SoC device is itself a combination of a high performance processor and Field Programmable Gate Array (FPGA) logic all on a single chip. This now allows us to have an operating system, data processing system, pulse sequencer, digital receiver and Tx/Rx control logic all on a single chip.

A prototype system was built using a SoC FPGA module running a Linux OS with a WIFI connection to an iPad running a web based control program. A 30 W Class-D RF power amplifier and preamp/duplexer was integrated to work with the 17 MHz, Mini-MOUSE sensor. DAC and ADC devices were used to provide the necessary Tx/Rx analogue/digital conversion and a 70 dB gain block was also included to provide the required signal amplification. One key feature of the new platform is that the data from the FPGA based digital receiver is automatically streamed to the main processor system memory via a DMA controller. This allows zero delay between acquisitions and one can also snoop at the data while it is being acquired. The fully integrated system, with rechargeable Lithium batteries to allow five hours operation, fits in a case measuring 150x120x65 mm and weighs 800 grams, Figure 1. Experiments showed successful T2 measurements on polymer composites and rubber samples.

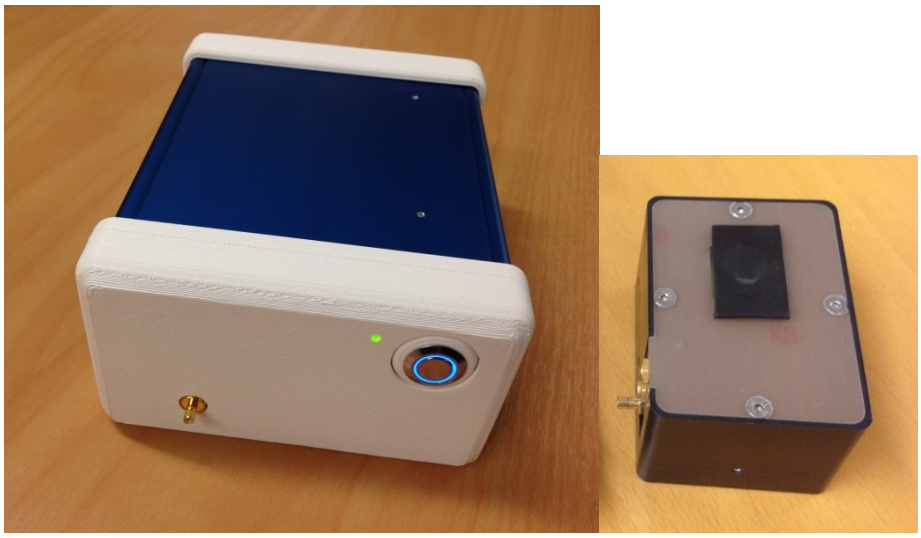

Figure 1 The Prototype Mobile NMR system with 17MHz, Mini-MOUSE sensor [1].

References

[1] D. Oligschlager, S. Gloggler, B. Blumich, etl, (2015), A Miniaturized NMR-MOUSE with a High Magnetic Field Gradient (Mini-MOUSE), Springer, Applied Magnetic Resonance, 181-202, 46.

Real-time Multidimensional NMR Inversion Using Compressed Sensing

Sen Gu[a], Lizhi Xiao[a], Guangzhi Liao[a]

[a]China University of Petroleum Beijing, 18 Fuxue Road, Changping, Beijing China 102249.

Currently, all interpretation software of the NMR logging for data processing are all carried out after data collected. But since the establishment of a sophisticated NMR laboratory for identification and analysis of fluid has gained increasing attention, the characterization of real-time, continuity and accuracy for NMR data processing has become more and more important, and it turns into a new trend in NMR logging data processing and development of technology in the field of oil exploration.

Therefore, the goal of this work is to realize real-time multidimensional NMR data processing, In order to achieve the goal we collect echo data continuously, and then get the multidimensional NMR spectrum at the same time, stop collect the data when the NMR spectrum is no longer significant changes. However, a large amount of data and long acquisition time limits its application in NMR logging. So we present a new method for Multidimensional NMR relaxometry that incorporates compressed sensing (CS) as a means to vastly reduce the amount of relaxation data without compromising data quality [1]. Unlike the conventional CS reconstruction in the Fourier space (k-space), the proposed CS algorithm is directly applied onto the Laplace space without compressing k-space to reduce the amount of data required for NMR relaxation spectra [2]. A fast 3D pulse sequence was adopted to get the data and extract 3D T_1-D-T_2 probability function [3].

We present a version of the FISTA algorithm to do the NMR inversion, which does not use any matrix factorization and memory efficient, was applied to the multidimensional NMR problem [4]. In comparison to the forward model, this fast and memory efficient algorithm is applied to obtain the Multidimensional NMR distribution with high resolution without large computer memory requirement and to show the advantage of Multidimensional NMR for fluid identification. From the Fig1, we can find that when the echo data is insufficient the quality of 3D spectra not maintain very well via the CS reconstruction. But when the echo data is more the NMR spectrum is not significant difference ,so we can stop collect the data, thus realizes real-time multidimensional NMR data processing and save time.

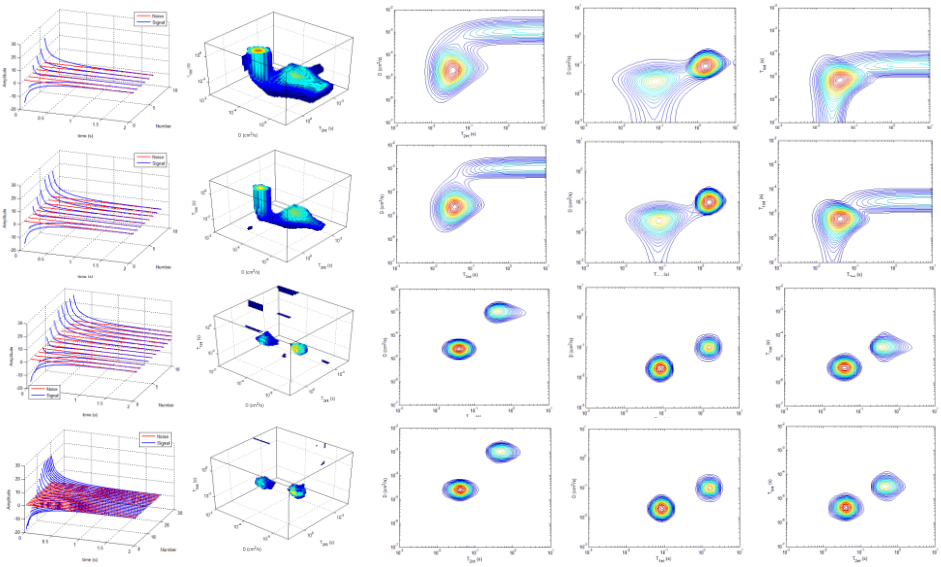

Figure 1 – Real-time Multidimensional NMR relaxometry from the stimulated data with same SNR (SNR=500) and different number of echo trains: 6, 8,12 and 18.

References:

[1] Ruiliang B, Alexander C, Wojciech C et al. Efficient 2D MRI relaxometry using compressed sensing, J. Magn. Reson, 2015, 255 : 88-99
[2] E J Candes and Y Plan. Tight Oracle Bounds for Low-rank Matrix Recovery from a Minimal Number of Random Measurements. Eprint Arxiv, 2010, 57(4): 2342-2359
[3] Liu H, Xiao L, Guo B et al. Heavy oil component characterization with multi-dimensional unilateral NMR, Pet. Sci, 2013, 10: 402-407
[4] Paul D Teal and Craig Eccles. Adaptive truncation of matrix decompositions and efficient estimation of NMR relaxation distributions, Inverse Problems, 2015, 31.

Fast Laplace Inverse Transform (FLINT)

P.D. Teal[a]

[a]Victoria University of Wellington, PO Box 600, Wellington 6140, New Zealand.

An important approach to the interpretation of nuclear magnetic resonance (NMR) measurements for analysis of porous materials is the estimation of the spectra of relaxation times. This is typically performed using a numerical inversion of a Laplace transform. The observed data $Z(\tau_1,\tau_2)$ for a T_1-T_2 two-dimensional measurement (for example) can be expressed in terms of the spectra of relaxation times $S(T_1,T_2)$ using an integral:

$$Z(\tau_1,\tau_2)=\iint k_1(\tau_1,T_1)k_2(\tau_2,T_2)S(T_1,T_2)\,dT_1 dT_2 \tag{1}$$

with kernels k_1 and k_2 depending on the form of the experiment. Experimental data is collected at discrete values of time, and so (1) is typically approximated using matrices as $Z=K_1SK_2^{\mathrm{T}}+E$ where E is measurement noise. Numerical inversion of a Laplace transform to obtain S is known to be an ill-conditioned procedure, so the inversion procedure typically uses a regulariser. In addition, the relaxation time spectra is often non-negative, so the solution takes the form

$$\hat{S}=\underset{S\geq 0}{arg\,min}\|Z-K_1SK_2^T\|_F^2+\alpha\|S\|_F^2 \tag{2}$$

where the subscript F represents the Frobenius norm.

The large size of the matrices K_1 and K_2 has in the past meant that solutions of (2) have required some form of data compression, typically performed using the singular value decomposition [1], and then use of the Butler-Reeds-Dawson algorithm. Advances in optimisation theory has made more efficient methods available. One of these is inspired by the Fast Iterative Shrinkage-Thresholding Algorithm (FISTA)[2], although the Frobenius norm regulariser here means that thresholding does not form part of the algorithm. Matrices S_0 and Y_1 can be initialised for example to have all elements set to 1, the Lipschitz constant L can be conservatively set to $L = 2\mathrm{trace}(K_1^{\mathrm{T}}K_1)\mathrm{trace}(K_2^{\mathrm{T}}K_2)$, $t_1=1$, and then the algorithm proceeds by iteration of the following steps:

$$S_k \Leftarrow max\left(0,\frac{L-2\alpha}{L}Y_k+\frac{2}{L}\left(K_1^T Z K_2-K_1^T K_1 Y_k K_2^T K_2\right)\right) \tag{3}$$

$$t_{k+1}\Leftarrow\frac{1+\sqrt{1+4t_k^2}}{2} \tag{4}$$

$$Y_{k+1}\Leftarrow S_k+\frac{t_k-1}{t_{k+1}}\left(S_k-S_{k-1}\right) \tag{5}$$

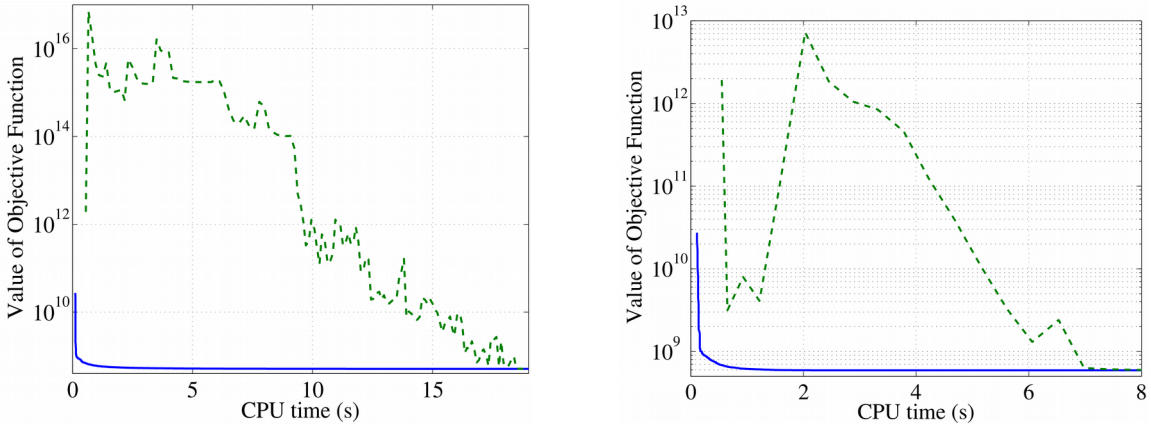

Figure 1 – Convergence comparison for measured data. The value of regularisation parameter α for the left panel is 10^{-3} and for the right panel 10^{2}. In both panels the proposed method is shown by the solid line, while the BRD method after data compression is shown by the dashed line.

Convergence is rapid and reliable and can be detected by a threshold on the residual. Further details are available in [3].

References

[1] Venkataramanan, L., Song, Y.-Q. & Hurlimann, M. (2002). Solving Fredholm integrals of the first kind with tensor product structure in 2 and 2.5 dimensions, IEEE Trans. Signal Processing 50(5): 1017–1026..

[2] Beck, A. & Teboulle, M. (2009). A fast iterative shrinkage-thresholding algorithm for linear inverse problems, SIAM J. Imaging Sciences 2(1): 183–202.

[3] P.D. Teal and C. Eccles. Adaptive truncation of matrix decompositions and efficient estimation of NMR relaxation distributions. *Inverse Problems*, 31(4):045010, April 2015.

The effect of microstructure of semi-permeable barriers onto diffusion MRI: A one-dimensional theoretical study

N. Moutal[a], D. S. Grebenkov[a]

[a]Laboratory of Condensed Matter Physics, CNRS – Ecole Polytechnique, F-91128 Palaiseau, France.

Diffusion of water molecules in biological tissues is hindered by cellular semi-permeable membranes. The geometrical complexity of the tissue prohibits analytical solutions of the Bloch-Torrey equation and thus exact formulas for relating the microstructure to the measurable pulsed gradient spin-echo (PGSE) signal. In this situation, one-dimensional models of semi-permeable barriers can help to uncover this relation and to understand the role of the diffusive exchange across the membranes. Moreover, these models can accurately describe some ordered structures such as vegetal cells or muscles [1].

We present an effective method to compute the eigenvalues and eigenfunctions of the Laplace operator in one-dimensional domains with multiple barriers [2,3]. The method allows us to compute the PGSE signal analytically for infinitely narrow gradient pulses, or numerically for arbitrary pulse sequences. In particular, this method generalizes earlier approaches [3-6] and allows us to study more sophisticated configurations of barriers such as microstructures inside larger scale structures. For instance, the signal for a multilayer structure with m-1 evenly spaced semi-permeable internal barriers (at distance l), enclosed within a larger-scale impermeable membrane, reads

$$S = 2\frac{1-\cos mq}{(mq)^2} + \frac{4q^2}{m^2}\sum_{k=1}^{\infty}\frac{1-(-1)^{km}\cos mq}{(k^2\pi^2-q^2)^2}e^{-\frac{Dtk^2\pi^2}{l^2}} + \sum_{\substack{1\le n\le m-1\\ k\ge 0}}\frac{4q^2(1-(-1)^n\cos mq)\left(\frac{\cos\alpha_n^k-\cos q}{\cos\psi_n-\cos q}\right)^2 e^{-\frac{Dt{\alpha_n^k}^2}{l^2}}}{m^2\left({\alpha_n^k}^2-q^2\right)^2\left[\left(1+\frac{1}{2\tilde\kappa}\right)\sin\alpha_n^k+\frac{\alpha_n^k\cos\alpha_n^k}{2\tilde\kappa}\right]\frac{\sin\alpha_n^k}{\sin^2\psi_n}}$$

where α_n^k are solutions of the following equation (1)

$$\cos\alpha_n^k - \frac{\alpha_n^k\sin\alpha_n^k}{2\tilde\kappa} = \cos\psi_n \quad (2)$$

$\psi_n = \frac{n\pi}{m}$ (with $n = 1 \dots m-1$), and q=γgδl, γ being the gyromagnetic ratio, g and δ the gradient strength and duration, κ the inter-barrier permeability, D the diffusion coefficient, and $\tilde\kappa = \frac{\kappa l}{D}$. Figure 1 shows the dependence of the signal on the number m of layers in two regimes: high permeability and low permeability.

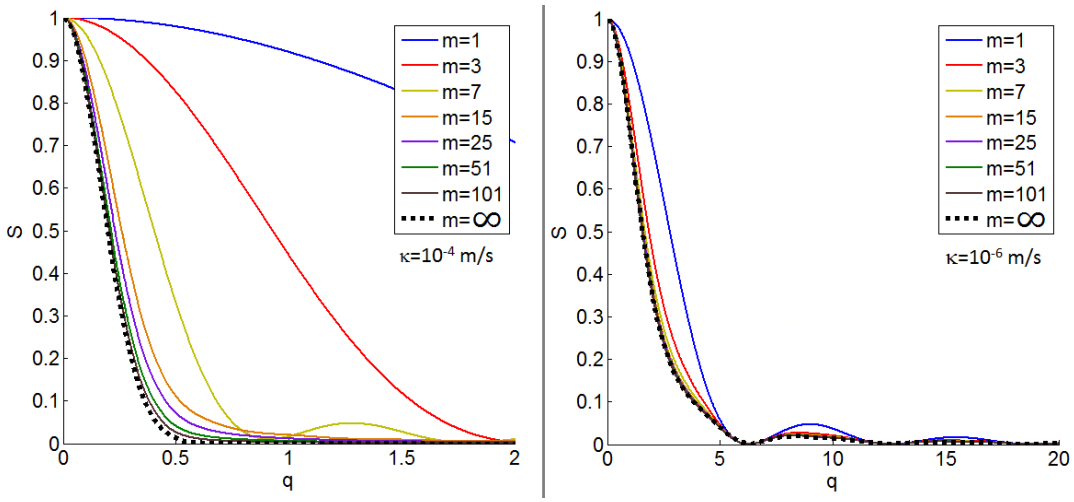

Figure 1 – PGSE signal computed analytically under the narrow pulse approximation (with Δ=1s) in a multilayer structure with m-1 evenly spaced semi-permeable barriers (at distance l=4μm) of permeability κ=10^{-4} m/s (left) and κ=10^{-6} m/s (right), with reflecting boundary conditions at the exterior endpoints. The signal is plotted against q=γgδl. One can see the dependence on the number of layers m. The signal for an infinite array of barriers (i.e. the periodic case considered in [5]) is plotted by black dotted line.

In conclusion, the proposed method presents new insights into the intricate relation between the microstructure and the PGSE signal and helps to reveal the role of permeability, especially in the low- and high-permeability limits.

References

[1] Van As H. Intact plant MRI for the study of cell water relations, membrane permeability, cell-to-cell and long-distance water transport. *J. Exper. Botany* **58**, 743-756 (2007)

[2] Grebenkov D. S. Pulsed-gradient spin-echo monitoring of restricted diffusion in multilayered structures, *J. Magn. Reson.* **205**, 181-195 (2010)

[3] Grebenkov D. S. Exploring diffusion across permeable barriers at high gradients. II. Localization regime, *J. Magn. Reson.* **248**, 164-176 (2014)

[4] Tanner, J. E. Transient diffusion in a system partitioned by permeable barriers. Application to NMR measurements with a pulsed field gradient. *J. Chem. Phys.* **69,** 1748 (1978)

[5] Novikov E. G. , van Dusschoten D., and Van As H. Modeling of Self-Diffusion and Relaxation Time NMR in Multi-Compartment Systems. *J. Magn. Reson.* **135**, 522-528 (1998)

[6] Sukstanskii, A., Yablonskiy, D. and Ackerman, J. Effects of permeable boundaries on the diffusion-attenuated MR signal: insights from a one-dimensional model. *J. Magn. Reson.* **170,** 56–66 (2004)

What are, and what are not, Inverse Laplace Transforms

E. Fordham[a], L. Venkataramanan[b], J. Mitchell[a], A. Valori[c]

[a]Schlumberger Gould Research, High Cross, Madingley Road Cambridge CB3 0EL, UK; [b]Schlumberger-Doll Research Centre, One Hampshire Street, Cambridge, MA 02139, US; [c]Schlumberger Dhahran Carbonate Research, Dhahran Techno Valley, Dhahran, Saudi Arabia.

Time-domain NMR, in one and higher dimensionalities, makes routine use of inversion algorithms to generate results called "T_2-distributions" or joint distributions in two (or higher) dimensions of other NMR parameters, T_1, diffusivity D, pore size a, etc. Even in otherwise authoritative texts [1], these are frequently referred to as "Inverse Laplace Transforms" although the standard inversion of the Laplace Transform long-established in many textbooks of mathematical physics [2, 3, 4] does not perform (and cannot perform) the calculation of such distributions. The operations performed in the estimation of a "T_2-distribution" are the estimation of solutions to a Fredholm Integral Equation (of the First Kind), a different and more general object whose discretization results in a standard problem in linear algebra, albeit suffering from well-known problems of ill-conditioning and computational limits for large problem sizes [5]. The "First Kind" qualification is important in this regard because FIE's of the Second Kind typically exhibit less ill-conditioned behaviour. The Fredholm Integral Equation is not restricted to exponential kernels; the same solution algorithms can be used with kernels of completely different form. On the other hand, (true) Inverse Laplace Transforms, treated analytically, can be of real utility in solving the diffusion problems highly relevant in the subject of NMR in porous media [6].

The inaccurate terminology can be highly confusing for students at all levels.

This poster will show explicitly that a "T_2-distribution" $P(R_2)$ is not an "Inverse Laplace Transform". If the customary expression for the total magnetization decay

$$M(t) = \int_0^\infty P(R_2) e^{-tR_2}\, dR_2 \tag{1}$$

is regarded as a (forward) Laplace Transform, then, contrary to superficial appearances, the (real) time variable t in $M(t)$ corresponds to the *complex* Laplace variable s in the (forward) Laplace Transform $F(s)$ and not to the variable t:

$$F(s) = \int_0^\infty f(t) e^{-st}\, dt \tag{2}$$

Similarly, the time variable t in $F(s)$ corresponds not to the variable t in $M(t)$ but to the relaxation rate R_2. Evaluating $P(R_2)$ using the textbook Inverse Laplace Transform [2, 3, 4] based on the contour integral first described in 1916 [7] is not possible, because data on $M(t)$ for *complex* t are required. Since "complex time" t has no meaning in the context of time-domain NMR, $M(t)$ is simply undefined for other than real t, and this approach fails.

Alternative algorithms for evaluating Inverse Laplace Transforms from data at discrete points confined to the *real* axis are known, such as the Stehfest algorithm [8], based on generating functions in [9]. This takes the form of an infinite sum over discrete points on the real axis and is useful when the forward transform $F(s)$ is known analytically, but the inverse $f(t)$ is not. However the sampling points do not necessarily correspond to experimental echo times, and [8] suffers from the familiar instabilities in the presence of experimental error, so is again of no direct use for the evaluation of $P(R_2)$.

For the evaluation of T_2-distributions $P(R_2)$, we return to solutions of Fredholm Integral Equations, with regularization and positivity constraints, as the solution method set out in [5]. These reduce to solution of standard linear algebra problems when discretized [5], and for many practical algorithms, exponential and non-exponential kernels are equally acceptable, and likewise of utility in the subject [10]. The FIE's with non-exponential kernels have not even a superficial resemblance to Inverse Laplace Transforms, but are directly related to the methods in [5], widely used for generating T_2-distributions and their multi-dimensional generalizations.

Returning to (true) Inverse Laplace Transforms, the poster will give examples of their utility in the solution of diffusion problems, and examples of numerical estimation where the forward transform is known analytically.

References

[1] Callaghan, P.T. (2011) Translational Dynamics and Magnetic Resonance, OUP
[2] Matthews, J. & Walker R.L. (1970) Mathematical Methods of Physics, Benjamin
[3] Jeffreys, H. & Jeffreys, B.S. (1956) Methods of Mathematical Physics, CUP
[4] Arfken, G. (1970) Mathematical Methods for Physicists, Academic Press
[5] Venkataramanan, L., Song, Y.Q. & Hürlimann, M.D.(2002) IEEE Trans. Signal Processing, 50(5), 1017.
[6] Grebenkov, D.S. (2007) Rev. Mod. Phys. 79, 1077–1137
[7] Bromwich, T.J. I'A. (1916) Proc. London Math. Soc. 2(15) 401–448
[8] Stehfest, H. (1970) Comm. ACM, 13(1), 47–49
[9] Gaver, D.P. (1966) Oper. Res. 14(3), 444–459
[10] Mitchell, J. (2016) Invited Lecture, MRPM13 (this conference)

Local analysis of single-phase flow through complex porous media using flow propagators

Y. Zheng[a], I. Shikhov[a], M. N. d'Eurydice[b], C. H. Arns[a]

[a]The University of New South Wales, Australia; [b]Victoria University of Wellington, New Zealand

Flow propagators have been frequently used in porous media characterization and to characterize fluid flow within. Scheven et al., Codd et al. [1, 2] and others measured flow propagators in various media and discussed how dispersion or other effects, such as relaxation and internal gradients, affect its shape. In addition, numerical simulations were used by many researchers to match their measurements [3]. However, these works mainly focused on homogeneous media like beads pack and clean sandstones. Heterogeneous cores were also studied by some groups but their interpretations lacked quantitative analysis of how pore geometries affect fluid transport which shapes the flow propagators.

In this work, we compute regional steady state flow propagators to investigate the relationship between local propagators and global ones. We use bead packs to represent different sample regions. Four kinds of featured regions, micro pore region (0.5mm diameter beads), macro pore region (1.5mm diameter beads), micro-macro pore region (flow from 1.5mm beads to 0.5mm beads) and macro-micro pore region (opposite flow direction) are measured locally to quantitatively analyse the flow transport. We combine Lattice Boltzmann Method (LBM) and random walk techniques to carry out the simulations. The LBM method is used to compute the velocity field, and water molecular transport along the streamlines to simulate convection flow, then random walk method is used to simulate diffusion. We further simulate the local flow propagators in carbonate images, and study effect of relaxation on flow propagators. Figure 1 depicts an example comparison of flow propagators for the bead packs used for validation of the method.

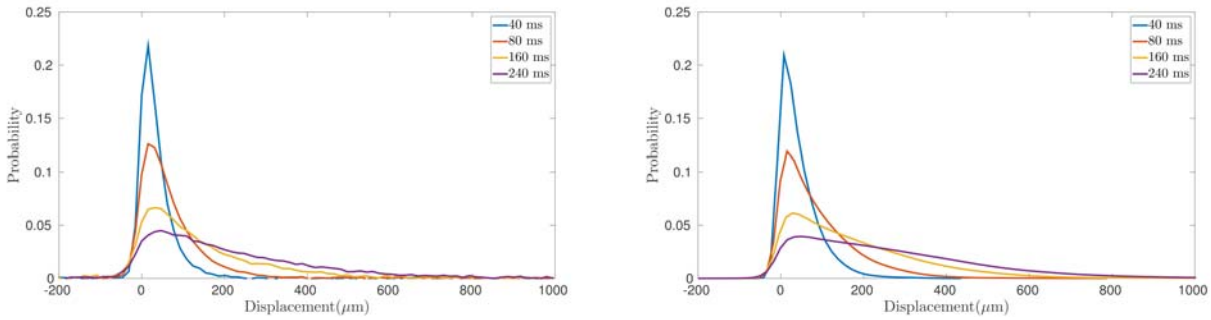

Figure 1 – Flow propagators in 0.5mm beads pack at different times, experiment results(left) and simulations(right) .

References

[1] Scheven, U. M., J. G. Seland, and D. G. Cory. "NMR propagator measurements on flow through a random pack of porous glass beads and how they are affected by dispersion, relaxation, and internal field inhomogeneities." Physical Review E 69.2 (2004): 021201.
[2] Codd, S. L., and S. A. Altobelli. "A PGSE study of propane gas flow through model porous bead packs." Journal of Magnetic Resonance 163.1 (2003): 16-22.
[3] Maier, Robert Sullivan, et al. "Simulation of flow through bead packs using the lattice Boltzmann method." Physics of Fluids (1994-present) 10.1 (1998): 60-74.
[4] Arns, C. H., et al. "NMR petrophysical predictions on digitized core images." Petrophysics 48.03 (2007).

Performance Evaluation of Improved 2DUPEN algorithm

V. Bortolotti[a], L. Brizi[b,c], P. Fantazzini[b,c], G. Landi[d], F. Zama[d]

[a]Department of Civil, Chemical, Environmental, and Materials Engineering, University of Bologna, Italy; [b]Department of Physics and Astronomy, University of Bologna, Italy; [c]Museo Storico della Fisica e Centro Studi e Ricerche Enrico Fermi, Roma, Italy; [d]Department of Mathematics, University of Bologna, Italy.

The inversion of two-dimensional NMR relaxation data involves a very large number of measurement points, making the solution difficult for both storage requirements and computation times. The 2DUPEN algorithm, described in [1], can be improved by introducing suitable weighting factors obtained by a windowing procedure and by compressing the data using the Singular Value Decomposition (SVD). The Improved 2DUPEN (I2DUPEN) method performs the solution of the following weighted penalized Least Squares problem:

$$\min_f \left\{ \|B\,K\,f - B\,s\|^2 + \sum_{i=1}^{N} \lambda_i \cdot (L\,f)_i^2 \right\}$$

where $K \in R^{M \times N}$ is the discretized exponential kernel, $s \in R^M$ and $f \in R^N$ are the vector reordering of the data $S \in R^{M_1 \times M_2}$ and the unknown distribution $F \in R^{N_x x N_y}$ respectively. The matrix $L \in R^{N \times N}$ is the discrete Laplacian operator, $B \in R^{M \times M}$ is a diagonal matrix of weights related to the statistics of the data and λ_i are the local regularization parameters defined by the UPEN principle. As an example, we consider a test problem that simulates an IR-CPMG acquisition of 128×2048 data with uniformly distributed noise of level 10^{-2}. The reconstruction of a 64×64 map using the whole data set (i.e. B is the identity matrix) is obtained after 1684 seconds with relative error 4.186×10^{-2} using an Intel i7-6500U processor and 16 GB of Ram.

By exploiting the structure of the kernel, $K = K_1 \otimes K_2$ with $K_1 \in R^{M_1 \times N_x}$ and $K_2 \in R^{M_2 \times N_y}$ and by computing their SVD ($K_1 = U_1 S_1 V_1^t$, $K_2 = U_2 S_2 V_2^t$) we can write the problem in its compressed equivalent form $\|Kf - s\|_2 = \|\hat{K}f - \hat{s}\|_2$ where $\hat{K}f$ and $\hat{s}$ are the vector reordering of the matrices $S_1 V_1^t F V_2 S_2^t$ and $U_1^t S U_2$ respectively with $K_1 \in R^{(r_1 r_2) \times N}$ and $\hat{s} \in R^{(r_1 r_2)}$. The values r_1, r_2 are the number of non zero singular values of the matrices K_1, K_2 respectively. Hence using the whole set of singular values in our example we have $\hat{s} \in R^{N^2}$ and $\hat{K}f \in R^{N^2}$ with $N^2 = 4096$. The spectral structure of the matrices is characterized by a very large number of small singular values, as reported in figure 1 (left), hence setting to zero the singular values smaller than a threshold T>0, we can reduce the length of the projected data vector $\hat{s}$ while preserving the quality of the reconstruction. In our example we still obtain a good quality reconstruction (relative error 3.976×10^{-2}) by using $T=10^{-2}$ with $r_1 \cdot r_2 = 240$ after 1213 seconds (see Figure 1 center and right).

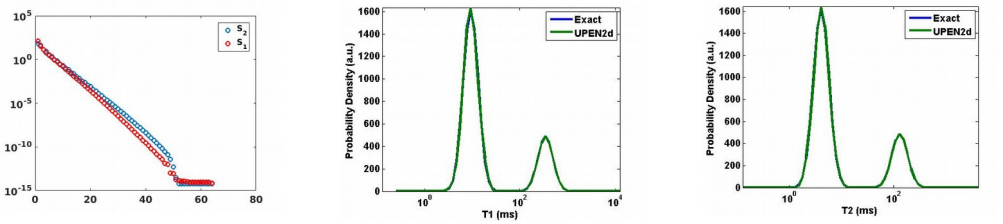

Figure 1 – Singular values (left) T_1 (center), T_2 (right) reconstructions with threshold $T=10^{-2}$

If the noise is additive, random, and, approximately, normally distributed, and if systematic data errors are smoothly varying with time, then averaging data points into sufficiently narrow windows does not change significantly the result with respect to that obtained by using all points. In our example the windowing was implemented by reducing the points in the CPMG blocks to 118 non uniformly distributed values having a data set $S \in R^{128 \times 118}$. Defining the matrix B as $B = \hat{B} \otimes I$ with $\hat{B} \in R^{118 \times 118}$ and the identity matrix $I \in R^{128 \times 128}$ then BKf is the vector reordering of the matrix $K_1 F (\hat{B} K_2)^t$. It is possible to compress the data by applying a threshold T to the Singular Values of the matrices K_1 and $(\hat{B} K_2)$ (reported in Figure 2 (left)).

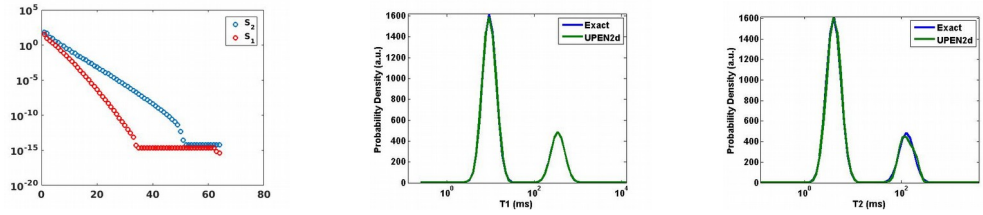

Figure 2 – Weighted Singular values (left). Weighted T_1 (center), T_2 (right) reconstructions with threshold $T=10^{-2}$.

For example, using $T=10^{-2}$ we obtain the solution represented in Figure 2 (center and right) after 840 seconds with relative error 5.936×10^{-2}. Many experiments, performed both on synthetic data sets as well as on real data, confirm that coupling the windowing strategy together with the truncated singular values decomposition allows us to obtain substantial improvements in the computation times while preserving good quality results (i.e. precise reconstruction of the height and amplitude of peaks).

References

[1] V. Bortolotti, R.J.S. Brown, P. Fantazzini, G. Landi, F. Zama, submitted, 2016.

Hydrodynamics and 2D NMR characterization of wettability in saturated rocks

J. Wang, L. Xiao, L. Guo, G. Liao, Y. Zhang, F. Xiao

State Key Laboratory of Petroleum Resources and Prospecting, China University of Petroleum, Beijing, China

The hydrodynamics in porous media is extremely complex due to surface interaction such as wettability and heterogenous pore structure. However, it is critical for oil production plan and oil recovery. Researches have been done on qualitatively interpretating NMR response of wettability [1, 2, 3], and the NMR simulation were made by assuming the shape of fluid and its distrution. But the real distribution of fluid is complex because of wettability and pore geometry. This makes the interpretaion of NMR response diffucult. The wettability and viscosity isexamined in this research by combining the simulation of distribution of oil and water in saturated rockand two dimensional Laplace NMR method [2, 4, 5]. The explicit force LBM with multiple relaxation method can be applied to high viscosity fluid and wettability simulation. Then based on the results of fluid distribution, two dimensional nuclear magnetic resonance response is simulated in saturated rocks. This method can provide deep interpretation of the wettability and viscosity characterization of NMR response.

An example of fluid distribution influenced by wettability and saturation(*Figure 1*) is simulated by this method, and *2D* NMR simulation in a rock core based on fluid distribution are implemented. The distribution simulation of water and oil in saturated rock provides us the information of how the fluids interact with the pore wall and their distributions, which contributes to the understanding of NMR response simulation.

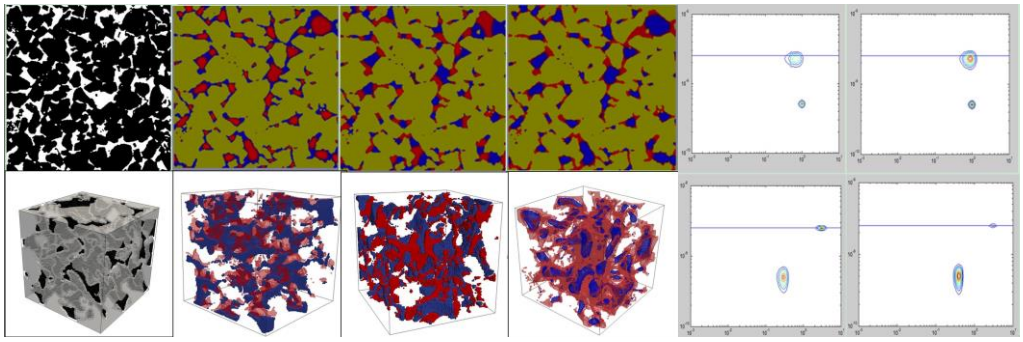

Figure 1 - Fluid distribution affected by wettability in rock core. Red is oil and blue is water. Colum1 is rock sample and colums 2-4 is fluid distributin affected by water wetting, mixted wetting and oil wetting.colum 5-6 is NMR simulation with different wettablity and saturation. Row 1 is water wetting with increasing water saturation and row 2 is oil wetting with increasing oil saturation. Colum 5 are fluid distribution and *2D* NMR simulation result of oil wetting with high viscosity.

When only wettability and saturation are considered, the NMR simulation results show the surface relaxation effects and diffusion coefficient of the wetting phase will decrease. It is because that interacting with pore walls, surface relaxation of wetting fluid accelerates its relaxation. Confined by the walls, the diffusion coefficient also declines[2]. With saturation increasing, T_2 relaxation time and diffusion coefficent shift to high value, because the ratio of contacting surface area to volume decrease and volume increase. Thus, influence of mixed wettability on fluid distribution and 2*D* NMR characterization is sumlated and the relationship is built between wettability index and surface relaxation in *Equation(1.2)*, where ρ_{eff} and saturation can be obtained by fitting *Equation (1.1)* on T_2-*D* map.The equation is different from the definiton of wettability. But they can be related. Based on those simulation and theory, we will do some experiment to testify the simulation and relationship.

$$D(t) = D_0(1-\gamma\frac{aL_D+(L_D/L_M)^2}{aL_D+(L_D/L_M)^2+\gamma}) \tag{1.1}$$

Where $a = 4/(9\sqrt{\pi})(T_{2S}\rho_{eff})$, $\gamma = 1-D_\infty/D_0$, $D_\infty = D_0/(\phi F)$ $L_D = \sqrt{D_0 t}$, $\rho_{eff} = (S_{contcact}/S_{total})\rho$

$S_{contcact}$ is contacting area and S_{total} is whole area of the pore.

$$1/T_{2S} = \rho_{eff}W_{index}/S_w(S/V) \tag{1.2}$$

Where S_w is saturaiton of fluid.

References

[1] Evseev N, Dinariev O, Hurlimann M, et al.. Petrophysics, 2015, 56(01): 32-44.
[2] Minh C C, Crary S, Singer P M, et al. SPWLA 56th Annual Logging Symposium. Society of Petrophysicists and Well-Log Analysts, 2015.
[3] Bergman D J, Dunn K J, Schwartz L M, et al. Physical Review E, 1995, 51(4): 3393.
[4] Arns C H, AlGhamdi T, Arns J Y. New Journal of Physics, 2011, 13(1): 015004.
[5] Zielinski L, Ramamoorthy R, Minh C C, et al. Society of Petroleum Engineers, 2010.

NMR solid state spin-echo simulation for water absorption in SWCNT

Long GUO, Lizhi XIAO*, Zijian JIA

State Key Laboratory of Petroleum Resources and Prospecting, China University of Petroleum, Beijing 102249, China.

Nano scale absorption has invoked extensive interest for its potential applications in shale gas development, catalysts, and drug delivery. Studies showed that the interactions between Single Wall Carbon Nanotube (SWCNT) and guest molecules can be detected by NMR with solid state echo. This solid-echo depends on the fact that water molecules encounter the carbon nanotube and stick for a short time. Therefore, it is a critical for us to simulate collision frequency of moleculars confined inside the SWCNT. A solid (quadrapolar) echo refocuses dipolar and quadrupolar couplings. It is generated by a 90 pulse applied at a during time, τ, after the 90 excitation pulse. The maximum echo amplitude can be acquired at a during time τ after the second pulse. The echo delay time τ should be smaller than the inverse coupling strength. The water adsorption on the interior surface of the SWCNT has been measured using ^{1}H-NMR [1]. Our aim is to calculate the homo- and heteronuclear contributions to the van Vleck moments [2] of absorbed water molecules in SWCNT with lattice Boltzmann method (LBM) [3]. This study would contribute to the research of adsorption in doped carbon nanotubes.

The spin Hamiltonian in frequency units for a solid containing two dipolar-coupled spin-1/2 species I and S can be written in the high-field approximation as:

$$H = H_0 + H_{II} + H_{IS} + H_{SS} \tag{1}$$

where:

$$H_0 = -\gamma_I B_0 \sum_j I_{jz} - \gamma_S B_0 \sum_\alpha S_{\alpha z} \tag{2}$$

is the Zeeman interaction with the external magnetic field of magnitude B_0 applied along z-axis; I and S are the quantized spin vectors of hydrogen atom and impure atom (usually is Fe) in SWCNT; j and a are the numbers of hydrogen atoms and impure atoms, respectively. H_{II}, H_{IS}, H_{SS} are the truncated dipolar Hamiltonian for the interaction between the resonant spins II, IS and SS, respectively. After mathematical derivation [2] in time domain, the decay of the transverse magnetization following a resonant 90 - τ - 90 pulse sequence is given by:

$$E(t,\tau) = 1 - \frac{M_2^I (t-\tau)^2}{2!} + \frac{M_4^I (t-\tau)^4}{4!} \ldots - M_2^{IS} t\tau \tag{3}$$

where E is echo amplitude related to the time t and interval time τ. In equation (3), the second order expansion terms can be expressed as:

$$M_2^I = M_2^{II} + M_2^{IS} = \frac{1}{3}\left[I(I+1)\frac{1}{N_I}\sum_{j,k} B_{jk}^2 + S(S+1)\frac{1}{N_I}\sum_{k,\beta} C_{k\beta}^2 \right] \tag{4}$$

where j, k represent different hydrogen atoms, β represents different impure atoms. **B** and **C** are the factors related to the relative positions of molecules. N_I is the number of hydrogen absorbed on SWCNT. The explicit expressions of M_4^I and other high-order terms are omitted in this summary. In equation (3) and (4), the key parameter is N_I, the number of molecules adsorbed by the pore walls in time τ. The molecules adsorption and desorption processes can be simulated by diffusion approaching and departing the wall, respectively. The density distribution can be determined by the chemical potential distribution in SWCNT [3]. Compared to molecular dynamics (MD), LBM can solve the adsorption problem in a larger temporal and spatial scales.

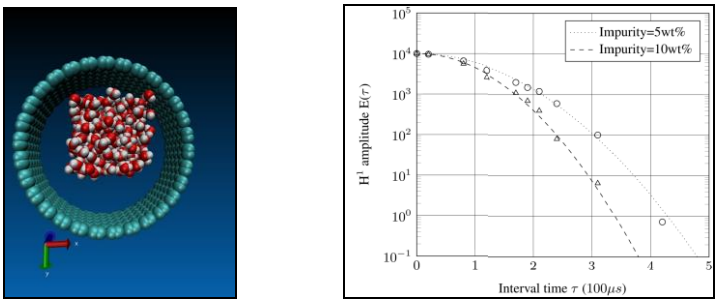

(a) (b)

Figure 1 (a) Configurations of water moleculars inside SWCNT, (b) 90-τ-90 maximum echo amplitude E(τ) as a function of interval time τ, simulations (dashed line) and experiments (marks) at 253K.

References

[1] Sekhaneh, W., Kotecha, M., Dettlaff-Weglikowska, U., Veeman, W. S. Chem. Phys. Lett., 428(2006) 143-147.
[2] Boden N., Gibb M., Levine Y. K., and Mortimer M. Journal of Magnetic Resonance., 16(1974), 471-482.
[3] Maximilien Levesque, Magali Duvail, Ignacio Pagonabarraga, Daan Frenkel, and Benjamin Rotenberg, Phy. Rev. E, 88(2013), 013308.

Micrometer Lithium Ion Diffusion in a Garnet-Type Cubic $Li_7La_3Zr_2O_{12}$ (LLZO) for Pellet and Powder Samples studied by ^7Li NMR Spectroscopy

Kikuko Hayamizu[a], Shiro Seki[b] and Tomoyuki Haishi[c]

[a]Institute of Applied Physics, University of Tsukuba, Tsukuba 305-8573, Japan; [b]Central Research Institute of Electric Power Industry, Yokosuka 240-0196, Japan; [c]MRTechnology, Inc. 2-1-6 Sengen, Tsukuba 300-0047, Japan.

A garnet-type conductor $Li_7La_3Zr_2O_{12}$ (LLZO) and related materials have been attracted much attention owing to their large ionic conductivity and possible application to all-solid lithium ion batteries with safety. The crystal structures and lithium pathways have been studied by XRD and neutron diffraction methods. $^{6,7}Li$ relaxation times have been measured in the wide ranges of temperature and frequency. These studies are concerned with atomic scale information. Ionic conductivity is one of the most important information for practical application of these materials, and is related to longer-scale pathways where grain boundaries are important issues. The pulsed-gradient spin-echo (PGSE) NMR can provide direct information on ion displacement on time scale of 10^{-2} to 1 s in a micrometer order distance. We have successfully applied the PGSE ^7Li NMR method to measure lithium ion diffusion on sulfide-type lithium solid conductors [1-3], and found the lithium diffusion in the solid conductors is not uniform and distributed in time and space. We observed similar effects in the Li^+ migration in the solid conductor of $Li_{6.6}La_3Zr_{1.6}Ta_{0.4}O_{12}$ [4].

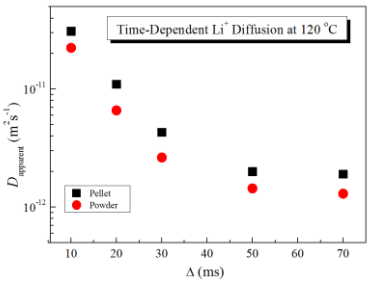

Figure 1. Time-dependent ^7Li diffusion of the cubic LLZO in pellet and powder forms.

In this study, mobile lithium ions in a cubic garnet $Li_7La_3Zr_2O_{12}$, LLZO (Al-stabilized) were studied by ^7Li NMR spectroscopy for pellet and powder samples, the latter of which was ground from the pellet. The lithium diffusion was measured by the PGSE ^7Li NMR method between 70 and 130 ºC by varying the measuring parameters. When the observation time (Δ) was shorter than 20 ms, the echo attenuation showed diffractive diffusion patterns with fast apparent diffusion constant ($D_{apparent}$), indicating that the Li^+ diffusing space is not free and is restricted. For longer Δ, the values of $D_{apparent}$ became gradually slower to approach an equilibrated value as shown in Fig. 1. Also the $D_{apparent}$ values depend on the pulse field gradient (PFG) strength (g) and became smaller as the g became larger. These experimental results strongly suggest the Li^+ ions migrate in polydispersitive manners. One-dimensional image profiles (Fig. 2) for the mobile Li^+ of the pellet increased with the increase of temperature. The area intensity of the ^7Li images showed a good correspondence to the number of Li^+ carrier ions.

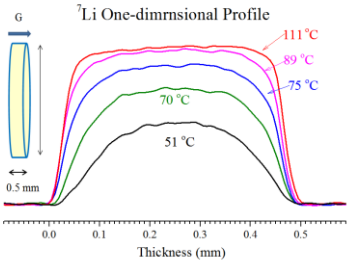

Figure 2. ^7Li one-dimensional profiles of a LLZO plate of diameter 3mm and thickness 0.5 mm measured from 51 to 111 ºC.

References

[1] K. Hayamizu, Y. Aihara, Solid State Ionics, 238 (2013) 1-7.
[2] K. Hayamizu, Y. Aihara, N. Machida, Solid State Ionics 259 (2014) 59–64.
[3] K. Hayamizu, Y. Aihara, T. Watanabe, T. Yamada, S. Ito, N. Machida, Solid State Ionics, 285 (2016) 51-58.
[4] K. Hayamizu, Y. Matsuda, M. Matsui, N. Imanishi, Solid State Nucl. Magn. Reson. 70 (2015) 21-27.

Water transport in Nafion membranes under various conditions studied by NMR

J.-C. Perrin[a,b], A. El Kaddouri[a,b], M. Klein[a,b], S. Leclerc[a,b], J. Dillet[a,b], L. Guendouz[c], O. Lottin[a,b]

[a]Université de Lorraine, LEMTA, UMR7563, Vandoeuvre-lès-Nancy, F-54500, France,[b]CNRS, LEMTA, UMR7563, Vandoeuvre-lès-Nancy, F-54500, France; [c]Institut Jean-Lamour, UMR 7198, CNRS, Université de Lorraine, Vandoeuvre-lès-Nancy, F- 54500, France.

In a Proton Exchanging Membrane Fuel Cell (PEMFC), the membrane is at the heart of the assembly and is the place where electrochemical reactions happen. As water mobility governs these reactions, the Nafion polymer has been studied by NMR techniques (imaging, self diffusion…), but mostly outside a fuel cell. However, in an operating fuel cell, the membrane is exposed to multiple mechanicals constraints (hydration, swelling…). Therefore, we wanted to study the effect of such conditions on the water transport in the polymer.

Three boundary conditions were investigated using different NMR techniques:

- Stretching: Self diffusion experiments were performed on membranes under traction. Using a specially designed traction apparatus, we were able to measure diffusion anisotropy and to compare the results with experiments on membranes stretched outside the spectrometer. We demonstrated that this anisotropy is much higher in the case of in-situ traction in comparison with membranes stretched at high temperature before the experiment [1]. We also developed a simple deformation model of the membrane in order to analyze the experimental results.
- Compression: We used a home-made pressure chamber compatible with NMR experiments which allows us to apply on the membrane a pressure up to 140 bars. We then performed chemical shift, self diffusion and Single Point Imaging (SPI) [2, 3] experiments to see the effect of this pressure on the water transport. First results show that this pressure induces a decrease in water content and a slight reduction off the diffusion coefficient. Unlike stretching experiments, we were not able to observe any diffusion anisotropy.

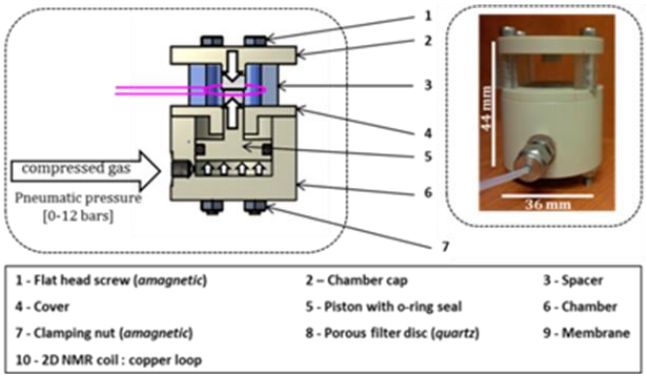

Figure 1 – Pressure chamber designed for MRI.

- Hydration and drying: We inserted the membrane inside a hydration cell inside the magnet. This device allows us to control the air humidity with the possibility to have different conditions on each side of the sample. We then performed SPI experiments across the membrane plane during hydration or drying phases. This allows us to visualize area in the membrane center with lower hydration and to extract drying and hydration kinetics constants from these experiments.

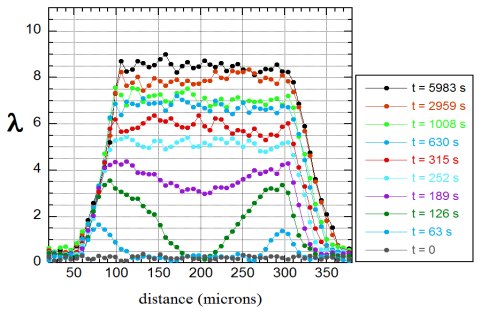

Figure 2 – 1D images of a membrane during hydration

References

[1] M. Klein, J.C. Perrin, S. Leclerc, L. Guendouz, J. Dillet, O. Lottin, Macromolecules. 46 (2013) 9259–9269.
[2] Z. Zhang, A. Marble, B. MacMillan., K. Promislow, J. Martin., H. Wang, B. Balcom, J. Magn. Reson. 194; (2008) 245-253.
[3] M. Klein, J.C. Perrin, S. Leclerc, L. Guendouz, J. Dillet, O. Lottin, ECS Trans. 58 (2013) 283–289.

P50

Low field NMR relaxivity as a fast characterization method for mesoporous alumina

H. Fordsmand[a], M. Lutecki[a]

[a]Haldor Topsoe A/S, Haldor Topsøes Allé 1, DK-2800 Kgs. Lyngby, Denmark

Mesoporous alumina is widely used as catalyst and carrier material in heterogeneous catalysis. It is typically prepared by calcination of nanocrystalline pseudoboehmite into γ- and/or θ-alumnina in a pseudomorph transition. Mesoporous alumina is consequently a refractory material with a very high porosity and specific surface area. In its unique role as both catalyst and support, another important property of mesoporous alumina is the presence of surface hydroxyl groups. The properties of the mesoporous alumina such as for example porosity, pore size, and surface acidity are therefore critical to the performance of the mesoporous alumina either as a carrier or a catalyst. However, traditional characterization techniques such as for example N_2-sorption porosimetry and IR spectroscopy are often lengthy and require careful drying pretreatment because of the high surface area and hygroscopic nature of mesoporous alumina. H_2O low field NMR relaxometry is a fast procedure for probing the interaction of protons imbibed inside pores with the surface of the mesoporous alumina. The preparation procedure is very simple, and the technique is consequently a potent alternative to characterization in production as well as research.

Pseudoboehmite samples were calcined from 400 to 900°C under dry and humid conditions. The calcined samples were subsequently characterized by mercury intrusion porosimetry, N_2 sorption measurements, NH_3-TPD, and LF T_1-T_2 2D NMR relaxometry. A 20 MHz Bruker mq20 LF instrument was used for the NMR relaxometry measurements. T_1 and T_2 surface relaxivities were calculated from relaxometry, surface area, and porosimetry data.

$$\rho = \frac{V}{TS} \tag{1}$$

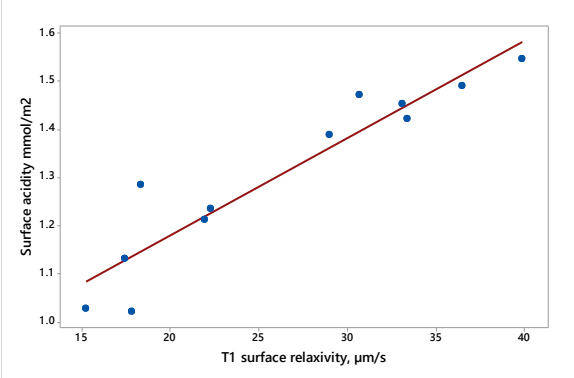

Figure 1. Correlation of NH_3 surface acidity with T_1 surface relaxivity of water for mesoporous alumina.

The results showed that longitudinal surface relaxation correlated strongly with surface acidity suggesting a strong interaction with protonated surface species. Longitudinal relaxometry is consequently a fast tool for probing the acidity of alumina.

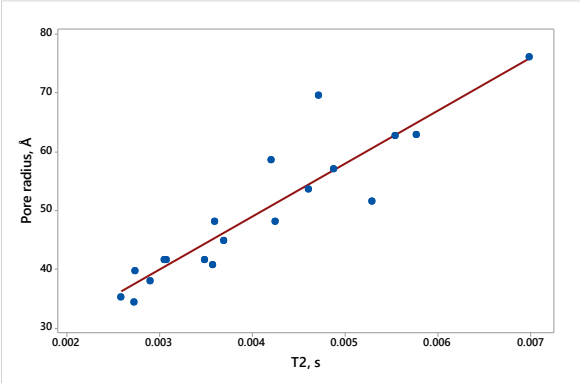

Figure 2. Correlation of mean pore size determined by Hg intrusion with T_2 relaxation constant for water in mesoporous alumina.

Transverse surface relaxation was less influenced by surface properties and correlated best with pore size. T_2 relaxometry is consequently a fast porosimetry method.

$$r = c * T2 \tag{2}$$

Liquid and gas phase velocity measurements of foam using motion-sensitized SPRITE

A. Adair[a], B. Newling[a]

[a]Univ. of New Brunswick, Dept. of Physics, Fredericton, Canada, E3B 5A3.

Although foam is not a porous medium in the traditional sense, its study by MRI shares many of the features typical of magnetic resonance in porous media. In addition, the study of its flow behaviour has applications in porous media research, such as enhanced oil recovery. Common flow measurement techniques are often optical or invasive. Foam, which is optically opaque and physically delicate, is better studied by using a non-optical and non-invasive measurement technique (e.g., magnetic resonance imaging). For this study in particular, the SPRITE (Single Point Ramped Imaging with T_1 Enhancement) MRI pulse sequence (a pure phase-encoding technique) was used to image foam as it flowed through a pipe constriction [1, 2].

The velocity field of the foam flow was measured with a preparation-readout style measurement – PFG (pulsed field gradient) waveforms were used to motion-sensitize the preparation phase and a 3D Conical SPRITE pulse sequence was used to image the sample during the readout phase [3]. 3D PFG-SPRITE measurements have previously been performed on other samples (including liquid flow in rock cores), but not on foam flow [4].

Motion-sensitized SPRITE measurements can suffer from phase errors (and hence velocity errors) due to eddy currents which result due to the rapid amplitude-switching gradient pulses. The pre-equalization method was used to modify the input PFG waveforms, given the system impulse response, so that the sample experienced the desired gradient waveforms [5].

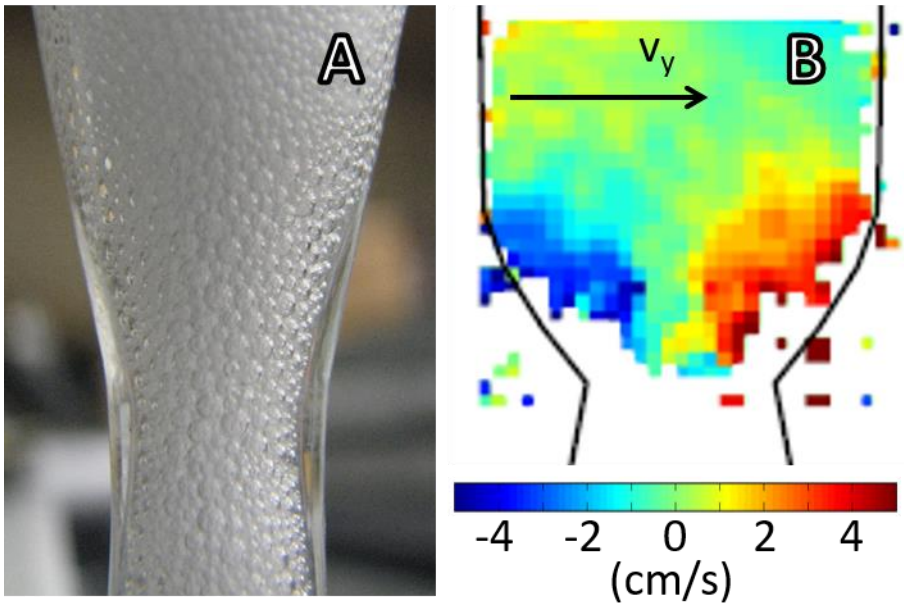

Figure 1 – (A) A photograph of foam as it flows vertically upwards through a pipe constriction. (B) A map of the y-component of velocity for the liquid phase of the foam as it exits from the constriction throat [2].

The foam sample was created by bubbling SF_6 (sulfur hexafluoride) through a water mixture. Therefore, it was possible to measure both the gas and liquid phases of the foam (under identical flow conditions) by switching between hydrogen and fluorine RF probes. A photograph of a typical foam as it flows through the pipe constriction is shown in Fig. 1A. A velocity map (of the y-component) of the liquid phase of the foam as it exits the constriciton throat is shown in Fig. 1B. Motion-sensitizing PFG can be applied to any imaging gradient direction; therefore, all three spatial components of velocity can be measured, if desired. For this experiment, velocity maps of foam flowing through a pipe constriction were created for both the gas and liquid phases. A comparison of the behaviour of the two phases is presented.

References

[1] B. J. Balcom, et al., J. Magn. Reson. Ser. A. 123 (1996) 131-134.
[2] K. Bos, K. G. Wilson, B. Newling, Diffus. Fund. 18 5 (2013) 1-4.
[3] M. Halse, et al., J. Magn. Reson. 165 (2003) 219-229.
[4] K. Romanenko, D. Xiao, B. J. Balcom, J. Magn. Reson. 223 (2012) 120-128.
[5] F. G. Goora, B. G. Colpitts, B. J. Balcom, J. Magn. Reson. 238 (2014) 70-76.

Investigation of the influence of DNP spin probes on the NMR relaxation and diffusion properties of water molecules in Nafion

O. Neudert[a], T. Überrück[b], J. Granwehr [b,c], S. Han[d], S. Stapf[a], B. Blümich[b]

[a]Technical University Ilmenau, Institut für Physik, Unterpörlitzer Straße 38, 98693 Ilmenau; Germany, [b]RWTH Aachen University, Institut für Technische und Makromolekulare Chemie, Worringerweg 1, 52074 Aachen, Germany; [c]Forschungszentrum Jülich, Institut für Energie- und Klimaforschung, Ostring O10, 52425 Jülich, Germany; [d] University of California Santa Barbara, Department of Chemistry and Biochemistry, Santa Barbara, CA 93106, USA.

Although polyelectrolyte membranes (PEMs) have been used in industrial processes for decades, the exact ion-conduction mechanisms are frequently unknown. Especially the sulfonated tetrafluoroetyhlen based polymer Nafion, which is the most common material for PEM fuel cells, is under continuing debate in the scientific community. An in-depth understanding of its properties could lead to an increase in fuel cell efficiency and further optimization of the polymer material itself. In this debate nuclear magnetic resonance (NMR) is employed as a versatile, non-invasive technique to analyse the relaxation and diffusion properties as well as exchange processes of water inside the membrane.

Recently Han *et al.* showed that Overhauser dynamic nuclear polarizitation (ODNP) is able to extend the existing NMR toolbox, giving new insights into the proton conduction pathways by using different TEMPO derivates as paramagnetic spin-probes to highlight certain regions inside the membrane [1]. Although their results are promising, the effect of the spin-probes on the general properties of the membrane is not known in detail and hence the results of ODNP enhanced measurements of PEMs warrant further investigation.

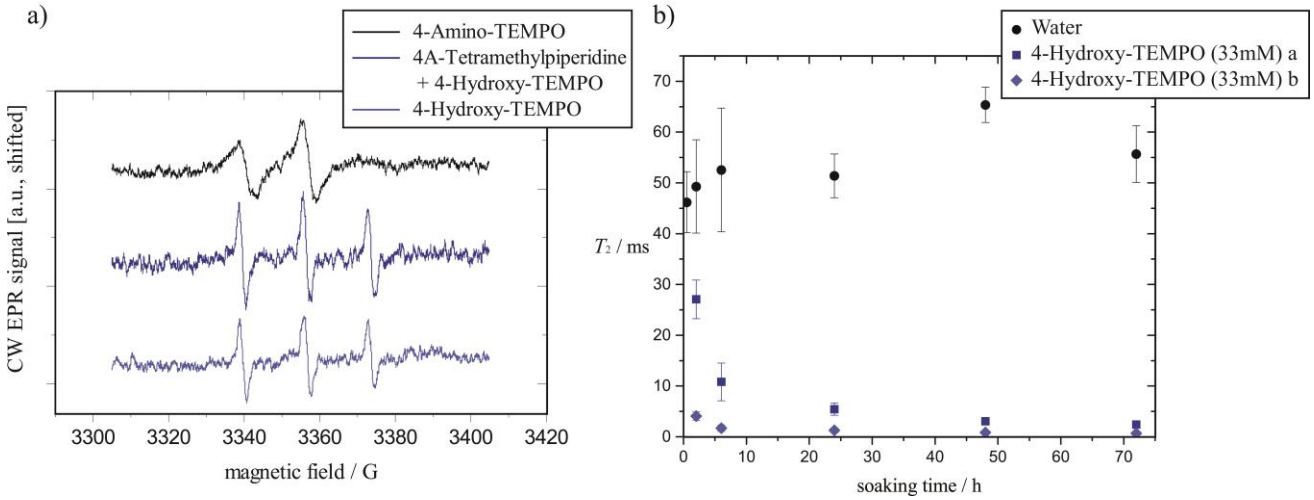

Figure 1 – a) X-band continuous-wave (CW) EPR spectra of nitroxide spin probes in Nafion membrane. The intensity distribution and the linewidths of the three nitroxide resonances provide evidence of different mobility and hence different locations of the TEMPO-derivates inside the membrane. b) Decay of the T_2-relaxation components of water during the equilibration process of a Nafion/4-Hydroxy-TEMPO system. As reference a second T_2 measurement series for Nafion soaked in pure water is shown.

In this work, fully hydrated Nafion membranes were studied, containing the paramagnetic nitroxide molecule TEMPO or one of its derivates (4-Hydroxy-TEMPO, 4-Amino-TEMPO), which have previously been used as spin-probes in the ODNP measurements by Han *et al*. Due to their different functional groups they reside in different molecular environments within the membranes. While 4-Amino-TEMPO associates with the sulfonate groups of Nafion, i.e. is bound to the inner membrane surface, TEMPOL resides within the membrane channels where it shows a considerably higher mobility (Fig. 1a). Both thermal and DNP polarized NMR measurements of the nuclear spin relaxation and diffusion were performed at various magnetic field strengths and different relative radical concentrations. Furthermore, temporal aspects were studied, regarding the equilibration time of the membrane/spin-probe system (Fig. 1b) and the activity of the spin-probes over time. In order to differentiate between paramagnetic and diamagnetic relaxation effects caused by the spin-probes, they were compared to their diamagnetic equivalents Tetramethyl-piperidine, 4-Amino-Tetramethyl-piperidine and 4-Hydroxy-Tetramethyl-piperidine. With the in depth investigation of the para- and diamagnetic effects of DNP spin probes on Nafion this work helps to understand the complex interactions in such systems and will be the basis for future DNP enhanced experiments on PEMs or even fuel cells.

References

[1] J. Song, O.H. Han, S. Han, Nanometer-Scale Water- and Proton-Diffusion Heterogeneities across Water Channels in Polymer Electrolyte Membranes, Angew. Chem. Int. Ed. 54 (**2015**) 3615-3620.

In situ NMR Imaging: A Tool for Characterizing Ion Transport Properties in Li-Ion Battery Electrolyte Solutions

S. Krachkovskiy,[a] J. Bazak,[a] B. Balcom,[b] I. Halalay,[c] G. Goward[a]

[a]Department of Chemistry, McMaster University, Hamilton, Ontario, Canada [b]Department of Physics, University of New Brunswick, New Brunswick, Canada [c]General Motors Global R & D, Warren, Michigan, USA

The operation of battery management systems requires that the transient conditions experienced by a battery cell in electrified vehicle applications can be accurately described through battery modeling [1]. Reliable data on the transport properties of electrolyte solutions, as functions of both salt concentration and temperature, are a prerequisite for accurate electrochemical modeling. Complicating the acquisition of such reliable data is the fact that Li-ion battery (LIB) electrolyte solutions can experience large concentration polarizations during battery operation, due to fairly low values of the Li^+ cation transference number (t^+) and the salt diffusivity (D), particularly during battery operation at high charge/discharge rates or at low temperatures. While modern instrumentation makes specific conductivity and viscosity measurements routine, this is not the case for diffusivity and transference number measurements. In order to determine the latter two transport properties, we undertake *in situ* MRI [2] for the *in-operando* visualisation of the steady-state ion concentration in LIB electrolytes during the application of a constant current. Our results confirm that the concentration gradient developed is proportional to the applied current as described by the diffusion-migration equation under steady-state conditions,

$$-D(c)\frac{\partial c}{\partial x} = -\frac{(1-t^+(c))i}{F} \quad (1)$$

where i is the current density and F is the Faraday constant. Taking into account that $\frac{\partial c}{\partial x}$ is the salt concentration gradient obtained from imaging, the task of determining $t^+(c)$ and $D(c)$ is reduced to measuring the concentration dependence of the diffusivity $D(c)$.

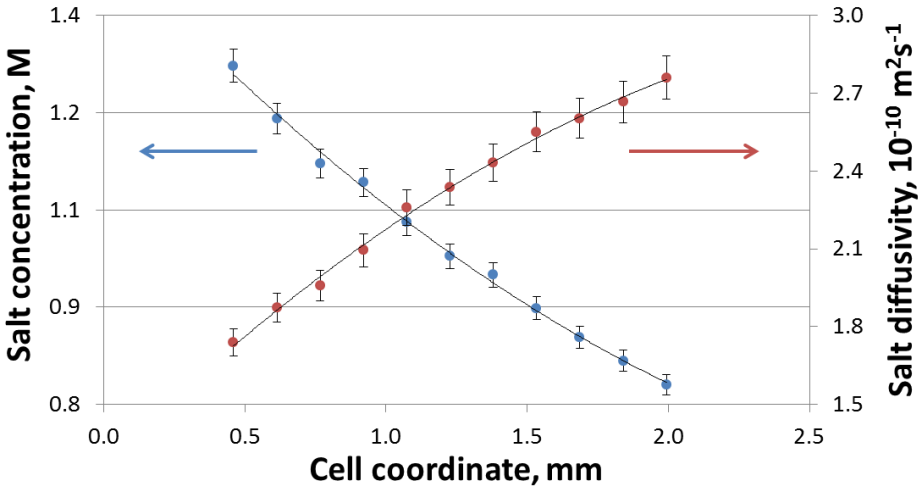

Figure 1 –Steady-state lithium salt concentration (blue) and diffusivity (maroon) profiles in 1 M $LiPF_6$ / EC:DMC (1:1 v/v) at a current density of 9 A/m^2.

By combining a PFG diffusion experiment and MRI, we can determine the salt concentration and the salt diffusivity of the electrolyte during the application of a constant current (Fig. 1). The diffusion coefficient has a significant dependence on the salt concentration, with the values of D measured at opposite ends of the cell varying by more than 60%. The lithium transference number varies less with salt concentration [3]. From the experimentally derived D and concentration profiles one obtains $t^+ = 0.31 \pm 0.03$, by using Eqn. (1).

References

[1] T.R. Tanim, C.D. Rahn, and C.-Y. Wang, *J. Dynamic Syst. Meas. and Control*, **137**, article # 011005 (2014).
[2] C.E. Muir, B.J. Lowry, and B.J. Balcom, *New J. Phys.*, **13**, article # 015005 (2011).
[3] A.K. Sethurajan, S.A. Krachkovskiy, I.C. Halalay, G.R. Goward, and B. Protas, *J. Phys. Chem. B*, **119**, 12238 (2015).

Monitoring Steady State Moisture Distribution during Wick Action in Mortar by MRI

Razieh Enjilela[a], Prisciliano F. de J. Cano-Barrita[a,b], Andrew Komar[c], Andrew Boyd[c], Bruce J. Balcom[a]

[a]MRI Research Center, Department of Physics, University of New Brunswick, Fredericton, New Brunswick, Canada; [b]Instituto Politecnico Nacional-CIIDIR Unidad Oaxaca, Mexico; [c]Department of Civil Engineering and Applied Mechanics, McGill University, Montreal, Canada.

The movement of water or water carrying aggressive ions is one of the leading causes of deterioration of concrete structures built in aggressive environments worldwide. One dimensional Centric Scan SPRITE [1] with T_2^* mapping [2] MRI measurements were undertaken to observe the water content distribution in 10 cm mortar specimens with a staedy state water content due to wicking and evaporation [3]. Bulk FID and T_2^* mapping results show a bi-exponential behavior of the MR signal lifetime T_2^* in all samples, indicating at least two different water populations. The short T_2^* lifetime, assigned to interlayer water, and its associated amplitude are constant along the sample. The long T_2^* lifetime, related to water in the pore space, and its associated amplitude change with local moisture content (Fig. 1).

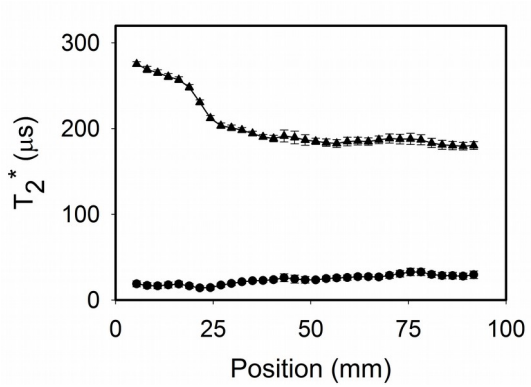

Figure 1 – T_2^* lifetime components versus position for 10 cm mortar sample (w/c = 0.35). Long (▲) and short (●) T_2^* lifetime.

In the steady state the wet front was displaced deeper into the sample as the water to cement (w/c) ratio increased (Fig. 2). The profiles were processed to extract the transport parameters controlling the wick action by assuming a diffusion based model containing a sink term [3] and considering an exponential diffusivity function. There is a good agreement between measured and predicted profiles at moisture contents higher than 0.3 for three mortar samples (w/c = 0.35, 0.40, and 0.45). There seems to be additional mechanism taking place at the wet front besides capillary action at lower moisture content for low water to cement ratios (w/c = 0.35, 0.40).

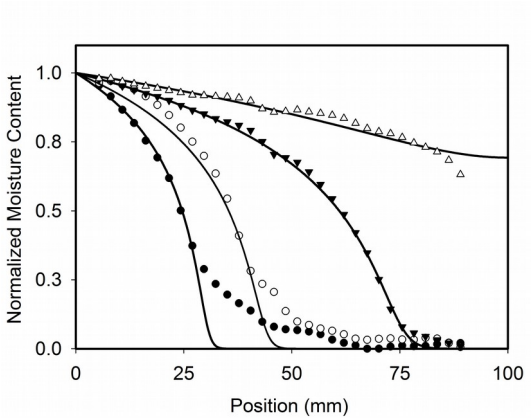

Figure 2 – Experimental and fitted steady state moisture distribution profiles for mortars (●) w/c = 0.35, (○) w/c = 0.40, (▼) w/c = 0.45, and (Δ) w/c = 0.60. The signal intensity (moisture content) was normalized by the highest signal at the wet end for each sample before fitting the experimental data to a literature model [3].

1D Centric scan SPRITE T_2^* mapping was successfully used for quantitative imaging of two water populations in mortar samples during steady state wick action. Processing the profiles permitted extraction of the transport parameters controlling the wicking process.

References

[1] M. Halse, D. J. Goodyear, B. MacMillan, P. Szomolanyi, D. Matheson, B. J. Balcom, J. Magn. Reson. 165 (2003) 219–229.
[2] S. D. Beyea, B. J. Balcom, P. J. Prado, A. R. Cross, C. B. Kennedy, R. L. Armstrong, T. W. Bremner, J. Magn. Reson. 135 (1998) 156–164.
[3]. D. A. Lockington, J. Y. Parlange, M. Lenkopane, Transp. Porous Media. 68 (2007) 29-36

P55

Multidimensional relaxation and diffusion studies of a halogen free ionic liquid

M. A. Javed [a], S. Ahola [a], K. Aslam [a], O. Mankinen [a], A. Filippov [b], F. U. Shah [b], S. Glavatskih [c], O. N. Antzutkin [b], V.-V. Telkki [a]

[a] NMR Research Group, University of Oulu, P.O.Box 3000, FIN-90014 Oulu, Finland; [b] Chemistry of Interfaces, Luleå University of Technology , SE-97187 Luleå Sweden; [c] System and Component Design, KTH Royal Institute of Technology, SE-10044 Stockholm, Sweden.

Halogen-free, boron based ionic liquids (ILs) composed of chelated orthoborate anions and phosphonium cations exhibit good lubrication properties including wear and friction reducing potential, low melting points and a high thermal and hydrolytic stability [1]. Interestingly, one of these ILs, trihexyltetradecylphosphonium bis(mandelato)borate, $[P_{6,6,6,14}]$[BMB], has shown two significantly distinct diffusion coefficients at temperatures below 340 K, which was explained by the presence of two coexisting liquid phases in the IL that maybe correlated with outstanding friction and wear reducing properties of this IL [2].

NMR relaxation and diffusion experiments provide versatile information about the dynamics and structure of substances such as ionic liquids, proteins, polymers, liquid crystals and porous media. They also improve the chemical resolution by separating different components in complex systems without spectral resolution. Multidimensional experiments greatly enhance the chemical resolution and information content in NMR relaxation and diffusion studies [3].

The present variable temperature relaxation and diffusion studies aim to characterize the structural phases of [P6,6,6,14][BMB] IL. The presence of two distinct diffusion components suggests that there are at least two coexisting phases at lower temperatures and a single homogeneous liquid phase at higher temperatures above 340 K. The D-T_2 correlation experiments correlate the signals observed in 1D T_2 and diffusion experiments. The results reveal that the slow diffusing component has shorter relaxation time while fast diffusing component has longer relaxation time. T_2-T_2 and D-D exchange experiments reveal the chemical exchange between the phases. The presence of cross peaks indicates the exchange between the two phases and makes it possible to calculate the exchange rates, eventually revealing the structure of phases.

References

[1] F. U. Shah, S. Glavatskih, D. R. MacFarlane, A. Somers, M. Forsyth, O. N. Antzutkin, *Phys. Chem. Chem. Phys.*, 13, 12865-12873 (2011).
[2] A. V. Filippov, F. U. Shah, M. Taher, S. Glavatskih, O. N. Antzutkin, *Phys. Chem. Chem. Phys*., 15, 9281-9287 (2013).
[3] Y. Q. Song, J. Magn. Reson., 229, 12-24 (2013).

Investigation of CH_4 Motional Behavior in Isoreticular M_2MOF-74

VJ. Witherspoon[a], J. Bachman[a], J. Long[a,c,e], B. Blumich[b], JA. Reimer[c,d]

[a]Department of Biomolecular and Chemical Engineering, Universityc of California, Berkeley, Berkeley, CA , USA; [b]Institute for Technical and Macromolecular Chemistry, RWTH Aachen Universuty, Aachen, Germany; [c]·Department of Chemistry, University of California, Berkeley, Berkeley, Berkeley, CA , USA [d] Environmental Energy Technologies Division, Lawrence Berkeley National Laboratory, Berkeley, Berkeley, CA , USA [e] Materials Sciences Division, Lawrence Berkeley National Laboratory Berkeley, Berkeley, CA , USA

Metal organic frameworks, MOFs, are a novel class of porous materials with proven potential for use as solid adsorbents for gas separation and storage processes. We surmise that it is important to probe the translational motion of gases confined within MOFs in order to better understand interactions between host and adsorbent thereby leading to the rational design of MOFs for specific adsorption applications. MOF adsorbents probed by pulsed field gradient NMR have been theoretically and experimentally related to the transport diffusivities and have led to a better understanding of the translation dynamics taking place in MOFs [1,2], including improving the accuracy of molecular dynamic simulations, and our ability to predict macroscopic transport behaviour [3].

We have investigated structure-property relationship between MOFs and gaseous adsorbents in IR-MOF-74, M_2(Mg,Ni,Zn)dobdc$_4$ through the characterization of the adsorbate diffusive and relaxation behaviour. The ^{1}H 13-Interval Pulsed Field Gradient Stimulated Echo, [4], based pulsed sequence has been applied to the systems using a Bruker Advance 700 MHz spectrometer and the Diff30 Mic5 probe.

For the first time the diffusion and relaxation pressure dependence of CH_4 was observed in IRMOF-74 series. We have observed relaxation and diffusometry phenomenon deviating from the traditional behaviour of CH_4 in porous media.

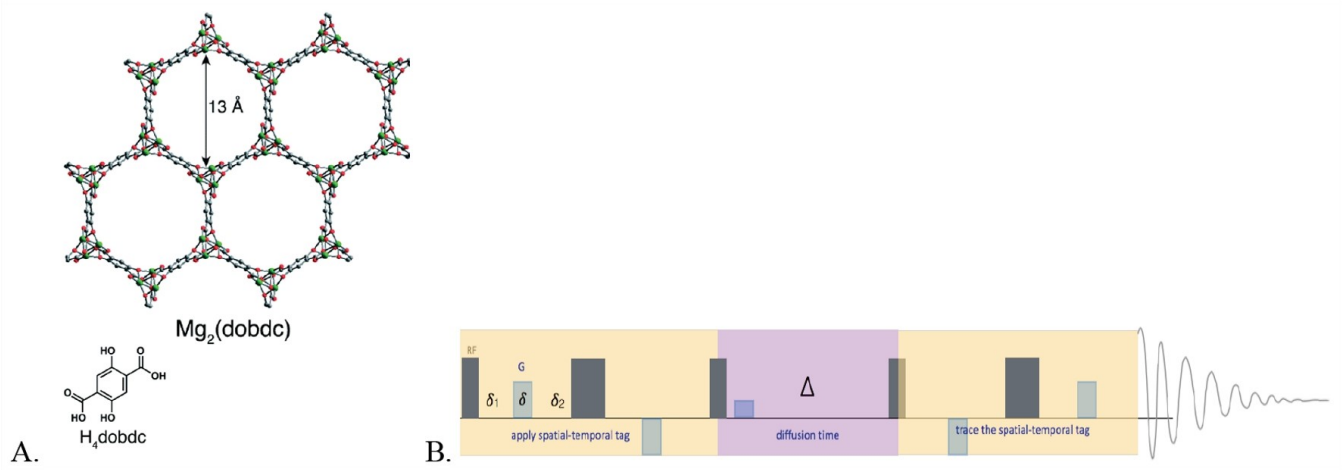

Figure 1. A. Image of M-MO4-74 (M_2dobdc) characterized by hexangonal in plane channels and open metal sites [5]. B. PFG sequence for assessing the diffusion of gases. [4]

References

[1] *LC. Lin, J.Kim, X.Kong, E.Scott,T.McDonald,J.Reimer, B. Smidt, Angew. Chem. Int. Ed. 2013, 52, 4410 –4413*
[2] *F. Stallmach, S.Gröger, V. Kunzel, J. Kärger, O.M. Yaghi, M. Hesse, U. Müller . Angew. Chem. Int. Ed. 2006, 45, 2123 –2126*
[3] *F. Rittig, T.S. Farris, J.M. Zieliinski, AIChE Journal, 2004 50, 3*
[4] *R.M. Cotts, M.J.R. Hoch, T. Sun, and J.T. Markert, Journal of Magnetic Resonance 1989, 833, 252-266*
[5] J.A. Mason, M. Veenstra and J. Long, Evaluating Metal Orgamic Frameworsk for natural gas storage, Octorber 2013

P57

Fast Field Cycling NMR applied to understand dynamics of polypropylene and polyethylene polymers

[a]M. Pasin, [a]G. Ferrante, , [a]R. Steele, [b]A. Marchi Netto, [b]M. Farah, [c]M. Flämig, [c]E.A. Rössler

[a]*Stelar Srl, Via E. Fermi 4, 27035 Mede (PV) Italy;*

[b]*Braskem SA, Via Oeste, lote 5, Passo Raso, Triunfo-RS ZIP 95853-000, Brazil;*

[c]*Universität Bayreuth, D 95440 Bayreuth, Germany.*

Fast Field Cycling NMR (FFC) is a low-field magnetic resonance technique which measures the dependence of the spin-lattice relaxation rate $1/T_1$ on the magnetic field (or equivalently the frequency) over a wide range of magnetic fields (T_1 dispersion or NMRD). The technique has made strong progress in recent years covering now a frequency range of about 10kHz-42MHz. This gives important information on a wide range of molecular motions (dynamics), such as rotation and diffusion, present in a substance or complex mixture.[1,2]

By measuring an NMRD profile, important information on slow motions can be obtained. For example, FFC may be used to efficiently study dynamics of polymers or generally of complex fluids and can be represented in a format which can be compared to classical rheology results, that is, FFC may be interpreted as a molecular rheology technique.[3,4]

Measuring a large temperature range and exploiting frequency-temperature superposition (as done in rheology), master curves are constructed which may cover more than 10 decades in frequency. Thereby the temperature dependence of the dynamics in terms of shift factors or correlation times is revealed. In this study we performed FFC NMR measurements on different kinds of polyethylene (PE) and polypropylene (PP), in both the semi-crystalline phase and in the melt, and compared the results with those of other polymers like polybutadiene (PB) and polypropylene-ethylene (PEP). Rheological measurements on these polymers are reported, too. We explored how FFC NMR can be applied to distinguish between different kinds of polypropylenes and polyethylenes with optimal and non-optimal processing behaviour and rheology and to improve understanding of their dynamics.

References

[1] R. Kimmich, E. Anoardo, *Progress in Nuclear Magnetic Resonance Spectroscopy* **2004**, *44*, 257-320.
[2] R.M. Steele, J-P. Korb, G. Ferrante, S. Bubici, *Magnetic Resonance in Chemistry* **2015**, DOI: 10.1002/mrc.4220.
[3] R. Meier, D. Kruk, E.A. Rössler, ChemPhysChem 14, 3071-3081 (2013)
[4] M. Hofmann, C. Gainaru, B. Cetinkaya, R. Valiullin, N. Fatkullin, E.A. Rössler, *Macromolecules* **2015**, *48*, 7521−7534.

Revealing the porous structure of cement materials via the NMR relaxometry and diffusometry of cyclohexane molecules

A. Bede, C. Badea, I. Ardelean

Technical University of Cluj-Napoca, Department of Physics and Chemistry, 400114, Cluj-Napoca, Romania.

Nuclear magnetic resonance (NMR) relaxometry and diffusometry techniques are widely used for the characterization of porous materials. The NMR relaxometry techniques rely on the proportionality between the relaxation rate and the surface to volume ratio of the investigated pores [1, 2]. Thus, with an appropriate calibration approach they provide us information on the pore size and their distribution. The NMR diffusometry techniques on the other side provide information on the pore size and connectivity without the need of a previous calibration [3,4]. If however, the porous materials are cement based, the NMR techniques are more difficult to be applied due to the internal gradients arising inside these materials as an effect of their magnetic impurity content. The internal gradients influence both the transverse relaxation measurements and the diffusion measurements by altering the effective gradients seen by the nuclear spins. Due to the fact that the internal gradients are determined by the magnetic impurity content of the sample and by the magnetic field strength most NMR studies in the literature are reported on white cement and using low field instruments. Moreover, owing to the natural presence of water inside cement materials most NMR relaxation and diffusion refer to water molecules and saturated conditions.

In our investigations we extend the studies on cement materials to the cyclohexane molecules partially saturating a white cement paste prepared with different water-to-cement ratios between 0.4 and 0.7 respectively. The cyclohexane was chosen as filing liquid due to its nonpolar (aprotic) molecules which experience weaker interactions with the surface containing OH groups [2] and thus providing longer relaxation times. The transverse relaxation measurements were performed using the well-known CPMG pulse sequence with an echo time interval of 0.1 ms [4, 5].

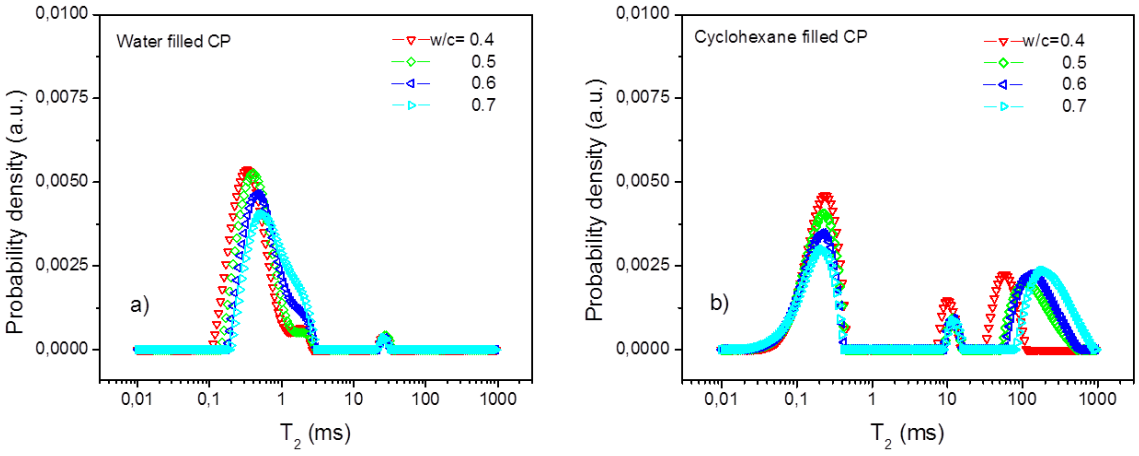

Figure 1 – Relaxation time distribution of liquid water (a) and cyclohexane (b) molecules confined inside a hydrated cement paste after 1 year of hydration. The cement paste (CP) was prepared at different water-to-cement ratios (between 0.4 and 0.7) as indicated on the figure. The first peak corresponds to the intra-C-S-H pores, the second to the inter-C-S-H pores and the third to the capillary pores respectively [5].

Figure 1 shows the relaxation time distributions of water (Fig.1a) and cyclohexane (Fig.1b) molecules confined inside cement paste pores. It is observed a better distinction between the different pore reservoirs for the cyclohexane filled samples as compared with the water filled ones. It is also observed that the intra-C-S-H pores remain saturated with water originating in the preparation approach while the inter-C-S-H and capillary pores are filled by cyclohexane. The relaxation studies on cyclohexane molecules clearly demonstrate an increase in the size of the capillary pores by increasing water-to-cement ratio from 0.4 to 0.7. Under the same conditions the size of inter-C-S-H pores remains unaffected. The increase in the pore size introduced by water-to-cement ratio could be also demonstrated by the diffusion measurements which further revealed a decrease in the tortuosity. In the case of cement paste containing nano-SiO_2 particles the NMR relaxation studies on cyclohexane molecules has also clearly estabilished the relationship between the size of capillary pores and the amount of nanoparticles.

References

[1] P.F. Faure, S. Rodts, Magn. Reson. Imaging. 26 (2008) 1183–1196.
[2] J.-P. Korb, Curr. Opin. Colloid Interface Sci. 14 (2009) 192–202.
[3] I. Ardelean, R. Kimmich, Annu. Rep. NMR Spectro.49 (2003) 45-115.
[4] A. Pop, I. Ardelean, Cem. Concr. Res. 77 (2015) 76–81.
[5] P. McDonald, V. Rodin, A. Valori, Cem. Concr. Res. 40 (2010) 1656–1663.

A COMPUTATIONAL APPROACH FOR UNDERSTANDING NUCLEAR SPIN DIFFUSION IN POROUS MEDIA

E. Lucas-Oliveira[a], A. G. Araújo-Ferreira[a], W. A. Trevisan[a,b], M. N. D'Eurydice[a,c], C. A. Fortulan[d], T. J. Bonagamba[a]

[a]São Carlos Institute of Physics, University of São Paulo, PO Box 369, 13560-970, São Carlos, SP, Brazil. [b]CENPES-Petrobras, 21941-915, Rio de Janeiro, RJ, Brazil. [c]School of Chemical and Physical Sciences - Victoria University of Wellington, PO Box 600, Wellington, New Zealand (current address). [d]São Carlos School of Engineering, University of São Paulo, PO Box 359, 13560-970, São Carlos, SP, Brazil.

Over the past two decades, with the advent of Exchange NMR techniques, it became necessary to correlate the observed results with the material microstructure, composition and molecular fluid dynamics. Since this requires specific boundary conditions for solving the diffusion equation, the theoretical solution is restricted to some specific models. For more complex cases, computational physics methods are often required to simulate the evolution of the Exchange NMR signal resulting from molecular dynamics within the porous matrix.[1,2]

The main equation that associates longitudinal (T_1) and transverse (T_2) relaxation time distributions with the pore sizes was identified analytically by Brownstein & Tarr for some special geometries. Since then, three diffusion regimes were defined: slow, intermediate and fast. The correct identification of these regimes is important, as there is a clear relationship between relaxation time and pore size for a system in the fast diffusion regime.[2]

Herein, the simulations were performed using random walk to describe the dynamics of the water molecules within a porous matrix. The NMR signal contributions are calculated taking into account the interactions of the nuclei with the pore walls and among themselves. To preserve the complexity of translational diffusion through the sample microstructures, 3D X-ray micro-CT images (μCT) were acquired to represent the digital porous media.[3]

Classic and sophisticated NMR experiments can be reproduced by the developed software, such as CPMG, Inversion-Recovery, and Exchange. For example, the simulation of T_2 distributions measured by CPMG for special pore geometries provides pore size distributions in good agreement with the theory proposed by Brownstein & Tarr.

Figure 1 describes some simulated experiments**. Figure 1(a)** shows the simulated and experimental data observed for the T_1xT_2 correlation experiment, obtained from a synthetic alumina porous medium.[4] This synthetic porous medium has three different pores sizes, ranging from 100 nm to 100 μm orders of magnitude, since the digital data was obtained with μCT resolution over 1-μm resolution, only pores sizes higher than μm scale were detected. Due to this reason, just two pore sizes show up from simulation.

One of the most important parameters estimated from these simulations is the surface relaxivity ρ_{eff}, defined by $1/T_2 = \rho_{eff}(S/V)$, in which S/V is the pore surface to volume ratio and $\rho_{eff} = \rho_1 + \rho_2$, where ρ_1 and ρ_2 are the longitudinal and transverse surface relaxivities, respectively.[3] To estimate the surface relaxivity from simulations we used, as reference, the longer relaxation times, because the μCT image precision for the larger pores is higher. We found $\rho_{eff} = 17$ μm/s for the synthetic alumina and with this parameter the pore size distribution was calculated. The T_1xT_2 correlation reveals that T_1/T_2 ratio is not constant and increases for shorter times. This is a consequence of comparable bulk and surface relaxations for the larger pores, whereas surface relaxation dominates for smaller pore scales.

Figure 1(b) illustrates the simulation of a T_2xT_2 Exchange experiment. In order to evaluate the program, an artificial digital porous medium with two distinct regions was constructed. This porous medium consists of a centered sphere connected with a mesh of smaller pores. The exchange between sites can be characterized by exchange rates k_{ij} and the equilibrium of detailed balance, $\boldsymbol{M}_i k_{ij} = \boldsymbol{M}_j k_{ji}$. From the simulation of the T_2xT_2 Exchange experiment, k_{ij} and k_{ji} rates were calculated as a function of the total magnetization of the smaller pores. Results confirm that detailed balance is preserved.[4,5]

The obtained results, in a good agreement with the standard models, indicate the potential of computational physics in the analyses of the NMR in complex porous materials.

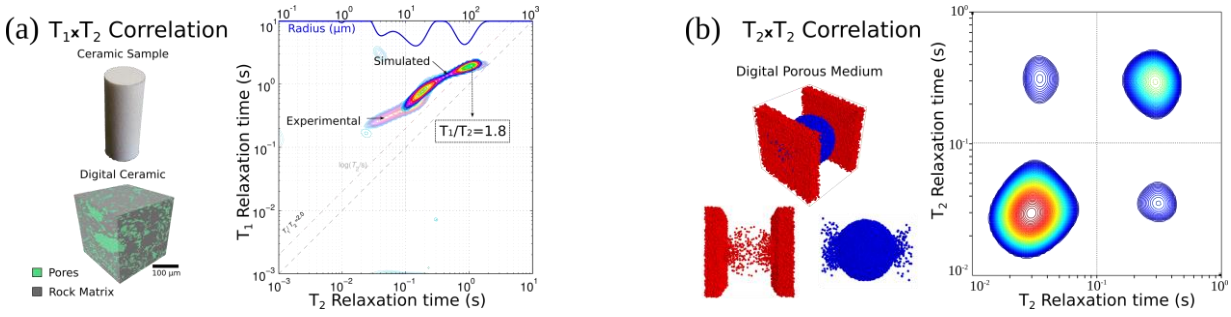

Figure 1 - (a) The digital porous medium reconstructed by μCT images, represents 1mm^3 of the synthetic ceramic sample (left hand side). The simulated data represents the evolution of 10^6 particles. With the experimental data, we found the T_1/T_2 ratio for the larger pores and this reference condition allowed estimating $\rho_{eff} = 17$ μm/s and, consequently, $\rho_1 = 6$ and $\rho_2 = 11$ μm/s. (b) Digital porous medium designed for simulation (left hand side). It shows the particle distribution after 100 ms mixing time. The exchange process appears on the map as correlation peaks (non-diagonal).

References

[1] Y.-Q. Song, Magnetic resonance of porous media (MRPM): A perspective. Journal of Magnetic Resonance 229 (2013) 12-24.
[2] K.R. Brownstein, C. Tarr, Importance of classical diffusion in NMR studies of water in biological cells. Physical Review A 19 (1979) 2446.
[3] C.H. Arns, T. AlGhamdi, J.-Y. Arns, Numerical analysis of nuclear magnetic resonance relaxation–diffusion responses of sedimentary rock. New Journal of Physics 13 (2011) 015004.
[4] M.N. D'Eurydice, E.T. Montrazi, C.A. Fortulan, T.J. Bonagamba, T_2-filtered T_2-T_2 Exchange NMR. Submitted to Journal of Chemical Physics.
[5] R. Dortch, R. Horch, M. Does, Development, simulation, and validation of NMR relaxation-based exchange measurements. The Journal of chemical physics 131 (2009) 164502.

T_2-Encoded Fast-Field-Cycling Relaxometry

O. Neudert[a], C. Mattea[a], S. Stapf[a]

[a]Ilmenau University of Technology, Institute of Physics, PO Box 100565, 98684 Ilmenau, Germany.

Fast-Field-Cycling (FFC) NMR relaxometry, which employs fast electronic switching of the current in an electromagnet, is an unparalleled technology that enables magnetic-field dependent measurements of nuclear spin-lattice relaxation times as short as 1ms over a broad range of magnetic field strengths, typically between 50 µT and 1 T. An essential limitation of the technique, however, lies in the limited homogeneity and stability of the acquisition field strength, which prohibits spectrally-resolved detection of the NMR signal. The lack of spectral resolution occasionally leads to an overlap of different signal contributions which may complicate the interpretation of relaxation data in systems with multiple components. Multi-exponential T_1 relaxation data analysis or Laplace Inversion can be used to approach this problem. However, these methods usually require excellent data quality, especially when more than 2 components are present and/or when relaxation times are very similar.

In this contribution, the feasibility of spin-spin relaxation time measurements at the acquisition field strength (392 mT) of a commercial FFC relaxometer (STELAR Spinmaster FFC2000) was investigated. For this purpose, CPMG-based acquisition schemes acquiring one data point per echo were tested. It was found that by using very short echo times reliable measurements of the spin-spin relaxation time are possible in the range of 0.5 ms to 200 ms (figure 1). Based on these findings, a two-dimensional method was implemented, which combines relaxation field-dependent T_1 measurements with CPMG acquisition at the fixed detection field. A multiexponential analysis of the CPMG signal decay was used to extract T_1 relaxation recovery curves for each component, which were fitted individually using a monoexponential model. Thereby advantage is taken of the spin-spin relaxation contrast to distinguish different signal components and to extract spin-lattice relaxation dispersion curves for each of them.

A combination of three water-filled controlled pore glass samples with different pore sizes was used to test the method. All three components were distinguished successfully using the two-dimensional T_2-encoded FFC relaxometry approach, reproducing reference data obtained with single-component samples (figure 2).

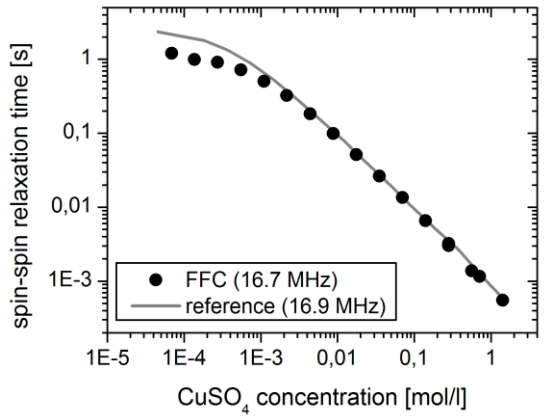

Figure 1 – T_2 measurement of $CuSO_4$-doped water using the FFC relaxometer ("FFC") and a permanent magnet array ("reference").

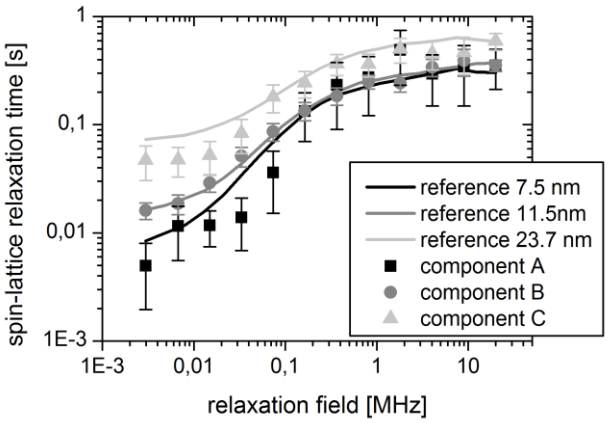

Figure 2 – T_1 relaxation dispersion measurement of three water-filled controlled pore glass materials (lines) and a mixture of them (symbols).

Acknowledgements

This research was funded by the Carl Zeiss Foundation.

Comparison of NMR porosity and water imbibition porosity (WIP): A case study of Paleocene limestone and associated rocks from Eastern Dahomey Basin.

O.B. Olatinsu[a], B. Clennell[b], L. Esteban[b]

[a]Department of Physics, Faculty of Science, University of Lagos, Lagos, Nigeria; [b]CSIRO Energy Oil, Gas and Fuels Program, 26 Dick Perry Avenue, Kensington, 6151, Perth, Australia.

This study presents the results of porosity measurement on four representative rock types (limestone, sandstone, shale and glauconite) from eastern Dahomey Basin. Standard magnetization CPMG decay curves were measured with a number of scans ranging from a minimum of 2000 to a maximum of 20,000 scans to achieve a good signal-to-noise ratio of the NMR response [1, 2]. The connected water-filled porosity (ø in %) of the rock was estimated from three methods: (i) NMR proton signal (T_2 total raw amplitude), (ii) integration from the T_2 distribution [3] and (iii) water inhibition porosity (WIP) based on sample mass and volume under dry and saturated conditions (or partially saturated at 52 % relativhumidity).

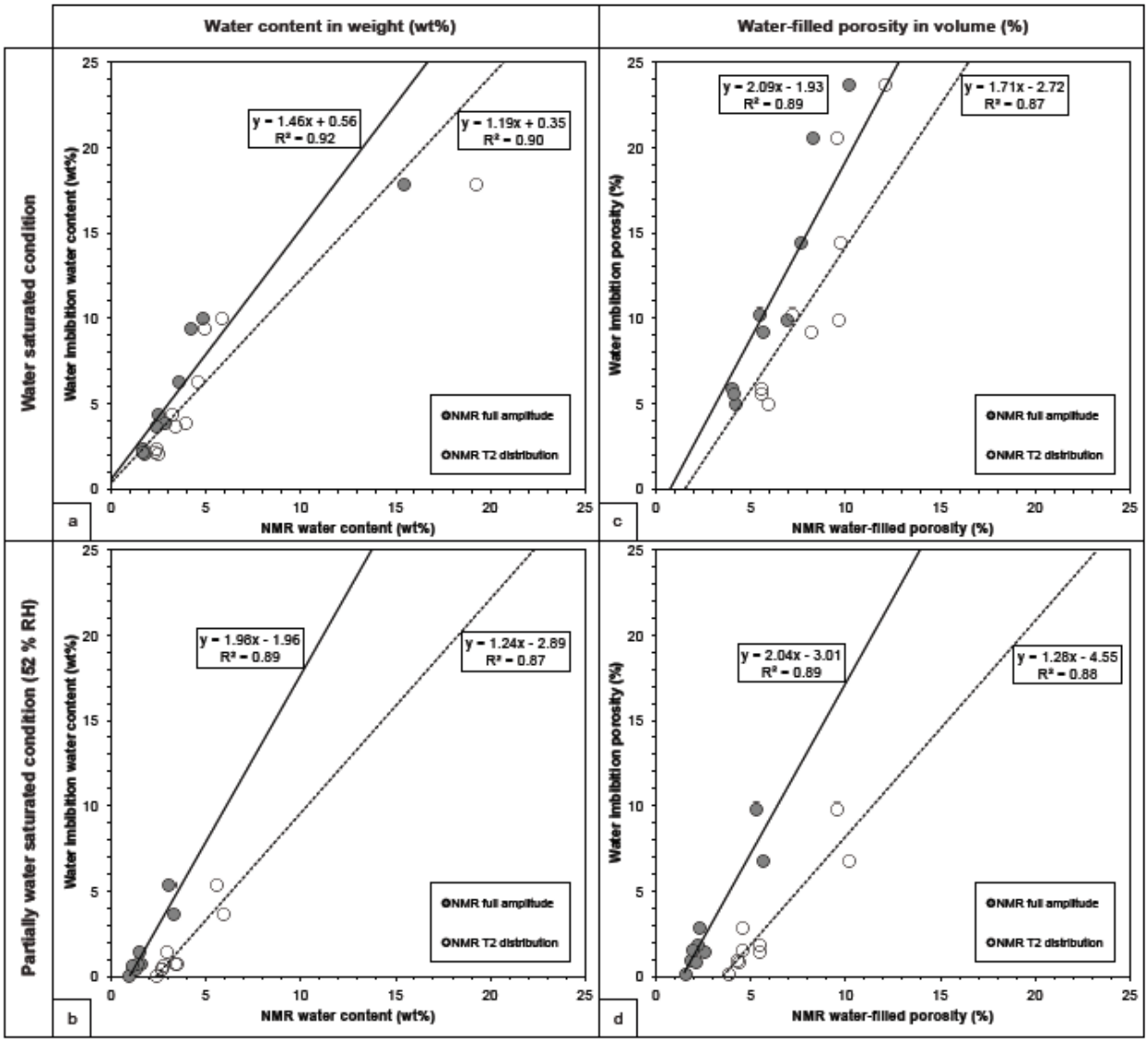

Figure 1 – Water content analysis comparisons between NMR and WIP methods on the sample collection: Dashed linear regression curves from NMR T_2 distribution analysis are closer from a 1 to 1 fitting between NMR and WIP techniques than the black linear regression curves obtained from full NMR amplitude. In all the cases, the linear regression coefficient is excellent around 0.9.

The water content from both techniques, WIP and NMR, show a very high degree of correlation (Fig. 1). Generally for all the rock types studied, the water content and equivalent water-filled porosity from both techniques on the saturated samples follow a trend with a regression factor of approximately 90 %. The water content from NMR derived from T_2 distribution show better agreement with WIP than the water content derived from NMR full amplitude signal. Similar trend is observed on the partially saturated samples under 52 % RH for the water content and equivalent water-filled porosity; although the trend is less obvious as all the dataset is squeezed toward low water content.

References

[1] C . Casieri, F . De Luca,. L Nodari, U. Russo,. C. Terenzi, *Chemical Physics Letters*, 496 (2010), 223-226.
[2] A. Dillinger, L. Esteban.. *Marine and Petroleum Geology*, 57 (2014), 455-469.
[3] T. Chuah, M.Sc Thesis, Rice University, Houston, Texas, USA. (1996), 131p.

Obtaining Surface Relaxivity from NMR-only Data

Z. Luo, J. Paulsen, V. Vembusubramanaian, and Y. Song

Schlumberger-Doll Research, Cambridge, MA.

NMR relaxation (such as T2) has been applied to obtain pore size distribution for many years. T1 and T2 are closely related to the pore size through a parameter called surface relaxivity (ρ). However, this parameter is not typically measured for each sample, and thus the accurate pore size is not known in the right unit. Zielinski et al. [1] have shown that it is possible to use the diffusion-relaxation (DT2) measurement to obtain rho from NMR data alone. This is because both relaxation and diffusion are affected by the presence of pores:

$$\frac{1}{T_2} = \frac{1}{T_{2b}} + \rho\frac{S}{V_p}$$

and

$$\frac{D(\Delta)}{D_0} \approx 1 - \frac{4}{9\sqrt{\pi}}\frac{S}{V_p}\sqrt{D_0\Delta}$$

where Δ is the diffusion time, $D(\Delta)$ is the time dependent diffusion coefficient, S/V_p is the surface-to-volume ratio of the material. T_{2b} is the bulk T2 value. Qualitatively speaking, a comparison of the T2 and D results should allow the determination of ρ. Zielinki et al reports a method that takes into consideration the full T2 and D distributions of the sample.

However, their analysis requires predetermined parameters such as the bulk diffusion coefficient, bulk T2, tortuosity and heterogeneity length scale of the pore structure. Moreover, their restricted diffusion model can be internally inconsistent, potentially failing for samples with wide pore size distribution (PSD) or large pores. To address these issues, we propose a new method based on analyzing multiple DT2 maps with varied diffusion times [2]. With multiple diffusion times, the values of the apparent diffusion coefficient correctly describe a wider range of restricted diffusion behavior in samples with wide PSD and large pores, and so do not require predetermined parameters. Experiments on glass beads packs and rocks are used to validate the new method.

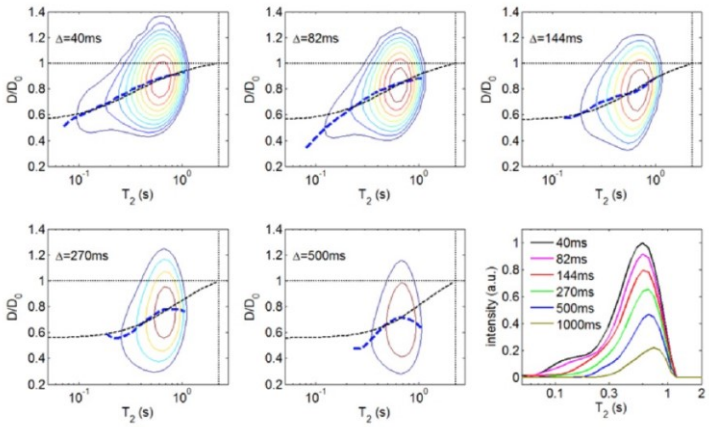

Figure 1. DT2 maps at different diffusion times obtained for a Berea sandstone.

References

[1] L. Zielinski, et al. Restricted Diffusion Effects in Saturation Estimates from 2D Diffusion-Relaxation NMR Maps, SPE Annual Technical Conference and Exhibition, (2010).

[2] Luo, Z.-X., Paulsen, J. L., Song, Y.-Q. (2015). Robust determination of surface relaxivity from nuclear magnetic resonance DT2 measurements. J Magn Reson 259(C), 146–152.

Wettability determination of porous media from T1-T2 method

C. Liang[a], L. Z. Xiao[a], C. C. Zhou[b], L. Guo[a], Z. J. Jia[a]

[a]State Key Laboratory of Petroleum Resource and Prospecting, China University of Petroleum, Beijing, China

[b]Research Institute of Petroleum Exploration and Development, Beijing, China

Wettability is a significant factor which influences the distribution of multiphase fluids in reservoir rocks. In paticular wettability evaluation of tight rock is a big challenge because of low permeability and complex pore structure. Wetting behavior is dominated by the basic fluid-solid and fluid-fluid intermolecular forces in the neighborhood of surfaces[1]. The energy exchange between the spin system and the rotational and translational motion of fluid molecules near solid surfaces are measured by NMR relaxation. Therefore NMR method has gradually developed into a powerful tool for rock wettability qualitative and quantitative analysis. The change of wettability can be observed by a shift of oil peak in the T2 spectrum from the bulk T2 distribution of live oil on 1D NMR[2]. Meanwhile D-T2 map is used to wettability interpretation depend on effective surface relaxivities[3].

In this research the wettability index of porous media is estimated from T1-T2 correlation. Three groups of glass beads(diameter = 400-600μm) with different wettabilities were studied. Group A、B、C respectively contained 100% cleaned uncoated glass beads(water-wet)、50% cleaned uncoated glass beads and 50% treated glass beads (oil-wet)、100% treated glass beads. Glass bead media was saturated with distilled water which bulk T2 relaxation is 2.5s. Fig 1 shows that with the number of oil-wet glass beads increasing, T1-T2 distribution shifts to longer relaxation time and T1/T2 value deviates from the line of T1/T2=1. The ratio of T1 and T2 indicates wettability changes. Futhermore the T1-T2 mapping of porous media with different wettabilities were simulated by LBM (Lattice Boltzmann method)[4] in packed-sphere model with two kinds of wetting balls which diameter is 400μm. The simulation results (fig.2) agreed with previous experiments. In conclusion (1) wetting fluids show T1/T2>1;(2) the wettability index can be obtained from the ratio of T1 and T2; (3) mud invasion and crude oil viscosity and other effects may be considered in downhole wettability measurement.

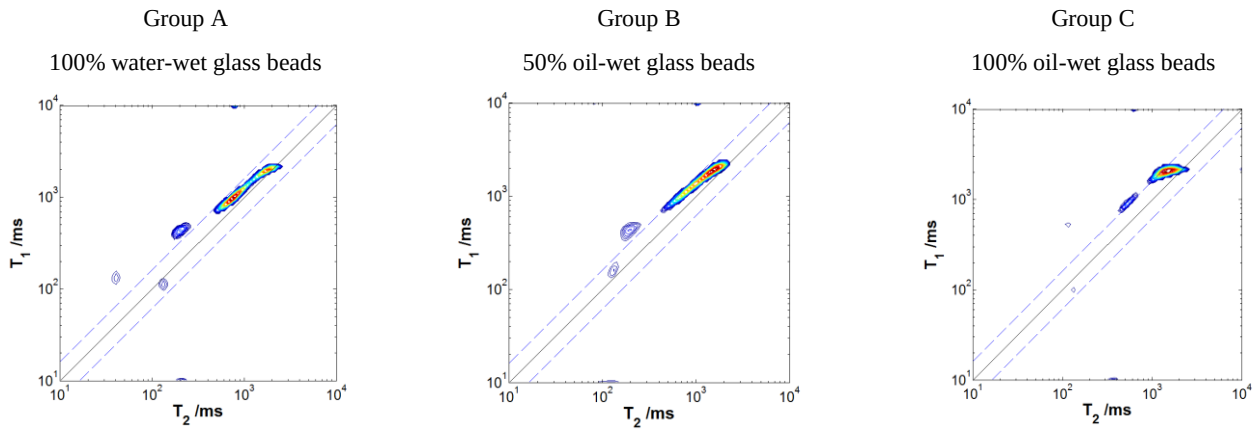

Figure 1 T1-T2 distribution of glass-bead porous media in three groups with different wettabilities

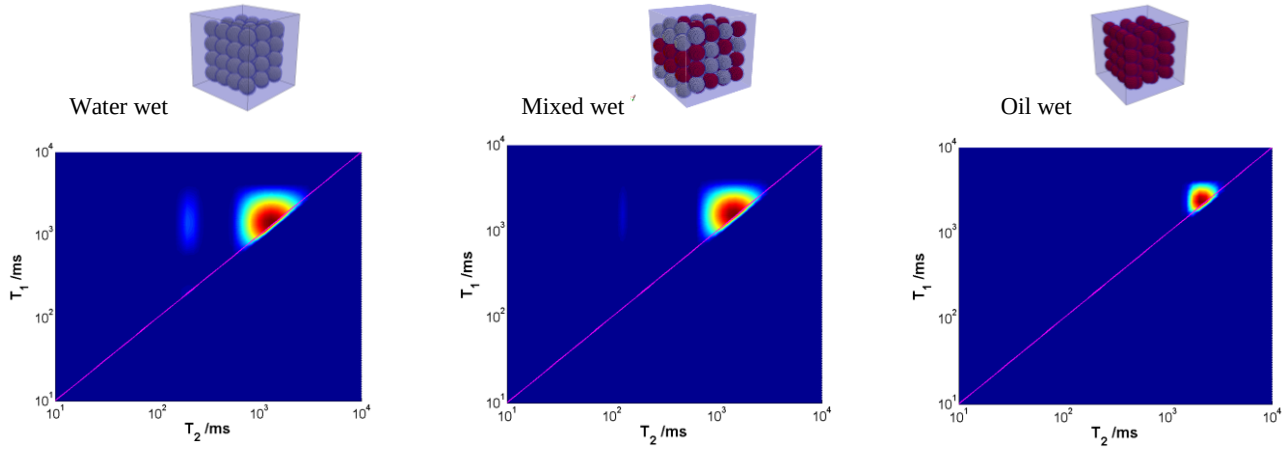

Figure 2 T1-T2 distribution simulated in different wettabilities by LBM method

References

[1] Hirasaki G J. Wettability: fundamentals and surface forces[J]. SPE Formation Evaluation, 1991, 6(02): 217-226.
[2] Abdallah W, Buckley J S, Carnegie A, et al. Fundamentals of wettability[J]. Oilfield Review, 2007, 19(2):44-61.
[3] Minh C C, Crary S, Singer P M, et al. Determination of Wettability from Magnetic Resonance Relaxation and Diffusion Measurements on Fresh-State Cores[C]//SPWLA 56th Annual Logging Symposium. Society of Petrophysicists and Well-Log Analysts, 2015.
[4] Long. Guo, Lizhi. Xiao, Guangzhi. Liao. LBM binary mixtures for simulating NMR measurements. Internatioal conference on magnetic resonance microscopy, 2015.

Free Induction Decay rates in suspensions and water-saturated densely packed particles with varying volume fractions of solid phases

O. Kishenkov, L. Menshikov, A. Maximychev

Moscow Institute of Physics and Technology, 9 Institutskiy per., Dolgoprudny, Moscow Region, 141700, Russian Federation.

Nuclear Magnetic Resonance is used for the assessment of porous media in geophysics and oil exploration [1, 2, 3, 4]. The study of the connection between the geometric properties of porous media and the Free Induction Decay of the liquid phase is a challenge in the field [4]. Varian Inova 500 NMR spectrometer with the proton frequency 500 MHz was used to acquire the Free Induction Decay rates of the samples of two types:

(a) water suspensions of 1.5 μm glass particles with the volume fraction of the solid phase from 0.03 % to 0.32 %;

(b) water saturated densely packed spherical glass particles with the sizes in the range 60–440 μm and water saturated densely packed glass particles with irregular shape and the sizes in the range 95–275 μm (Figure 1).

The images of the samples were acquired with the use of the Quanta FEI setup. It was found that the dependence of the Free Induction Decay rate of the liquid phase of the samples on the square root of the volume fraction of the solid phase of the samples is linear for the square root of the volume fraction of the solid phase in the range from 10^{-2} to almost 1 (Figure 2). A model of the suspension of spherical particles in liquid was proposed and used for the interpretation of the experimental results. It was found that the experimental data and the theoretical data agree within the 50% error.

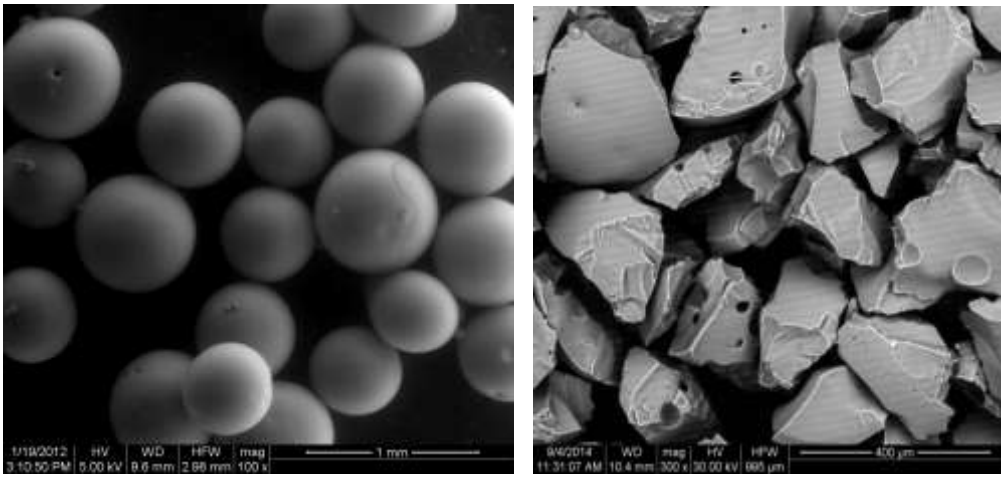

Figure 1 – spherical glass particles and glass particles with irregular shape.

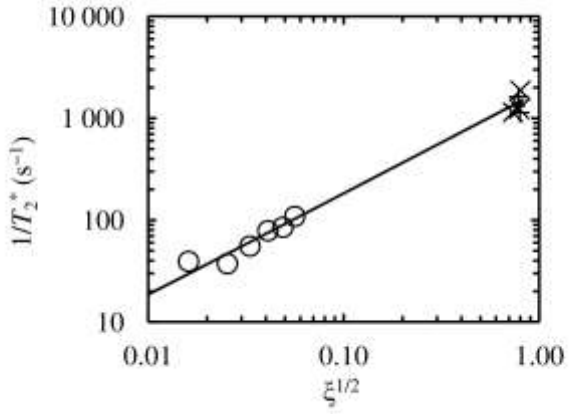

Figure 2 – the dependence of the FID rate $1/T_2^*$ on the square root of the volume fraction of the solid phase of suspensions (○) and water-saturated densely packed glass particles with spherical (+) and irregular (×) shape is linear.

References

[1] B. Blümich Essential NMR for Scientists and Engineers, Springer, Berlin, 2005.
[2] J. Jestin, L. Barre, J Disper Sci Tech. 25 (2004) 341–347.
[3] K. Dunn, G. Bergman Nuclear Magnetic Resonance: Petrophysical and Logging Applications, Pergamon, 2002.
[4] E. Grunewald, R. Knight, Near Surface Geophysics, 9 (2011) 169–178.

Superdiffusion in Porous Media

A.M. Perepukhov[a], D.A. Alexandrov[a], A.V. Maximychev[a], L.I. Menshikov[a,b,c], P.L. Menshikov[b],

[a] Moscow Institute of Physics and Technology, Institutskii per. 9, Dolgoprudny, Moscow Region 141700, Russia; [b]National Research Centre "Kurchatov Institute", 1, Akademika Kurchatova sq., Moscow, 123182, Russia; [c] Northern (Arctic) Federal University, Severnaya Dvina Emb. 17, Arkhangelsk 163002, Russia

For a liquid sample with unrestricted diffusion in a constant magnetic field gradient g, transverse relaxation rate $1/T_2$ for CPMG measurements is increased on a value $1/T_{2D} = 1/3(\tau\gamma g)^2 D$, where γ is magnetogyric ratio, τ is half the echo spacing, and D is the diffusivity. Here the linear dependence of $1/T_2$ on τ is reported, which we observe in porous material with adsorbing properies. It results from the bulk mediated surface diffusion [1].

CPMG data were carried on relaxometer Bruker the Minispec with magnetic field B_0=0.5 T for free water and water filled porous media composed of glass beads with diameters d=57 μm. Transverse relaxation rates were measured both with applied constant magnetic field gradient G = 2 G/cm, and without it (Fig. 1).

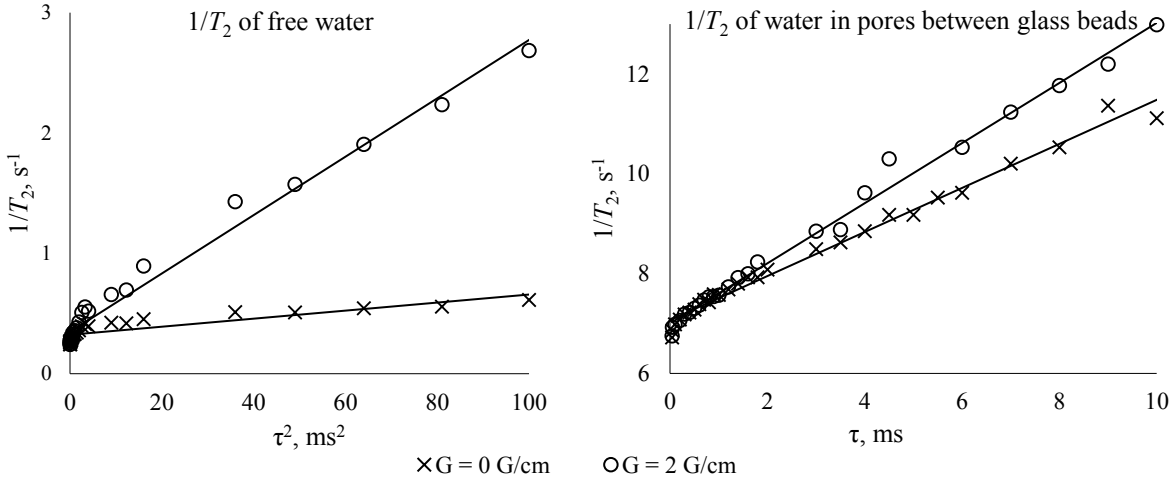

Figure 1 – Results of CPMG measurements. Transverse relaxation rate of protons in free water versus τ^2 (left). Transverse relaxation rate of protons versus τ in the water filled porous material composed of glass beads with diameters d=57 μm (right). Applied constant gradient 2 G/cm is on (○) and off (×).

In frames of the model [1] we derive the expression

$$\frac{1}{T_2} = \frac{1}{T_{20}} + \frac{\pi}{8}\cdot\frac{\tau}{{\tau_0}^2}, \tau_0 = \sqrt{\frac{2V_T\tau_A}{D\gamma g}} \quad (1)$$

that correlates with our observations. Here V_T is thermal velocity of molecules and τ_A is the adsorption time.

The internal magnetic field gradient (G_χ) produced by glass beads is $G_\chi = 2\pi B_0|\Delta\chi|/d \approx 2$ G/cm [2], where $\Delta\chi \approx 4\cdot10^{-7}$ is the difference in susceptibilities of porous material (glass) and pore fluid (water). Due to its random direction the resulting gradient in pores is $g = (G^2+G_\chi^2)^{1/2} \approx 2.8$ G/cm. From here and (1) follows that the gradient applying should lead to the increase of the curve slope in a factor $g/G \approx 1.41$ that agrees with the observed value 1.37.

In [3,4] the inhomogeneity of magnetic field due $\Delta\chi$ was considered in non-adsorbent materials. It was shown that normal (Fickian) diffusion is masked in this case by the quasilinear dependence on τ of the observed transverse relaxation rate. The diffusion displacements of molecules in typical time ~ ms are small compared with the pore sizes in our case. It means that $1/T_{2D} = 1/3(\tau\gamma)^2 < G_\chi^2 > \sim 0.2$ s^{-1}, where the avereging over the pore bulks is produced. From here and Fig.1 follows that effect [3,4] is negligible in our case due to large pore sizes and the anomalous (Levy) diffusion resulting from the mechanism [1] predominates.

References

[1]. O. V. Bychuk, B. O'Shaughnessy, J. Chem. Phys. 101 (1994) 772 - 780
[2]. J. A. Glasel, K. H. Lee, J. Amer. Chem. Soc. 96(1974)970– 978
[3]. R. J. S. Brown, P. Fantazzini, Phys. Rev. B, 47(1993)14823 - 14834
[4]. P. Fantazzini, R. J. S. Brown, J. of Magn. Res. 177(2005) 228 - 235

Particle motion in porous materials during capillary suction

C.J. Kuijpers[a], H.P. Huinink[a], N. Tomozeiu[a,b], O.C.G. Adan[a,c]

[a]Applied Physics Department, Eindhoven University of Technology, PO Box 513, 5600MB Eindhoven, The Netherlands; [b]A&PS, R&D Department, Océ Technology BV, PO Box 101, 5900 MA, Venlo, The Netherlands; [c]Organization of Applied Scientific Research, TNO The Netherlands, P.O. Box 49, 2600 AA Delft, The Netherlands.

For environmental reasons the printing industry is developing water-based inks. These inks are complex mixtures containing among others, water, a co-solvent and particles (pigments). As many printing media are porous, the penetration depth of the particles plays a crucial role in the print quality. In this study we present results on the migration of Fe_2O_3 nanoparticles during capillary suction. The chosen particle is a model system for the pigment particle in ink-jet inks.

We therefore investigate the behavior of water-based particle mixtures that penetrate in a porous material by using NMR imaging and relaxometry complemented with rheology measurements and visual observations. We use Al_2O_3 samples as a well-defined model porous material for printing media to quantify the penetration of each component. To study the effect of pore size we use Al_2O_3 samples with three different pore sizes: 200 nm, 1.1 µm and 16 µm. The smallest being 200 nm, which is similar to the pore size found in a paper coating and is of the same order as the imbibing Fe_2O_3 nanoparticles (30 nm) and the largest much bigger than the particle size at 16 µm. We also study the intermediate regime with an average pore size of 1.1 µm that is similar to the average pore size found in normal printing paper. We investigated the dependency of the penetration depth of Fe_2O_3 particles on the viscosity of the penetrating liquid by adjusting the glycerol concentration. Furthermore, the effect of the pore size on the penetration speed of both liquid and particles as well as the penetration depth of the particles is evaluated.

The penetration depth of the particles and the local concentrations are measured with T_2 relaxation analyses using an in-house developed 1D-NMR imaging system [1]. Both the liquid front and the particle front are measured with a resolution of 0.9 mm. The particle front can be followed due to the signal loss in the vicinity of the Fe_2O_3 particles (Figure 1) due to the shortening of the T_2 [2]. By measuring the T_2 relaxation time locally with a CPMG sequence we can derive the concentration of the particles throughout the sample in every profile.

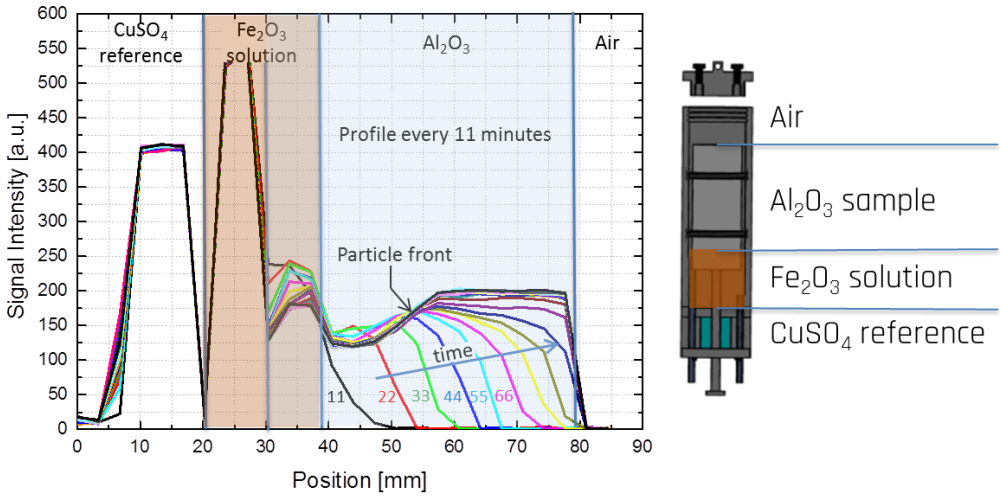

Figure 1 – ^1H profiles of an uptake experiment of 10wt% Fe_2O_3 in H_2O penetrating into 200 nm porous Al_2O_3 (left) and the used measurement geometry (right).

In all of the studied pore sizes we observed a separation of the particle front with respect to the liquid front due to particle media interaction. In the smallest pore size, the particles only penetrate a small distance into the sample due to particle trapping. The particles get stuck to the wall which limits their transport. Remarkably this does not influence the penetration speed of the liquid which progresses in the sample with the same rate it would in the absence of the nanoparticles. Secondly, using visual observations, we observe a very sharp particle front which is also observed in the intermediate pore size case. There we find that the particle front scales with t^{β}, where β has a value between 0.5 and 1. In the 16 µm pore size we still observe a separation of the particle front from the liquid front but the particle front is no longer sharp. The diffuse particle front penetrates at a speed linearly dependent on time (β=1).

References

[1] K. Kopinga, L. Pel, Rev. Sci. Instrum. 65 (1994), 3673-3681
[2] B. Issa, I. M. Obaidat, B. A. Albiss, Y. Haik, Int. J. Mol. Sci. (2013) 21266-21305

Detecting microbially induced calcite precipitation (MICP) in a model well-bore using downhole low-field NMR

Catherine M. Kirkland[a,b], Sam Zanetti[a], Adrienne J. Phillips[a,e], Elliot Grunewald[c], David O. Walsh[c], Sarah L. Codd[a,d],

[a] Montana State University, Center for Biofilm Engineering, PO Box 173980, Bozeman, Montana, USA, 59717. [b] Montana State University, Department of Chemical and Biological Engineering, PO Box 173920, Bozeman, Montana, USA 59717. [c]Vista Clara Inc., 12201 Cyrus Way Ste. 104, Mukilteo, Washington, USA, 98275. [d] Montana State University, Department of Mechanical and Industrial Engineering, Montana State University, PO Box 173800, Bozeman, Montana, USA. [e]Department of Civil Engineering, Montana State University, PO Box 173900, Bozeman, Montana, USA.

Microbially induced calcite precipitation (MICP) has been widely researched in recent years due to its relevance for engineering applications including subsurface barriers for hydrodynamic control and sealing of reservoir cap rocks [1]. Subsurface applications of MICP are inherently difficult to monitor non-destructively and with spatio-temporal resolution. Nuclear magnetic resonance (NMR), however, is commonly used to characterize the pore size distributions, porosity, and permeability of subsurface geologic formations [2]. These are the same physical properties affected by MICP, indicating that NMR well-logging tools may have potential for monitoring subsurface engineering applications of MICP. This investigation used a low-field NMR well-logging probe to monitor MICP in the pore spaces of a sand-filled radial-flow bioreactor. Signal amplitude and T_2 relaxation were measured over an 8-day experimental period to identify the change in signal response due to MICP. No significant changes were recorded during the 3-day control period. Following inoculation with the ureolytic bacteria, *Sporosarcina pasteurii*, and subsequent injections of urea and calcium substrate pulses for 4 days, the NMR measured water content in the reactor decreased by approximately 24%. T_2 relaxation distributions bifurcated from a single mode centered about approximately 785 ms into a very fast decaying population (T_2 less than 10 ms) and a larger population with relaxation times greater than 1000 ms.

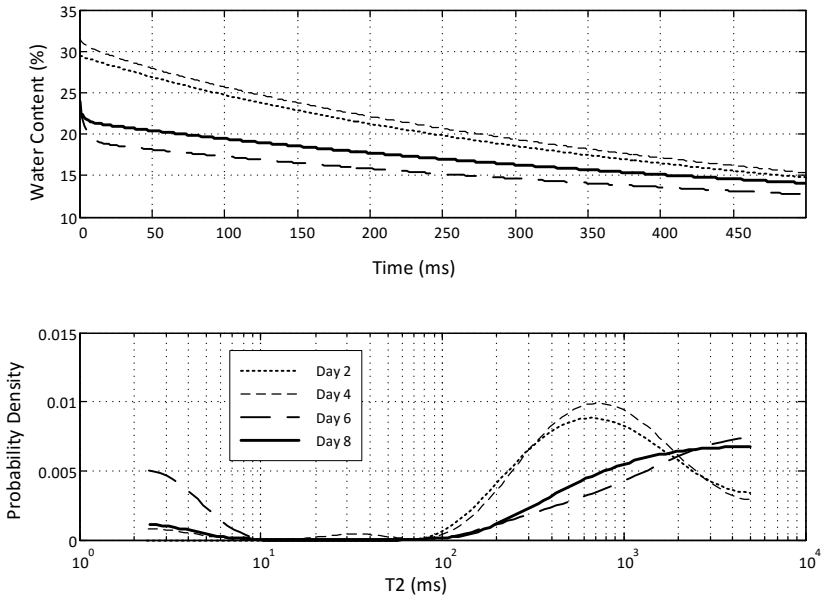

Figure 1 - Selected multi-exponential signal decay curves and T_2 distributions. Day 2 data was collected during the control period prior to inoculation. MICP began on Day 4 and continued to Day 7. The Day 8 data was collected just prior to destructive sampling. The signal amplitude (water content) decreased by approximately 24% over the experimental period while the T2 distribution split into a large population with slow relaxation and a small population with very fast relaxation.

The reduction in signal amplitude indicates that pore water was displaced by calcite precipitation in the voids. Furthermore, the longer T_2 relaxation times suggest that calcite formation on the quartz sand mineral surface reduced the surface relaxivity, ρ, by shielding paramagnetic impurities from the pore fluid. The combination of changes in pore volume and surface minerology accounts for the changes in the T_2 distributions following MICP. Destructive sampling and subsequent analysis with ICP-MS and gravimetric methods confirmed an evenly-distributed porosity reduction of approximately 16% due to calcite precipitation. These results indicate that the low-field NMR well logging probe is sensitive to the physical and chemical changes caused by MICP in a laboratory bioreactor.

References

1. A.J. Phillips, R. Gerlach, E. Lauchnor, A.C. Mitchell, A.B. Cunningham, L. Spangler, Biofouling 6 (2013) 715-733.
2. L.L. Latour, R.L. Kleinberg, P.P. Mitra, C.H. Sotak, J. Magn. Reson., Series A, 1 (1995) 83-91.

P68

Assessment of multiscale hybrid network structures of defibrillated plant fiber dispersions

Gert-Jan Goudappel, Krassimir Velikov, Ruud den Adel, John van Duynhoven

Unilever Discover Vlaardingen, Olivier van Noortlaan 120, 3133 AT Vlaardingen, The Netherlands

When exposed to mechanical defibrillation plant fiber dispersions form a mesoscale porous hybrid network composed of rigid cellulose fibrils and soluble/flexible pectin chains. The energy input during the shear treatment determines to which extent the cell walls are defibrillated resulting in microstructurally different hybrid networks having different macroscopic viscosity and water binding capacity. Understanding these relations is of particular interest for formulation of defibrillated plant fiber dispersions in foods and detergents products.

The objective of this study is to understand the multiscale structure of the hybrid cellulose/pectin networks formed upon defibrillation of citrus fibers dispersions. Quantitative NMR was used to measure in situ the shear-induced release of soluble pectin from citrus fibers. At nm scale level (1-100 nm) small angle X-ray scattering experiments were performed (ID02 beamline ESRF Grenoble) to analyze the packing distances between cellulose elementary fibrils and micro fibrils. ^{19}F diffusion NMR on ^{19}F labelled dendrimers was used to probe network heterogeneity at sub-micron level, while ^{1}H T_2 relaxation NMR was used to look at a scale of tens of µm and provide a quantitative measure for the degree of defibrillation. The critical role of pectin was underpinned by enzymatic pectin degradation experiments.

Chirality and kinetics of a self-assembled Fe_4L_6 metallosupramolecular cage with guests

S. Komulainen,[a] J. Jayapaul,[b] J. Zhu,[a] K. Rissanen,[c] L. Schröder,[b] V.-V. Telkki[a]

[a]NMR Research Group, University of Oulu, P.O.Box 3000, FIN-90014 University of Oulu, Finland; [b] ERC Project BiosensorImaging, Leibniz-Institut für Molekulare Pharmakologie (FMP), 13125 Berlin, Germany; [c]Department of Chemistry, Nanoscience Center, University of Jyväskylä, P. O. Box 35, 40014 Jyväskylä, Finland

In supramolecular chemistry the host-guest systems are one of the most fascinating fields of study. Especially the study of C_2-symmetric bis-bidentate ligands with octahedral metal ions forming tetraedric M_4L_6 cages as potentials hosts for wide range of molecules has gained lots of attention in recent years. As metal ions are essential components of the self-assembly, the M_4L_6 cage structure strongly depends on the coordination geometry of the metal ion. The host structure can encapsulate variable sized guest molecules with different polarity (neutral molecules, gases, anions and cations) and they can be utilized, e.g., in self-sorting of guest mixtures. The chirality of these M_4L_6 cages (Fig. 1B) has been studied intensively as with four metal centers three different diastereomers can form in solution: homochiral ΔΔΔΔ/ΛΛΛΛ(T), heterochiral ΔΔΔΛ/ΛΛΛΔ(C_3) and achiral ΔΔΛΛ/ΛΛΔΔ(S_4). The homochiral T symmetry in which all the metal-to-metal faces are the same leading to minimized strain is the most commonly observed. The careful design of ligand geometry and steric properties can lead to symmetry break and favor of more strained C_3 or S_4 diastereomer. Also the guest molecules change the equilibrium between these diastereomers.

Tetrahedral Fe_4L_6 cage (Fig. 1A) with disulphonic acid substituents is water-soluble and it has many promising applications as a chemically stabilizing molecular container and biosensor cage. [1] Here we report NMR analysis revealing T, C_3 and S_4 diastereomers of the cage, which play a major role in the encapsulation of guest molecules. The encapsulation of cyclohexane at 323 K changed the conformation from T to C_3, having a twisted $C_{3'}$ intermediate conformation during the entering. While C_3 conformation was favored with cyclohexane (85 %), it totally disappeared in the case of Xe guest and only T (75 %) and S_4 (25 %) were present. Competition between these two guest molecules revealed that, when strongly binding cyclohexane was added to the cage solution including Xe, it could not disturb the in-out exchange of xenon. On the other hand, when Xe was added to the cage solution including cyclohexane, Xe could not enter the cage. Thermodynamic analysis of the encapsulation of Xe guest indicated that the process is entropy driven as the enthalpy is positive due the twisting of the cage during Xe entering.

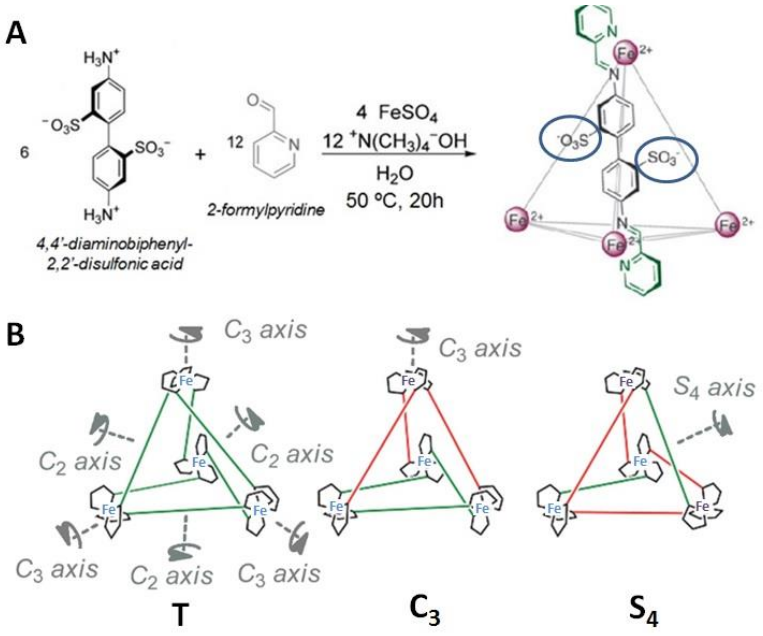

Figure 1 – a) Synthesis of water-soluble tetrahedral Fe_4L_6 cage. b) Three diastereomers of the cage.

References

[1] J. Roukala, J. Zhu, C. Giri, K. Rissanen, P. Lantto, V.-V. Telkki, *J. Am. Chem. Soc.* 2015, 137, 2464–2467

The Mechanism of NMR relaxometry of Tight Porous Media with Multi-scale Digital Rock

G. Liao[a], L. Xiao[a], J wang[a], L. Guo[a], W. Chen[a]

[a] State Key Laboratory of Petroleum Resources and Prospecting, China University of Petroleum, 102249, Beijing, China

With the contrast between the molecule diffusion coefficients and relaxation time of fluids (oil and water), multidimensional NMR method has been considered to be a powerful tool to identify oil and water phases saturated in porous media. However, it is difficult to calculate the fluid properties quantificationally because of the restricted diffusion of fluid molecules and the internal magnetic field gradients caused by the differences of susceptibility between fluid and solid matrix in extrmely tight samples. Multi-scale (milli-micro-nano) X-ray CT imaging technology has been employed to build a model of porous media to study the interface effect between the solid phase and fluid phase. Magnetization transfer occurred between hydrogen nuclear in bound state and movable state is estimated quantificationally. The new fast pulse sequence and multidimensional inversion algorithm are proposed, which is proved with NMR experiments with didderent tight rock.

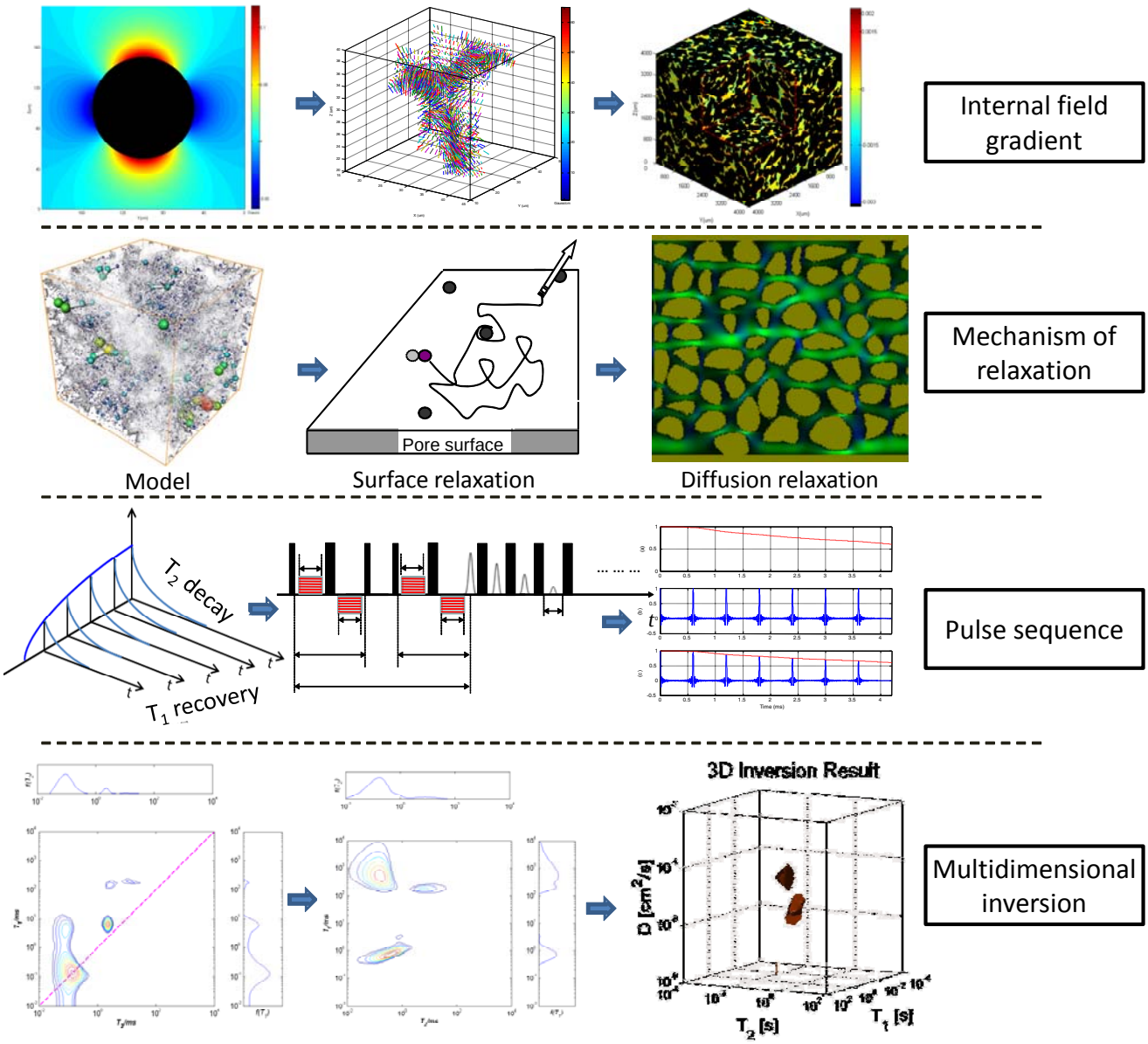

Figure 1 – Caption figure. Caption Figure. Caption figure. Caption Figure. Caption figure. Caption Figure.

Acknowledgement

We gratefully thank the financial supports from CNPC Science and technology innovation foundation (2014D-5006-0304), National Natural Science Foundation of China(Grant No. 41504101), 863 Program"(2013AA064605).

References

[1] Hürlimann M. and Venkataramanan L., Quantitative measurement of two dimensional distribution functions of diffusion and relaxation in grossly inhomogeneous fields. Journal of Magnetic Resonance, 2002. 157(1): 31-42.
[2]Song Y. Q., Using Internal Magnetic Fields to Obtain Pore Size Distributions of Porous Media, Concepts in Magnetic Resonance, 2003, 18A(2): 97-110.
[3]Sun B Q, Dunn K J. A global inversion method for multi-dimensional NMR logging. Journal of Magnetic Resonance, 2005, 172(1): 152-160.
[4] Arns C, Sheppard A, Sok R, et al. NMR Petrophysical Predictions on Digitized Core Images, Petrophysics, 2007, 48(3):202-221

Development of a compact bench-top system for Fast Field Cycling NMR relaxometry in rock cores and large volume samples

M. Polello, R. Rolfi, A. Provera, Y. Xia, G.Ferrante

Stelar, Via E. Fermi 4, 27035 Mede (PV)

Recent NMR works demonstrate that Fast Field Cycling (FFC) and multi-frequency NMR relaxometry offer unique insights for the study of rock cores and heavy crude oils [1-6].

Nevertheless the exploitation of this powerful NMR technique can become very challenging in some applications, not only because of the intrinsic limits of NMR at low field but also because of a lack of a suitable instrumental platform.

Aim of this work is the development of a simple and compact bench-top NMR sytem for Fast Field Cycling NMR relaxometry, capable of measuring T1 dispersion curves from earth field up to 0.2T (8 MHz, 1H Larmor frequency) in large samples and, in particular, in standard 1" rock cores.

With this objective in mind, some novel design concepts and manufacturing technologies have been introduced, in particular in the development of a very compact air-cored low inductivity wide bore electromagnet as well a high speed/high precision power supply and field controller.

Moreover, the measurement of the NMRD profiles at low fields of samples with poor S/N or with low sensitivity hetero-nuclei would usually require a high number of accumulations and, therefore, a long measurement time. This can lead also to a low accuracy and precision of the NMR experiments because of the limited field stability of the magnet and power supply system.

In this work we want to present some technical solution aiming to challenge and mitigate these limitations. In particular:

- reduce the FFC experiment time
- make the investigation of low sensitivity samples easier and faster
- increase measurement accuracy
- allow the acquisition of NMRD profiles in the presence of limited field stability.

References

[1] J.-P. Korb, G. Freiman, B. Nicot, P. Ligneul, *Phys. Rev. E80*. 061601-12 (**2009**)
[2] L. Zielinski, M.D. Hurlimann, Energy & Fuels, 2, 5090-5099 (**2011**)
[3] J.-P. Korb, B. Nicot, A. Louis-Joseph, S. Bubici and G. Ferrante, J. Phys. Chem. C 118, 23212-23218 **(2014)**
[4] L. Benamsili, J.-P. Korb, G. Hamon, A. Louis-Joseph, B. Boussiere, H. Zhou, R.G. Bryant, Energy & Fuels dx.doi.org/10.1021/ef401871h (**2013**)
[5] G. Ferrante, H. Kwak, S. Bubici and J-P. Korb "New insights in water surface dynamics and pore-connectivity in carbonates by using multi-frequency NMR relaxation techniques" at MRPM12- Magnetic resonance on porous media conference, Wellington-NZ
[6] G.Ferrante, S.Sykora *Technical aspects of fast Field Cycling* Advanced in inorganic chemistry vol.57, 405-470 (**2005**)

New instrumental platforms for the exploitation of the field-dependence of T_1, T_2 and 2D correlation spectra T_1-T_2 for probing the dynamics and wettability of petroleum fluids in rock cores and shale oils

Jean-Pierre Korb[1,2], Gianni Ferrante[3], Rebecca Steele[3], and Donald Pooke[4]

[1]*Physique de la Matière Condensée, Ecole Polytechnique-CNRS, 91128 Palaiseau, France*

[2]*Phenix-UMR CNRS UPMC 8234, 75252 Paris, France.*

[3]*Stelar, Via E. Fermi 4, 27035 Mede (PV), Italy*

[4]*HTS-110, 69 Gracefield Road, PO Box 31-310, Lower Hutt 5040, New Zealand*

Recent NMR works demonstrates that Fast Field Cycling (FFC) and multi-frequency NMR relaxometry offer unique insights for the study of rock cores and heavy crude oils [1-5]. Nuclear magnetic relaxation dispersion (NMRD) profiles, acquired through FFC NMR relaxometry by scanning a wide range of magnetic fields, provides unique information on the surface dynamics of confined petroleum fluids in porous rocks, thus information on "wettability" and pore connectivity in carbonates can be obtained [6]. A new method has been introduced for estimating the wettability of rock/oil/brine systems using non-invasive *in situ* NMRD [1, 2]. This technique yields unique information about the extent to which a fluid is dynamically correlated with a solid rock surface. Unlike conventional relaxation studies at fixed magnetic field, this approach directly probes the dynamical surface affinity of fluids which measures the dynamical correlation (microscopic wettability) between diffusive fluids and fixed paramagnetic relaxation sources at the pore surfaces.

The method was first applied to carbonate reservoir rocks [1], and recently applied to probe *in situ* the dynamics and wettability of oil, water and gas trapped in the complex microstructure of shale-oil rocks [3]. This allowed characterization of local wettability at organic and mineral pore surfaces and in turn, the possibility to interpret the *2-D* T_1-T_2 correlation spectra that could be made down-hole, thus providing an invaluable tool for investigating oil and gas recovery in these important porous rocks.

The T_1-distribution dispersion of crude oils as a function of the relaxation field is a powerful new technique to study asphaltene aggregation directly in heavy crude oils of various compositions [4]. In petro-physical contexts, knowledge of the field/frequency dependence of relaxation can improve interpretation of T_1 and T_2 measurements in common oilfield use, assess wettability of water in reservoir rocks and improve characterization of asphaltene aggregates.

Herein, we describe how new FFC instrumentation for standard 10 mm and large diameter samples up to 1.5", in combination with a variable-field (0-5 Tesla) cryogen-free superconducting magnet was developed for rock core analysis and petroleum applications. Characterization of 1" carbonate rock cores and different crude oils, brines and complex mixtures, through acquisition of NMRD profiles from a few kHz up to 40 MHz, was possible. Complex two-dimensional T_1-T_2 experiments were also acquired using a variable field cryogen-free superconducting magnet, for studying a potential exchange of proton magnetization between the various proton pools [6].

References

[1] J.-P. Korb, G. Freiman, B. Nicot, P. Ligneul, *Phys. Rev. E80*. 061601-12 (**2009**)
[2] L. Zielinski, M.D. Hurlimann, Energy & Fuels, 2, 5090-5099 (**2011**)
[3] J.-P. Korb, B. Nicot, A. Louis-Joseph, S. Bubici and G. Ferrante, J. Phys. Chem. C 118, 23212-23218 **(2014)**
[4] J.-P. Korb, A. Louis-Joseph, L. Benamsili, *J. Phys. Chem. B*, *117*, 7002–7014 (**2013**)
[5] L. Benamsili, J.-P. Korb, G. Hamon, A. Louis-Joseph, B. Boussiere, H. Zhou, R.G. Bryant, Energy & Fuels dx.doi.org/10.1021/ef401871h (**2013**)
[6] G. Ferrante, H. Kwak, S. Bubici and J-P. Korb "New insights in water surface dynamics and pore-connectivity in carbonates by using multi-frequency NMR relaxation techniques" at MRPM12- Magnetic resonance on porous media conference, Wellington-NZ

Tortuosity estimate through paramagnetic gas diffusion in multi-phase fluid systems saturating reservoir rock using T_2 (z, t) low-field NMR

I.Shikhov[a] and C.H. Arns[a]

[a] School of Petroleum Engineering , University of New South Wales, Sydney, 2052, Australia

Petrophysical interpretation of ^1H NMR relaxation responses from saturated rocks may be affected by the presence of oxygen dissolved in fluids. Oxygen shortens longitudinal and transverse relaxation times of proton-rich fluids due to the NMR paramagnetic relaxation enhancement (PRE) [1]. This effect may require a thorough correction to avoid misinterpretation of NMR signals. On the other hand, oxygen concentration diffusion resolved in time and space can be employed similarly to standard tracer techniques to study pore connectivity and wettability in multiphase systems.

We utilize relaxation time contrast between air-saturated and oxygen-free fluids to evaluate concentration diffusion rates of oxygen within two fluid phases saturating rock and to estimate the time required to establish equilibrium concentrations. The PRE effect on observed relaxation time is assumed to be a linear sum of oxygen-free bulk fluid relaxation rate and PRE related rate [1], [2] is given by

$$\frac{1}{T_{1,2\ obs}} = \frac{1}{T_{1,2B\ pure}} + \frac{1}{T_{1,2O_2}} \ . \qquad (1)$$

We employ a spatially-resolved T_2 (z, t) experiment [3] to derive a time-dependent oxygen concentration change C_{O2} (z,t) along the fully- and partially-saturated carbonate core plug exposed to air saturated oil at its inlet. This provides an effective mutual diffusion coefficient of oxygen and accordingly a tortuosity estimate. The difference in oxygen solubility in aqueous and oil phases as well as rock wettability state were used to isolate NMR response of oil phase.

The oxygen diffusion-based tortuosity is compared to conductivity-based tortuosity (both experimental and simulated) [4]. The latter is calculated on a full-size (2-in long and 1 inch in diameter) high-resolution micro-tomographic image of Mount Gambier limestone (the same core as in NMR experiments) by solving the stationary Laplace equation for conductivity.

We demonstrated the applicability of 1D relaxation technique to model for evaluation of pore connectivity in partially saturated water-wet rocks and tortuosity estimates per phase.

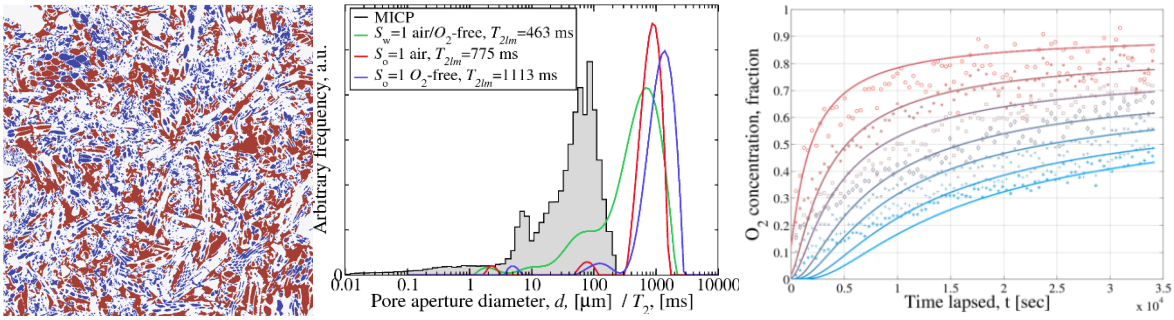

Figure 1 Left: Slice through CT image modified using capillary drainage transformation (CDT) to set fluid distributions assuming fully water-wet rock; So=48.9%; Middle: Comparison of experimental T_2 distributions of a core fully saturated with water or oil in equilibrium with air / oxygen free state (MICP pore-aperture distribution is given for reference); Right: Change of oxygen concentration $C(z, t)$ as normalized fraction of solubility with time at different distances from the core inlet evaluated from the $T_2(z, t)$ experiment for the case of So=100%.

References

[1] G. Chiarotti, G. Cristiani, L. Giulotto, L., Il Nuovo Cimento, 1(5) (1955) 863–873.
[2] S. Chen, G. Zhang, H. Kwak, C.M. Edwards, J. Ren, J. Chen, SPE ATCE, SPE90553 (2004) Houston, TX, USA.
[3] F. Furtado, P. Galvosas, F. Stalmach, U. Roland, J. Kärger, F.-D. Kopinke, Environ. Sci. & Technol., 45 (2011) 8866-8872.
[4] L.J. Klinkenberg, Bull. Geol. Soc. Am., 62 (1951) 559-562.

A new application of ionic liquid in predicting tortuosity factor in hierarchically porous silica monolith by means of PFG NMR

S.Hwang[a], R. Valiullin[a], J. Haase[a] and J. Kärger[a]

[a] University of Leipzig, Faculty of Physics and Geosciences, Linnéstrasse 5, 04103 Leipzig, Germany

Ionics liquids (ILs) are organic salts in the liquid state with low melting points, usually less than 100℃. Due to their novel physicochemical characteristics such as high polarity, good thermal stability and very low vapour pressure, ILs have been used in various fields of catalysis and organic/inorganic syntheses. However, in the present work, we will describe a new application of ILs in predicting tortuosity factors in hierarchically porous materials with a 3D pore network using NMR cryoporometry and diffusometry. The tortuosity factor, τ, can be expressed as [1]:

$$\frac{1}{\tau} = \frac{D_{\text{pore}}}{D_{\text{bulk}}} \tag{1}$$

where τ is the tortuosity, D_{bulk} is the diffusivity in the unperturbed bulk phase and D_{pore} is the effective diffusivity in the pores.

The concept of NMR cryoporometry is to detect a temperature shift of the melting point of a probe liquid under confinement. In the present work we have used 1-Butyl-3-methylimidazolium trifluoromethanesulfonate, which is an IL and also called [BMIM][OTf], as a probe liquid for NMR cryoporometry and investigated how its melting point changes when it is confined in hierarchically porous silica monoliths [2], possessing micro- and/or meso-pores along with a 3D bicontinuous macro-pore network. With the use of Hahn echo sequence, the temperature of a solid-liquid transition on [BMIM][OTf] can be found by measuring the signal intensity of the liquid phase only, i.e. no signal from the solids.

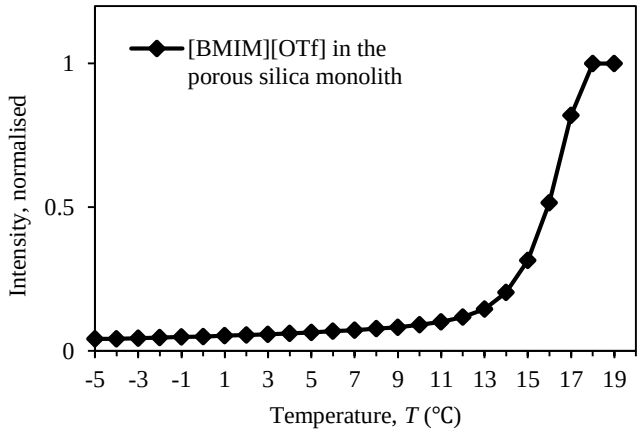

Figure 1 – Melting curve plotted by the normalised intensity of Hahn echo signal of [BMIM][OTf] adsorbed in the meso- and macro-pores of a hierarchically porous silica monolith

[BMIM][OTf] in the bulk phase is known to exhibit the complete melting at approximately 18℃. The [BMIM][OTf] in the silica monolith also gives the melting point of 18℃ as shown in Figure 1. Despite of a relatively large Gibbs-Thomson coefficient, k_{GT}, of 340 K·nm for the [BMIM][OTf], this negligible temperature shift may result from a great proportion of macro-pores present in the silica monolith. However, the long tail at lower temperatures in Figure 1 indicates the presence of meso-pores in which the confined molecules of [BMIM][OTf] exhibit a shift of their melting point towards lower temperatures, thereby remaining in the liquid state even at around 9℃. We now conduct PFG NMR experiments with the 13-interval sequence at 9℃ at which the molecules in the macro-pores are still in the solid state, in order to determine the effective diffusivity in meso-pores, D_{meso}, and then, the tortuosity of the meso-pores, τ_{meso}. This kind of approach using ionic liquids can be very useful in probing hierarchically porous, complex systems and in characterising their textural properties.

References

[1] J. Kärger, D.M. Ruthven, D.N. Theodorou, Diffusion in Nanoporous Materials, Wiley-VCH, Weinheim, 2012
[2] Y. Hu, et al.,Adv. Funct. Mater. 17 (2007) 1873–1878.

Molecular translational dynamics in glycerol/water mixtures by MGSE method

J. Stepisnik [a], C. Mattea [b], S. Stapf [b]

[a] Department of physics, University of Ljubljana, FMF, Institute "Jožef Stefan", Ljubljana, Slovenia, Jadranska 19,1000 Ljubljana; [b] Department of Technical Physics II, TU Ilmenau, P.O. Box 100 565, 98684 Ilmenau, Germany.

The knowledge of translational dynamics is important to understand the mechanism of glycerol/water in maintaining the structure of biological macromolecules and its cryoprotective role in living beings. New experimental insight into molecular interactions in this system could be achieved by the *Modulated Gradient Spin Echo method* (MGSE). This NMR method allows direct observation of the molecular velocity autocorrelation spectrum (VAS). Originally, MGSE was realized with a combination of CPMG RF-train and the interspersed gradient pulses or waveforms. The upper frequency of this technique is limited by the gradient coil induction to about 1 kHz. By applying the CPMG train simultaneously with a steady gradient field, the upper frequency is increased to a few tens of kHz depending on the available strength of magnetic field gradient.

By using the NMR mouse and 100 MHz NMR instrument, the MGSE measurements of glycerol/water solutions provide the VAS in the frequency range from 100 Hz to 10 kHz (figure 1). The results show that VAS of water molecules exhibits features not described by any known model.

While the spectra of glycerol/water mixtures, which are similar to that of water at low glycerol concentration, changes in a completely new form at the higher glycerol concentration, the unusual form of the spectrum can be attributed to frequent contacts between water/water and water/glycerol molecules. Calculation of VAS by using a simple model of coupled Langevin equations gives the spectra that fits well to the experimental data assuming stromg damped harmonic interactions.

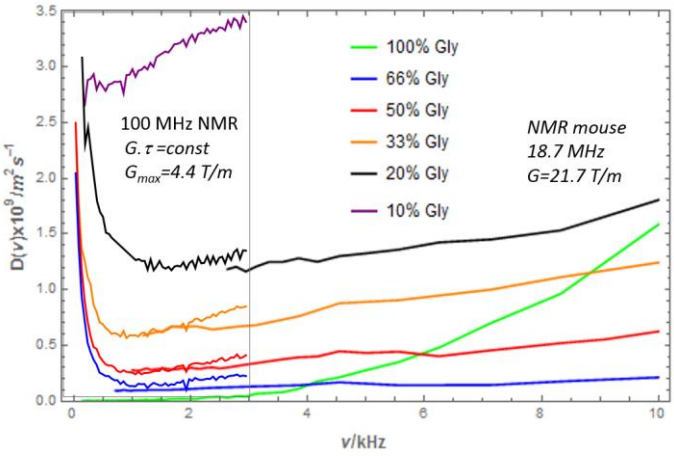

Figure 1 – Velocity autocorrelation spectrum $D(\nu)$ of glycerol/water mixtures at different concentrations.

References

[1] R. Kubo, The fluctuation-dissipation theorem, Rep. Prog. Phys. 29, 1966, 255-84.
[2] J. Stepišnik, Analysis of NMR self-diffusion measurements by density matrix calculation, Physica104B (1981) 350.
[3] P.T. Callaghan, J. Stepišnik, Generalized analysis of motion using magnetic field gradients, Advances in Magnetic and Optical Resonance ed. Waren S. Waren, Vol. 19, p. 324-397, (1996), Academic Press.
[4] J. Stepišnik, S. Lasič, A. Mohorič, I. Serša, A. Sepe, Spectral characterization of diffusion in porous media by the modulated gradient spin echo with CPMG sequence, J. Magn. Reson., 182, (2006) 195.
[5] J. Stepišnik, A. Mohorič, C. Mattea, S. Stapf, I. Serša, Velocity autocorrelation spectra in molten polymer measured by NMR modulated gradient spin-echo, EuroPhysics Letters, 106 (2014) 27007.

NMR diffusometric droplet sizing in nanoemulsions

J.-H. Sommerling[a], A.J. Simon[a], G. Guthausen[a], G. Leneweit[b], H. Nirschl[a]

[a]Institute for Mechanical Process Engineering and Mechanics, Pro²NMR, Karlsruhe Institute of Technology, Straße am Forum 8, 76131 Karlsruhe, Germany; [b]Abnoba GmbH, Hohenzollernstraße 16, 75177 Pforzheim, Germany

Droplet size distributions (DSD) in emulsions can be measured with pulsed field gradient (PFG) nuclear magnetic resonance (NMR) experiments. The basic principal of the method is the differentiation of free and hindered diffusion in the closed drop geometry of emulsions. The use of PFG NMR is of great advantage for emulsions with high turbidity, as it is mostly the case with highly dispersed phase fractions or opaque continuous phase, where optical methods are very limited. The approach is mostly established for emulsions with droplets larger than one micrometer, while data for nanoemulsions is limited. When measured, the signal decay is usually correlated with the diffusion coefficient, as described by Stejskal-Tanner [1]. In the case of DSD, different approaches are known to deduce DSD from the experiments, differing in the mathematical approach with according constraints, limitations and processing speeds.

In this work several modelling approaches were evaluated and compared, one being the model after Murday and Cotts (MC) [2] assuming a lognormal distribution [3] and another being the regularization, using a generalized cross validation (GCV) [4]. The influence of droplet diffusion due to Brownian motion was considered, estimating the droplet movement according to the Stokes-Einstein law. The measured data was analysed applying Stokes-Einstein law extended to a droplet size distribution. Both effects, diffusion of molecules inside the droplets and movement of the whole droplet contribute to the signal decay in a PFG-NMR experiment. In order to identify the strength of contribution several parameters influencing the diffusion were adapted. Overall the effects of droplet movement were investigated by measurements at different temperatures, two defined droplet size distributions and switching continuous and dispersed phase. These investigations allow to distinguish between the effects of droplet movement itself and molecular diffusion inside the droplets, leading to specific contributions to the signal decay.

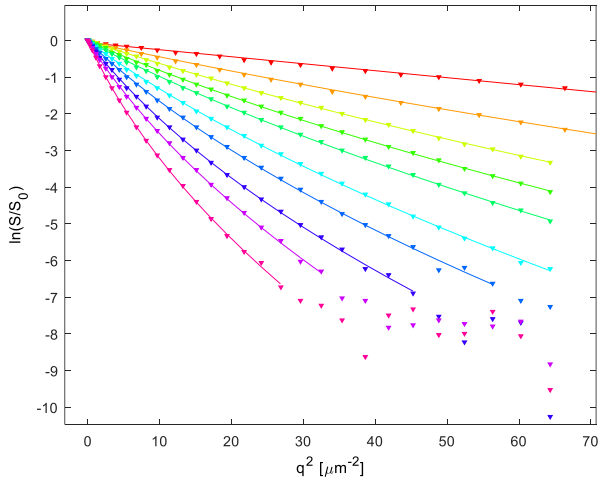

Figure 1 – Signal decay of an emulsion varying the gradient delay Δ visualizing the time dependency due to droplet movement.

Pharmaceutical emulsions containing squalene oil, water and phospholipids or polyglycerin-polyricinoleat (PGPR) as emulsifier were chosen as model system [5]. O/W emulsions with phospholipids are common and can be produced with sizes ranging from several micrometers to 100 nanometers [6, 7]. These emulsions can be diluted for characterisation in laser diffraction or photon correlation spectroscopy. W/O emulsion with the same composition can be stabilized with PGPR, also allowing to produce nanoemulsions.

References

[1] E.O. Stejskal and J.E. Tanner. Spin diffusion measurements: Spin echoes in the presence of a time dependent field gradient. *The Journal of Chemical Physics*, 42(1):288–292, 1965.

[2] J.S. Murday and R.M. Cotts. Self diffusion coefficient of liquid lithium. *The Journal of Chemical Physics*, 48(11):4938–4945, 1968.

[3] K.J Packer and C. Rees. Pulsed nmr studies of restricted diffusion. i. droplet size distributions in emulsions. *Journal of Colloid and Interface Science*, 40(2):206 – 218, 1972.

[4] K.G. Hollingsworth and M.L. Johns. Measurement of emulsion droplet sizes using pfg nmr and regularization methods. *Journal of Colloid and Interface Science*, 258(2):383 – 389, 2003.

[5] L.C. Collins-Gold. Parenteral emulsions for drug delivery. *Advanced Drug Delivery Reviews, 5 (1990) 189-208*, 1990.

[6] Christopher B. Fox, Ryan C. Anderson, Timothy S. Dutill, Yasuyuki Goto, Steven G. Reed, and Thomas S. Vedvick. Monitoring the effects of component structure and source on formulation stability and adjuvant activity of oil-in-water emulsions. *Colloids and Surfaces B: Biointerfaces*, 65(1):98 – 105, 2008.

[7] Peter van Hoogevest and Armin Wendel. The use of natural and synthetic phospholipids as pharmaceutical excipients. *European Journal of Lipid Science and Technology*, 116(9):1088–1107, 2014.

Restricted diffusion and higher order relaxation modes – A combined approach utilizing DT_2 to extract pore-sizes without calibration

M. Müller-Petke[a], R. Dlugosch[a], A. Obert[a,b]

[a]Leibniz Institute for Applied Geophysics, Hannover, Germany; [b]University of Würzburg, Germany.

One of the primary applications of NMR in Geosciences is estimating pore-size distributions (PSD). Generally, two types of experiments can be used; (i) relaxation time measurements (mostly T_2) or (ii) diffusion measurement. Relaxation time data can provide PSDs but calibration is necessary as surface relaxavity (ρ) is typically unknown. Diffusion measurements can yield pore-size information without calibration in case of restricted diffusion, i.e. for small pore-sizes. Further, diffusion measurements commonly provide estimates of mean pore-sizes instead of PSDs.

Recently, approaches have been presented to overcome some of these limitation. A methodology that allows for estimating a mean pore-size and ρ directly from relaxation time measurements without calibration has been presented in [1] in the case of narrow PSDs and large pores. This approach refers to non-fast diffusion conditions that cause higher order relaxation modes (HoRM). Combined diffusion and relaxation time experiments (DT_2) have been used to estimate surface relaxivities [2] and therefore pore-sizes without calibration. The authors proposed an improved physical model to calculate restricted diffusion for broad PSDs. However, the impact of non-fast diffusion is neglected.

We have developed a forward algorithm that allows to calculate DT_2 data including both non-fast diffusion conditions and the improved model for restricted diffusion. This is motivated by (i) accurately modelling the physics for material that contains large pores and (ii) the expectation that restricted diffusion for smaller pores and non-fast diffusion present in larger pores almost perfectly supplement each another when estimating pore-sizes. Consequently, we postulate improved pore-size (and ρ) estimates using this model. To evaluate this postulation, we first defined a complex pore model consisting of four isolated pores (20 µm, 50 µm, 150 µm and 0.5 mm) with different relative intensities (1, 0.1, 0.1, 1). Second, for this pore model we calculated the corresponding DT_2 values using the improved model that includes HoRM (Fig. 1d). Based on these DT_2 values synthetic data is calculated (Fig. 1a). Finally the synthetic data is inverted for a smooth DT_2 distribution (Fig. 1e) as in [2] smooth DT_2 distributions are used to estimate pores-sizes. Even though the data can be well explained (Fig. 1b) by the estimated model, details of the true model are not well resolved (both HoRM and the mid-range pores). It appears plausible to estimate reliable pore-sizes and ρ for the smallest pore (20 µm) as restricted diffusion is present but uncertainties for the largest pore (0.5 mm) will potentially be high as restriction is weak (but needs to be evaluated in more detail) and the two mid-range pores are not captured at all. Thus, even though sucessfully used in [2], smooth inversion appears inappropriate to extract all necessary details, especially HoRM that would help to improve pore-size estimation for larger pores as shown in [1].

In anology to our experience when extracting HoRM from smooth T2 distributions this is, not suprising considering the limited resolution of a smooth inversion. We therefore extended our inversion algorithm from [1] to directly estimate pore-sizes and ρ from DT_2 data without inverting for a smooth distribution. Not unexpectedly, two discrete pores (20µm and 0.4mm) are already sufficient to explain the synthetic data (Fig. 1c). Note, the discrete DT_2 model (Fig. 1f) is a calculated DT_2 distribution from the estimated pore-sizes. We found large pores to be well estimated, thanks to HoRM, but as a mixture of the two largest pores. The small pore is well estimated too, thanks to restricted diffusion. The mid-range pore (150µm) is, still not detected. However, currently this is rather a proof-of-concept and detailed analyses and comparison of uncertainties are necessary. Nevertheless, we expect further improvements using at least two different diffusion observation times.

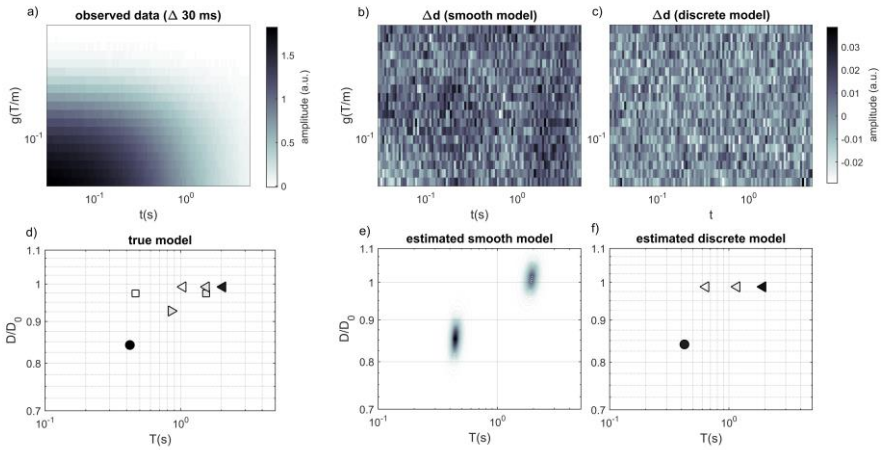

Figure 1 – Synthetic modelling and inversion assuming a multi-pore model. Modelling: pore-sizes [20 - ●, 50 - ▶, 150 - ■, 500 - ◀] µm and 20 µm/s surface relaxivity. Gray scale of the symbols represent the intensity of the DT_2 value. Higher order relaxation modes appear for 150µm and 0.5mm with the symbol for the corresponding pore-size. Measurement paramter: 30ms big delta, 3ms little delta, gradient [0.05-0.5] T/m, 0.5% Gaussian noise.

References

[1] M. Müller-Petke, R. Dlugosch, J. Lehmann-Horn, M. Ronczka, Geophysics 80/3 (2015), D195-D206.
[2] Z.-X. Luo, J. Paulsen, Y.-Q. Song, J. of Mag. Res. 259 (2015), 146 - 152.

Self-diffusion in Polymer Solutions Measured with PFG NMR

Xiaoai Guo[a,d], Esther Laryea[b], Manfred Wilhelm[a], Burkhard Luy[c], Hermann Nirschl[d], Gisela Guthausen[c,d]

[a]Karlsruhe Institute of Technology (KIT), Institute for Chemical Technology and Polymer Chemistry, Karlsruhe, Germany; [b]Karlsruhe Institute of Technology (KIT), Institute for Thermal Process Engineering, Germany; [c]Karlsruhe Institute of Technology (KIT), Institute for Biological Interfaces IBG-4, Karlsruhe, Germany; [d]Karlsruhe Institute of Technology (KIT), Institute for Mechanical Process Engineering and Mechanics, Karlsruhe, Germany.

Polymer size and molecular-weight distribution (MWD) are important parameters in polymer characterisation. DOSY experiments are in principle capable of revealing both the molecular weight and its distribution via the self-diffusion coefficient distribution (DCD). Systematic characterization of polymer solutions and determination of these parameters is essential for an in-depth understanding of the polymeric macromolecular structures and their dynamic and transient properties. In this work PFG-NMR self-diffusion experiments on two different polymers (PS, PMMA in $CDCl_3$) covering a wide range of molecular weights M_w, polydispersities PDI and concentrations C have been performed to study the influence of molecular weight and polydispersity on the diffusion measurement. The acquired NMR (Bruker Avance 200 MHz SWB tomograph equipped with a Diff30 probe with 5 mm inner diameter at 20°C) signal attenuation S is expressed in one model as

$$S(k) = S_0 \int_0^\infty P_G(D) \exp(-kD)\, dD = S_0 (1 + k\sigma_G^2 / D_{mean})^{-D_{mean}^2/\sigma_G^2} \quad (1)$$

where $P_G(D)$ is the gamma distribution function [1] describing the distribution of diffusion coefficient D with the mean value D_{mean} and the width σ_G, k is defined as $k = (\gamma g \delta)^2(\Delta - \delta/3)$, γ is the proton magnetogyric ratio, g is the gradient, δ is the gradient pulse duration and Δ the diffusion time.

Figure 1a shows exemplarily the measured diffusion coefficients for different polymer samples (M_w = 7589 to 263022 g/mol) in $CDCl_3$ at different concentrations ranging from 0.2 wt% to 7.3 wt%. It is seen that the higher M_w and C, the smaller D_{mean}. At concentrations lower than 2 wt% there is almost no significant dependence of the diffusion coefficient on C. Further increase in the concentration leads to the decrease in the diffusion coefficient due to polymer interaction [2]. Moreover, to determine MWD, PDI of the polymer can be related to the DCD (D_{mean}, σ_G) determined from the NMR experiment, given by

$$PDI = \frac{M_w}{M_n} = \frac{\langle M^2 \rangle}{\langle M \rangle^2} = (1 + \sigma_G^2 / D_{mean}^2)^{1/\alpha^2} \quad (2)$$

where α is a scaling parameter [1], which may depend on the properties of polymer and solvent.

Figure 1b illustrates the relation between α and $C{\cdot}M_w$ for the polymers corresponding to those in Fig.1a. It is interesting to find that the scaling parameter α approaches a constant 0.51 ± 0.06 for the polymers (PS, PMMA in $CDCl_3$) studied in the present experiments at the concentration up to 7.3 wt%. This value agrees fairly well with those for other polymers, e.g. α = 0.53 - 0.55 for PEO polymers in D_2O [3].

The present study has confirmed that PFG NMR can be used to determine the MWD from the DCD by analyzing the acquired NMR signal decay with a gamma distribution model as well as the carefully predetermined scaling parameter. Above the critical concentration, PFG-NMR gives additional insight into the polymer interactions. Data processing will be compared with other models, e.g. the tailored norm regularisation method [4].

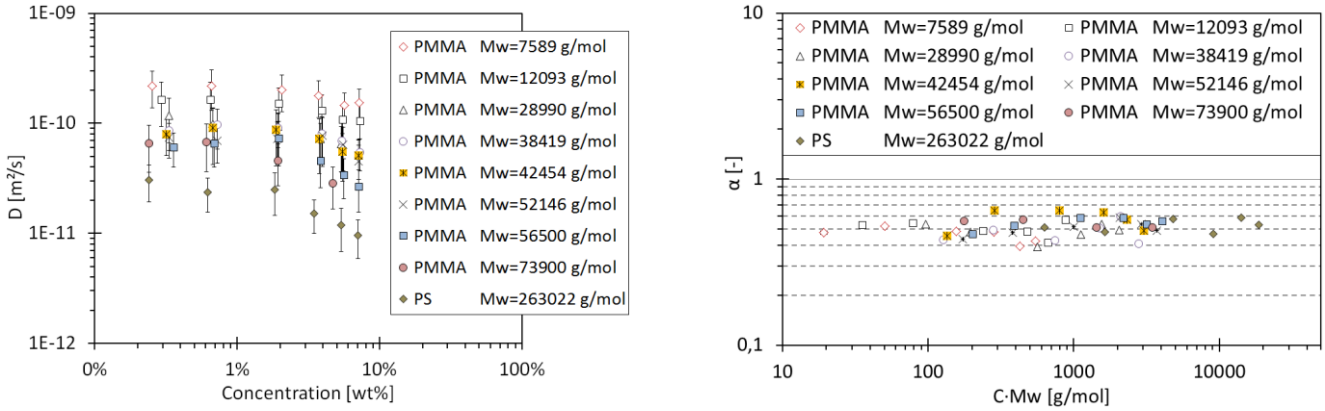

(a) (b)

Figure 1 –(a) Diffusion coefficients with the mean value D_{mean} and the width σ_G and (b) scaling parameter α for different polymer samples at different concentrations ranging from 0.2 wt% to 7.3 wt%.

Acknowledgements

We gratefully acknowledge the financial support from the German Research Foundation (DFG SFB 1176 Project Q2).

References

[1] M. Röding, D. Bernin, J. Jonasson, A. Särkkä, D. Topgaard, M. Rudemo, J. Magn. Reson. 222 (2012) 105-111.
[2] R. Kimmich, NMR - Tomography Diffusometry Relaxometry. Springer Verlag, Berlin, 1997.
[3] B. Hakansson, M. Nyden, O. Söderman, Colloid. Polym. Sci. 278 (2000) 399-405.
[4] M. Urbanczyk, D. Bernin, A. Czuron, K. Kazimierczuk, Analyst 141 (2016) 1745-1752.

^{1}H PFG NMR for Characterizing Interactions of Potential Electrolytes and Electrode Materials

S. Merz[a], P. Jakes[a], H. Tempel[a], H. Kungl[a], M.F. Graf[a], R.-A. Eichel[a,b], J. Granwehr[a,c]

[a]Forschungszentrum Juelich, Institute of Energy and Climate Research, Fundamental Electrochemistry (IEK-9), 52425 Juelich, Germany; [b]RWTH Aachen University, Institute of Physical Chemistry, 52074 Aachen, Germany; [c]RWTH Aachen University, Institute of Technical and Macromolecular Chemistry, 52074 Aachen, Germany

With regard to post lithium-ion battery technologies, metal–air batteries are currently receiving revived interest, particularly focusing on secondary systems because this type of battery possess two- to tenfold higher theoretical energy densities compared to lithium-ion technologies [1]. Since metal–air batteries require a continuous oxygen exchange from the ambient atmosphere through the cathode, the major challenging factors of metal-air systems as secondary batteries are the limitations due to the wetting properties of the cathode and the evaporation/carbonization of the electrolyte. To overcome these issues, new ionic liquid electrolytes or mixtures of water and ionic liquids are being investigated.

Knowledge of electrolyte mobility in pores and interactions with pore surfaces at the electrode is required to systematically improve pore structure and surface morphology in order to provide an optimized surface area for a particular electrolyte [2]. Monitoring electrolyte–electrode interactions requires a detailed description of the pore morphology and permeability, where NMR methods allow us to conclude on diffusion processes in solvation layers. As shown in Figure 1, diffusion processes of ionic liquid electrolytes in electrode materials can be contradistinctive to the expected behavior of liquids in porous materials. For a fully saturated porous air electrode [Figure 1a] a broad line is observed whereas distinct peaks and an increased mobility are prominent for a partly saturated system [Figure 1b]. This indicates that motion of ionic liquids in porous hosts is more complex than what is commonly exhibited by fluids; hence a multimodal investigation is essential for an adequate description of mobility and wetting. The directly accessible information of molecular displacement afforded by ^{1}H PFG NMR is an invaluable tool to gain insights on different ionic liquid distribution and motion in porous electrodes.

To characterize porous electrode materials and feasible electrolyte compositions for metal–air systems a series of ionic liquid/water electrolyte mixtures is assessed in terms of their interactions with carbon black electrode material. The diffusion behavior of the ionic liquid/water electrolyte mixtures is studied by PFG NMR for pressed Vulcan carbon black of different porosities and cathode layers prepared via electrospinning of polyacrylonitrile solutions with subsequent carbonization. The results are compared with nitrogen adsorption (BET) and water vapour methods to gain additional information on the wetting behaviour and triple phase boundaries.

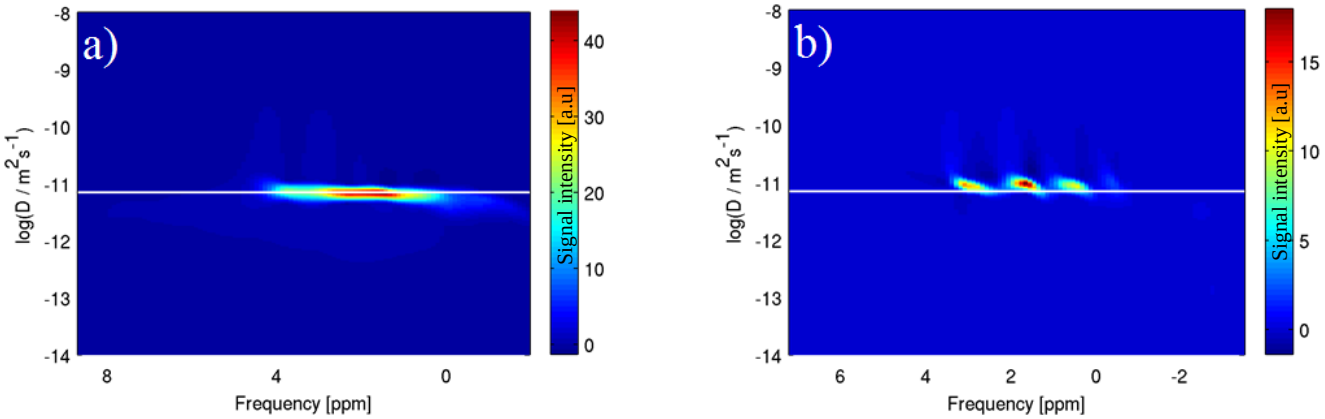

Figure 1 – Diffusion coefficient distribution of an ionic liquid electrolyte inside pressed carbon black electrode material measured by ^{1}H-PFG NMR: (a) fully loaded with ionic liquid (b) loaded with 1/3 of the initial amount.

We gratefully acknowledge funding by the “German Federal Ministry of Education and Research” (BMBF, grant number 03SF0499F “LUZI”)

References

[1] D. Linden, TB Reddy; Handbook of Battery. McGraw-Hill, 2001.

[2] Grey, C.P. and N. Dupré, Chemical reviews, 2004. 104(10): p. 4493-4512.

Diffusion of carboxylate molecules in nanosilica suspensions: from the monomer to polyelectrolytes

Caterina Dolce[a], Guillaume Mériguet[a]

[a] Sorbonne Universités, UPMC Univ Paris 06, CNRS, Laboratoire PHENIX case 51, 4 place Jussieu, F-75005 Paris, France.

Diffusion in crowded media occurs in various contexts, ranging from intracellular biological processes [1], protein-DNA attractions [2], to polymers diffusing among fixed nanoparticles [3]. The diffusion is expected to decrease due to the excluded volume of obstacles. Additional interactions between diffusing molecules and crowding particles, such as electrostatic interactions, can lead an additional hindrance. The present work aims at answering the following question: *how does the diffusion depend on the properties of the crowding medium?*

To address the latter question, we have measured the self-diffusion of carboxylated molecules by Pulsed Field Gradient NMR experiments in a crowded medium. For that purpose, we designed an experimental system made of of carboxylated molecules of various sizes, from a simple carboxylate (propionate) up to polyelectrolytes (sodium polyacrylate, PAANa), diffusing in aqueous dispersions of silica nanoparticles. The molecules and particles are both negatively charged and their charge can be continuously adjusted with pH.

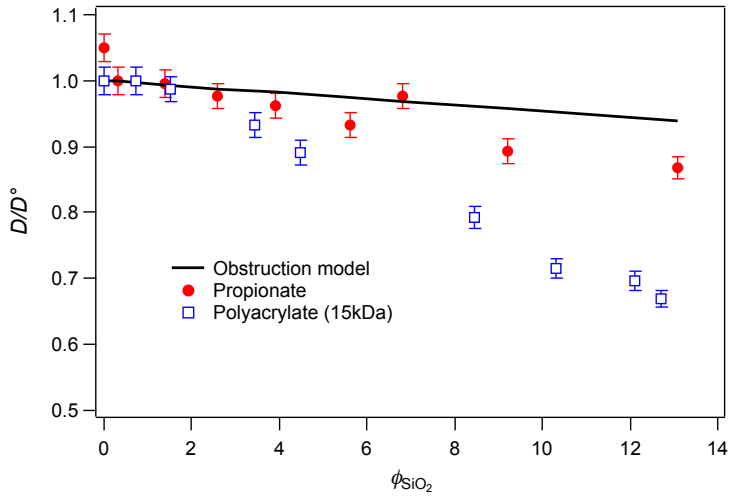

Figure 1 – Evolution of the normalized diffusion coefficient with the volume fraction of silica particles

The preliminary results show a steeper decrease of the diffusion in the presence of negatively charged obstacles than with uncharged obstacles, showing the additional hindrance of the electrostatic interactions. This effect increases with the concentration of silica nanoparticles (see fig 1). The influences of the size of the diffusing molecules and the charge of the molecules and the particles, both controlled by the pH of the suspensions, will be discussed and compared with models from the literature [4].

References

[1] H. Zhou, G. Rivas, and A. Minton, Annu. Rev. Biophys. 37 (2008) 375.
[2] G-W. Li, O. Berg, and J. Elf, Nat. Phys. 5 (2009) 294.
[3] J. Huang, Z. Mao, and C. Qian, Polymer 47 (2006) 2928.
[4] B. Jönsson, H. Wennerström, P. G. Nilsson, and P. Linse, Colloid Polym. Sci. 264 (1986) 77

Spatially resolved, under-sampled propagators and imaging of carbonate rock dissolution

A.A. Colbourne, A.J. Sederman, M.D. Mantle, L.F. Gladden

Magnetic Resonance Research Centre, Dept. of Chemical Engineering and Biotechnology, University of Cambridge, Cambridge, CB3 0HE, UK

Dissolution of a porous rock matrix by an acidic flow causes a change in the pore structure and subsequently the pattern of fluid flow [1,2]. The governing factors for the changing of the pore space are related by the Péclet (Pe) and Damköhler (Da) dimensionless numbers, comparing the transport properties of the fluid in the porous medium with the reactive properties of the solid matrix and the incident fluid [2,3]. Fluid flow rate plays a primary role in determining under what dissolution regime the reaction progresses: from more uniform dissolution at high Pe and low Da, through different "wormholing" regimes to face or compact dissolution at very low Pe and high Da. Here we use NMR propagators as well as imaging and relaxation measurements to monitor the changes in the pore space and fluid flow as a function of reaction progress of the dissolution of Ketton limestone core-plugs with 10 L of 0.01 M HCl at 2, 5, 10 and 50 mL / min.

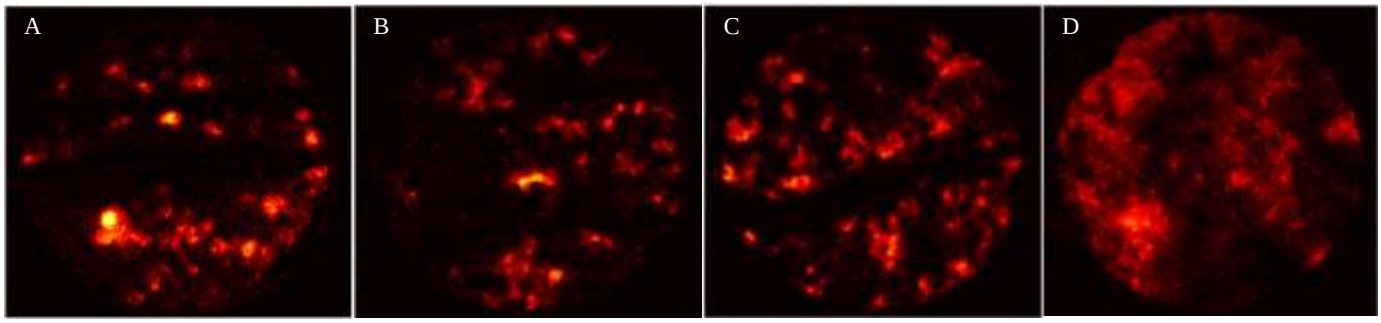

Figure 1 – 2D difference images of a 5 mm thick, cross-sectional slice centred 4 mm from front of the rock core plug. Cores are 38 mm in diameter. Images are shown ofter a total volumemetric flow opf reactant of 10 L at flowrates of A) 2 mL min^{-1}, B) 5 mL min^{-1}, C) 10 mL min^{-1} and D) 10 mL min^{-1}. Increasing flow rate correlates with increasing delocalisation of dissolution.

Figure 1 shows the dependence of reaction mode on flow-rate: fewer, larger wormholes are observed at lower flow rates, these increase in number until at 50 mL min^{-1} where the wormholes formed are "ramified" in nature. Undersampled NMR propagators are used to monitor the transport in the rock core plugs during reactive flow, and investigate the fluid behaviour related with the different reaction modes.

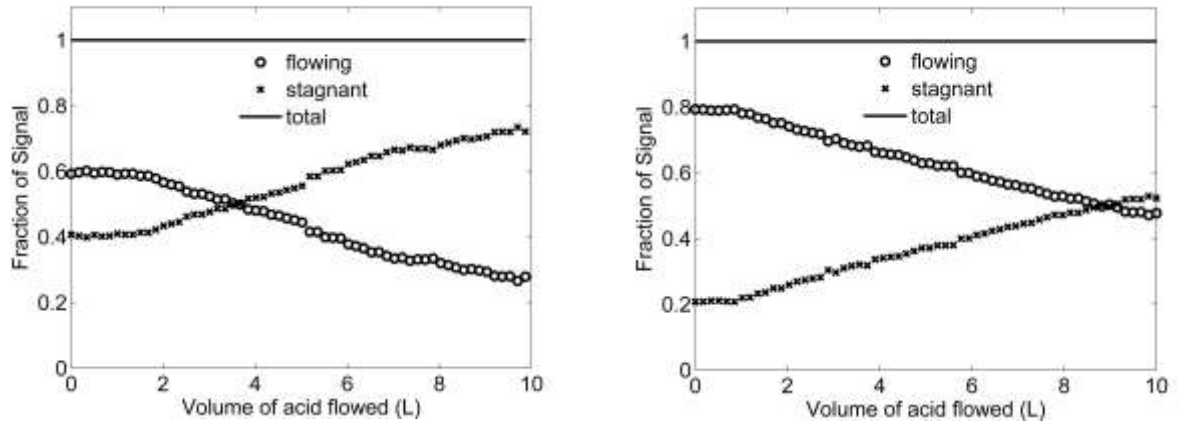

Figure 2 – Normalised sums of the flowing and stagnant regions in the 2 and 10 mL / min propagator measurements at the same logitudinal position as the 2D images in *Figure 1*.

The propagator can be separated into a peak from the stagnant region corresponding approximately to a gaussian centred on zero displacement – the width proportional to the diffusion coefficient – and a flowing region corresponding to the remaining signal. *Figure 2* shows how the proportion of fluid in the flowing and stagnant regions changes as a function of reaction progress: a steady reduction in the proportion of flowing spins and corresponding increase in stagnant spins. The beginning of this transition signals the point at which fresh acid has penetrated to a particular region of the core. The behaviour thereafter gives information on the mode of reaction present.

References

[1] Hoefner, M. L., and Fogler, H. S. (1988) Pore evolution and channel formation during flow and reaction in porous-media, *AIChE Journal 34*, 45-54.
[2] Daccord, G., Lietard, O., and Lenormand, R. (1993) Chemical dissolution of a porous-medium by a reactive fluid. 2. convection vs. reaction, behaviour diagram, *Chemical Engineering Science 48*, 179-186.
[3] Blunt, M. J., Bijeljic, B., Dong, H., Gharbi, O., Iglauer, S., Mostaghimi, P., Pauluszny, A., Pendtland, C., (2013), Pore scale imaging and modelling, *Advances in Water Resources*, 51, 197-216.

Enhanced Gas Recovery NMR Measurements

M.L. Johns[a], M Zecca[a], A Honari[a], S.J Vogt[a], B.. Bijilic[b] and E.F May[a]

[a] School of Mechanical and Chemical Engineering M050, University of Western Australia, 35 Stirling Highway, Crawley 6009, Western Australia, Australia.
[b] Department of Earth Science and Engineering, Imperial College London, Prince Consort Road, London SW7 2BP, United Kingdom.

Enhanced Gas Recovery (EGR), in which injected (and hence sequestered) CO_2 is used to increase natural gas production, has never been practiced industrially from the start of a gas field development despite presenting both significant operational (increased natural gas production) and environmental (secure CO_2 sequestration) benefits [1]. Primarily this lack of adoption is due to uncertainty regards the extent of mixing of the injected supercritical CO_2 and the nascent natural gas, possibly resulting in unacceptable contamination of the natural gas product. Reservoir simulations that accurately capture the CO_2–natural gas mixing processes are essential if EGR is to be adopted. The mixing process is adequately captured by the full dispersion coefficient ($\underline{\underline{D}}$):

$$\underline{\underline{D}} = \left(\frac{D}{\tau}\right)\underline{\underline{I}} + \frac{\alpha_T}{\phi}\left|\underline{v}\right|\underline{\underline{I}} + \frac{(\alpha_L - \alpha_T)}{\phi\,|\underline{v}|}\underline{v}\,\underline{v}^T, \qquad (1)$$

where the molecular diffusivity for CO_2-CH_4 mixtures, the longitudinal dispersivity, transverse dispersivity and the tortuosity are denoted by D, α_L, α_T, and τ respectively. Here we report on the use of NMR measurements to determine α_L, α_T, and τ and their validation for EGR CO_2–natural gas core flooding processes under reservoir/supercritical conditions.

Specifically we use *in-situ* time-resolved NMR 1D axial profiles to determine the dispersion coefficient ($\underline{\underline{D}}$) for a CO_2-CH_4 core flood; via comparison with traditional effluent analysis using IR [2] we are able to quantify and eliminate the erroneous contribution of entry/exit and edge effects in the core flood. We also measure tortusoity (τ) using traditional PFG techniques and use this measurement to validate the dispersion coefficient measurement as velocity approaches zero. This is performed for both a range of sandstone and carbonate rock cores. The final dispersivity data ($\underline{\underline{D}}$ - Peclet number (Pe) relationship) will be presented in a format which is readily incorporated into EGR simulations.

We subsequently have proceeded to adapt our apparatus and methodology to also incorporate residual or connate water [3]. Multi-dimensional MRI was used to confirm the even distribution of residual water in the rock cores; a variable direction centrifuge procedure was established to ensure this. NMR T_2 relaxation measurements were used to confirm the pore size distribution occupied by the residual water phase – sample results are shown in Figure 1. Residual water was found to distinctly occupy the smaller pores, which resulted in an increase in gas dispersion (of up to an order of magnitude) for all rock cores considered. We will conclude by detailing methodology to determine the tortuosity of these partially saturated rock cores, again using PFG techniques.

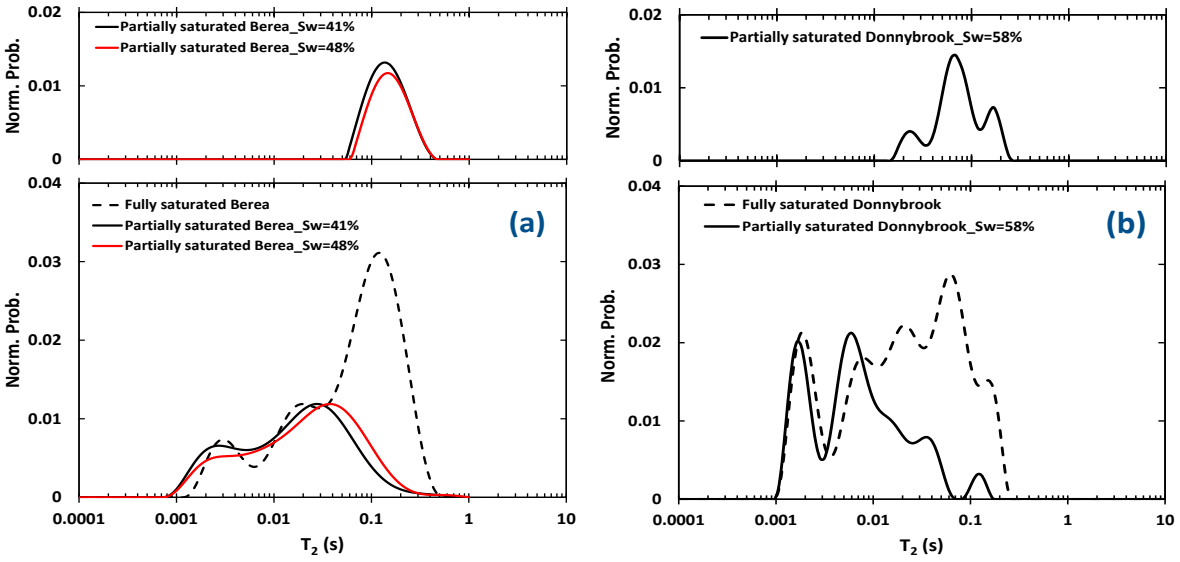

Figure 1 – Distributions of T_2 relaxation (and hence ~pore size) for **(a)** Berea and **(b)** Donnybrook sandstones. The upper panel (created by subtraction of the solid trace from the dashed trace in the lower panel) shows the T_2 (and hence ~pore size) distribution essentially occupied by the supercritical gas phase.

References

[1] Hughes T.J., Hanari, A., Graham, B.F., Chauhan, A.S., Johns, M.L. and May, E.F. (2012) CO_2 Sequestration for Enhanced Gas Recovery: New Measurements of Supercritical CO_2-CH_4 Dispersion in Porous Media and a Review of Recent Research, *Int. Jnl. Greenhouse Gas Control,* **9**, 457-468.
[2] Hanari, A., Vogt, S.J., May, E.F and Johns, M.L. (2015) Gas-Gas Dispersion Coefficient Measurements using Low-Field MRI**,** *Transport in Porous Media*, **106,** 1, 21-32.
[3] Hanari, A., Zecca. M., Vogt, S.J., Iglauer, S., Bijeljic, B., Johns, M.L. and May, E.F. (2016), The Impact of Residual Water on CH_4-CO_2 Dispersion in Consolidated Rock Cores, *Int. Jnl. Greenhouse Gas Control****, in press***

Improvement of NMR-based Measurement Accuracy in Tight Sandstone Porosity and Pore Distribution

Y. L. Zhang, Y. W. Gao, F. Wu, Y. Yang, P. Q. Yang

Shanghai Niumag Electronic Technology Co., Ltd.,200333,Shanghai,China.

Introduction

Nuclear magnetic resonance (NMR) technology is an effective method for studying fluid state of sandstone reservoir, but that tight sandstones are characterized as fine porosity and fast transverse relaxation[1]. As matter of fact, the instinct limitation of the shortest echo interval of classic CPMG sequence makes itself less accurate to meet the assessment standard in petroleum industry.The main reason what leads to low nuclear magnetic porosity in tight sandstone is that the short relaxation component(T2 < TE) is undervalued. So for measuring nuclear magnetic porosity and distribution of tight sandstone, need a method can reduce the influence of non-uniform magnetic field (the main magnetic field, the core internal gradient field) and dead time of coil, as far as possible to near zero moment of nuclear magnetic resonance (NMR) signal .In order to improve testing accuracy, the MSE-CPMG sequence is used to measure tight sandstone originally.

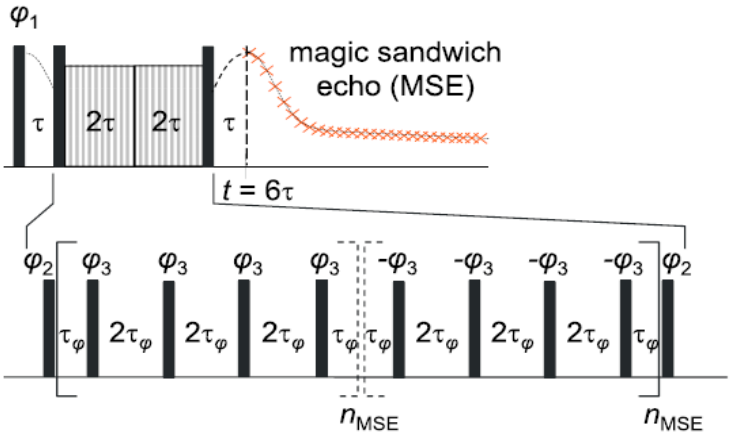

Figure 1 –Timing diagram for the MSE-CPMG sequence.

In experiment, for the initial time of MSE sequence sampling is approximate 20us which sharply enhanced the capability in detecting of ultrashort T2 relaxation components and can reflecte the information of the pore fluid more completely compared to classic CPMG sequence that use 200us for the first sample. Furthermore, the spectral inversion of MSE-CPMG presented characteristics of short T2 relaxation components in a way better than that of CPMG sequence.

Table 1. NMR porosity and porosity by weighting of 10 tight sandstones.

Sample	Porosity by Weighing (%)	NMR porosity by CPMG (%)	Relative error (%)	NMR porosity by MSE (%)	Relative error (%)
1	7.03	5.76	-17.99	6.76	-3.71
2	6.97	5.26	-24.55	6.29	-9.68
3	6.89	5.59	-18.87	6.81	-1.15
4	6.89	5.39	-21.75	6.41	-6.95
5	6.63	4.82	-27.38	5.99	-9.70
6	5.37	4.06	-24.41	4.94	-7.88
7	6.48	4.86	-25.01	5.90	-8.89
8	6.58	5.19	-21.14	6.19	-5.83
9	6.78	5.29	-22.00	6.23	-8.13
10	8.98	7.43	-17.23	8.57	-4.58

The results of NMR experiment for 10 tight sandstone show that the relative error of nuclear magnetic porosity and water-filled porosity is controled under 10%, the method of MSE-CPMG sequence increased measurement precision in water of tight sandstone pore significantly, satisfied the requirement of the oil industry standards.The method displays certain practicability and opens the opportunities to be integrated into NMR techniques in detection of tight sandstone reservoir.

References

[1]Timur A. Effective porosity and permeability of sandstones investigated through Nuclear Magnetic Resonance principles[C]. SPWLA 9th Annual Logging Symposium, New Orleans, LA, 1968, Paper K.

Low-field (LF) NMR-based Characterization of active pore distribution during natural gas accumulation

F.Wu[a], Y. L.Zhang[a], Y. W.Gao[a], Z. Y. Xie[b], P. Q.Yang[a]

[a]ShanghaiNiumag Electronic Technology Co., Ltd.,200333,Shanghai,China;[b]Langfang Branch of Research Institute of Petroleum Exploration and Development,065000,Langfang,China.

In the process of gas reservoir formation, the regulation of pore remained in the rock is the key point in natural gas geology, but the traditional experimental technology cannot provide the displacement process of natural gas in different size of the pore. The low filed NMR as a unique technique to characterize the distribution of pore fluid has been widely used in Petrophysics[1]. With the help of the low field NMR real time displacement measurement platform,we obtained the active pore distribution during natural gas accumulation, and quantitative evaluated the effect of the displacement differential pressure, pore pressure and time on natural gas accumulation. The platform and the method create favorable conditions for the research of natural gas reservoir formation mechanism.

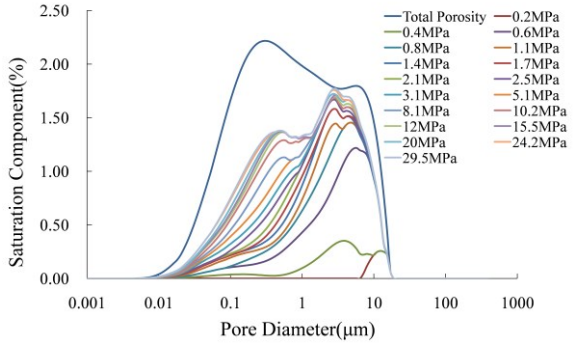

Figure 1 –The displacement process of natural gas in different size of the pore.

Use NMR measureing the displacement process of rock under different displacement pressure difference by the T2 relaxation distribution of the remaining fluid, to deduce the gas pore of methane under the differential pressure, through the transformation model of relaxation time and pore diameter (Equation 1), obtaining methane gas saturation distribution of pore under different displacement pressure difference (figure 1).Then provide the displacement process of natural gas in different size of the pore(figure 2).

$$\frac{1}{T_2} = \rho\frac{S}{V} = a\frac{1}{r} \tag{1}$$

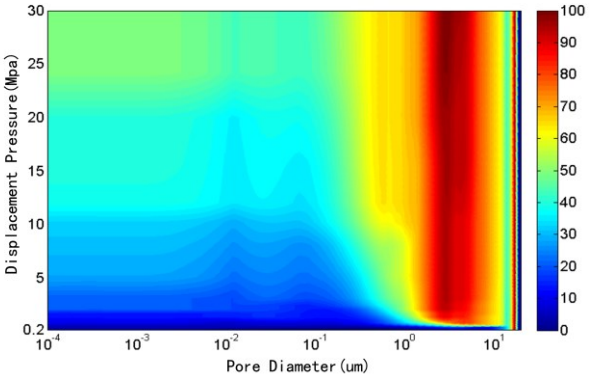

Figure 2 –the active pore distribution during natural gas accumulation.

The experiment obtained the active pore distribution during natural gas accumulation.It can be divided into three step, step 1 when displacement differential pressure is less than 2.5 MPa, gas mainly exist in the pore of 1 ~ 10 um with the increase of displacement pressure difference, the methane gas saturation increases rapidly and the gas saturation of pore those diameter is less than 1 um changes little in the process .Second step 2 after the macropore is close to saturation (displacement differential pressure 2.5 MPa), the gas began to pour into small pore, but there will have a certain amount of residual water can't be displacement out (displacement pressure 2.5 ~ 12 MPa).Step 3 experimental differential pressure is not enough to the rest of the water in the small pore, T2 relaxation distribution has changed little, defineing the rest of water as for bound water (displacement differential pressure 12 ~ 30 MPa).

References

[1] Dunn K J, LaTorraca G A, Warner J L, et al .On the calculation and interpretation of NMR relaxation time distributions[C]. SPE Annual Conference, New Orleans, LA, 1994, Paper 28367.

High temperature fast field cycling study of crude oil

A.Lozovoi[a], M.Hurlimann[b], R.Kausik[b], S.Stapf[a], C.Mattea[a]

[a] Department of Technical Physics II, TU Ilmenau, P.O. Box 100 565, 98684 Ilmenau, Germany; [b] Schlumberger-Doll Research, One Hampshire Street, Cambridge, Massachusetts 02139, United States

Nuclear magnetic resonance (NMR) has been widely used to study crude oil both in bulk and in rock reservoirs. Among other NMR methods, fast field cycling (FFC) relaxometry is of a particular interest for the laboratoty research of oils, since it provides an opportunity to obtain information about the oil composition and molecular dynamics from a distribution of longitudinal relaxation times T_1 as a function of Larmor frequency. Creating conditions similar to the oil wells, e.g. pressure, temperature, etc., allows one to predict the behaviour of the aforementioned oil characteristics in a borehole. This information helps to significantly improve the efficiency of oil extraction and transportation.

Conventional FFC probes do not provide an opportunity to perform measurements at the in-situ well temperature, which can exceed ∽170-175°C. Therefore, the prediction of the features of the T_1 distributions at that temperature has been made based solely on theoretical modeling and extrapolations from laboratory measurements. To improve the situation in this field and carry out direct experiments at these conditions, a high-temperature probe suitable for use in Stelar Spinmaster FFC2000 has been designed and constructed. This allows FFC experiments to be performed at temperatures up to 200°C.

Crude oil samples with known SARA (saturate, aromatic, resin, asphaltene) composition analysis were provided by Schlumberger-Doll Research for the high-temperature FFC study. As is well known, crude oils are a complex mixture of different molecules with a broad range of sizes, shapes and properties, resulting in a complex molecular dynamics. Consequently, their NMR response cannot be described by a single relaxation time and one has to assume a broad distribution of T_1. One way of obtaining it is an application of the one-dimensional inverse Laplace transform (ILT) [1].

The focus of this research was put on investigating the effect of asphaltene molecules in crude oils on the T_1 relaxation time distribution at well-like high temperatures. This is of particular interest since the influence of even small amount of asphaltene on the rheological properties of oil is signifant because of the tendency of these molecules to form porous aggregates. The mechanism of aggregation is not clearly understood and several models for this process can be found in the literature [2]. In this work, oils with different asphaltene content (12.9%, 6.6%, 0%) were studied. The measured longitudinal relaxation decays were recalculated into the distributions of T_1 with the use of an ILT procedure. Resulting relaxation spectra for a range of frequencies from 0.01 MHz to 25 MHz at temperatures up to 170°C are shown in Figure 1.

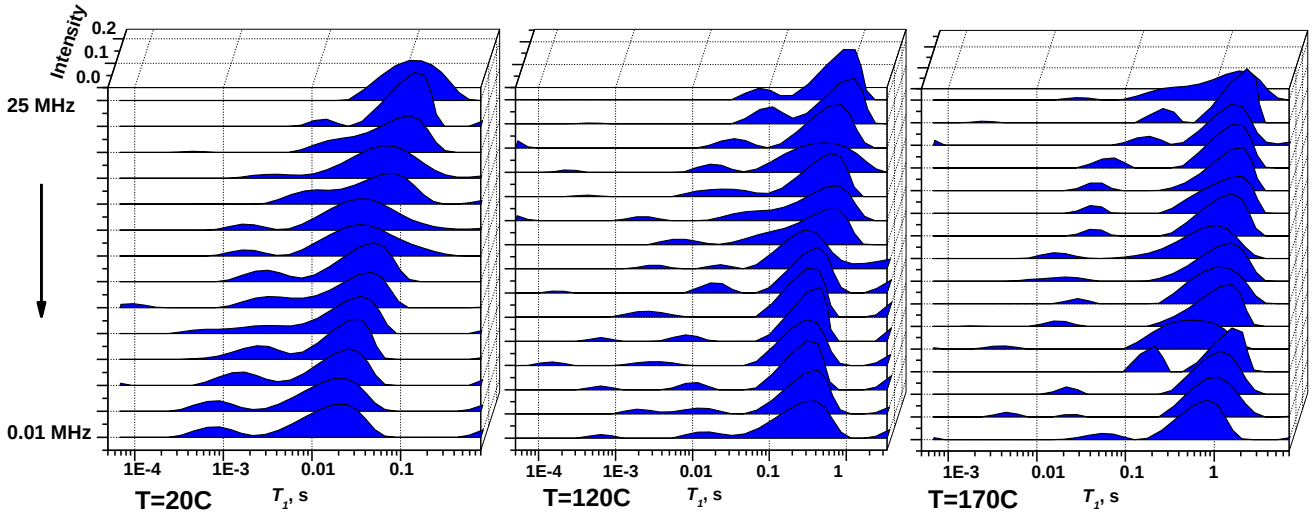

Figure 1 – T_1 relaxation times distributions for crude oil with 12.9% asphaltene content for 3 temperatures obtained with the use of Inverse Laplace Transform

References

[1] Freed, D. E., Hurlimann, M. D. (2010). One- and two-dimensional spin correlation of complex fluids and the relation to fluid composition. Comptes Rendus Physique, 11(2), 181–191.

[2] Zielinski, L., Saha, I., Freed, D. E., Hurlimann, M. D., Liu, Y. (2010). Probing Asphaltene Aggregation in Native Crude Oils with Low-Field NMR. Langmuir, 26(7), 5014–5021.

PETROPHYSICAL STUDY OF RESERVOIR ROCKS BY MAGNETIC RESONANCE IMAGING WITH SPIRICAL SPRITE METHOD

B. Bam[a], B. Balcom[b], B. MacMillan[b], F. Marica[b]

[a]Upstream and Technical Services, EPLAB/LAIP, ENI S.p.A., Milan, Italy; [b]MRI Research Center, Department of Physics, University of New Brunswick, Federicton, Canada.

Nuclear Magnetic Resonance (NMR) has played an important role in formation evaluation for the last 25 years, contributing to both log and laboratory measurements, and providing fast and accurate ways of measuring petrophysical properties such as irreducible satuaration and wettability, capillary pressure and pore size distribution, fluid distribution and relative permeability curves. For this work, a high field 100 MHz MRI and a low field 8.55 MHz NMR relaxometry were used. We used the 3D SPIRICAL SPRITE pulse sequence (Single Point Ramped Imaging with T_1 Enhanced) [1]. 16 samples from 8 reservoirs (sandstones, fratctured carbonates, tight oil and shaley sands) were selected and measured for porosity, irreducible saturation, core flooding parameters and T_2 distribution maps. All measurements were carried out at MRI Research Centre, University of New Brunswick (UNB) as part of a collaboration between ENI and UNB. The results demonstrate that the SPRITE method provides accurate measurements also in complex rocks. The study confirmed also that low field NMR is better than high field in tight sands having short T_2's and strong inhomogeneities of the internal magnetic fields due to the presence of clay minerals.

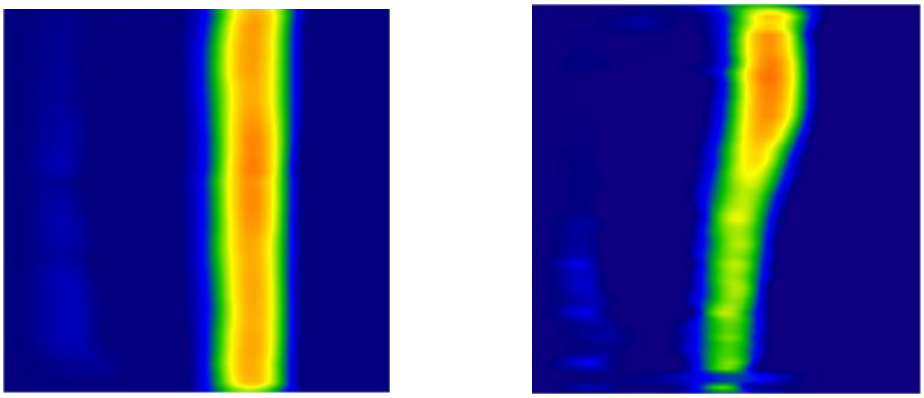

T_2 (µs) **T_2 (µs)**

Figure 1. T_2 distribution map of sample A329 before and after centrifugation

References

[1] B. Balcom, R. MacGregor, S. Beyea, D. Green, "Single Point Ramped Imaging with T1 Enhancement (SPRITE)", Journal of Magnetic Resonance A (1996) 118, 122-125.

Hydrodynamics and 2D NMR characterization of wettability and viscosity in saturated rocks

Jie Wang, Lizhi Xiao, Long Guo, Guangzhi Liao, Yan Zhang, Fengkai Xiao

State Key Laboratory of Petroleum Resources and Prospecting, China University of Petroleum, Beijing, China

In porous media, such as rock, influenced by wettability, oil viscosity and pore geometry, the hydrodynamics is extremely complex and it is difficult to characterize. However, it is critical for developing oil production plan and oil recovery. Researches have been done on qualitative interpretating NMR response of wettability [1,2,5] and NMR simulation by assuming the shape of fluid distrution. But the real distribution of fluid is complex because of wettability and pore geometry. This makes the interpretaion of NMR response diffucult. This paper is focused on the combination of the simulation of distribution of oil and water in saturated rock under the influence of wettability and viscosity and two dimensional NMR characterization of the complex system[2,3,4]. The explicit force LBM with multiple relaxation method can be applied to high viscosity fluid and wettability simulation. Then based on the results of fluid distribution, two dimensional nuclear magnetic resonance response is simulated in saturated rocks. This method can provide deep interpretation of the wettability characterization on NMR response. Figure 1 is the digital rock sample and the fluid distribution affected by wettability.

An example of fluid distribution influenced by wettability and saturation is simulated by this method, and 2D NMR simulation in a rock core based on fluid distribution are implemented. The simlation results is shown in fiigure 2 columns 1-4.The distribution simulation of water and oil in saturated rock provides us the information of how the fluids interact with the pore wall and their distributions, which contributes to the understanding of NMR response simulation. When only wettability and saturation are considered, the results show the surface relaxation effects and diffusion coefficient of the wetting phase would decrease. It is because that interacting with pore walls, surface relaxation of wetting fluid accelerates its relaxation. Confined by the walls, the diffusion coefficient also declines[2]. With saturation increasing, T2 relaxation time and diffusion coefficent shift to high value, because the ratio of contacting surface area to volume decrease and volume increase. Besides, influence of mixed wettability on fluid distribution and 2D NMR characterization is sumlated and the relationship is built between wettability index and surface relaxation. Based on those simulation and theory, we would do some experiment to testify the simulation.

At last, viscosity is also included. Viscosity has little influence on fluid distribution. But it would lead to much more residual oil and cost much more time and higher pressure to displace. Wettablity also increase the capillary pressure of rock core as shown in figure 1 cloums 5. As a nonwetting phase, the higher viscosity shifts the T2-D map to smaller T2 distribution and diffusion coefficient. But as the wetting phase, when we increasing the viscosity, the T2D map shows the complex changes as shown in figure 2 column 5 which would be talked about in future wrok.

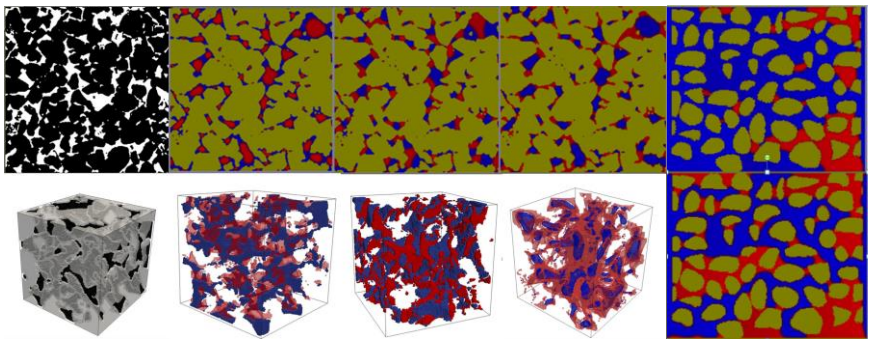

Figure 1-Fluid distribution affected by wettability in rock core, red is oil and blue is water. Colum1 is rock sample, colums 2-4 is fluid distributin affected by oil wetting, mixted wetting and oil wetting.colum 5 is displacement with different viscosity and wettability.

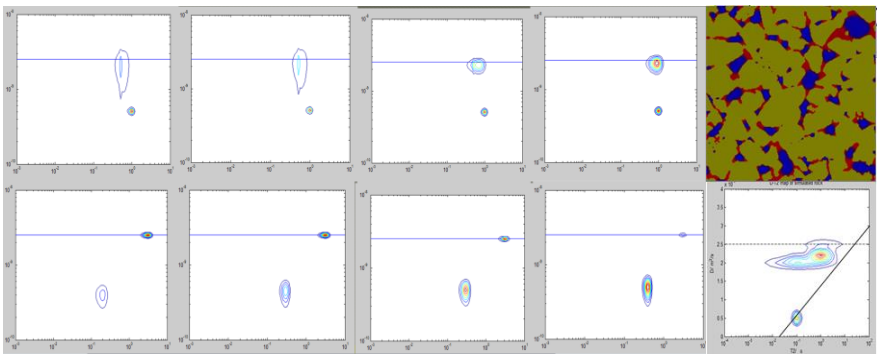

Figure 2-NMR simulation of different wettablity and saturation. Row 1 water wetting with increasing water saturation and row 2 is oil wetting with increasing oil saturation. Colum 5 is high viscosity oil distribution and as wetting phas 2D NMR simulation result.

References

[1] Evseev N, Dinariev O, Hurlimann M, et al.. Petrophysics, 2015, 56(01): 32-44.
[2] Minh C C, Crary S, Singer P M, et al. SPWLA 56th Annual Logging Symposium. Society of Petrophysicists and Well-Log Analysts, 2015.
[3] Arns C H, AlGhamdi T, Arns J Y. New Journal of Physics, 2011, 13(1): 015004.
[4] Song Y Q, Zielinski L, Ryu S. Physical review letters, 2008, 100(24): 248002.
[5] Bergman D J, Dunn K J, Schwartz L M, et al. Physical Review E, 1995, 51(4): 3393.

Pore scale analysis of NMR response in laminated rock with digital rock

Zhi Tian[a], Lizhi Xiao[a], Guangzhi Liao[a], Jie Wang[a]

[a]China University of Petroleum Beijing, 18 Fuxue Road, Changping, Beijing China 102249

Nuclear Magnetic Resonance (NMR) well logging is an effective method for oil and gas exploration, which could detect the information of rock pore fluid directly, thereby providing valuable parameters such as porosity, permeability and pore size distribution to realize the reservoir parameters determination, fluid identification and evaluation. However, it's still facing some problems that using wireline NMR logs to identificate and evaluate thinly laminated reservoirs due to its complicated responses and the limitation of tool's resolution, and pore coupling between micro-pores and macro-pores also impede NMR rock typing. In order to analyze the NMR properties of laminated sandstones, a pore scale thinly bedded digital rock model is reconstructed via process based method [1]. Firstly, the dynamic grain sedimentation process is simulated by sphere grain packing under the action of gravity and other external forces, and then following by the compaction and diagenesis algorithm. As shown in Fig.1(a), it's the forward pore scale laminated formation model reconstructed of two different kinds of rocks with different grain size distributions, and Fig.1(b) represents the pore network distribution of the digital rock. And then Lattice Boltzmann Method (LBM) is used to determine the fluid concentration with different water saturations. Finally, the random walk algorithm is adopted to simulate the echo train signals acquisition with CPMG pulse sequence under certain magnetic field gradient, which is widely and universally used in downhole wireline NMR logging [2, 3].

We analyze the sensitivity of NMR T_2 distribution to the presence of micro-pores and macro-pores bedded sedimentary formation. The results of brine saturated laminated formation under different surface relaxivity and magnetic field gradient contrast shows that NMR T_2 relaxation response do not influenced by the pore size distribution, but also the diffusional pore coupling, transverse relaxation shows clear bimodal distribution when the surface relaxivity of micro-pore layer is relatively large, while decreasing the the surface relaxivity of micro-pore layer will escalate the pore couping, which cause the T_2 distribution becomes unimodal. In order to further convince the diffusional coupling, a fractal discrete fracture network (FDFN) model is adopted to generate several fractures between different layers[4]. The results shows that the fracture-pore diffusinal coupling will also change the morphology of T_2 distribution. Correctly understanding of this pore coupling phenomenon will substantially lead to better interpretation of wireline NMR logs in thinly beded or other inhomogeneous reservoirs with complex pore structure. And then we also simulate the T_2-D maps of the laminated rock under different water saturations, which can be further used to investigate the quantitative relationship between NMR signal and fluid saturation.

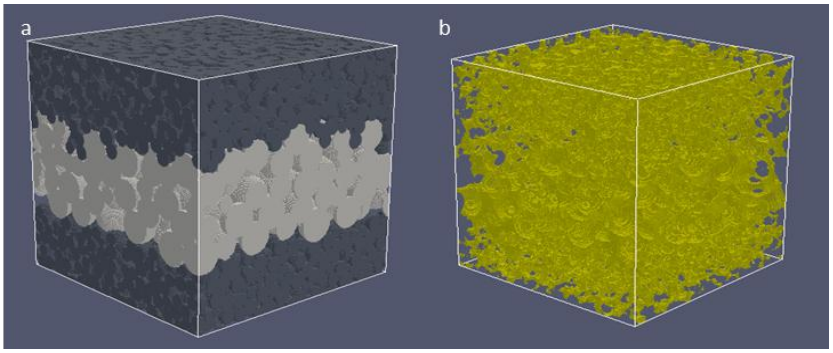

Figure 1 –laminated digital rock model and its pore network

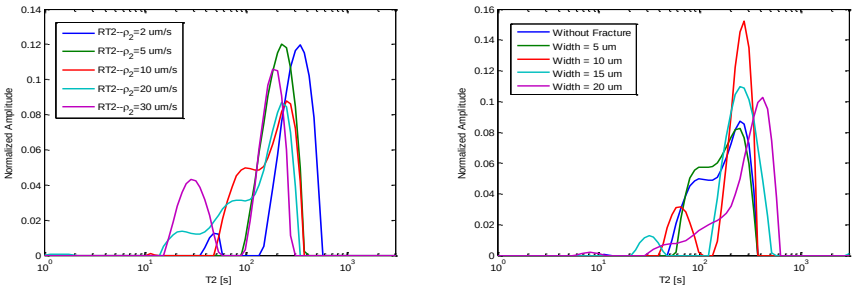

Figure 2 –laminated rock: T_2 distribution (a) of different suface relaxivity contrasts, (b) including planar fractures of different thickness

References

[1] Oren P E, Bakke S. Transport in Porous Media, 2002.
[2] Toumelin E, Torresverdin C, Sun B, et al. J. Mag. Res. 2007, 188(1): 83-96.
[3] N.H.Alhwety, N.I.Sayedakram, I.Shikhov et al. Diffusion-fundamentals. 2014.
[4] Chi L, Heidari Z. Geophysics, 2014, 80(1): 31-42

Permeability of water flow in CH_4 hydrate-bearing quartz sand

E.Kossel[a], C. Deusner[a], N. Bigalke[a,b], M. Haeckel[a]

[a]GEOMAR Helmholtz Centre for Ocean Research Kiel, Wischhofstr. 1-3, Kiel, Germany; [b]present address: GEOTEK, 4 Sopwith Way, Daventry, Northamptonshire, NN11 8PB, United Kingdom.

Gas hydrates are crystalline compounds where water molecules form a cage structure occupied by small gas molecules. Natural gas hydrates occur at high pressures and low temperatures in permafrost and sub-marine environments. They contain vast amounts of natural gas that is predominantly composed of methane [1]. The occurrence of a solid crystalline phase in the sediment pore space reduces the volume available for fluid transport and consequently the permeability of the geological formation. Although the permeability is a key factor for understanding and predicting mass transport in gas hydrate settings, it is not well understood how the formation or dissociation of gas hydrates in the pore space of marine sediment alters the permeability and the flow characteristics of the involved phases. State-of-the-art petrophysics simulation codes use theoretically derived permeability equations that are hardly backed by experimental data. The reason for the insufficient validation of the model equations is the difficulty to create gas hydrate bearing sediments in the laboratory that have undergone formation mechanisms equivalent to the natural process and have a well-defined gas hydrate saturation.

We designed an experimental set-up that enabled us to measure changes of water permeability in CH_4 hydrate-bearing quartz sand with known gas hydrate saturation and distribution. It is based on a NMR-transparent flow-through pressure cell that can sustain pressures up to 15 MPa and is temperature controlled in the range from 5 °C to 15 °C [2]. We formed methane hydrates in quartz sand from a methane-saturated aqueous solution and used a multi slice spin echo imaging pulse sequence to get time-resolved images of the sample volume during water flow. The acquisition time for one set of images was 128 seconds. Maps of the gas hydrate saturation were obtained by calculating the normalized difference of the images and a gas hydrate free reference image. These maps were included into 3-D Finite Element Method simulations. In our simulations, we tested five different permeability equations and constrained the equation parameters by finding the best possible matches between simulation results and experimentally measured pressure differences during water flow. The tested permeability equations were the modified Stone equation [3], the van Genuchten/Parker equation [4,5,6], the pore filling Kozeny grain equation [7], the Civan [8] equation and an equation that is used within the CMG Stars reservoir simulator [9]. All suitable permeability equations include the term $(1\text{-}S_H)^n$, where S_H is the gas hydrate saturation and n is the constrained exponent. The most basic equation for the description of the permeability behavior of water flow through gas hydrate bearing sand turned out to be

$$k = k_0 (1 - S_H)^n . \quad (1)$$

In our experiments, n was determined to be 11.4 (±0.3).

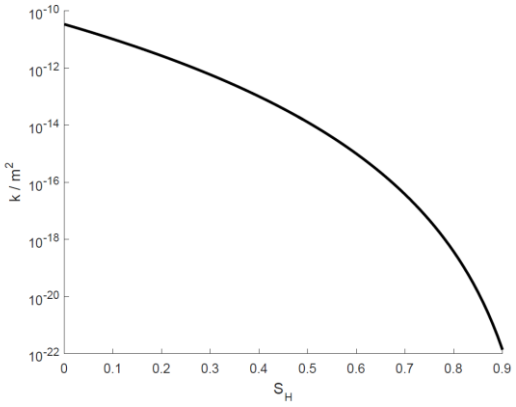

Figure 1 – Water permeability as function of gas hydrate saturation.

References

[1] E. D. Sloan, and C. A. Koh, Clathrate hydrates of natural gases, 3rd ed., CRC Press, New York, 2008.
[2] E. Kossel., C. Deusner, N. Bigalke, and M. Haeckel, Diffusion Fundamentals, 18(15), 1-4, 2013.
[3] H. L. Stone, Journal of Petroleum Technology, 22(2), 214-218, 1970.
[4] Y. Mualem, Water Resources Research, 12(3), 513-522, 1976.
[5] M. T. van Genuchten, Soil Science Society of America Journal, 44(5), 892-898, 1980.
[6] J. C. Parker, R. J. Lenhard, and T. Kuppusamy (1987),Water Resources Research, 23(4), 618-624,1987.
[7] J. Kozeny, J., Sitzungsberichte Akademie der Wissenschaften, 136, 271-306, 1927
[8] F. Civan, F., AIChE Journal, 47(2), 271-287, 2001.
[9] CMG, STARS advanced process and thermal reservoir simulator (user's guide), Calgary, Canada, 2009.

P90

A New Method for measuring the wettability of porous media by In-situ NMR Water Vapor Isotherm Technique

Hyung T. Kwak and Ahmad M. Harbi
Saudi Aramco

Yuan Chong, Zhi-Xiang Luo, Patrick R. Doyle, Alfred Kleinhammes, and Yue Wu
Department of Physics and Astronomy, University of North Carolina, Chapel Hill, NC 27599-3255, USA

The wettability of the porous structure within rocks, is one of the key parameters that determine the hydrocarbon recovery factors and the fluid flow through those rocks. Consequently, wettability is one of the essential input variables for geophysical models that predict fluids flow through reservoir rocks. Wettability is often used as a distinguishing characteristic of materials, designating them as hydrophobic, or hydrophilic. However, wettability is not just a material parameter characteristic of a given rock, e.g. sandstone or carbonate, but depends on other factors as well, such as surface roughness, surface area, existence of primary adsorption sites, and specific ion effect.

NMR Water Vapor isotherm could provide insight into the molecular dynamics at the interface by analyzing different total amount of adsorbed water vapor and shapes of the measured water vapor isotherm as a function of relative vapor pressure for hydrophilic and hydrophobic surfaces. Since the NMR water vapor isotherm is affected not only by water molecule affinity but also by other factors controls wettability of pore surface, it should be able to measure wettability of interior pore surface of porous materials. Additional advantage of NMR water vapor isotherm wettability measurement is it can accurately measure the wettability of nano sized pore surface since gas is injected instead of liquids from other conventional wettability measurement methods.

The experimental results shows the clear differences in the NMR water vapor isotherm curves from water- and oil-wet model porous materials. The experimental results along with the concept of a new method for quantifying wettability index will be presented.

Asphaltene porous aggregates in crude oil investigated by aromatic and fluorine containing tracers: a relaxometry and DNP study

Siegfried Stapf[1], Amin Ordikhani-Seyedlar[1], Artur Lozovoi[1], Carlos Mattea[1], Oliver Neudert[1], Ravinath Kausik[2], Denise E. Freed[2], Yi-Qiao Song[2], Martin D. Hürlimann[2]

[1]Dept. of Technical Physics II, TU Ilmenau, PO Box 100 565, 98684 Ilmenau, Germany; [2]Schlumberger-Doll Research, One Hampshire Street, Cambridge MA 02139, USA

Asphaltenes are a class of medium-sized PAHs present in most crude oils that are conventionally NMR-invisible due to their short relaxation times. Quantification of asphaltenes requires an elaborate process of precipitation that cannot be done in the borehole, yet a sudden change of composition or concentration of asphaltenes poses a severe threat to the production infrastructure. An indirect detection appears possible by the effect that asphaltene has on the general viscosity and relaxivity of the remaining molecules, the so-called maltenes. However, while the relation of NMR relaxation times and diffusion coefficients with overall viscosity and molecular size in a typical oil composition has been established, this relation breaks down in the presence of significant amounts of asphaltene. DFT and experimental data suggest that aromatic molecules, probably supported by a process called π–π-stacking, have longer interaction times with the asphaltene aggregates, leading to shorter NMR relaxation times and enhanced DNP factors employing the radicals contained in asphaltenes.
In this study, we systematically separate the influence of PAH and radical concentration, aromaticity and molecular size on the relaxation dispersion and the important T_1/T_2 ratio of fluid components. A particular strong influence is identified for molecules containing ^{19}F nuclei; we thus suggest fluorinated tracer compounds for a time-efficient downhole assessment of asphaltene concentration in crude oil.

The relation of NMR relaxation times and diffusion coefficients with overall viscosity and molecular size in a typical fluid composition has been established for bulk oils [1-3]. A major obstacle for the task of compositional analysis remains, however, the widely unknown role of molecular shape and chemistry, most importantly aromaticity, on the NMR relaxation behaviour. This is particularly important in asphaltene-containing oils where the relaxation of solvent maltene protons, is significantly affected by interactions with radical-containing asphaltenes [4]. However, aromatic and aliphatic maltenes are expected to interact differently with asphaltene aggregates [5], and size-dependent residence time variations within the porous aggregates become important [6]. While fundamental studies have attempted to provide a molecular dynamics description of relaxation times that take advantage of data obtained at variable magnetic fields [7], they still suffer from a lack of distinction of dynamics between molecules of various architecture, and from the generally broad relaxation times distribution in natural oils.

^{19}F containing tracer molecules were applied at low concentrations to natural oils of different asphaltene content [8], and the tracer's relaxation time ratio T_1/T_2 as well as the field dependence of relaxation times, $T_1(\omega)$, were obtained. This strategy has the advantage of specifically determining the behaviour of different tracers, where molecular weight and aromaticity are considered as variables. One main finding of this study is the significant increase of T_1/T_2 for aromatics in the presence of asphaltenes compared to alkanes [9]. The results are interpreted in terms of selective maltene-asphaltene interaction based on frequency dependent relaxation results. The strong contrast of relaxation times allows for a simplified quantification of either asphaltene concentration or maltene aromaticity in crude oils. The role of asphaltene has further been quantified by concentration-dependent measurements of protonated and fluorinated test molecules in a deuterated solvent, and of non-aggregating polycyclic radical (BDPA) and neutral molecules mimicking asphaltene (violanthrone-78), respectively. The shape of the $T_1(\omega)$ dispersion is in agreement with the assumption of an efficient RMTD process possibly supported by overall aggregate tumbling on a μs timescale. Results of the enhancement in dynamic nuclear polarization (DNP) experiments, making use of microwave saturation of the naturally occurring radicals in oils, confirm the significant difference in interaction strength of asphaltenes with aromatic and aliphatic molecules, or even with individual moieties in the molecules [10]. The use of suitable tracer molecules for relaxation measurements, and a comparison of DNP enhancement employing naturally occurring asphaltene radical species, bears the potential to facilitate the conventional but time-consuming SARA analysis of crude oil.

[1] D.E. Freed, J. Chem. Phys. **126**, 174502 (2007).
[2] D.E. Freed, J. Phys. Chem. **113**, 4293-4302 (2009).
[3] D.E. Freed, M.D. Hürlimann, Comptes Rendues Physique **11**, 181-191 (2010).
[4] J.-P. Korb, A. Louis-Joseph, L. Benamsili, J. Phys. Chem. B **117**, 7002-7014 (2013).
[5] O. Castellano, R. Gimon, U. Soscun, Energy Fuels **25**, 2526-2541 (2011).
[6] M. Derakhshesh, A. Bergmann, M. R. Grey, Energy Fuels **27**, 1748-1751 (2013).
[7] L. Zielinski, M.D. Hürlimann, Energy Fuels **25**, 5090-5099 (2011).
[8] S. Stapf, A. Ordikhani-Seyedlar, N. Ryan, C. Mattea, R. Kausik, D. E. Freed, Y.-Q. Song, M. D. Hürlimann, Energy Fuels **28**, 2395-2401 (2014).
[9] S. Stapf, A. Ordikhani-Seyedlar, C. Mattea, R. Kausik, D. E. Freed, Y.-Q. Song, M. D. Hürlimann, Microp. Mesop. Mat. **205**, 56-60 (2015).
[10] A. Ordikhani-Seyedlar, O. Neudert, S. Stapf, C. Mattea, R. Kausik, D. E. Freed, Y.-Q. Song, M. D. Hürlimann, Energy Fuels, *in press*

Optimising Digital Filters in low-field NMR

E. Fordham[b], A.Valori[a], J. Mitchell[b]

[b]Schlumberger Gould Research, High Cross, Madingley Road Cambridge CB3 0EL, UK; [a]Schlumberger Dhahran Carbonate Research, Dhahran Techno Valley, Dhahran, Saudi Arabia.

Optimising parameters for NMR is delicate. In virtually all cases, the best choice depends not only on the sample and hardware, but also on the experimental objective. In all imaging experiments (from MRI to astrophysics), the inverse relationship between Field Of View and resolution is obvious and typically easy to understand. Similar compromises occur in time domain NMR, albeit less straightforward to visualise.

Digital filters are an intrinsic part of the receiver chain in modern NMR and MRI instruments based on highly oversampled analogue to digital conversions [1]. Depending on the vendor, some digital filtering in the receiver chain may be user-programmable, although this is not widely practised on benchtop systems [2].

Spectroscopy and MRI typically deal with relaxation rates much slower than relaxation in porous media. This requires a completely different approach to the art of filtering in the two applications. Understanding digital filters is important for noise/interference suppression, but also for correct pulse sequence timing (dead times, group delays), especially for CPMG with very short echo times (shale applications). Delay times can be minimised by careful design of "fast" filters. Also, digital filtering is only the last stage of reception; signal spectra are also affected by hardware characteristics, in particular the bandwidth of the probe-preamplifier system. The introduction of Active Damping Feedback Preamplifiers (ADFP) (or *Q*-switching) in modern instruments, has increased dramatically the physical bandwidth of typical commercial probes. This makes wise setting of digital filters even more critical.

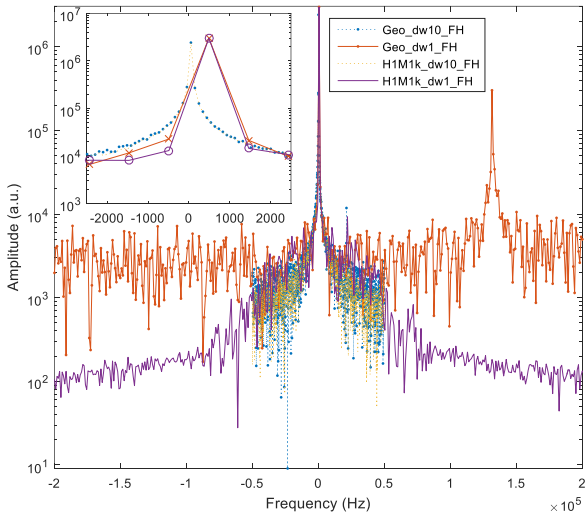

Figure 1 –: Water-Fluorinert measured with different Dwell times (1µs and 10µs) and different filters (Geo and H1M1k). The inset is an expansion of the zero frequency area. The spectra acquired with DW=1µs and the filter Geo is contaminated by about 40% 19F signal)

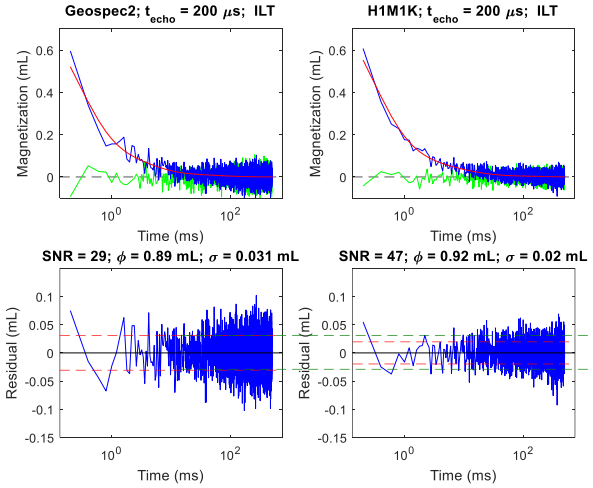

Figure 2 –: Different signal to noise performances of the two filters considered (both at DW=1µs and 32 scans)

In this paper we will discuss the effects of different acquisition parameters and digital filtering on Signal to Noise ratio (Figure 2), instrument dead time, instrument sensitivity and calibration, artefact generation and 19F-1H signal cross-contamination. The latter is a special risk in systems where PTFE is widely used for coil formers and sample holders, and per-fluorinated oils are used for heat transfer and pressure applications. Examples will be shown of completely misleading petrophysical interpretations, for the unwary.

Figure 1 shows the 2MHz spectrum of signal of a water-Fluorinert mixture acquired with two different DWell times (1µs and 10µs) and two different filters (Geo and H1M1k). The signal with the filter Geo at DW=1µs is heavily contaminated (40%) by 19F. Although DW=10µs would avoid this, faster sampling has advantages for fast decaying signals, e.g. detection of echo shapes, artefacts in short echo spacing CPMG, and enhancing SNR. Strategies for reconciling these conflicting objectives will be discussed.

References

[1] Moskau, D. Concepts in Magnetic Resonance, 15(2), (2002). 164–176.
[2] Mitchell, J., Gladden, L. F., Chandrasekera, T. C., & Fordham, E. J. Progress in Nuclear Magnetic Resonance Spectroscopy, 76(0), (2014) 1–60.